INTEGRATED SURFACE WATER GROUNDWATER MODELING IN THE UPPER RIO GRANDE IN SUPPORT OF SCENARIO ANALYSIS

by

Jesse Roach

A Dissertation Submitted to the Faculty of the

DEPARTMENT OF HYDROLOGY AND WATER RESOURCES

In Partial Fulfillment of the Requirements
For the Degree of

DOCTOR OF PHILOSOPHY
WITH A MAJOR IN HYDROLOGY

In the Graduate College

THE UNIVERSITY OF ARIZONA

2007

THE UNIVERSITY OF ARIZONA
GRADUATE COLLEGE

As members of the Dissertation Committee, we certify that we have read the dissertation

prepared by Jesse Roach

entitled INTEGRATED SURFACE WATER GROUNDWATER MODELING IN THE UPPER
RIO GRANDE IN SUPPORT OF SCENARIO ANALYSIS

and recommend that it be accepted as fulfilling the dissertation requirement for the

Degree of Doctor of Philosophy

_____ Date: March 19, 2007
Dr. Kevin Lansey

_____ Date: March 19, 2007
Dr. Thomas Maddock III

_____ Date: March 19, 2007
Dr. Vincent Tidwell

_____ Date: March 19, 2007
Dr. Phillip Guertin

_____ Date: March 19, 2007
Dr. Janie Chermak

Final approval and acceptance of this dissertation is contingent upon the candidate's submission
of the final copies of the dissertation to the Graduate College.

I hereby certify that I have read this dissertation prepared under my direction and recommend
that it be accepted as fulfilling the dissertation requirement.

_____ Date: March 19, 2007
Dissertation Director: Dr. Kevin Lansey

STATEMENT BY AUTHOR

This dissertation has been submitted in partial fulfillment of requirements for an advanced degree at the University of Arizona and is deposited in the University Library to be made available to borrowers under rules of the Library.

Brief quotations for this dissertation are allowable without special permission, provided that accurate acknowledgment of source is made. Requests for permission for extended quotation from or reproduction of this manuscript in whole or in part may be grated by the head of the major department or the Dean of the Graduate College when in his or her judgment the proposed use of the material is in the interests of scholarship. In all other instances, however, permission must be obtained from the author.

SIGNED: _____

Jesse Roach

ACKNOWLDEGEMENTS

TABLE OF CONTENTS

TABLE OF CONTENTS - *continued*

TABLE OF CONTENTS - *continued*

TABLE OF CONTENTS - *continued*

LIST OF FIGURES

LIST OF FIGURES - *continued*

LIST OF FIGURES - *continued*

LIST OF FIGURES - *continued*

LIST OF FIGURES - *continued*

LIST OF FIGURES - *continued*

LIST OF FIGURES - *continued*

LIST OF FIGURES - *continued*

LIST OF TABLES

LIST OF TABLES - *continued*

ACRONYMS

AEBES	Actual Elephant Butte Effective Supply
AET	actual evapotranspiration
AF	acre feet
AG	agriculture or agricultural
AMSL	above mean sea level
BDA	Bosque del Apache
BoR	Bureau of Reclamation
CFS	cubic feet per second
EAC	elevation-area-capacity
EBEIS	Elephant Butte Effective Index Supply
EBID	Elephant Butte Irrigation District
EPA	Environmental Protection Agency
ET	evapotranspiration
ETTB	ET Toolbox
GDD	growing degree day
GIS	Geographical Information System
GPD	gallon per day
GW	groundwater
LFCC	low flow conveyance channel
MAF	million acre feet
MRG	Middle Rio Grande
MRGCD	Middle Rio Grande Conservancy District
NMRGCB	New Mexico's Rio Grande Compact Balance
OIS	Otowi Index Supply
PET	potential evapotranspiration
RMSE	root mean square error
RGC	Rio Grande Compact
SA	sensitivity analysis
SAHRA	Semi-Arid Hydrology and Riparian Areas
SJC	San Juan Chama
SVP	Shared Vision Planning
SW	surface water
SWE	snow water equivalent
URGWOM	Upper Rio Grande Water Operations Model
USACE	U.S. Army Corps of Engineers
USGS	United States Geological Survey

ABSTRACT

New and growing demands to finite and fully allocated water resources in the semi-arid southwestern United States mean that existing water resources must be managed with increasing efficiency to minimize shortages and associated social conflict. Computer based simulations can provide a powerful tool to aid in policy related decisions. This dissertation describes the development of a simulation model of the Rio Grande surface water and groundwater system for use in scenario evaluation. The primary model goal is to integrate cross disciplinary science at a basin scale, and make it easily accessible to a wide range of stakeholders. To achieve this at a river basin scale, three existing groundwater models and one surface water model were simplified and combined in a system dynamics framework using the commercial software package Powersim Studio 2005. To this physical model, a simple human behavioral model and user interface was added. The resulting scenario evaluation tool runs 40 year simulations on a laptop computer in tens of seconds, with inputs that are easily changed by non-expert users via a graphic, user friendly interface.

CHAPTER 1: INTRODUCTION

As human demands for fresh water grow beyond sustainable supplies, and acceptable

water resources are diminished by overdraft and reductions in water quality, water

scarcity is becoming a global issue (Rosegrant et al. 2002). In situations where

exploitation of water resources is not limited by lack of storage and conveyance

infrastructure, improved resource management is perhaps the single best tool available to

cope with growing demands. This dissertation will outline the development of a basin

scale hydrological simulation model designed to improve water management decisions by

informing stakeholders and decision makers with relevant integrated hydrological

science. In this, the first chapter of the report, the overall context driving water scarcity

will be introduced at a global level, as well as at the level of the Rio Grande system in

northern and central New Mexico which provides the focus area for the model. The need

for simulation models will be addressed, the concept of system dynamics modeling

introduced, and the goals and unique characteristics of the Rio Grande model outlined. In

Chapter 2, the overall surface water system model component will be covered, followed

by the groundwater system component in Chapter 3. Chapter 4 will cover scenario

analysis using the integrated model and a simple human behavioral model. Chapter 5

will provide conclusions, suggested improvements on the current model, and directions

for future work.

1.1 Challenges to Water Management

1.1.1 Challenges on a Global Level

Significant modern challenges to water management at a global level include growing resource scarcity, groundwater overdraft, climate change related uncertainties, resource contamination, and soil salinization (Jury and Vaux 2005). The ability of the world's finite fresh water resources to supply ever growing demands without increasing these impacts is in doubt among a wide range of researchers (e.g. Zehnder et al. 2003, Gleick et al. 2003, Rosegrant et al. 2002). As growth of human water demands stress resources, less water is available for the hydrologic environment or food production, resulting in environmental degradation and political unrest, especially in the world's poorer and more populous arid and semi-arid regions, among the likely results (Jury and Vaux 2005, Wolf 1999). While these problems are global in nature, the acute symptoms of fresh water scarcity will be regional in nature, and not necessarily limited to the developing world. The upper Rio Grande basin in the semi-arid southwestern United States is an example of a basin already feeling the impact of growing demands in the context of finite and fully allocated supplies.

1.1.2 Challenges in the Rio Grande

Large portions of the western United States, including New Mexico are characterized by a lack of abundant water resources, with annual precipitation less than 12 inches typical as seen in Figure 1-1. The main river system draining New Mexico is that of the Rio Grande, an important renewable supply of water that has supported

Precipitation: Annual Climatology (1971–2000)

Precipitation (in.)

0	16–20	36–40	80–100
<4	20–24	40–50	100–120
4–8	24–28	50–60	120–140
8–12	28–32	60–70	140–160
12–16	32–36	70–80	160+

Source: http://www.wcc.nrcs.usda.gov/climate/prism.html
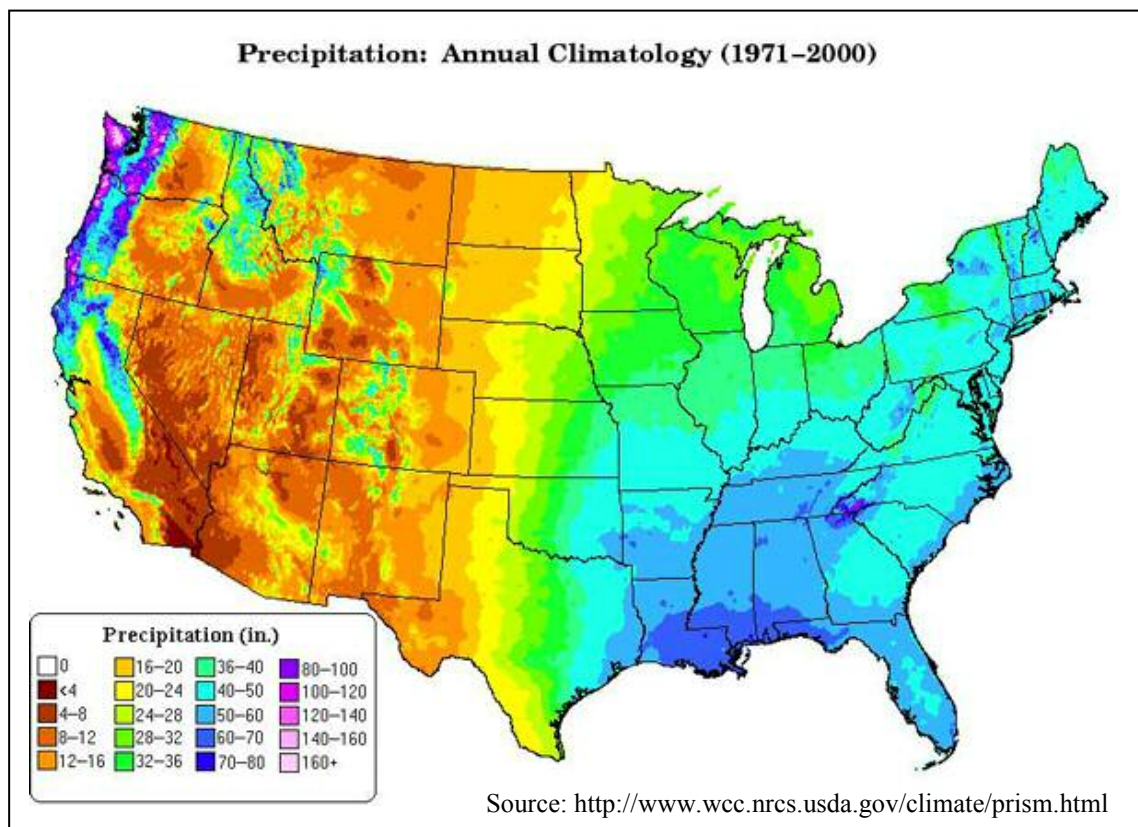
Figure 1-1. PRISM annual average precipitation estimates for the United States 1971 - 2000.

agriculture based human civilizations for thousands of years (e.g. Horgan 1954). Since

the adoption of the Rio Grande Compact by the states of Colorado, New Mexico at the

end of 1939 (Colorado et al. 1938), releases from Caballo reservoir (see Figure 2-1 for

location) have exceeded those demanded for downstream use in only six years (Shafike

2007). In other words, in all but the wettest of periods, the available surface water

resources in the upper Rio Grande are dedicated for human use. In typical years, every

drop of water is used, sometimes several times, before, in most cases, ending up in the

atmosphere as a result of evapotranspiration (ET) from rivers, reservoirs, fields, lawns, or

riparian vegetation. The era of seeking new surface water supplies and increasing surface

water storage to serve growing demands is long past in the Rio Grande. In addition to scarce water resources, the semi-arid southwestern United States, including the Rio Grande basin is experiencing rapid population growth. According to the United States Census Bureau, the state of New Mexico increased in population from approximately 1.5 million in 1990, to 1.8 million in 2000, a 20% increase, with 85% of that growth occurring in urban areas (United States Census Bureau 2007). With surface water rights dedicated largely to agriculture, the rapid urban growth was supported by increased groundwater use, which in many areas exceeded natural recharge and is therefore not a sustainable long-term growth strategy. The United States Department of the Interior, Bureau of Reclamation (2005) noted that rapid population growth in combination with scarce water resources is a recipe for social conflict over water. As shown in Figure 1-2, Bureau of Reclamation considers the upper Rio Grande basin in New Mexico one of 10 areas in the United States where the likelihood of water scarcities and associated social conflict by the year 2025, is "highly likely". Indeed, social conflict in the basin is already occurring, with a well publicized lawsuit between environmental groups on behalf of the endangered Rio Grande Silvery Minnow affirming the right of the Bureau of Reclamation to reduce deliveries of San Juan Chama water (see Section 2.2.2) to contractors including the city of Albuquerque in order to provide minimum river flows for protection of the minnow (Gardner, 2006). Who gets the water in times of shortage may have to be, as in this case, settled in the courts, but this is surely not the preference of water managers, and perhaps something science can help limit.
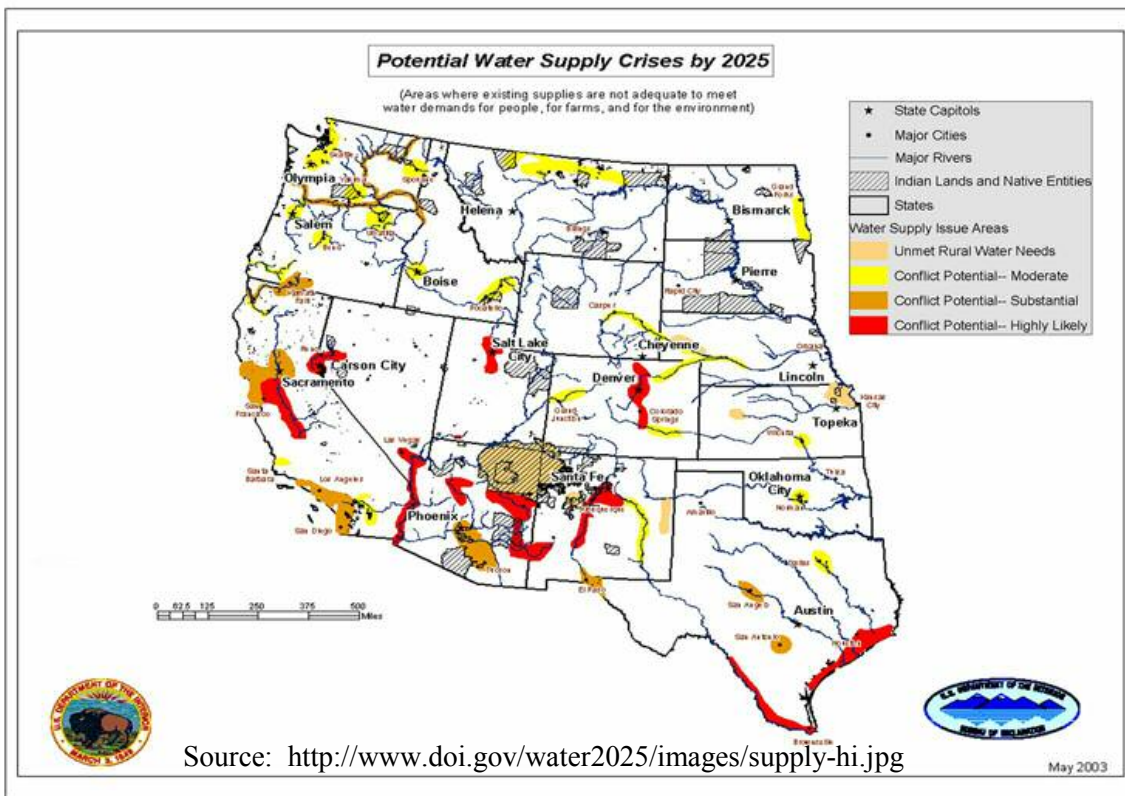
Figure 1-2. Areas in the western United States with significant potential for near term water supply shortages. Figure taken from the United States Department of Interior, Bureau of Reclamation Water 2025 report (BoR 2005).

1.2 The Role of Science in Addressing Water Management Challenges

Whether at the global, national, or river basin level, science has a role to play in addressing the challenges facing water managers. Jury and Vaux (2005) state that the task of scientists in addressing the world's emerging water problems is

> "…to do a better job of explaining, communicating, and educating water managers, decision makers, and members of the public. Only through effective programs of communication and outreach will existing science be used to its fullest potential in the development of comprehensive strategies for addressing the many water problems that confront the world."

In its Water 2025 report, the Bureau of Reclamation (2005) puts forth a variety of qualitative strategies to address population growth driven increases in water demands to the finite supplies of the western United States. The four "reality-based tools" proposed by Water 2025 are: 1) Conservation, Efficiency, and Markets, 2) Collaboration, 3) Technology, and 4) Removal of Institutional Barriers and Increases in Interacgency Cooperation. It is notable that all four of these tools are ways to potentially increase efficiency in management and use of existing water supplies, but that a mechanism to test the quantitative value of each in a given location does not exist. The science, that likely exists in many of the basins considered in Water 2025 report has not been used to evaluate the tools proposed on a case by case basis. If these strategies are to be adopted, it will be important to know which will provide the most bang for the buck. In other words, some sort of simulation tool relevant to basins of interest would be valuable for use in determining which of these tools to bring to bear first in a given river basin.

In terms of tools specific to the Rio Grande basin in New Mexico, Belin et al. (2002) provide a comprehensive and well thought out list of potential water management tools to help manage finite water resources in the face of rapidly growing population. However, as in the case of the tools recommended by the Bureau of Reclamation for the western United States, the laundry list provided by Belin et al. (2002) does not include a mechanism for measuring the relative impact each suggestion might have, or the relative costs associated with the implementation of each. A tool that could bring the extensive hydrologic science that has been done in the Rio Grande basin to bear on the qualitative policy suggestions would be very useful to water managers. It would be nice to test each policy option on a model of the system to see if it would work as expected.

This dissertation documents the development of a computer model simulation tool that can be used to evaluate water policy options in the Rio Grande, and in the process help explain and educate stakeholders to the existing science in the basin. The simulation model described here serves two main purposes: 1) the integration of science across geographic regions and scientific disciplines, and 2) the repackaging of this science into a form that is readily accessible to stakeholders and the interested public. Simulation models have been built that accomplish one of these tasks, but the model described here is unique in its ability to accomplish both tasks to a significant degree.

1.2.1 Integration of Cross Disciplinary Science at a Basin Scale

Water cycles through and across earth's atmosphere, land surface, and subsurface on temporal and spatial scales that vary dramatically. For this reason, hydrometeorology,

surface water hydrology, and groundwater hydrology are often treated as separate

disciplines, and to this day, tight integration of atmospheric processes, surface water

processes, and groundwater processes is a difficult endeavor whose success remains on

the cutting edge of physical hydrology (e.g. Kumar et al. 2006). However, to truly

understand why water moves through the upper Rio Grande basin in the way it does, in

addition to the physical laws that describe surface water and groundwater movement, the

legal institutions and human behaviors that govern how water is stored, used, and moved

through the variety of engineering structures in the basin including reservoirs, diversions

and wells must also be understood. Interdisciplinary models that include the best

available science from both physical and social science are still relatively rare, and at the

cutting edge of multidisciplinary hydrology. Many models strong in the social sciences

are simplified on the physical side to allow for solution and optimization of an objective

function (e.g. Ward et al. 2001). On the other hand, models strong in the physical are

often focused on either surface or groundwater, and include no human behavioral model

at all, assuming no changes to human behavioral related factors, or relying on exogenous

data to serve as behavioral related inputs for scenario evaluation (e.g. USACE et al. 2002,

McAda and Barroll 2002). There is a general lack of models with a strong spatially

distributed physical basis, and the platform to incorporate legal and economic aspects of

hydrology. The model described in this dissertation represents the most advanced

multidisciplinary model in existence in the upper Rio Grande basin.

1.2.2 *System Dynamics Modeling*

Recent successful efforts to bring the physical and social aspects of hydrology together on a common platform have utilized system dynamics modeling (e.g. Tidwell et al. 2004, Yalcin and Lansey 2004, Simonovic and Fahmy 1999). System dynamics is a modeling approach that breaks down the systems to be modeled into a set of stocks and flows, where stocks are reservoirs or stockpiles of material, and flows are movement of material in and out of the stocks. Originally formalized to model industrial processes and behaviors (Forrester 1961), system dynamics is ideally suited to situations where the component pieces of a system may behave relatively simply independently, but the relationships and feedbacks between systems through time may lead to behavior that would not have been predicted a priori. Relationships between systems can become more important than the individual system behavior. A classic example of the whole being greater than the sum of the parts. As explained by Jay Forrester (1987), the man generally credited with creation of the field, "system dynamics modeling can be effective because it builds on the reliable part of our understanding of systems while compensating for the unreliable part", and may help correct "incorrect intuitive solutions to complex systems". Beyond these classical advantages to considering the whole rather than the parts, a wide range of systems, from social to physical can be relatively easily modeled within commercially available object oriented software packages[1]. The software is intuitive and easy to learn, allowing scientists from different disciplines to collaborate on multidisciplinary modeling efforts. Hydrologic components, both physical and social can

---

[1] Powersim (www.powersim.com), Vensim (www.vensim.com), and Stella (www.iseesystems.com) are three widely used object oriented software packages designed for system dynamics modeling.

be organized on a common platform to be part of a single system whose overall behavior depends on the relationships and feedbacks between the model components. The model described in this dissertation is a system dynamics model developed entirely on one software platform, composed of multiple physical and social components, whose interdependent behaviors define the overall hydrologic system behavior.

1.2.3 Bringing Science and Stakeholders to the Table

Commercially available system dynamics software has also helped create a field of decision making methodology that relies on stakeholder engagement in development of models for use in planning decisions. Formally called mediated modeling (van den Belt 2004) or Shared Vision Planning (SVP) (USACE 2007), this approach uses collaborative model building to engage and educate stakeholders towards consensus based and scientifically sound water resource management decisions. Stakeholders are engaged and empowered in the collaborative model building exercise to create an integrative decision support tool. In this way stakeholders, including the interested public, and the best available science can be closely involved in creating the decision support product. The intuitive and object oriented nature of the system dynamics software, as well as the ability to create easily understood user interfaces for changing input data and observing model output are important to the ability of stakeholders to use the final model product to make their decision. Finally, for the model to be useful in a group decision making process, it must run quickly enough to be evaluated in real time: ideally on the order of seconds to tens of seconds on a laptop computer. This approach

was used successfully in the Rio Grande system in and around Albuquerque by the

Middle Rio Grande Water Assembly in their formulation of a regional water plan

(Tidwell et al. 2004). The resulting decision support model incorporated dozens of

policy options, and was an important tool in the final decision making process. However,

from a technical perspective, the model was lumped both spatially and temporally to a

significant degree. The model described in this dissertation is in many ways an extension

of the Tidwell et al. model, reduced temporally from an annual to a monthly timestep,

expanded in spatial extent, and reduced in spatial unit from a lumped three county region

to river reach units based on surface gage locations.

1.3 Combining Science Integration and Stakeholder Accessibility

As computing power continues to grow, simulation of complex systems is becoming a more and more practical and practiced way to scope alternatives and catch planning mistakes in a virtual formulation of a system in order to avoid potentially costly mistakes in the real world (e.g. Harris 2004). Laptop computers make these simulations portable, and if the models include a user friendly interface, make possible direct interaction with the simulations by the public or non-expert stakeholder. This is the idea of the upper Rio Grande model described in this dissertation. With a basin scale spatial extent, river reach spatial units, and a monthly timestep, the model is able capture the salient behaviors of the surface water, groundwater, and human behavioral systems being modeled. The model is unique in the degree of integration between these systems at a basin scale, and in this way contributes to the hydrologic science in the basin. And while it is detailed enough to be meaningful to science questions in the basin, the model is also able to run a forty year scenario in about 10 seconds on a laptop computer. This speed and portability allow the model to be used in group discussion or decision making settings. Some modelers have discovered that it can be difficult to use a single model for public education and outreach as well as technical insights (Ford 1996), however if a model is robust enough to provide system level insights to professionals, and runs fast enough for rapid, real time interactions, making it an effective education tool is arguably a matter of interface development.

In support of this argument, the monthly timestep Rio Grande model documented in this dissertation is currently under review by the technical team of the Upper Rio Grande Water Operations Model (URGWOM), which consists of scientists and modelers from the United States Geological Survey, the United States Army Corps of Engineers, the United States Bureau of Reclamation, and the New Mexico Interstate Stream Commission. The collaboration with the URGWOM tech team was funded by Sandia National Laboratories, and occurred through a series of (currently ongoing as of April 2007) bi-monthly meetings which started in early 2006. Initial meetings were dedicated to familiarizing the URGWOM tech team with Powersim Studio 2005, the commercially available software package used to build the monthly time step model. Subsequent meetings focused on demonstrating the specific framework, assumptions, and methods used to build the monthly model (which also represent the bulk of this dissertation). During this second phase, the model was changed, added to, and improved upon significantly, based on the knowledge of the URGWOM technical team. Finally, once requested changes and enhancements were complete, the members of the technical team reviewed the model individually prior to an external model review. Once the review process is complete, it is likely that the monthly timestep Rio Grande model documented in this dissertation will be included in the URGWOM suite of tools for public outreach and education, as well as for internal use by the URGWOM tech team for system level scoping, scenario analysis, and result comparison to the daily timestep surface water routing and operations focused URGWOM.

CHAPTER 2: SURFACE WATER COMPONENT

2.1   Introduction

As fresh-water resources in the western United States and the world are pushed beyond their sustainable limits by new and growing demands, increased efficiency in management of water resources is of critical importance if water managers are to reduce social conflict and environmental damages often associated with water scarcity. As pointed out by Jury and Vaux (2005), science can play a role in improving water management efficiency, but the science must be integrated, multidisciplinary, interdisciplinary, basin-scale in scope, and, most important, communicated effectively to water managers. Computer models and simulations can provide a very effective way to integrate interdisciplinary science on large temporal and spatial scales. If the simulations are rapid and user-friendly, the computer model itself becomes a vehicle for informing policy decisions with science. Rapid, basin scale, multidisciplinary computer simulations represent a tremendous tool for informing water management with scientific knowledge.

Models to aid in improved water management efficiency must address dynamics in the surface water and groundwater systems, and their associated feedbacks. This chapter will focus on the development of a physically based monthly timestep model of surface water dynamics that can be used as the hydrologic foundation for real-time scenario evaluation by stakeholders, policy makers, and the interested public. Components contributing to the surface water balance include river routing, reservoir operations, open water evaporation, riparian evapotranspiration, river diversion, return flows, and groundwater interaction. These processes are subject to agricultural,

municipal, industrial and environmental demands as managed by the built infrastructure and operated with respect to defined policies, water rights, and water management institutions. The focus area for this model is the Rio Grande surface water and associated groundwater systems in northern and central New Mexico.

2.2   Model Development

2.2.1   *Spatial and Temporal Extent and Resolution*

The physical setting of the model is the Rio Grande system extending from the surface water gage near Lobatos, Colorado (managed by the Colorado State Engineer), 6 miles upstream of the Colorado–New Mexico state line (USACE et al. 2002), to the outlet of Caballo Reservoir, some 363 river miles downstream. Two major tributaries, the Rio Chama and Jemez Rivers, are also modeled. The spatial resolution of the model was defined by surface water gage locations with periods of significant historic record. Consistent with an existing routing and operations model known as the Upper Rio Grande Water Operations Model (URGWOM) (USACE et al. 2002) the river system was divided into 17 conceptual spatial units referred to as reaches. For a detailed physical description of each reach, consult the URGWOM Physical Model Documentation (USACE et al. 2002). In addition to the river reaches, seven reservoirs are modeled explicitly, three in the Chama drainage (Heron, El Vado, Abiquiu), one on the Jemez River (Jemez), and three on the Rio Grande (Cochiti, Elephant Butte, Caballo). The physical extent of the model, including reservoir and gage locations, is shown in Figure 2-1. The surface water gages used for input and calibration are listed in Tables 2-1 and 2-2 respectively, along with relevant physical information.

The model runs on a monthly timestep, and uses the period from 1975 through 1999 for calibration, 2000 through 2004 for validation, and runs forward from 2005 in scenario evaluation mode. During the calibration period, parameters in the model are manipulated to match observed stream flows at calibration gages (Table 2-2) as closely as

possible at each timestep with cumulative modeled and observed flows equal for the 25-year calibration period. During the validation period, the calibrated model is run using observed hydrologic and climatic conditions as inputs, and the behavior of the model is compared to observations at the internal stream gages (Table 2-2). This comparison sheds some light on the relative certainty of the model for making predictions with a set of known inputs. Finally, the scenario evaluation mode is used to run the model several decades into the future with user-determined hydrologic and climatic inputs, with the goal of exploring possible hydrologic outcomes to a variety of user-determined scenarios. The monthly timestep allows the model to be small enough and fast enough to run multiyear scenarios in a matter of seconds on a personal computer, while still capturing the seasonal variability that characterizes the surface water system.

Inputs will be discussed in more detail in Section 2.2.3; however, an overview of temporally varying inputs is provided here. Major temporally varying inputs include total gaged surface water flows at the model boundary (Table 2-1), and monthly climate data including temperature (average max, average min, and mean), mean relative humidity, mean windspeed, total solar radiation, total precipitation, reservoir ice cover, and reservoir pan evaporation. Observed historic values for these data are used for calibration and validation input, and are shuffled by historic year to generate coupled hydrologic and climatic inputs for scenario evaluation. Human groundwater extraction and wastewater returns to the river are based on historic data for the calibration and validation period, and modeled as a function of human water use patterns during scenario evaluation. Other temporally varying input data include agricultural and riparian areas by

plant type. In this case, estimates of historic values are used during calibration and validation, while user inputs determine the values for future runs. Treatment of human water use patterns is described in Chapter 4. In the current model formulation, mountain front and tributary recharge inputs to the groundwater system are essentially constant through time, however current land surface modeling efforts at New Mexico Tech University (Tidwell et al. 2006, Chapter 4) will allow these major groundwater inputs to be connected to climate patterns in future model versions.

As will be evident throughout this paper, development of this monthly model of the surface water system was aided tremendously by the data collection and conceptual model development of URGWOM. As discussed in Section 1.3 as well, coordinated development of this tool with the URGWOM team has occurred to create a fast, simple, and interactive complement to their daily model.
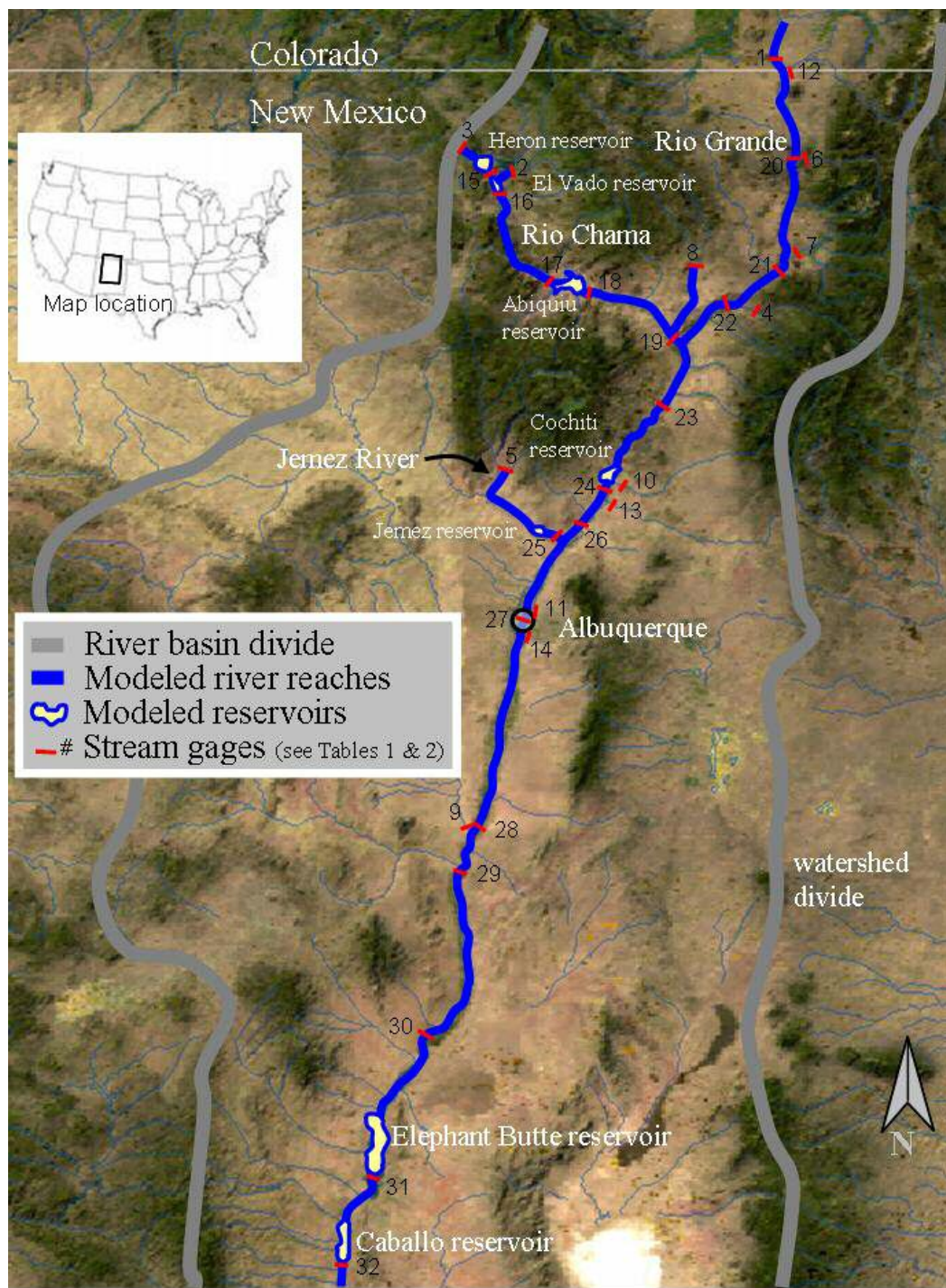
Figure 2-1. Physical extent of model and reach locations as defined by gage locations. Gages are identified with numbers corresponding to specific gage information in Tables 2-1 and 2-2. Gages numbered 1–14 provide input to the model, and are numbered beginning with the largest 1975–1999 input to the model, followed by the second largest, etc. Gages numbered 15–32 provide movement and calibration information within the model extent.

Table 2-1. Gages used for input.
The numbers in the final column refer to the gage locations as shown in Figure 2-1.
The Rio Grande near Lobatos gage is operated by the Colorado Department of Water Resources (CDWR), and the Azotea tunnel outlet gage is operated by the United States Bureau of Reclamation (BoR). All other gages are operated by the United States Geological Survey (USGS). Data from www.usgs.gov and URGWOM documentation (USACE et al. 2002).

Gage	USGS Gage#	Average Annual Input 1975-99 [af/yr]	% of Gaged Inputs [%]	Contrib Drainage Area [mi^2]	Datum Elev [ft amsl]	~Lat [dd]	~Long [dd]	Fig 2-1 ID#
Rio Grande near Lobatos	CDWR	386200	34%					1
Rio Chama near La Puente	8284100	295300	26%	480	7083	36.66	106.63	2
Azotea tunnel outlet	BoR	97100	9%					3
Embudo Creek at Dixon	8279000	72500	6%	305	5859	36.21	105.91	4
Jemez River near Jemez	8324000	65100	6%	470	5622	35.66	106.74	5
Red River below Fish Hatchery	8266820	58300	5%	185	7105	36.68	105.65	6
Rio Pueblo de Taos below Los Cordovas	8276300	57900	5%	380	6650	36.38	105.67	7
Rio Ojo Caliente at La Madera	8289000	56900	5%	419	6359	36.35	106.04	8
Rio Puerco near Bernardo	8353000	23100	2%	6220	4722	34.41	106.85	9
Santa Fe River above Cochiti	8317200	8700	1%	231	5505	35.55	106.23	10
North Floodway Channel near Alameda	8329900	7300	1%	88	5015	35.20	106.60	11
Costilla Creek near Garcia	8261000	6500	1%	200	7821	36.99	105.53	12
Galisteo Creek Below Galisteo Dam	8317950	4200	0%	597	5450	35.46	106.21	13
Tijeras Arroyo near Albuquerque	8330600	300	0%	128	4999	35.00	106.65	14

Table 2-2. Gages used for calibration. The numbers in the final column refer to the gage locations as shown in Figure 2-1. The Willow Creek below Heron and Rio Grande below Caballo gages are operated by the United States Bureau of Reclamation (BoR). All other gages are operated by the United States Geological Survey (USGS). Data from www.usgs.gov and URGWOM documentation (USACE et al. 2002).

Gage	USGS Gage#	Contrib Drainage Area [mi²]	Datum Elev [ft amsl]	Average Annual Flow 1975-99 [af/yr]	River Mile (above mouth) [mile]	~Lat dd	~Long dd	Fig 2-1 ID#
Willow Creek below Heron	BoR			96900				15
Rio Chama below El Vado	8285500	777	6696	373900	76	36.58	106.72	16
Rio Chama abv Abiquiu Reservoir	8286500	1500	6280	396700	47	36.32	106.60	17
Rio Chama below Abiquiu Dam	8287000	2047	6040	414800	31	36.24	106.42	18
Rio Chama near Chamita	8290000	3044	5654	464500	3	36.07	106.11	19
Rio Grande near Cerro	8263500	5500	7110	418700	1693	36.74	105.68	20
Rio Grande blw Taos Junction Bridge	8276500	6790	6050	619100	1658	36.32	105.75	21
Rio Grande at Embudo	8279500	7460	5789	685200	1643	36.21	105.96	22
Rio Grande at Otowi	8313000	11360	5488	1200600	1614	35.87	106.14	23
Rio Grande below Cochiti	8317400	11960	5226	1095300	1588	35.62	106.32	24
Jemez River blw Jemez Canyon Dam	8329000	1038	5096	54900		35.39	106.53	25
Rio Grande at San Felipe	8319000	13160	5116	1166600	1573	35.44	106.44	26
Rio Grande at Albuquerque	8330000	14500	4946	1072300	1540	35.09	106.68	27
Rio Grande Floodway nr Bernardo	8332010	19230	4723	953300	1487	34.42	106.80	28
Rio Grande Floodway at San Acacia	8354900	23830	4655	838600	1473	34.26	106.89	29
Rio Grande Floodway at San Marcial	8358400	24760	4242	779100	1425	33.68	106.99	30
Rio Grande blw Elephant Butte Dam	8361000	26510	4241	757500	1382	33.15	107.21	31
Rio Grande blw Caballo Dam	BoR			752400				32

2.2.2 Conceptual Model

The upper Rio Grande river system is fed primarily by snow melt from the San Juan and Sangre de Cristo mountains, which define the northwestern and eastern boundaries of the basin respectively. Water moves into the river system via surface water inflows and return flows, groundwater seepage, and direct precipitation onto open water. Water is also diverted from the San Juan River system, through tunnels under the continental divide and into the Rio Chama system. This inter-basin water, moved from the Colorado Basin to the Rio Grande Basin, is known as San Juan Chama (SJC) water. Water is lost from the river system by surface water diversions, leakage to the groundwater system, and open water evaporation to the atmosphere. Riparian evapotranspiration (ET) removes water from a shallow groundwater system, which is in rapid exchange with the river. Water diverted for agricultural irrigation use can be lost to the groundwater system through conveyance system leakage (ditches and canals) and crop seepage, and lost to the atmosphere via crop ET and open water evaporation. In some reaches groundwater discharges to the surface water system by seepage into agricultural drains.

With respect to water balance, land use, and groundwater use, the river system within the model extent is significantly different above Cochiti Reservoir than it is below. In general, the reaches upstream of Cochiti Reservoir tend to gain water from groundwater and tributary inflows faster than it is lost to the atmosphere, while in the reaches downstream of Cochiti atmospheric losses are greater and tributary inputs modest. As a result, flows tend to increase above Cochiti and decrease below, as shown in Figure 2-2.

Perhaps partially as a result of this change from gaining to losing, the groundwater
system south of Cochiti is fairly well studied and characterized, while the
characterization of the groundwater system upstream, especially upstream of the
confluence of the Rio Chama and Rio Grande, is more limited. Finally, the majority of
land within the model extent that is practicably irrigable by surface water diversion and
gravity application lies below Cochiti Reservoir, resulting in significant amounts of water
moving through agricultural conveyance systems (canals, ditches, and drains) below that
point, as shown in Table 2-3.
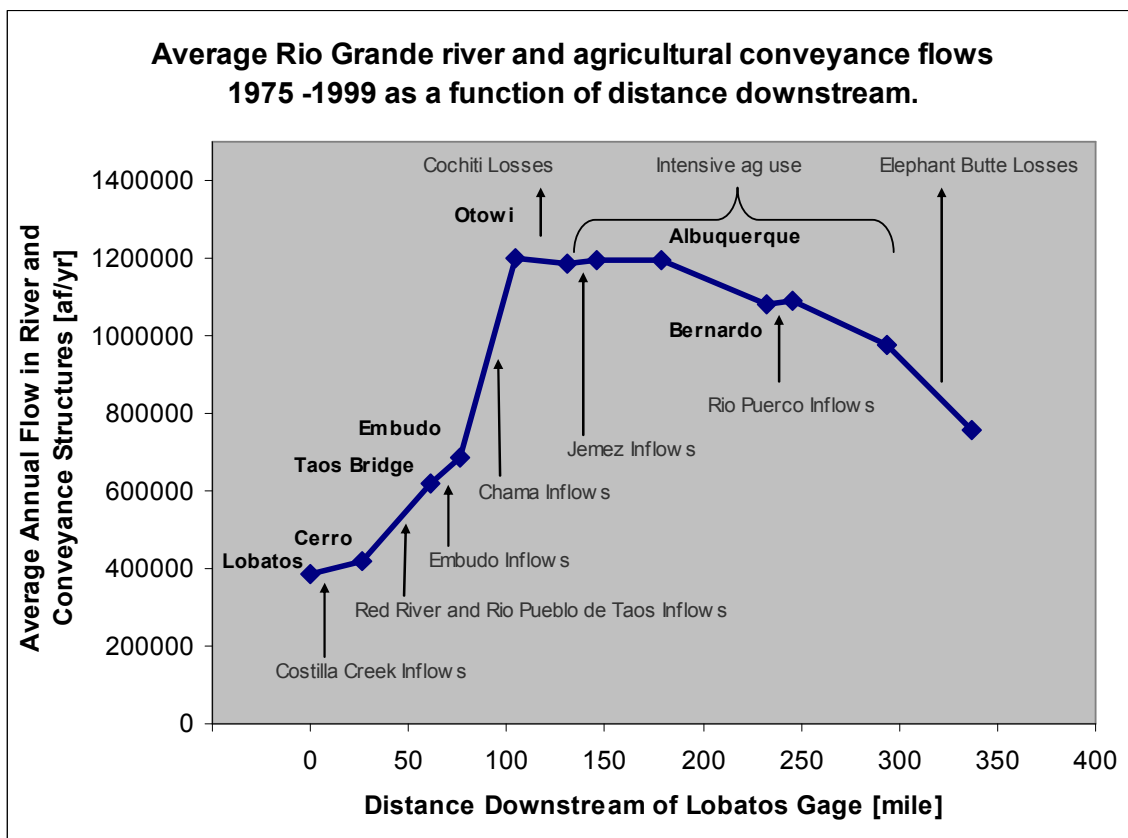
Figure 2-2. Average river and agricultural conveyance flows along Rio Grande 1975–
1999. In general, river gains above Cochiti and loses below. The Otowi to below
Cochiti reach appears to lose because of Cochiti Reservoir losses.

Table 2-3. Percent of total flow past points south of Cochiti Reservoir that is in agricultural conveyance system. Irrigation season is March – October. Flows in the conveyance system are a largest percent of total in the late summer and fall as river flows drop, but agricultural demand remains high. Data from USGS gages listed in Table 2-2, as well as combined conveyance flow data from URGWOM model data (USACE et al. 2002).

Location	Irrigation season % flows in conveyance system 1975-99	August - October % flows in conveyance system 1975-99
Cochiti Pueblo	9%	19%
San Felipe	3%	6%
Albuquerque	12%	27%
Bernardo	13%	32%
San Acacia	22%	26%
San Marcial	19%	34%
Average	13%	23%

2.2.3 Mathematical Model

2.2.3.1 Governing Equations

2.2.3.1.1 River Reach Mass Balance

Employing mass balance, the amount of water that flows out of a given river reach can be expressed mathematically as a function of inflows, outflows, and change in storage within the reach. At a monthly timestep, the change in storage in a river reach is assumed to be negligible with respect to the other flows through the reach, and precipitation gains to open water are also assumed to be negligible. The governing equation for a generic reach (*j*) is shown in Equation 2-1 below.

$$Q^j_{msout} = Q^j_{m\sin} + Q^j_{sw} + Q^j_{gwsw} - Q^j_{evap} \qquad (2\text{-}1)$$

In Equation 2-1, Q^j_{msout} represents mainstem flow out of the bottom of reach j, which is the location of the gage representing the lower end of the reach. The term $Q^j_{m\sin}$ represents mainstem flow into reach *j*, from the reach above or a gage on the model

boundary. If reach i is immediately above reach j, the flow out of reach i is the same as

the flow into reach j: $Q^i_{msout} = Q^j_{m\sin}$. The term Q^j_{gwsw} represents the net sum of all

interactions between the river and groundwater system in the reach, and is positive for a

groundwater gaining reach, and negative for a groundwater losing reach. The term Q^j_{evap}

represents open water evaporative losses. The term Q^j_{sw} represents the net sum of all

surface water inflows into and diversions out of the reach, as shown in Equation 2-2

below. The surface water inflows, diversions, and returns, may be gaged or ungaged.

$$Q^j_{sw} = Q^j_{swgaged} + Q^j_{swungaged} - Q^j_{swdiversion} + Q^j_{swreturn} \tag{2-2}$$

The terms $Q^j_{swgaged}, Q^j_{swungaged}, Q^j_{swdiversion}, Q^j_{swreturn}$ represent gaged and ungaged surface

water inflows (tributaries) and surface water diversions and returns respectively. Below

Cochiti Reservoir, the agricultural conveyance system is modeled as a parallel unit of

mass balance to the river system. For these reaches, the diversion and return flow terms

in Equation 2-2 serve as inflows and outflows for the conveyance system. Assuming that

direct evaporation losses from conveyance features is negligible, mass balance in the

conveyance system south of Cochiti Reservoir is modeled using Equation 2-3.

$$Q^j_{swdiversion} + Q^i_{convtf} = Q^j_{cropET} + Q^j_{convgw} + Q^j_{swreturn} + Q^j_{convtf} \tag{2-3}$$

Equation 2-3 states that surface water can enter the conveyance system by diversion from

the associated reach ($Q^j_{swdiversion}$), or by through flow from the conveyance system

immediately upstream (Q^i_{convtf}). Water is lost from the conveyance system to the

atmosphere by ET from crops (Q^j_{cropET}). Conveyance water moves to the groundwater

system as seepage from crops and canals, or moves from the groundwater system back to the conveyance system as seepage into drains. The groundwater exchange terms are lumped into a single conveyance to groundwater term (Q_{convgw}^{j}) in Equation 2-3 that can be positive or negative depending on the relative magnitude of the conveyance to groundwater system exchanges. Surface water flows out of the conveyance system to the river ($Q_{swreturn}^{j}$), or to the downstream conveyance system (Q_{convtf}^{j}).

As will be described in more detail in the following sections, the general strategy used to solve reach based mass balance (Equation 2-1) during the calibration period is to set the mainstem inflow term ($Q_{m\sin}^{j}$) using historic gage data. Open water evaporation losses (Q_{evap}^{j}) are estimated using channel geometry information and a reference ET from historic climate data input to a modified Penman Montieth equation. The groundwater exchange (Q_{gwsw}^{j}) is from a coupled, dynamic groundwater model, or a static exchange based on historic winter gage data, depending on data available for a given reach. The surface water term (Q_{sw}^{j}) is found using Equation 2-2, whose terms are set to historic gage values where available, and modeled otherwise. Crop ET losses for all reaches (Q_{cropET}^{j}) are modeled with a Penman Monteith based reference ET. In most reaches, the ungaged surface water inflow term ($Q_{swungaged}^{j}$) is used as a closure and calibration term. Downstream of Cochiti, the conveyance system is modeled using historic diversion ($Q_{swdiversion}^{j}$) and through flow ($Q_{convtf}^{i}, Q_{convtf}^{j}$) data, solving for unknown return flows ($Q_{swreturn}^{j}$) after evaporative losses and groundwater exchanges are accounted for.

Groundwater to conveyance system flows (Q^j_{convgw}) are modeled with a coupled

groundwater model, leaving return flows ($Q^j_{swreturn}$) as the only unknown in Equation 2-3.

In reaches where the river system and conveyance system are coupled to a groundwater

model, calibration involves a combination of ungaged surface inflows and/or parameter

adjustments associated with the surface water groundwater connection, to best match

historic gage data. Table 2-4 summarizes important information associated with the

modeled reaches, including degree of groundwater coupling. The carriage water factor is

explained in Section 2.2.3.2.9.

During validation and scenario evaluation, main stem flows into the reach ($Q^j_{m\sin}$)

are set to gage data for reaches beginning on the model boundary, and to outflows from

the reach above otherwise. Surface water diversions ($Q^j_{swdiversion}$) are modeled based on

agricultural demand and historic diversion patterns. Water available to return ($Q^j_{swreturn}$)

or flow into the next conveyance reach (Q^i_{convtf}, Q^j_{convtf}) is partitioned based on reach

specific historic proportions. All other terms in Equations 2-1 through 2-3 are calculated

as in the calibration period.

2.2.3.1.2 Reservoir Mass Balance

Seven reservoirs are included in the model. Table 2-5 summarizes basic

information associated with the reservoirs. Reservoir mass balance is calculated

according to Equation 2-4.

$$\Delta S^r = Q^r_{sw} + Q^r_{precip} - Q^r_{gw} - Q^r_{evap} - Q^r_{release} \qquad (2\text{-}4)$$

Table 2-4. Reach summary table. Irrigated agricultural acreage is an average of 1975–1999 values reported in URGWOM physical model documentation (USACE et al. 2002) and information from Rio Chama watermaster report 2002 (Wells 2002). See Table 2-10 for crop type distribution upstream of Cochiti. The carriage water factor is explained in Section 2.2.3.2.9. Riparian acreage is calculated from remotely sensed data for reaches above Cochiti and URGWOM values below, with the exception of Jemez, which uses values from a regional groundwater model of the Albuquerque Basin by Doug McAda and Peggy Barroll (2002).

Reach	Length [miles]	Gaged Tributaries	Irrigated Ag Acreage Modeled [acres]	Carriage Water Factor [%]	Riparian Acreage Modeled [acres]	Modeled Ag Convey-ance System	Coupled GW Model
Chama: Willow Creek to Heron	12	Azotea Tunnel (San Juan Chama)	0		0		None
Chama: Heron to El Vado	6	Rio Chama	0		1		None
Chama: El Vado to Abiquiu	29		300		20		Static
Chama: Abiquiu to Chamita	29	Ojo Caliente	4,540		80		Static
Lobatos to Cerro	26	Costilla Creek	0		300		Static
Cerro to Taos Junction Bridge	35	Red River Rio Pueblo de Taos	0		0		Static
Taos Junction Bridge to Embudo	15	Rio Embudo	190		100		Static
Embudo to Otowi	29		4,670		165		Dynamic
Otowi to Cochiti	27		0		1		Dynamic
Cochiti to San Felipe	15	Galisteo Creek	4,520	0.85	4,055	X	Dynamic
Jemez: Jemez Pueblo to Reservoir	30		5,370	0.2	3,985	X	Dynamic
San Felipe to Albuquerque	33	North Flood Channel	12,680	0.65	6,747	X	Dynamic
Albuquerque to Bernardo	53	South Flood Channel	53,700	0.4	20,114	X	Dynamic
Bernardo to San Acacia	14	Rio Puerco	680	0.2	6,639	X	Dynamic
San Acacia to San Marcial	48		10,490	0.2	21,591	X	Dynamic
San Marcial to Elephant Butte	42		0		7,635	X	Dynamic
Elephant Butte to Caballo	18		0		0		None

Table 2-5. Modeled reservoirs summary information.
Numbers from URGWOM (USACE 2002) with the exception of the El Vado capacity,
which is the maximum historic storage 1975–1999 (May and October 1986).

	Year Completed [AD]	Capacity [AF]	Dam Crest Elevation [ft amsl]	Primary functions
Heron	1971	401,300	7199	Storage San Juan Chama (SJC) water.
El Vado	1935	189,500	6914.5	Storage native and SJC water for irrigation.
Abiquiu	1963	1,198,500	6381	Flood control and storage SJC water.
Cochiti	1973	589,200	5479	Flood control.
Jemez	1953	262,500	5271.6	Flood and sediment control.
Elephant Butte	1916	2,023,400	4407	Storage for irrigation.
Caballo	1938	326,700	4190	Storage for irrigation.
Total		4,991,100		

The change in storage for a given timestep at reservoir r (ΔS^r) is the sum of inflows

minus outflows. Inflows include gaged and ungaged surface water inflows (Q^r_{sw}) to the

reservoir, and gains from precipitation that falls directly on the reservoir surface (Q^r_{precip}).

Outflows may include groundwater leakage from the reservoir (Q^r_{gw}), evaporation from

the reservoir (Q^r_{evap}), and all releases (including spills) ($Q^r_{release}$) from the reservoir. In

general, as will be discussed in more detail in the following sections, reservoirs were

calibrated with historic gaged surface water inflows and releases, and calculated

precipitation, evaporation, and groundwater leakage. Reservoir releases were set to

historic for the calibration period, and modeled with operation rules for the validation and

scenario evaluation periods. The following sections describe each of the terms in

Equations 2-1 through 2-4 in more detail.

2.2.3.2   Evapotranspiration

2.2.3.2.1   Reservoir Evaporation

For the 1975–1999 period, pan evaporation was measured for April through

October for the five reservoirs north of Albuquerque where evaporation pans freeze, and

during all months for Elephant Butte and Caballo. For the five upper reservoirs, where

pan evaporation cannot be consistently measured from November through March, winter

evaporation rate is estimated by Equation 2-5.

$$E^{r,m} = \frac{T_{max}^{r,m} + T_{min}^{r,m}}{2} * k^{r,m} \qquad (2\text{-}5)$$

where

$\quad E^{r,m}\quad =\quad$ evaporation rate from reservoir r during month m [L/T]

$\quad T_{max}^{r,m}\quad =\quad$ average daily maximum temperature for r during m [degree]

$\quad T_{min}^{r,m}\quad =\quad$ average daily minimum temperature for r during m [degree]

$\quad k^{r,m}\quad =\quad$ coefficient of proportionality for r during m [L/(degree*T)]

$k^{r,m}$ values are constant for a given reservoir in a given month, and are shown for

reservoirs above Elephant Butte in Table 2-6.

Table 2-6. Winter reservoir coefficient of proportionality ($k^{r,m}$) for upper reservoirs.

	$k^{r,m}$ [ft/°F/month]				
Reservoir \ Month	Nov	Dec	Jan	Feb	Mar
Heron, El Vado, and Abiquiu	0.0035	0.0026	0.0031	0.0037	0.006
Cochiti and Jemez	0.0047	0.0032	0.0038	0.0046	0.0074

For the five upper reservoirs from April through October, and Elephant Butte and

Caballo during all months, the evaporation rate is estimated with Equation 2-6.

$$E^{r,m} = 0.7 * E_{pan}^{r,m} \qquad\qquad (2\text{-}6)$$

where

$E^{r,m}$ = evaporation rate from reservoir r during month m [L/T]

$E_{pan}^{r,m}$ = pan evaporation measured at reservoir r during m [L/T]

Volume and edge effects result in pan evaporation typically overestimating actual open water evaporation. To correct for this effect, actual open water evaporation rate is estimated by multiplying measured pan evaporation by a pan coefficient less than unity. URGWOM uses a pan coefficient of 0.7 for all reservoirs. The methodology represented by Equations 2-5 and 2-6 for a monthly timestep is the same as used by URGWOM at a daily timestep (USACE et al. 2002).

2.2.3.2.2   *Reference Evapotranspiration Rate*

Where pan evaporation is not measured, crop and open water evaporation are calculated using a reference ET rate. The daily timestep URGWOM model uses daily reference ET rates calculated by a United States Bureau of Reclamation (BoR) product developed specifically for the Rio Grande south of Cochiti, called the ET Toolbox (Brower 2004). The monthly model uses the same modified Penman Monteith equation used by the ET Toolbox:

$$ET_{ref} = \frac{\dfrac{\Delta}{\Delta + \gamma} * SR \quad + \quad \dfrac{\gamma}{\gamma + \Delta} * U * D}{LHV * \rho_w} \qquad\qquad (2\text{-}7)$$

where:

ET_{ref} = reference ET rate [L/T]

Δ = vapor pressure/temperature gradient [M/LT^{2}degree]

γ = psychrometric constant [M/LT^{2}degree]

SR = net solar radiation [M/T^3]

U = wind speed function = 15.36(1+0.0062*U2m) [L/T]

U2m = wind speed in km/day measured at 2 meters [L/T]

D = vapor pressure deficit [M/LT^2]

LHV = latent heat of vaporization for water [L^2/ T^2]

ρ_w = water density [M/L^3]

The numerator on the right side of Equation 2-7 has two terms, representing energy available per unit area per time for ET from solar- and gradient-driven evaporation respectively. The denominator converts the energy to water volume per unit area (depth) per time. Equation 2-7 represents reference ET as a function of climatic conditions. For the monthly model, each term above is specific to a given reach in a given month.

As explained in the ET Toolbox documentation (Brower 2004, page 52), the majority of the historic, daily climate data used in the ET Toolbox was derived from a combination of Los Lunas and Alcalde weather stations for all reaches between Cochiti and Elephant Butte reservoirs. For reaches south of Cochiti, ET Toolbox daily data were averaged to monthly for use in the model. North of Cochiti, historic climate data were used from weather stations at El Vado dam, Abiquiu dam, Cerro, Alcalde, and Cochiti dam as available. Where nearby data were not available, historic monthly average values were substituted. Table 2-7 summarizes climate stations used for historic data for reaches north of Cochiti.

Table 2-7. Historic climate data sources used for reaches above Cochiti. The 1st and 2nd replacement stations are stations or methods used when data is not available from original station. Reaches below Cochiti use ET Toolbox data set (Brower 2004).

Reach	Temp Station	Temp 1st Replace	Temp 2nd Replace	RH, Wind, and Solar Radiation Station	RH, Wind, and Solar Radiation 1st Replace
Chama: Willow Creek to Heron	El Vado Dam			Alcalde	Alcalde historic average
Chama: Heron to El Vado	El Vado Dam			Alcalde	Alcalde historic average
Chama: El Vado to Abiquiu	Abiquiu Dam			Alcalde	Alcalde historic average
Chama: Abiquiu to Chamita	Abiquiu Dam			Alcalde	Alcalde historic average
Lobatos to Cerro	Cerro	Cerro historic average		Alcalde	Alcalde historic average
Cerro to Taos Junction Bridge	Cerro	Cerro historic average		Alcalde	Alcalde historic average
Taos Junction Bridge to Embudo	Alcalde	Espanola	Alcalde historic average	Alcalde	Alcalde historic average
Embudo to Otowi	Alcalde	Espanola	Alcalde historic average	Alcalde	Alcalde historic average
Otowi to Cochiti	Cochiti Dam	Cochiti historic average		Alcalde	Alcalde historic average

2.2.3.2.3   Plant Coefficients

Reference ET is modified by empirically determined unitless coefficients to scale reference ET to a particular plant or environment type. Evaporation coefficients for riparian and crop vegetation were derived according to ET Toolbox methodology, which uses either a growing degree or monthly average method to estimate crop coefficients (Brower 2004). The monthly average method always applies the same crop coefficient to a given crop in a given month. The growing degree method is used to track the energy

that can contribute to plant growth and development through the growing season, and is

essentially a model of plant growth through a growing season as a function of air

temperature. Using the growing degree method, a given crop ET will be greater in a

warm year than a cool year. The growing degrees available for plant utilization in a

given month *m* by plant type *p* can be calculated as:

$$GD^{m,p} = \left(\frac{(T_{max}^{m,p} + T_{min}^{m,p})}{2} - T_{base}^{p} \right) * days^{m} \qquad (2\text{-}8)$$

where:

$GD^{m,p}$ = growing degrees in month *m* for plant type *p* [degrees/T]

$T_{max}^{m,p}$ = the average maximum monthly temperature for month *m*, or plant maximum temperature cutoff parameter for plant type *p*, whichever is smaller [degrees/T]

$T_{min}^{m,p}$ = the average minimum monthly temperature for month *m*, or $T_{base}^{m,p}$, whichever is larger [degrees/T]

$T_{base}^{m,p}$ = the base temperature parameter for plant type *p* [degrees/T]

$days^{m}$ = the number of days in month *m* [-]

Table 2-8a summarizes the crop and plant types represented in the model, the method

used for calculation of crop coefficients, the growing degree parameters for the plant type

where applicable, and the beginning and end months of growing season of the plant type.

Regardless of coefficient method, ET is only applied during the growing season of a

given plant type. ET Toolbox relationships between growing degree days and plant ET

coefficient as a function of plant species were used to go from growing degree days to

plant coefficient, and are summarized in Table 2-8b. Table 2-8b also summarizes the

polynomial coefficients used for growing degree based coefficient calculations. Table 8c

summarizes the monthly average values for associated plant types.

Table 2-8a. Plant types represented in the model, method for determining crop coefficients, associated growing degree parameters, and growing season start and end month. Data from ET Toolbox (Brower, 2004).

	Plant Type	Coefficient Method	Base Temp GD (F)	Max Temp Cutoff GD (F)	Start Month	Stop Month
Agricultural	Alfalfa	Growing Degree	5	50	Jan	Oct
	Chile Peppers	Growing Degree	10	30	May	Nov
	Corn	Growing Degree	10	30	May	Nov
	Cotton	Growing Degree	12	30	May	Oct
	Grapes	Growing Degree	10	30	April	Oct
	Melons	Monthly Table			April	Aug
	Misc. Fruit	Monthly Table			Jan	Dec
	Misc. Vegetables	Growing Degree	10	30	May	Nov
	Nursery Stock	Monthly Table			Jan	Dec
	Oats	Growing Degree	5	30	April	July
	Pasture Grass	Monthly Table			March	Sept
	Sorghum	Growing Degree	7	50	June	Dec
	Spring Barley	Growing Degree	5	30	May	Oct
	Tree Fruit	Monthly Table			Jan	Dec
	Wheat	Growing Degree	4	27	April	July
Riparian	Bosque	Growing Degree	15.5	50	April	Nov
	Cottonwood	Growing Degree	15.5	50	April	Nov
	Riparian Marsh	Monthly Table			Jan	Dec
	Riparian Grass	Monthly Table			Jan	Dec
	Salt Cedar	Growing Degree	15.5	50	April	Nov

2.2.3.2.4   Open Water Coefficients

Where pan evaporation is not directly measured, open water evaporation can be predicted by multiplying reference ET by a unitless open water evaporation coefficient, an approach that is analogous to the method described above for vegetation. The open water coefficient method is used to estimate direct evaporation from a river reach. The ET Toolbox uses monthly open water coefficients developed by M. E. Jensen in the lower Colorado system (Jensen 1998). To develop local open water coefficients, the reference ET calculated for each reach above a reservoir was compared to the pan

Table 2-8b. Growing degree coefficients for relevant plant types from Table 2-8a. Growing degrees (GD) are calculated by spatial location according to equation 2-8, and used in the polynomial $K_c = A + B*GD + C*GD^2 + D*GD^3 + E*GD^4 + F*GD^5$ with vegetation specific coefficients A-F shown in the table to find the vegetation coefficient. Data from ET Toolbox (Brower, 2004).

| | Plant\Coefficient | $K_c = A + B*GD + C*GD^2 + D*GD^3 + E*GD^4 + F*GD^5$ | | | | | |
		A	B	C	D	E	F
Agricultural Crop	Alfalfa	0.41	0.00111	-4.25E-07	3.56E-11	0	0
	Chile Peppers	0.12	0.00168	-2.46E-07	-4.37E-10	0	0
	Corn	0.12	0.00168	-2.46E-07	-4.37E-10	0	0
	Cotton	0.00042	0.0012	4.62E-07	-5.77E-10	0	0
	Grapes	-0.091	0.000881	-1.5E-07	-3E-11	0	0
	Misc. Vege	0.12	0.00168	-2.46E-07	-4.37E-10	0	0
	Oats	0.057	0.000323	3.94E-06	-3.26E-09	0	0
	Pecan 1000	0.18	5.69E-05	1.4E-07	-6.21E-11	0	0
	Pecan 2000	0.25	0.000305	4.61E-07	-2.97E-10	0	0
	Pecan 3000	0.32	0.000531	7.24E-07	-4.84E-10	0	0
	Pecan 4000	0.29	0.00111	1.85E-07	-3.23E-10	0	0
	Pinto Beans	0.2	-0.000212	5.72E-06	-4.77E-09	0	0
	Sorghum	0.089	0.00159	-7.46E-07	-8.36E-13	0	0
	Spring Barley	0.057	0.000323	3.94E-06	-3.26E-09	0	0
	Wheat	0.016	0.0006	-2E-08	-3E-11	0	0
Riparian	Bosque	0.08	0.00239	-2.86E-06	9.5E-10	9.5E-13	-6.46E-16
	Cottonwood	0.12	0.00225	-5.06E-06	5.85E-09	-2.79E-12	3.38E-16
	Salt Cedar	0.04	0.00253	-6.53E-07	-3.95E-09	4.69E-12	-1.63E-15

Table 2-8c. Monthly vegetation coefficients for relevant plant types from Table 2-8a. Bosque uses the growing degree method for all months except May, June, and July. Data from ET Toolbox (Brower, 2004).

| | Plant Type | Monthly Vegetation Coefficients [-] | | | | | | | | | | | |
		Jan	Feb	Mar	Apr	May	Jun	Jul	Aug	Sep	Oct	Nov	Dec
Agricultural Crop	Melons	0	0	0	0.42	0.42	1.01	1.01	0.87	0.7	0.4	0	0
	Misc. Fruit	0.4	0.4	0.43	0.62	0.8	0.86	0.86	0.86	0.86	0.86	0.86	0.76
	Nursery Stock	0.4	0.4	0.43	0.62	0.8	0.86	0.86	0.86	0.86	0.86	0.86	0.76
	Pasture Grass	0.65	0.65	0.65	0.65	0.65	0.65	0.65	0.65	0.65	0.65	0.65	0.65
	Tree Fruit	0.4	0.4	0.43	0.62	0.8	0.86	0.86	0.86	0.86	0.86	0.86	0.76
Riparian Plant	Bosque	GD	GD	GD	GD	1	1	1	GD	GD	GD	GD	GD
	Riparian Marsh	0.25	0.25	0.28	1.15	1.15	1.15	1.15	1.15	1.15	1	0.25	0.25
	Riparian Grass	0.65	0.65	0.65	0.65	0.65	0.65	0.65	0.65	0.65	0.65	0.65	0.65

evaporation measured at the reservoir. As discussed previously, URGWOM uses a pan coefficient of 0.7 for all New Mexico reservoirs. Thus, open water evaporation coefficients can be estimated with pan evaporation and reference ET:

$$C_{ow}^{r,m} = \frac{0.7 * E_{pan}^{r,m}}{ET_{ref}^{j,m}} \qquad (2\text{-}9)$$

where:

$C_{ow}^{r,m}$ =   implied open water coefficient associated with reservoir r in month m [-]

$E_{pan}^{r,m}$ =   pan evaporation measured at reservoir r during month m [L/T]

$ET_{ref}^{j,m}$ =   reference ET in reach j immediately upstream of reservoir r in month m [L/T]

Figure 2-3 shows average open water coefficient values for each reservoir in each month of the year. Pan evaporation was not recorded at Heron or El Vado for winter months in the 1975–1999 calibration period. The summer coefficients are lower for upper reservoirs (Heron and El Vado) in part because pan evaporation is measured at the reservoir, but reference ET is calculated based on nonrepresentative climate data from climate stations at lower elevations. To arrive at a single coefficient for each month, Heron and El Vado values were excluded, and the remaining monthly measurements averaged and rounded to the nearest tenth. Table 2-9 shows the adopted open water coefficients for this model, as well as the coefficients from Jensen. The two are fairly close except December through March when the Jensen coefficients are significantly lower than the adopted upper Rio Grande coefficients.
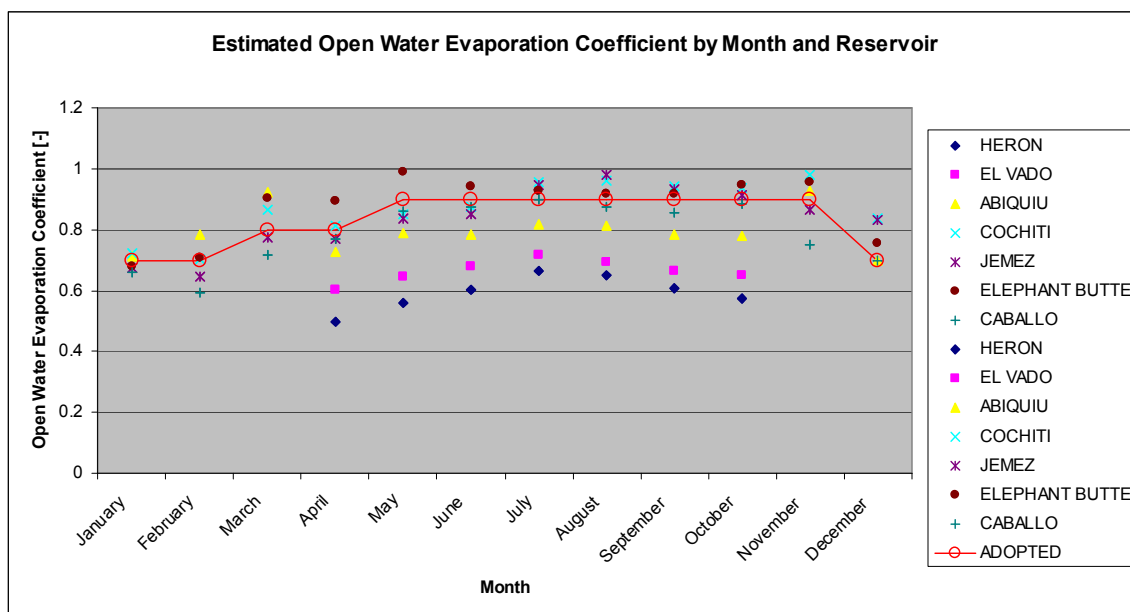
Figure 2-3. Inverse estimations of open water coefficients based on pan evaporation rates measured at reservoirs.

Table 2-9. Open water evaporation coefficients derived for the upper Rio Grande as compared to coefficients derived by Jensen (1998) in the lower Colorado River. The latter are used by ET Toolbox (Brower 2004), while the former are used in the monthly timestep model described in this dissertation. These coefficients are multiplied by reference ET to estimate open water evaporation.

Month	Open Water Evaporation Coefficient Upper Rio Grande	Open Water Evaporation Coefficient Jensen
January	0.7	0.52
February	0.7	0.57
March	0.8	0.67
April	0.8	0.79
May	0.9	0.84
June	0.9	0.89
July	0.9	0.89
August	0.9	0.85
September	0.9	0.89
October	0.9	0.86
November	0.9	0.87
December	0.7	0.57

2.2.3.2.5   Volumetric Evapotranspiration

Reference ET is multiplied by the plant or open water coefficient described above to get the ET rate for a specific plant type or open water. This value must be multiplied by the associated area of plant or water as shown in Equation 2-10, to get volumetric ET or evaporation for plants and open water respectively.

$$Q_{evap}^{r} = E^{r,m} * A^{r,m} * (1 - \text{cov}^{r,m}) \qquad (2\text{-}10a)$$

$$Q_{cropET}^{j} = ET_{ref}^{j,m} * \sum_{p} C^{j,m,c} * A^{j,m,c} \qquad (2\text{-}10b)$$

$$Q_{evap}^{j} = ET_{ref}^{j,m} * C_{ow}^{m} * A^{j,m,w} \qquad (2\text{-}10c)$$

$$Q_{ripET}^{j} = ET_{ref}^{j,m} * \sum_{p} C^{j,m,r} * A^{j,m,r} \qquad (2\text{-}10d)$$

where:

Q_{evap}^{r} = evaporation from reservoir r as defined in Equation 2-4 [L^3/T]

Q_{cropET}^{j} = crop ET in reach j as defined in Equation 2-3 [L^3/T]

Q_{evap}^{j} = open water evaporation in reach j as defined in Equation 2-1 [L^3/T]

Q_{ripET}^{j} = riparian ET in reach j for groundwater balance [L^3/T]

$E^{r,m}$ = evaporation rate from reservoir r during month m [L/T]

$ET_{ref}^{j,m}$ = reference ET in reach j during month m [L/T]

$C^{j,m,c}$ = ET coefficient in reach j during month m for agricultural crop c [-]

C_{ow}^{m} = open water evaporation coefficient during month m [-]

$C^{j,m,c}$ = ET coefficient in reach j during month m for plant r [-]

$A^{r,m}$ = surface area of reservoir r during month m [L^2]

$A^{j,m,c}$ = crop area in reach j during month m for agricultural crop c [L^2]

$A^{j,m,w}$ = open water area in reach j during month m [L^2]

$A^{j,m,r}$ = riparian vegetation area in reach j during month m for plant r [L^2]

$\text{cov}^{r,m}$ = percent of reservoir r covered by ice during month m [%]

Reservoir areas ($A^{r,m}$) are calculated based on storage volume in the reservoir using

Elevation-Area-Capacity (EAC) relationships specific to each reservoir (tables from

Roberta Ball, USACE personal communication 2003). Ice cover on a given reservoir

($\mathrm{cov}^{r,m}$) is a historically measured value, taken from the daily URGWOM data set and

averaged to monthly.

2.2.3.2.6   Crop Acreage

Vegetation areas for irrigated agricultural crops are taken from three different

sources. Crop acreages along the Rio Chama are taken from the Watermaster's Report

for the Rio Chama Mainstream 2002, with crop type percentages from the Rio Chama

Watermaster at the time (Stermon M. Wells, personal communication July 2003). For

acreages above Cochiti along the Rio Grande, approximate acreages of 200 and 5,000

acres for the reaches Taos Junction Bridge to Embudo and Embudo to Otowi respectively

are taken from the URGWOM Physical Model Documentation (USACE et al. 2002).

The same crop distribution as used for the Chama is assumed for the Rio Grande above

Cochiti. Table 2-10 summarizes crop acreage assumed for reaches above Cochiti for

1975–1999. Over 50,000 acres of agricultural land are irrigated by surface water below

Cochiti Reservoir and above Elephant Butte Reservoir (USACE et al. 2002, PHYMOD-

65). Irrigated crop acreages for the reaches in this "middle Rio Grande" stretch, with the

exception of lands irrigated from the Jemez river, are taken from URGWOM Physical

Model Documentation (*ibid*), which tabulated the data from the Middle Rio Grande

Conservancy District (MRGCD) sources, and broke it into river reach based units. Jemez

river total acreage of almost 5400 acres was taken from McAda and Barroll (2002) model

input files, with crop distribution assumed to be an average of URGWOM (USACE et al.

2002) crop distributions reported between Cochiti and Elephant Butte between 1975 and

1999. Based on this rich dataset, the model represents irrigated crop types and acreages

in the middle Rio Grande that are different for each year from 1975–1999. For the

validation period (2000–2006), 1999 crop acreage values are used, and the scenario

evaluation period uses user input to determine crop acreages, with 1999 acreages as a

default.

Table 2-10. Irrigated crop acreages for river reaches above Cochiti Reservoir.
The assumed crop distribution for each crop type is based on Rio Chama adjudicated
crop distribution patterns (Stermon Wells, personal communication July 2003). Chama
total acreage from the 2002 Chama Watermaster's report. Rio Grande total acreage
from URGWOM Physical Model Documentation (USACE et al. 2002). ETTB Category is
the ET Toolbox vegetation category to which each crop type was applied for
determination of crop coefficients.

Crop Type	ETTB Category	Assumed Crop Distribution %	El Vado to Abiquiu Reservoir Acres	Abiquiu Reservoir to Chamita Acres	Taos Junction Bridge to Embudo Acres	Embudo to Otowi Acres
Total	Total	100.0%	317	4862	200	5000
Alfalfa	Alfalfa	22.5%	71	1094	45	1125
Hay & Pasture	Pasture Grass	39.1%	124	1902	78	1956
Corn	Corn	10.7%	34	522	21	537
Orchard	Tree Fruit	10.7%	34	519	21	534
Grain	Wheat	6.4%	20	311	13	320
Garden	Misc Veg	4.0%	13	193	8	199
Fallow	None	6.6%	21	321	13	330

2.2.3.2.7   Riparian Vegetation Acreage

Vegetation areas for riparian vegetation upstream of Cochiti were calculated from

remotely sensed data. Some values were modified slightly during calibration based on

qualitative ground observations. The riparian vegetation areas north of Cochiti result in

losses that are small within the context of the overall water budget between gages, so no

time has been spent validating or improving the calculated values. Downstream of

Cochiti, with the exception of the Jemez and San Acacia to San Marcial reach, riparian

acreages from the URGWOM Physical Model Documentation (*ibid*) were used.

URGWOM does not use riparian area in the Jemez reach, so the Jemez riparian values

were taken from the McAda and Barroll (2002) Albuquerque basin regional groundwater

model. Gage data suggest losses in the San Acacia to San Marcial reach that were about

13,000 acre feet (AF)/yr greater than predicted with the model using URGWOM riparian

and crop acreages. Gage error may be part of the unexpectedly high water loss,

especially during the 1985 –1988 period when losses in the reach seem unusually high, or

it may be a result of active wetlands management in the Bosque del Apache wildlife

refuge, which effectively sits at the end of the agricultural irrigation system. For

modeling purposes gage error during the calibration period is assumed to be distributed

normally about zero, so no attempt was made to evaluate unusual gage error. Calibration

was achieved by increasing riparian acreage between San Acacia and San Marcial by

33% from 16,000 acres to 22,000 acres. Additional work will be necessary to discover

the source of this error. Riparian acreages used in the model are reported in Table 2-4.

2.2.3.2.8   *River Channel Open Water Area*

The open water area associated with each reach of the river channel is a function of flow

rate and channel cross-section geometry. Above Cochiti, the relationship between stream

width and flow associated with each gage is used as a proxy for the relationship in

associated reaches. Channel geometry at gage locations is not likely representative of the

entire reach above or below the gage, but additional data are not readily available, and

surface evaporation from the upper reaches is conceptually a relatively small term, so this

assumption is considered acceptable. Cross-sectional area at each gage as a function of

flow rate is reported in the URGWOM Physical Model Documentation (USACE et al.

2002). Stage as a function of flow rate is a key relationship associated with surface water

gages, and is available indirectly from field measurement data published online for each

gage operated by the United States Geological Survey (USGS).[2] With stage and cross-

sectional area available as a function of flow rate, a trapezoidal channel cross section was

assumed, and a base width and bank slope selected to fit the relationships between

flowrate, stage, and cross-sectional area observed at the gages. Table 2-11 summarizes

cross-sectional relationships adopted for select gages above Cochiti. A trapezoidal

channel did not satisfactorily describe historic field measurements of stage and flow at

either the Rio Grande gage below Taos Junction Bridge or the Chama gage near Chamita,

and so these gages were not included. Chama reaches from below El Vado Reservoir and

all Rio Grande reaches above Cochiti were assumed to follow the cross-sectional

relationships of the gages defining the beginning or end of the reach, or an average of

both as available. For example, in the reach from Lobatos to Cerro, for an average

monthly flow rate of 100 cubic feet per second (cfs), the calculated river stage using the

Cerro gage relationship would be $0.2145 * 100^{0.4742} = 1.9$ feet. The calculated width of

the river would be 56 feet (base width parameter) plus 6.5 (bank slope parameter)*1.9

---

[2]   E.g., for Rio Grande near Cerro gage:
        http://nwis.waterdata.usgs.gov/nm/nwis/measurements/?site_no=08263500&agency_cd=USGS

feet, or 68.35 feet. This width is then multiplied by the length of the reach (26 miles, see

Table 2-4) to get a total open water area of 0.34 mile^2 for Lobatos to Cerro at 100 cfs

flowrate ($A^{j,m,w}$ in Equation 2-10c).

Table 2-11. Channel geometry relationships adopted at selected gages, used to estimate stage and area as a function of flow rate in reaches above Cochiti Reservoir. Reaches between gages in this table used an average of both; other reaches used upper or lower gage data as available.

Gage	Stage [ft] from Q[cfs]	Cross Sectional Area [ft^2] from Q[cfs]	Fitted Base Width Parameter [ft]	Fitted Bank Slope Parameter (run/rise) [-]
Rio Chama below El Vado	0.27*Q$^{0.37}$	13*Q$^{0.48}$	75	8
Rio Chama above Abiquiu Reservoir	0.35*Q$^{0.36}$	11.5*Q$^{0.47}$	50	5
Rio Chama below Abiquiu Dam	0.4*Q$^{0.33}$	7*Q$^{0.54}$	28	12
Rio Grande near Cerro	0.2145*Q$^{0.4742}$	4.2943*Q$^{0.6976}$	56	6.5
Rio Grande at Embudo	0.15*Q$^{0.48}$	5.1771*Q$^{0.593}$	61	3
Rio Grande at Otowi	0.2*Q$^{0.41}$	3.2959*Q$^{0.6628}$	40	16

Below Cochiti, open water area associated with each reach of the river is calculated using

flow based relationships developed by the URGWOM technical team (USACE et al.

2002), shown in Table 2-12. The Jemez river was assumed to have a constant average

width of 25 feet, which when multiplied by a reach length of 30 miles (Table 2-4)

resulted in 91 acres of open water area.

2.2.3.2.9 *Potential Versus Actual ET in Model*

Equations 2-10b through 2-10d use reference ET to calculate potential ET for

agricultural, channel surface, and riparian ET. The potential ET is the maximum ET

expected for a given set of climatic conditions and growing history of a plant (if using

Table 2-12. Open water area of reaches below Cochiti Reservoir as a function of river flow. Relationships from URGWOM (USACE et al. 2002) physical model documentation page 39.

River Reach	River area [acres] as a function of flowrate (Q) in cfs	Bank full area [acres]
Cochiti to San Felipe	$110.85Q^{0.1988}$	625
San Felipe to Albuquerque	$84.281Q^{0.4099}$	2718
Albuquerque to Bernardo	$123.87Q^{0.4375}$	5175
Bernardo to San Acacia	$12.828Q^{0.5291}$	1054
San Acacia to San Marcial	$158.29Q^{0.3197}$	2913
San Marcial to Elephant Butte	$60.722Q^{0.5293}$	166

growing degree day (GDD) approach). The actual ET observed is less than potential if water availability is limiting. In the case of riparian vegetation, depth to groundwater can limit riparian ET. This is discussed in detail in Chapter 3. In the case of agricultural ET, crops are often grown in a moisture deficit state, that is, with less water applied than could potentially be transpired. Actual water delivery is restricted in timing and magnitude based on water rights, delivery infrastructure, and social institutions.

Due to limited diversion and return flow data, and relatively small irrigated acreages, actual ET is assumed to equal potential ET for all agricultural area upstream of Cochiti. The actual agricultural ET calculated in the model downstream of Cochiti is reduced from potential ET based on availability. A calibration factor of carriage water required to deliver water for use was used in middle valley reaches to reduce actual cumulative agricultural ET from 1975 through 1999 to cumulative agricultural ET values predicted by URGWOM for the same period. The calibrated carriage water requirements are shown in Table 2-4, and decrease as water moves downstream in the conveyance system. For example, the 85% requirement between Cochiti and San Felipe suggests that

only 15% of the water in the conveyance system can be used to satisfy agricultural ET demand, and the rest moves down to the next reach for use there. Without this calibration factor, the model would satisfy potential demand at the top of the conveyance system to the detriment of downstream users, which is not the observed tendency.

2.2.3.3 Groundwater Surface Water Interactions

2.2.3.3.1 *Groundwater Contributions Upstream of Rio Chama Confluence*

Relevant studies of the geohydrology of the groundwater system associated with the Rio Grande and Rio Chama river systems north of their confluence include a characterization of the aquifer geology by Wilkins (1986), a mass balance characterization of the Rio Grande system above Embudo by Hearne and Dewey (1988), and a regional groundwater model of the Taos area by Barroll and Burck (2005). The reaches above the Rio Chama/Rio Grande confluence tend to be gaining reaches (see Figure 2-2); however, quantitative estimates of the magnitude of that gain are limited. Hearne and Dewey (1988) constrained overall contributions with surface gage data, while Barroll and Burck (2005) calibrated groundwater flows to the Rio Grande between Arroyo Hondo and Rio Pueblo de Taos (part of the Cerro to Taos Bridge surface water reach, see Figure 2-1 and Table 2-2) using estimates based on direct stream flow measurements. Because the Hearne and Dewey work is spatially lumped above the Embudo gage and the Barroll and Burck work is spatially limited, additional data were developed for this modeling effort.

The magnitude of groundwater contributions for reaches upstream of the Rio Chama Rio/Grande confluence was estimated by analyzing winter gage flows. Historic gage data was filtered for winter months (November–February) when agricultural diversions and riparian ET are assumed negligible such that surface water losses are limited to direct evaporation from the river surface. Evaporative losses from the river channel for winter months during the calibration period (1975– 1999) were calculated with Equation 2-10c. In a given reach between an upstream and downstream gage, the calculated evaporative losses were removed from the upstream gaged flow, and gaged tributary flows, if any, including wastewater return flows (Espanola), were added to the upstream gaged flow. This "corrected" flow at the downstream gage was compared to the gaged flow to get a residual (observed–corrected) for each calibration winter month for each reach. The residual is positive when the downstream gage reading is larger than the corrected estimate. These residuals represent a combination of gage error, error in loss approximation, and ungaged gains between the gages. If gage and model errors are not overwhelming, the residuals should represent a proxy to ungaged inflows. No meaningful relationship was discovered between these ungaged inflow approximations and precipitation, snow pack, reservoir stage (Chama reaches), or stream flow. The ungaged groundwater inflows were set to constant values that result in an approximately equal number of negative and positive residuals in each reach for winter months 1975– 1999. The mathematical details and an example calculation are shown below.

The uncorrected winter residual for a given reach in a given month is the difference between the upstream gage plus tributary flow (inflows) and the downstream gage reading plus calculated evaporative losses (outflows):

$$R_{uw}^{j,m} = (Q_{down}^{j,m} + Q_{loss}^{j,m}) - (Q_{up}^{j,m} + Q_{trib}^{j,m}) \qquad (2\text{-}11)$$

where:

$R_{uw}^{j,m}$ = the uncorrected winter residual for reach j in month m [L^3/T]

$Q_{down}^{j,m}$ = the gaged flow at the bottom of reach j in month m [L^3/T]

$Q_{loss}^{j,m}$ = the modeled loss for reach j in month m [L^3/T]

$Q_{up}^{j,m}$ = the gaged flow at the top of reach j in month m [L^3/T]

$Q_{trib}^{j,m}$ = the gaged tributary input to reach j in month m [L^3/T]

For example, the January 1975 Lobatos (upstream gage) to Cerro (downstream gage) uncorrected winter residual was 29 cubic feet per second (cfs).

$$R_{uw}^{LBT2CROJan1975} = (Q_{down}^{j,m} + Q_{loss}^{j,m}) - (Q_{up}^{j,m} + Q_{trib}^{j,m}) = 198.8 cfs + 0.5 cfs - 170.3 cfs - 0 cfs = 29 cfs$$

The uncorrected winter residuals for the Lobatos to Cerro reach are shown in Figure 2-4a, and suggest that the reach is gaining. To estimate groundwater contribution magnitude, a constant groundwater inflow is added to the reach to get a corrected winter residual that is negative approximately as often as positive during the calibration period.

$$R_{cw}^{j,m} = (Q_{down}^{j,m} + Q_{loss}^{j,m}) - (Q_{up}^{j,m} + Q_{trib}^{j,m} + Q_{base}^{j}) \qquad (2\text{-}12)$$

where:

$R_{uw}^{j,m}$ = the corrected winter residual for reach j in month m [L^3/T]

Q_{base}^{j} = the base flow added to reach j in all months [L^3/T]

Figure 2-4b shows the corrected residual distribution for Lobatos to Cerro resulting from the addition of 39 cfs of constant base flow to the reach. Figures 2-5 through 2-9 show

the uncorrected and corrected residual distributions for the other reaches extending above

the Rio Chama/Rio Grande confluence. Adopted base flow values for each reach are

summarized in Table 2-13. These numbers are the best available, but are approximate.

Because of potential ungaged surface runoff during historic winter months, the

groundwater base flow estimates may include some fraction of ungaged surface flows.

Base flow values shown in Table 2-13 are used during all model periods.

The remainder of this section contains further explanation of the results for the three

reaches along the Rio Grande from Cerro to Otowi, and a summary of adopted base flow

values. The 34-mile reach from Cerro to Taos Junction Bridge includes a 17-mile stretch

from below the Arroyo Hondo tributary to above the Rio Pueblo de Taos tributary that

was the subject of seepage studies by the United States Geological Survey in 1963–1964,

and TetraTech, Inc., in 2003. These studies estimated groundwater surface water

interactions by measuring surface flows at several cross sections along the reach.

TetraTech estimated a net groundwater gain in the Rio Grande from Arroyo Hondo to

Taos Junction Bridge of approximately 22 cfs for the 17-mile stretch (1.3 cfs/mile), while

the USGS estimated gains of 17, 15, and 7.5 cfs for the same stretch in August 1963,

October 1963, and October 1964 respectively (1, 0.9, and 0.4 cfs/mile) (TetraTech, Inc.

2003). As a result of these analyses, Barroll and Burck (2005) calibrated groundwater

leakage to the Rio Grande between Arroyo Hondo and Rio Pueblo de Taos to be

approximately 1 cfs/mile. These estimates are quite a bit lower per mile than the 94 cfs

total inflow to the 35-mile reach (2.7 cfs/mile) suggested by the winter gage analysis for

the encompassing Cerro to Taos Bridge reach (see Figure 2-5b). There are two main

Lobatos to Cerro Winter Residuals Uncorrected

Occurance (y-axis): 0% to 70%

Values: < -100: 0%, -100 to -50: 0%, -50 to 0: 0%, 0 to 50: 64%, 50 to 100: 29%, > 100: 7%

Measured Flow Increase at Cerro [cfs]
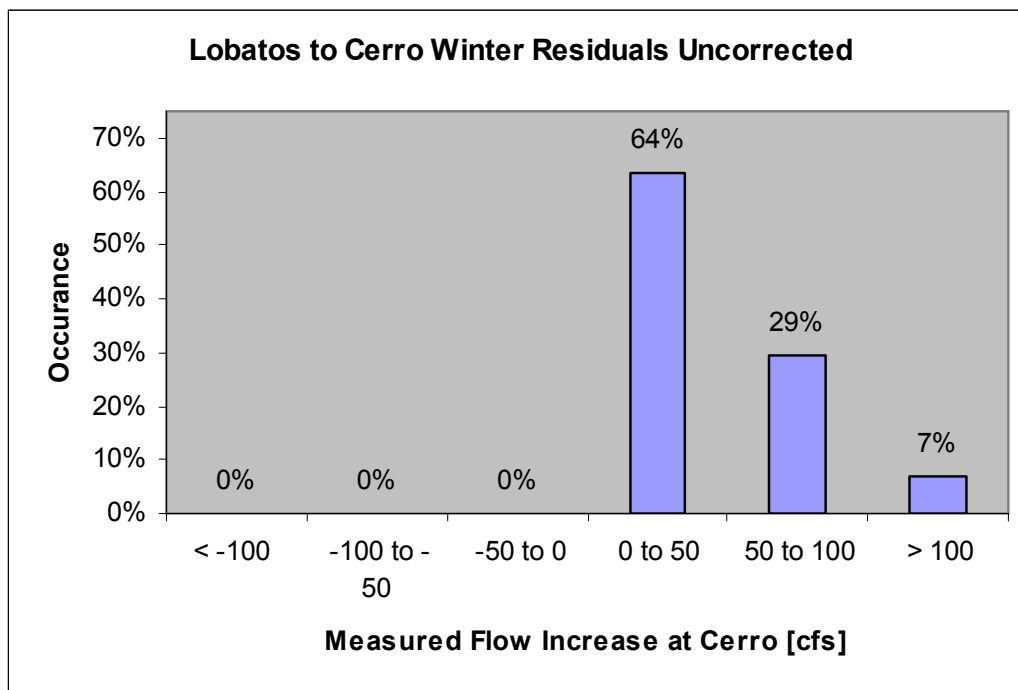
Figure 2-4a. Uncorrected winter residuals for Lobatos to Cerro reach 1975–1999.

Lobatos to Cerro Winter Residuals Base Flow Corrected (39 cfs constant inflow)

Occurance (y-axis): 0% to 60%

Values: < -100: 0%, -100 to -50: 0%, -50 to 0: 48%, 0 to 50: 43%, 50 to 100: 8%, > 100: 0%

Measured Flow Increase at Cerro (GW Corrected) [cfs]
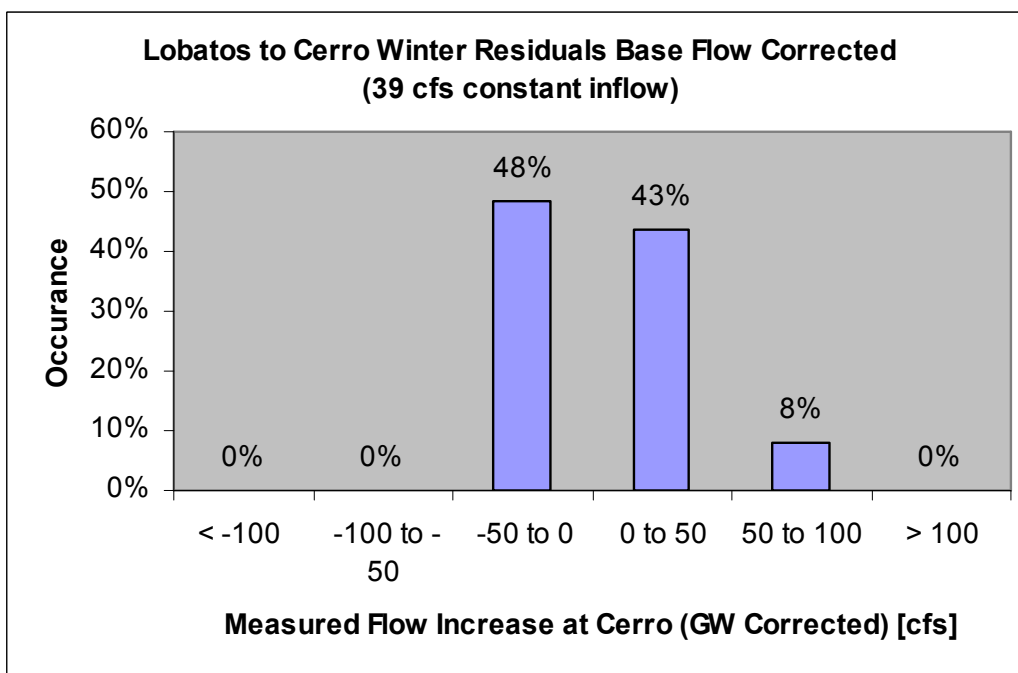
Figure 2-4b. Corrected winter residuals for Lobatos to Cerro reach 1975–1999 associated with a constant 39 cfs base flow addition.

Cerro to Taos Bridge Winter Residuals Uncorrected
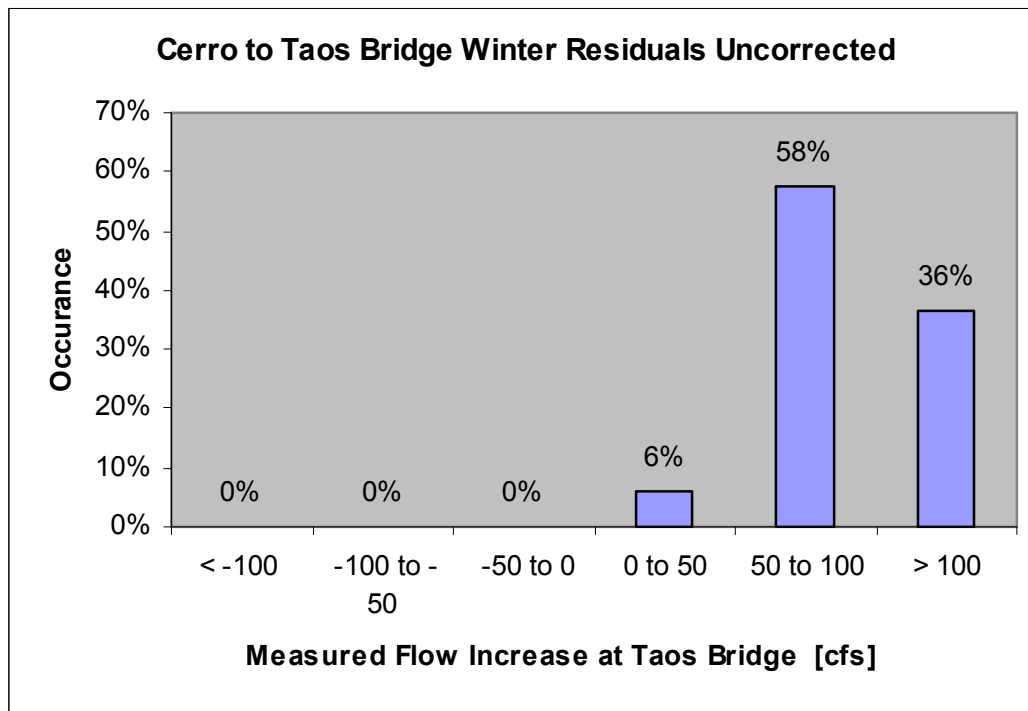
*Figure 2-5a. Uncorrected winter residuals for Cerro
to Taos Junction Bridge reach 1975–1999.*

**Cerro to Taos Bridge Winter Residuals Base Flow
Corrected (94 cfs constant inflow)**
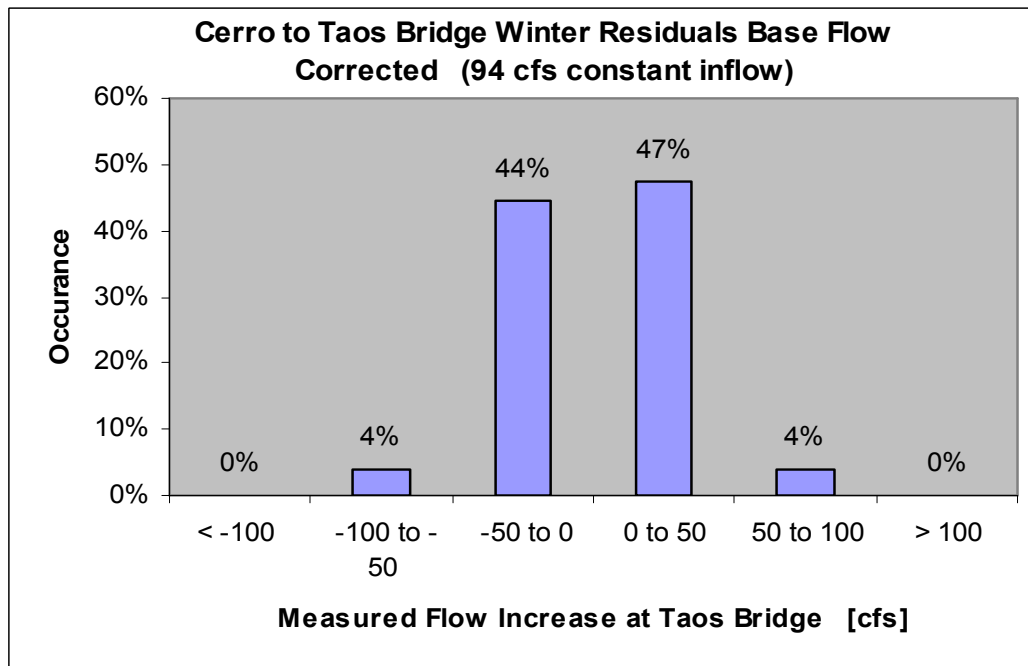
*Figure 2-5b. Corrected winter residuals for Cerro to Taos Junction Bridge
reach 1975–1999 associated with a constant 94 cfs base flow addition.*

Taos Bridge to Embudo Winter Residuals Uncorrected
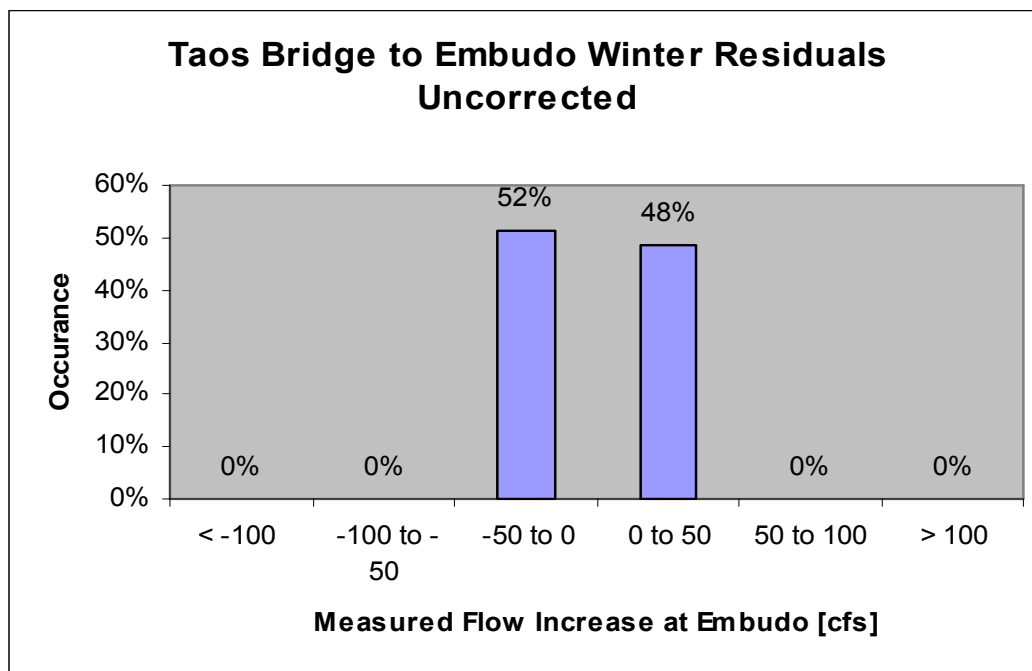
Figure 2-6. Uncorrected winter residuals for Taos Junction Bridge to Embudo reach 1975–1999. The uncorrected residuals are approximately distributed about zero, so no base flow was added to this reach.

Table 2-13. Base flow contribution added to modeled river reaches upstream of Rio Chama Rio Grande confluence. Values are based on winter gaged flows.

	Reach	Adopted Ungaged GW Contribution [cfs]	Reach Length [mile]	GW Contribution per Mile [cfs/mile]	Adopted Ungaged SW Contribution [cfs]
Chama	El Vado to Abiquiu	8	29	0.3	
	Abiquiu to Chamita	17	29	0.6	
	Chama Total	25	58	0.4	
Rio Grande	Lobatos to Cerro	39	26	1.5	
	Cerro to Taos Bridge	77	35	2.2	17
	Taos Bridge to Embudo	0	15	0.0	
	Embudo to Otowi	24	29	0.8	47
	Rio Grande Total	140	105	1.3	64

Embudo to Otowi Winter Residuals Uncorrected
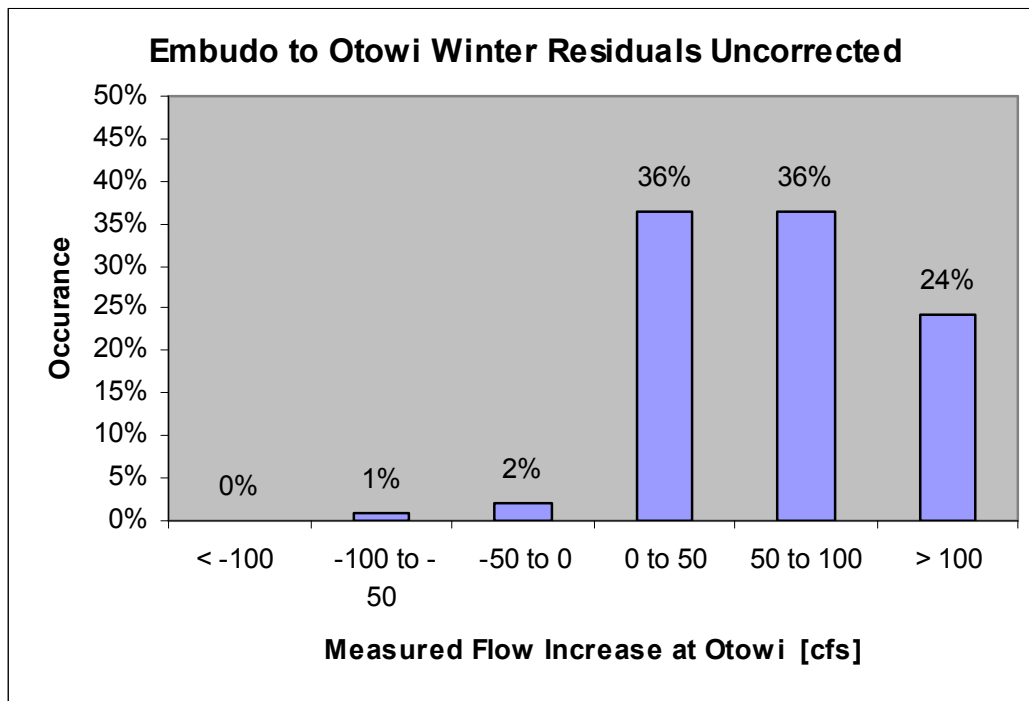
Figure 2-7a. Uncorrected winter residuals for Embudo to Otowi reach 1975–1999.

Embudo to Otowi Winter Residuals Base Flow Corrected (71 cfs constant inflow)
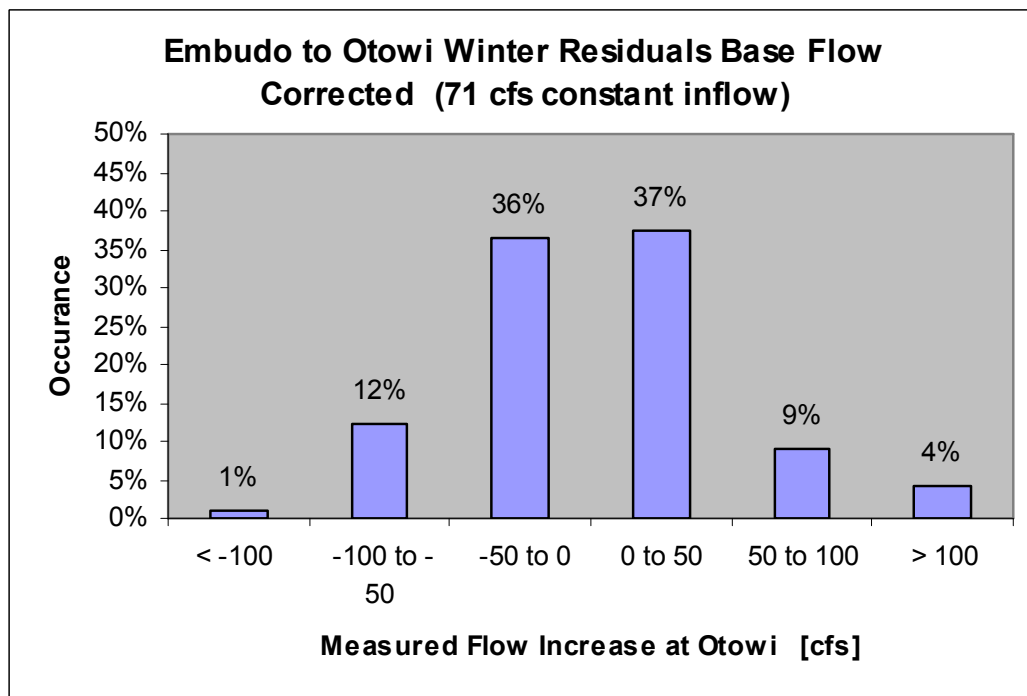
Figure 2-7b. Corrected winter residuals for Embudo to Otowi reach 1975–1999 associated with a constant 71 cfs base flow addition.
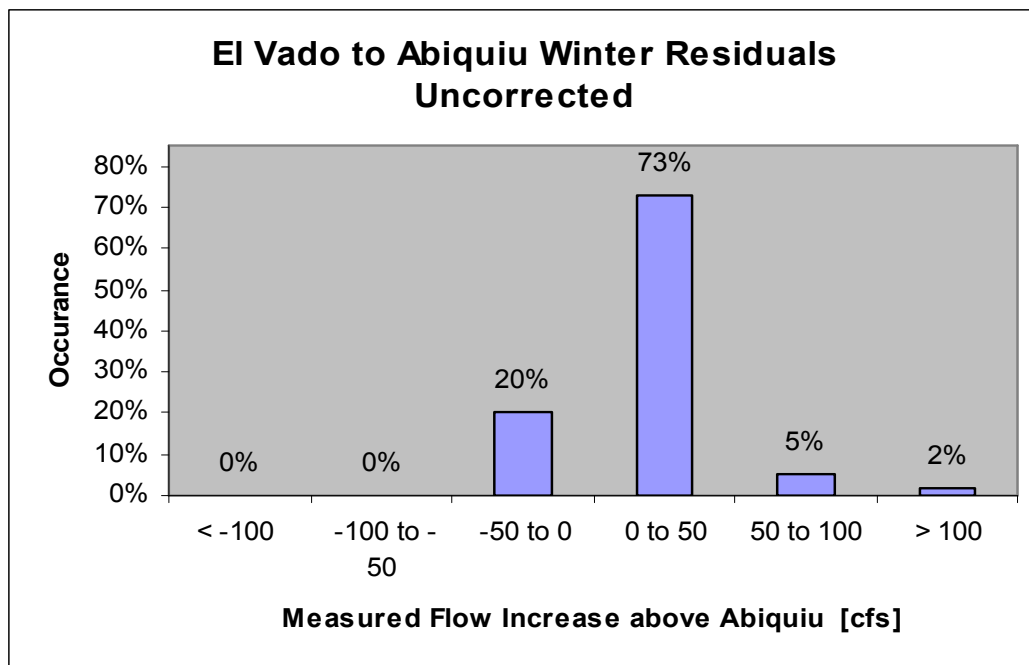
*Figure 2-8a. Uncorrected winter residuals for
below El Vado to above Abiquiu reach 1975–1999.*
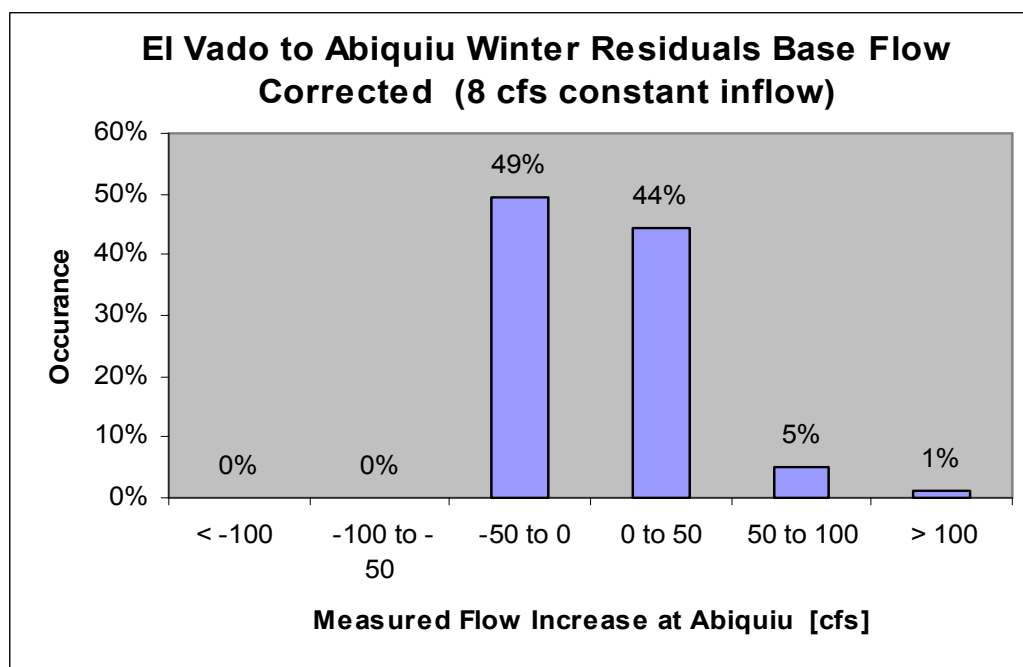
*Figure 2-8b. Corrected winter residuals for below El Vado to above Abiquiu
reach 1975–1999 associated with a constant 8 cfs base flow addition.*
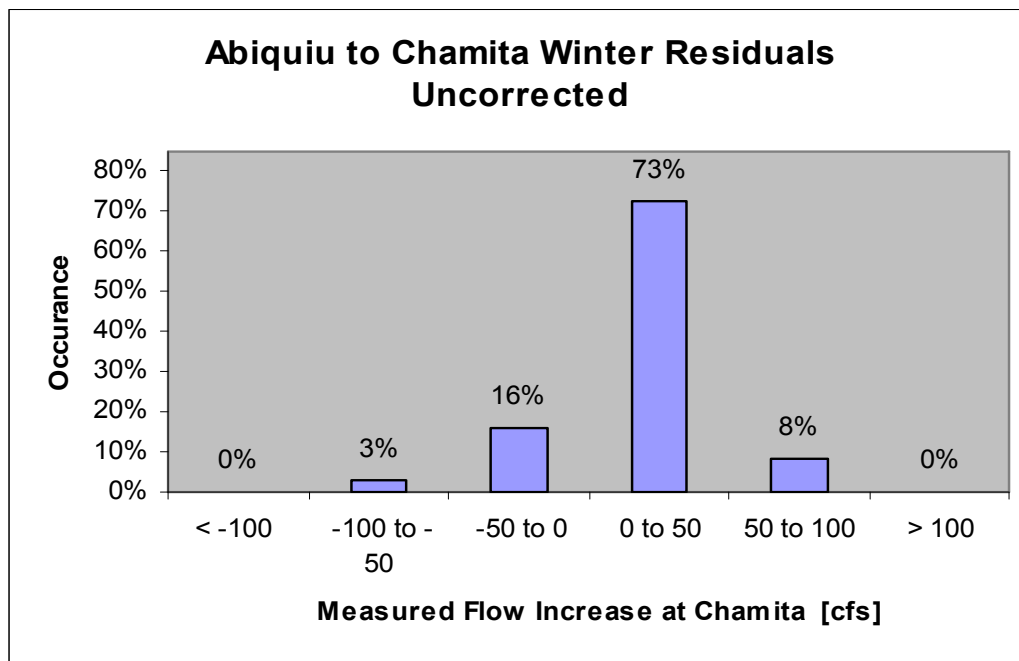
Figure 2-9a. Uncorrected winter residuals for below Abiquiu to Chamita reach 1975–1999.
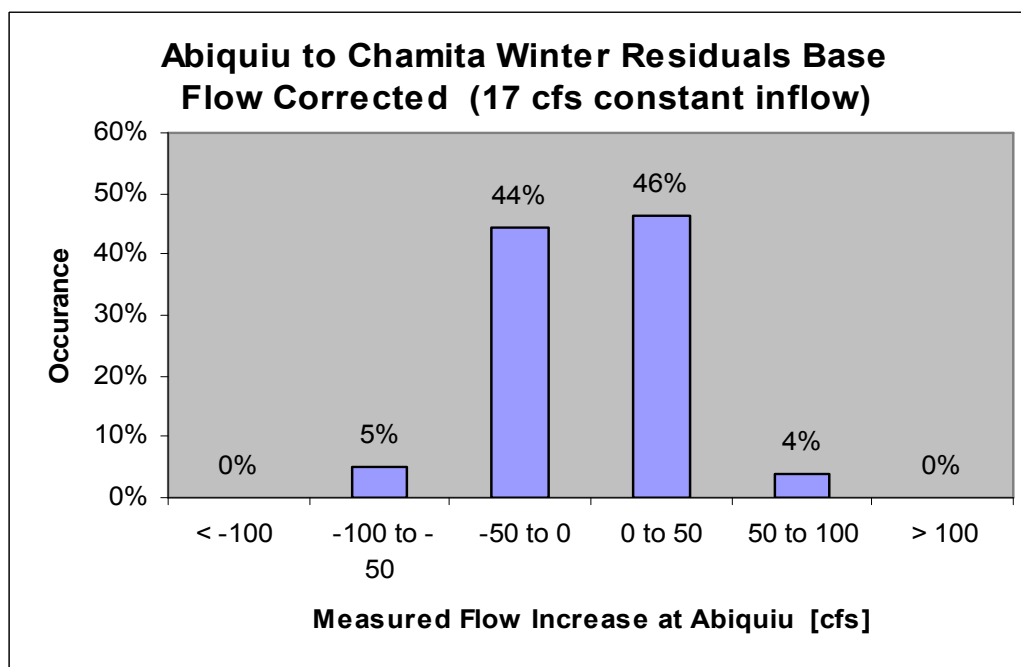
Figure 2-9b. Corrected winter residuals for below Abiquiu to Chamita reach 1975–1999 associated with a constant 17 cfs base flow addition.

reasons for the discrepancy.

Although it was not used to define a reach because of an incomplete historic record, the USGS operated a gage on the Rio Grande below the Arroyo Hondo confluence from March 1963 to September 1996, and from July 2002 to September 2004. Applying the same winter residual method described above to the reach from Cerro to Arroyo Hondo suggests that 78 cfs of base flow enters the Rio Grande in that stretch, leaving 16 cfs to enter the river between Arroyo Hondo and Taos Junction Bridge, a distance of 19 miles. This value compares well with the seepage studies and adopted value used by Barroll and Burck (2005). The 78 cfs of calculated base flow in the 16-mile stretch from Cerro to Arroyo Hondo is high because it includes tributary inputs from the Arroyo Hondo. Because of incomplete historic record, this tributary is not included as gaged inflow to the reach, but the USGS did operate a gage on the Arroyo Hondo near the Rio Grande confluence from 1912 to 1985.[3] Data from that gage suggest that average winter flows of the Arroyo Hondo are about 17 cfs. This reduces the estimated groundwater input to the Cerro to Arroyo Hondo stretch to approximately 60 cfs in 19 miles, a high value at 3.2 cfs/mile, but plausible for the area. The adopted groundwater contribution to the Cerro to Taos Bridge reach is 77 cfs, with the remaining 17 cfs attributed to surface water inflow from Arroyo Hondo.

The uncorrected winter residual distribution for the Taos Bridge to Embudo reach was centered about zero, so no groundwater correction was added to this reach (Figure 2-6). The corrected winter residual distribution for Embudo to Otowi suggests a very large

---

[3]   USGS gage ID number 08268500.

winter base flow of 71 cfs for the 29 mile reach. This number seems too large to local

hydrologists (Dr. Nabil Shafike, Senior Hydrologist, New Mexico Interstate Stream

Commission, personal communication 2006). Consistent with this notion, a regional

groundwater model underlying the Rio Grande from the Rio Chama/Rio Grande

confluence to Cochiti Reservoir (see Section 2.2.3.3.2.1) calculates groundwater inflows

between the confluence and Otowi gage of approximately 9 cfs (~ 0.6 cfs/mile) (Frenzel

1995). It is possible that the high winter gains between Embudo and Otowi includes

significant ungaged surface water inflow from the Santa Cruz and Pojaque

Rivers, and Santa Clara Creek. For the purposes of this study, 1 cfs/mile of groundwater

inflow was assumed along the Rio Grande between Embudo and the Rio Chama

confluence, for a total of 15 cfs above the confluence, and including the 9 cfs estimated

below the confluence, 24 cfs total groundwater contribution to the Embudo to Otowi

reach. The remaining 47 cfs of ungaged inflows suggested by the winter residual

analysis (Figure 2-7b) was attributed to ungaged surface water inflows (described in

Section 2.2.3.4.4).

2.2.3.3.2   *Groundwater Surface Water Interactions Downstream of the Rio Chama Confluence*

Understanding of the groundwater system downstream of the Rio Chama/Rio

Grande confluence is far greater than that upstream. Regional groundwater models have

been created for the Espanola Basin (Frenzel 1995), Albuquerque Basin (McAda and

Barroll 2002), and the Socorro Basin (Shafike 2005). Together these groundwater

models incorporate the regional Rio Grande river system from the Rio Chama confluence

to Elephant Butte Reservoir. As described in the next chapter of this dissertation, spatially aggregated, explicit finite difference groundwater flow models were created to capture the salient groundwater behavior represented by the Frenzel, McAda/Barroll, and Shafike models. The spatially aggregated versions run more rapidly than their spatially distributed counterparts, and are set up to run at a monthly timestep to facilitate connection to the surface water system described here. This section summarizes issues of coupling and calibration associated with connecting the groundwater models to the surface water, but for a more detailed description of model behavior the reader is referred to Chapter 3. Model parameters calculated during calibration were used during validation and scenario evaluation runs.

2.2.3.3.2.1   Espanola Basin Groundwater System

The Espanola Basin groundwater model created by Peter Frenzel (1995) covers the river system roughly from the Rio Grande/Rio Chama confluence to Cochiti Reservoir, and focuses specifically on pumping effects of the Los Alamos and Santa Fe well fields. Irrigated agriculture effects are not explicitly represented. Transient flows from the Frenzel model were used to calibrate a spatially aggregated 16-zone model that was linked dynamically to a similar Albuquerque basin groundwater model to the south, as well as to surface water reaches from the Rio Grande/Rio Chama confluence to Cochiti Reservoir. River stage was calculated as a function of monthly average flow in the Embudo to Otowi and Otowi to Cochiti reaches using the gage-based stage to flow relationships described in Section 2.2.3.2.8 and shown in Table 2-11. The modeled river

leakage was calibrated so that calibration average values would match the Frenzel calibration averages. See Section 3.4.2.

2.2.3.3.2.2   Albuquerque Basin Groundwater System

The Albuquerque basin regional groundwater model created by Douglas McAda and Peggy Barroll (2002) simulates regional groundwater flow associated with the Rio Grande river system roughly from Cochiti Reservoir to San Acacia. Transient flows from that model were used to calibrate a spatially aggregated 51-zone model that was linked dynamically to the 16-zone Espanola basin groundwater model, Jemez and Cochiti reservoirs, and surface water reaches from Cochiti to San Acacia. The Albuquerque groundwater basin does not communicate to any significant extent with the Socorro groundwater basin to the south in either the McAda/Barroll or Shafike (2005) models. Surface water stages in the river, canal, and drains are calculated with Manning's equation, and the spatially aggregated groundwater system is calibrated to match the McAda and Barroll model. The overall riparian ET combines atmospheric constraints on ET (reference ET) from the surface model with depth to groundwater constraints from the groundwater model using a calibration factor as described in Section 3.4.1. Values were calibrated to fall between the McAda/Barroll and URGWOM predicted values for the middle Rio Grande. Total mass balance was achieved for reaches above Bernardo by adding ungaged surface inflows. From Bernardo to San Acacia, calibration was achieved by increasing riparian ET from the groundwater system.

2.2.3.3.2.3   Socorro Basin Groundwater System

The Socorro basin regional groundwater model created by Nabil Shafike (2005) simulated regional groundwater flow associated with the Rio Grande river system from San Acacia to Elephant Butte Reservoir. As described in detail in the next chapter of this dissertation, steady state values for the Shafike model were used to calibrate a spatially aggregated 12-zone model that is dynamically linked to the surface water reaches from San Acacia to Elephant Butte. The Socorro groundwater basin does not communicate to any significant extent with the Albuquerque groundwater basin to the north in either the McAda/Barroll or Shafike models. Surface water stages in the river, canal, and drains are calculated with Manning's equation. San Acacia to San Marcial was calibrated by increasing the riparian acreage by 40%. See Section 2.2.3.2.7 for further discussion of this change. The San Marcial to Elephant Butte reach was calibrated to 1975–1999 gage values by manipulation of surface water groundwater exchanges. See Section 3.4.3.

2.2.3.4   Surface Water Flows

2.2.3.4.1   Gaged Streams

The majority of water enters the surface water system as gaged inflows, with the largest of these occurring at the top of the Rio Grande (Rio Grande near Lobatos gage) and Rio Chama (Rio Chama near La Puente gage), which together are responsible for 60% of gaged inflows to the model. Other tributary gages are included as reach inflows where they are available close to the confluence with any river reach. Relevant gaged tributary flows are added to the model during all model periods, with future run values based on historic year reshuffle as described in Section 4.2.2.1.

Flows from the gages in Table 2-1 are used as direct input into the model with three exceptions: the Ojo Caliente at La Madera gage, the Chama at La Puente gage, and the Embudo at Dixon gage. The La Madera gage is located 20 miles from the confluence of the Ojo Caliente and Chama, and gage readings are reduced by modeled potential losses between the gage and confluence. In the case of the La Puente gage, estimating flow at the gage with El Vado Reservoir behavior (see Section 2.2.3.5.4) and comparing to gaged flows suggests that the La Puente gage tends to overestimate high flows. In the case of the Embudo creek gage, 1975–1999 gage readings suggest that on average, more gaged water enters the Taos Bridge to Embudo reach (855 cfs in Rio Grande at Taos Bridge and 100 cfs from Embudo Creek for a total of 955 cfs) than leaves (946 cfs in Rio Grande at Embudo gage). Either losses in the 15-mile canyon reach are dramatically underestimated, or inflows are overestimated. The latter seems more likely. Flows from both the La Puente and Embudo Creek gages over a certain threshold are reduced by a calibrated percentage to result in flows consistent with downstream observations.

2.2.3.4.2   *Gaged Municipal Wastewater Returns*

Gaged wastewater return flows from municipal sources are included in the model for the cities of Espanola, Bernalillo, Rio Rancho, Albuquerque, Los Lunas, Belen, Socorro, and Truth or Consequences. 1975–1999 wastewater flow data are taken from URGWOM. Taos wastewater data are available; however, the Taos wastewater is assumed to discharge to the groundwater system, or the Rio Pueblo de Taos, which is a gaged tributary in the model. Los Alamos County and Los Alamos National Laboratory

wastewater data are also available; however, they are assumed to be accounted for in the groundwater contribution to the Otowi to Cochiti reach, which as discussed in Section 3.4.2.1.3.2 was based on seepage studies within that river reach (Frenzel 1995). Historic municipal wastewater data is used for calibration and validation, while future runs use returns based on human water use patterns based on historic trends and user input as described in Section 4.2.2.2.

2.2.3.4.3 *Surface Water Diversions and Returns*

Surface water diversion for agricultural irrigation is a historic and culturally important use of water in river systems in New Mexico, and historically represents the largest human user of water resources in the state (e.g. Wilson 1992). Along the Rio Grande proper, surface water is diverted from the river into agricultural conveyance systems for irrigation use in most reaches below Taos Junction Bridge. The same is true to some extent of all modeled reaches along the Rio Chama and Jemez River.

Along the Chama where historic diversion data are available, the diversion is set to historic, consumptive use is the potential crop ET up to diversion amount, and the return is the diversion less the consumptive use. Along the Rio Grande above Cochiti, and along the Jemez, historic diversion data are not readily available. For these reaches during all periods, as well as the Chama reaches during validation and scenario evaluation periods, we assume that half of the diversion is lost, and half returns to the system. The diversion amount is calculated as double the potential crop ET (see Section 2.2.3.2) up to available water, and the return is the diversion less the consumptive losses. Consumptive loss is the potential crop ET up to diversion amount.

Below Cochiti along the Rio Grande, calibration period diversions and conveyance

through flows are based on historic data. During validation and scenario evaluation

periods, diversions are based on 1975–1999 average diversions at each diversion point up

to available. The exception is the low flow conveyance channel (LFCC), which was

originally designed to reduce conveyance losses between San Acacia and Elephant Butte.

Utilized heavily between 1950 and 1986, growing awareness of endangered species

requirements and sediment buildup at its terminus have resulted in essentially zero

diversions to the LFCC since the late 1980s (Shafike 2005). Default diversion targets for

each diversion point are summarized in Table 2-14. As will be seen in Sections 2.3.1.4

and 4.3.5, this approach represents a weakness to the model approach, and should be

modeled as a function of irrigated crop acreage and user inputs in future model versions.

Table 2-14. Surface water diversion target to agricultural conveyance system below Cochiti for validation and scenario evaluation periods. Values are 1975–1999 average diversions rounded to the nearest 100 AF/mo. Low flow conveyance default diversions are assumed to be zero; however, this value can be changed by the user.

Diversion Target for Validation and Scenario Evaluation Periods [AF/mo]					
Diversion name	Cochiti	Angostura	Isleta	San Acacia	LFCC
in reach	CTI2SFP	SFP2ALB	ALB2BDO	BDO2SA	BD02SA
January	0	200	0	200	0
February	100	300	0	100	0
March	8300	11100	18700	6500	0
April	11200	14900	26000	8500	0
May	12300	17200	28400	8400	0
June	12100	17100	28900	8500	0
July	12000	18300	25500	7300	0
August	11700	16800	20200	4600	0
September	11100	16000	18300	3300	0
October	11200	15100	14600	3700	0
November	300	1100	200	300	0
December	0	100	0	300	0

(Month)

South of Cochiti, exchanges between the surface water agricultural conveyance system and the groundwater system are calculated as described in Section 2.2.3.3.2, and loss to the atmosphere is potential crop ET up to available, limited by carriage water requirements as discussed previously (Section 2.2.3.2.9) and summarized in Table 2-4. This is true for all modeling periods. After these interactions are considered, the water available to return to the river either flows through to the downstream agricultural conveyance system or returns to the river. A historically based fixed percentage of available water continues to the conveyance system in the next reach, and the rest returns to the river. As will be seen in Section 4.3.5, this is also a conceptual weakness in the current model structure, as the percent through flow remains constant during scenario runs when the system is changing significantly. The model may be improved in the future with better understanding and modeling of agricultural conveyance system operation. Nevertheless, the currently employed canal through flow percentages for each Rio Grande reach below Cochiti are summarized in Table 2-15. During the calibration period, the conveyance inflows are set to gage data, so the conveyance system effectively resets at each reach; however, during validation and scenario evaluation the conveyance through flows from an upstream reach (Q_{convtf}^{i} in Equation 2-3) become the conveyance inflows for the next reach downstream (Q_{convtf}^{j} in Equation 2-3).

Table 2-15. Amount of water in the agricultural conveyance system assumed to leave the reach in the conveyance system rather than returning to the river. Average of 1975–1999 observations.

Reach	Conveyance % Through Flow
Cochiti to San Felipe	23%
San Felipe to Albuquerque	63%
Albuquerque to Bernardo	45%
Bernardo to San Acacia	47%
San Acacia to San Marcial	58%
San Marcial to Elephant Butte	100%

2.2.3.4.4 *Ungaged Surface Water Inflows*

Combining Equations 2-1 and 2-2, and solving for ungaged surface water inflows:

$$Q_{swungaged}^{j} = Q_{msout}^{j} - Q_{m\sin}^{j} - Q_{swgaged}^{j} + Q_{swdiversion}^{j} - Q_{swreturn}^{j} - Q_{gwsw}^{j} + Q_{evap}^{j} \qquad (2\text{-}13)$$

The previous sections have defined all terms on the right side of Equation 2-13. Once all

terms on the right hand side of Equation 2-13 have been considered, most reaches and

reservoirs north of Bernardo need additional water to end up consistent with the observed

gage data. These reaches and reservoirs were calibrated to have no net error between the

gages during 1975–1999 by adding a modeled ungaged surface water inflow term. The

term was estimated as a percentage of a nearby gaged tributary. Using this approach,

input data for ungaged surface water inflows are based on available gages, and an explicit

error term can be calculated for mass balance between gages during calibration. Table

2-16 lists the reaches and reservoirs to which ungaged surface water inflows were added

as a calibration term, and the associated gage and calibration factor for the reach. This

ungaged inflow is in addition to any ungaged baseflow into the reach from groundwater

as described in Section 2.2.3.3.1 and shown in Table 2-13. For reaches upstream of

Cochiti, this term was only added during non-winter months (March through October).

For the reach between Elephant Butte and Caballo, the ungaged surface inflow is added

as a function of average precipitation rate at Elephant Butte and Caballo reservoirs.

Table 2-16. Dynamic ungaged surface water inflows to modeled river reaches. Added to close the mass balance. These values are in addition to any baseflow assigned to the reach (see Section 2.2.3.3.1 and Table 2-13). No ungaged inflows are added to reaches north of Cochiti during winter months (November through February).

Reach or Reservoir	Ungaged Inflow Added?	Ungaged Inflow Factor	Comments
Chama: Willow Creek to Heron	Yes	6.7%	Rio Chama near La Puente, Mar – Oct only
Chama: Heron to below El Vado	No		
Chama: El Vado to above Abiquiu Reservoir	Yes	36%	Rio Ojo Caliente at La Madera
Chama: below Abiquiu to Chamita	Yes	2.5%	Rio Ojo Caliente at La Madera
Lobatos to Cerro	No		
Cerro to Taos Junction Bridge	Yes	39%	Rio Pueblo de Taos below Los Cordovas
Taos Junction Bridge to Embudo	No		
Embudo to Otowi	Yes	165%	Rio Nambe below dam (USGS 08294210)
Otowi to below Cochiti	No		
Below Cochiti to San Felipe	Yes	275%	Galisteo creek below Galisteo dam
Jemez: Jemez Pueblo to Reservoir	Yes	65%	Flows < 200 cfs at Jemez River near Jemez
Jemez continued		4%	Flows > 200 cfs at Jemez River near Jemez
San Felipe to Albuquerque	Yes	340%	North floodway channel near Alameda
Albuquerque to Bernardo	Yes	40%	Rio Puerco near Bernardo
Bernardo to San Acacia	No		
San Acacia to San Marcial	No		
San Marcial to below Elephant Butte	No		
Below Elephant Butte to Caballo	Yes	26,000 acres	Multiplied by average of EB and Caballo precipitation values (L/T)

2.2.3.5   Reservoir Behavior

Section 2.2.3.1.2 and Table 2-5 give an overview of the characteristics of the

major reservoirs within the model extent, and Equation 2-4 outlines the governing mass

balance equation for reservoirs. Section 2.2.3.2 discusses how the evaporation term is

calculated for the reservoirs. This section will consider the leakage terms, the

precipitation terms, and the inflow and outflow terms for the seven modeled reservoirs.

2.2.3.5.1   Reservoir Groundwater Leakage

Groundwater flow into Elephant Butte Reservoir is modeled from the Socorro Basin

groundwater system. See Section 3.4.3. Reservoir leakage is modeled for Heron,

Cochiti, and Jemez reservoirs. Leakage from Heron is modeled according to URGWOM

(USACE et al. 2002) methodology.

$$Q_{gw}^{Heron} = (z^{Heron,m} - 7100\,ft) * 0.2134\frac{ft^2}{s} + 0.76\frac{ft^3}{s} \qquad (2\text{-}14)$$

where

Q_{gw}^{Heron} =   groundwater leakage out of Heron Reservoir [L^3/T].

$z^{Heron,m}$ =   the greater of 7,100 feet or the stage of Heron in feet for month m [L].

Reservoir leakage from Cochiti and Jemez reservoirs are calculated as a function of

reservoir stage and underlying aquifer head as described in Chapter 3.

2.2.3.5.2   Reservoir Precipitation

Reservoir precipitation gains for all reservoirs are calculated as the measured

precipitation depth at a given reservoir in a given timestep multiplied by the reservoir

area in that timestep. The precipitation gains go directly into storage in the given reservoir.

$$Q_{precip}^{r} = P^{r,m} * A^{r,m} * (1 - \text{cov}^{r,m})$$
(2-15)

where

Q_{precip}^{r} = precipitation gains to reservoir r as defined in equation 4 [L^3/T]

$P^{r,m}$ = precipitation rate measured at reservoir r during month m [L/T]

$A^{r,m}$ = the area of reservoir r during month m [L^2]

$\text{cov}^{r,m}$ = percent of reservoir r covered by ice during month m [%]

As discussed in Section 2.2.3.2.5, reservoir areas ($A^{r,m}$) are calculated based on storage volume in the reservoir using EAC relationships specific to each reservoir (tables from Roberta Ball, USACE personal communication 2003). Ice cover on a given reservoir ($\text{cov}^{r,m}$) is a historically measured value, taken from the daily URGWOM data set and averaged to monthly. For scenario evaluation runs, the ice cover is calculated using a simple regression relationship to average temperature during the previous month.

2.2.3.5.3 Reservoir Surface Water Inflows and Releases

Inflows to El Vado from Heron and Abiquiu from the Chama are set to appropriate gage data for the calibration period, and modeled for validation and scenario runs. Inflows to Heron from the SJC diversion tunnel (see Section 2.2.2), El Vado from the Rio Chama, Cochiti from the Rio Grande, Jemez Reservoir from the Jemez River, and Elephant Butte and Caballo reservoirs from the Rio Grande are modeled based on reach behavior between the nearest upstream gage and the reservoir. If the nearest upstream gage is a calibration gage (Table 2-2), it is set to observed values for the historic

calibration period, and modeled values for validation and scenario evaluation. Input gages (Table 2-1) are set to observed values for all periods, with scenario values from a reshuffle of historic data as described in Section 4.2.2.1. Reservoir inflows from modeled but ungaged reaches are calculated within the model for all periods. Ungaged inflows were added to Heron and Abiquiu reservoirs for calibration purposes as discussed in Section 2.2.3.4.4. In addition to modeled or gaged reservoir inflows, an error inflow (positive or negative at each timestep but net zero over time after calibration) is added to the reservoirs at each calibration timestep to force the modeled storage to observed storage. This error term is added to the reservoir to avoid compounding errors and maintain reservoir storage at historic observed levels during the calibration period. Reservoir releases for the 1975–1999 calibration period are set to observed historic releases. Reservoir releases for the validation and scenario evaluation periods are modeled using reservoir operation rules. The seven major reservoirs within the model extent are operated according to a complex set of legal and physical constraints with a broad range of objectives including interstate compact delivery requirements, downstream flood control, storage for agricultural and municipal demand, electric generation, and minimum stream flow. The full extent of operational requirements is represented in URGWOM. Predicted behavior of reservoirs under specific hydrologic scenarios by URGWOM was used to develop a simplified set of rules for operations. The reservoir operations rules that determine releases in the validation and scenario evaluation periods are summarized by reservoir in the next seven subsections.

2.2.3.5.3.1   Heron Reservoir Release Rules

Heron Reservoir is operated by the United States Bureau of Reclamation to store San

Juan Chama (SJC) water diverted from the Colorado river basin into the Rio Grande

Basin (see Section 2.2.2) for use by entities with contracts to the water. There are

currently 17 contractors with rights to almost all 96,200 AF of annual allocation of SJC

water (USDoI-BoR 2006). For simplicity, the URGWOM planning run and the monthly

model consider three of the contractors specifically: the City of Albuquerque, with annual

rights to 48,200 AF; the MRGCD, with annual rights to 20,900 AF; and the Cochiti

Recreation Pool, with annual rights up to 5,000 AF. All other contractors are lumped into

a "combined" contractor account with annual rights to 21,100 AF. The final 1,000 AF is

unallocated water reserved for future Native American water rights settlements and not

considered in the model. In January of each year, the contractor allocation of SJC water

in Heron available for use in that year is set to the annual right. Any amount not used by

the end of the year reverts to the general pool from which the allocations are reset at the

beginning of the next year. In practice, to avoid a dramatic release of unused contractor

water from Heron at the end of the year, there is some flexibility in release date granted

to the contractors to allow releases of the previous year's water in the first few months of

the next year. In simple terms then, Heron is modeled to pass through all native water,

and release SJC water based on modeled requests from contractors up to their annual

allocation. The legal framework of SJC operations mean that evaporative losses are not

charged to a given contractor, so the annual allocation of water is available to the

contractor at any time in the year. In other reservoirs where the contractors may be

allowed to store SJC water, the water is subject to evaporative losses. The result of this is that contractors are assumed to prefer to leave their allocation of water in Heron until they have use for it downstream, only moving it into downstream storage to avoid losing the water to the general pool at the end of the year.

2.2.3.5.3.2   El Vado Reservoir Release Rules

El Vado Reservoir is operated by the Middle Rio Grande Conservancy District (MRGCD) primarily to store native spring runoff to augment irrigation supplies later in the season when natural flows are low. The priority of surface water rights in New Mexico, as in most of the west is determined by the date of first beneficial use (e.g. Clark 1987). As a result, the native rights in the Rio Grande are the most senior in the basin, superseding all other rights and claims. The irrigation served by the MRGCD includes almost 9000 acres of native American lands with rights that are prior and paramount to all other irrigation rights[4]. Article VII of the Rio Grande compact prohibits additions to non prior and paramount native storage in El Vado if the total project water[5] stored in Elephant Butte and Caballo is less than 400,000 AF. MRGCD can also store its SJC water in El Vado, and lease space for storage of SJC water to other contractors. For modeling purposes, when irrigation demands below Cochiti are satisfied by Rio Grande flows, El Vado is operated to capture all native inflows that are physically and legally allowed, less a minimum release to irrigate approximately 5000 acres of agricultural

---

[4] As a rule of thumb, each acre of irrigated agriculture requires 3 feet of water per year, or 3 acre feet per acre.

[5] Project water in Elephant Butte and Caballo is all water in the reservoirs, less any SJC water in Elephant Butte for recreation pool purposes, and less any credit water from New Mexico or Colorado deliveries to Elephant Butte in excess of legal requirements. It is basically required delivery water from New Mexico.

lands (see Table 2-10) along the Chama. If Rio Grande flows are not sufficient to cover irrigation demands below Cochiti, native water is released from El Vado if available to satisfy those demands. If native water is insufficient, MRGCD-owned SJC water is released, and when that is gone also MRGCD calls for SJC releases directly from Heron Reservoir. Any MRGCD SJC allocation remaining in Heron at the end of the year is moved to El Vado. All releases of SJC water from Heron not intended for storage in El Vado are passed through. Combined SJC contractor storage in El Vado is allowed as a user input to the model.

2.2.3.5.3.3   Abiquiu Reservoir Release Rules

Abiquiu Reservoir is operated by the United States Army Corps of Engineers (USACE) primarily as a flood control reservoir, though storage of SJC water, primarily by Albuquerque, has become a significant part of operations. Native water is stored in Abiquiu only temporarily to prevent flows downstream from exceeding 1,800 cfs, 3,000 cfs, and 10,000 cfs below the reservoir, at the confluence with the Ojo Caliente, and at the confluence with the Rio Grande respectively. Stored native flood water is released as quickly as possible within the maximum flows listed above, with one exception called carryover storage. To ensure that flood waters that would have been largely unused had they not been stored are not used to supplement irrigation, if flows in the Rio Grande at Otowi are less than 1,500 cfs at any point after July 1 in an irrigation season, then any flood water stored during that irrigation season is delivered downstream after the irrigation season is over. For modeling purposes, native water is not stored except for flood control purposes, and released downstream as soon as possible within the

constraints of carryover storage. There is some discussion of native water storage at Abiquiu for stream augmentation purposes in the future, and this option is allowed as a user input. The model allows Albuquerque, MRGCD, and the combined contractor to store 130,000 AF, 2,000 AF, and 11,000 AF respectively in Abiquiu based on URGWOM values (Marc Sidlow, USACE personal communication 2006). This storage space is used by the contractors as available to avoid losses of allocated water in Heron at the beginning of each new year, and vacated first by the contractors when there is need for it downstream.

2.2.3.5.3.4   Cochiti Reservoir Release Rules

Cochiti Reservoir, like Abiquiu upstream, is operated by the USACE primarily as a flood control reservoir. The only native storage allowed in Cochiti is native flood control storage to limit Rio Grande flows between Cochiti and Elephant Butte reservoirs to a maximum of 7,000 cfs. This storage is temporary and evacuated as quickly as possible subject to the same carryover storage requirements described for Abiquiu reservoir in Section 2.2.3.5.3.3. The only SJC storage allowed in Cochiti is that amount necessary to maintain approximately 1,200 acres of reservoir area for recreation purposes. The 5,000 AF/yr SJC allocation to the Cochiti Recreation Pool is used to offset evaporative losses to the recreation pool in Cochiti. Additional storage is disallowed in Cochiti in part because large storage volumes in the reservoir lead to high leakage with adverse consequences to agricultural lands downstream of the dam (e.g., Smith 2001).

2.2.3.5.3.5   Jemez Reservoir Release Rules

Jemez Reservoir, like Abiquiu and Cochiti, is operated by the USACE primarily for flood control. The reservoir also acts as a sediment barrier to prevent sediment from discharging to the Rio Grande. For model purposes, the only storage allowed in Jemez is native flood control to aid in maintaining Rio Grande flows between Cochiti and Elephant Butte from exceeding 7,000 cfs. Flood storage in Jemez is subject to the same carryover storage requirements described for Abiquiu reservoir in Section 2.2.3.5.3.3.

2.2.3.5.3.6   Elephant Butte Reservoir Release Rules

Elephant Butte Reservoir is operated by the Elephant Butte Irrigation District (EBID) to store water delivered from New Mexico to Texas under the requirements of the Rio Grande compact. The water is released for irrigation in southern New Mexico and western Texas. The water released from Elephant Butte (and then Caballo) is consumed outside of the model boundary according to rules not included in the model. Elephant Butte reservoir rules are limited to flood control and a target release table. The available water up to the target value is released for each month. Available water includes water in the reservoir less SJC and New Mexico or Colorado credit water. (Water delivered to Elephant Butte from upstream in excess of contract obligation. See Section 2.2.3.5.3.8 below.) The model release targets from Elephant Butte by month are shown in Table 2-17.

*Table 2-17. Target releases used for Elephant Butte and Caballo reservoirs
to determine releases in validation and scenario evaluation modes.*

	Elephant Butte [AF]	Caballo [AF]
January	23600	7500
February	52100	28100
March	82700	109100
April	102700	89500
May	122800	101800
June	133000	128900
July	117500	135100
August	81000	107400
September	42100	67100
October	14600	15500
November	6600	0
December	18300	0
Total	797000	790000

2.2.3.5.3.7   Caballo Reservoir Release Rules

Caballo Reservoir, like the larger Elephant Butte just upstream, is also operated

by EBID. Caballo serves largely as additional storage to moderate releases from

Elephant Butte and add flexibility to EBID operations. There are no irrigation diversions

between Elephant Butte and Caballo, and in many ways, Caballo is simply an extension

of the larger Elephant Butte Reservoir. Release targets used in the model for Caballo

Reservoir are shown in Table 2-17.

2.2.3.5.3.8   Rio Grande Compact Calculations

An agreement between the states of Colorado, New Mexico, and Texas known as

the Rio Grande Compact (Colorado et al. 1938 and 1948), sets out a framework by which

these states share the waters of the basin. In simple terms, stream flows at four locations

in Colorado in a given year determine how much water must legally flow into New

Mexico from Colorado in that year. Similarly, an Otowi Index Supply (OIS) based on

stream flows along the Rio Grande at Otowi Bridge in New Mexico (see Table 2-2) in a

given year determine how much water must be legally delivered to Elephant Butte

reservoir for use in southern New Mexico and Texas in that same year. Changes to

depletions in the Rio Grande system in New Mexico above Otowi must be factored into

the OIS.   Because it has important implications for reservoir operations in New Mexico,

the Rio Grande Compact is included in the model. Three basic pieces of New Mexico

Rio Grande Compact balance calculations are calculations of the OIS, the calculation of

the Elephant Butte Effective Index Supply (EBEIS), and the Actual Elephant Butte

Effective Supply (AEBES). For model purposes, the OIS, which represents the amount

of water that would flow past the Otowi gage under conditions extant in 1929 when

negotiations on the Compact were initiated. The San Juan Chama project, and El Vado

and Abiquiu reservoirs were all constructed after 1929, so their effect is calculated out of

the observed Otowi flows to get the OIS:

$$OIS = Q_{native}^{otowi} + dS_{native}^{res} + E_{native}^{res} \qquad\qquad (2\text{-}16)$$

where

> OIS is Otowi Index Supply [L^3/T].
> Q_{native}^{otowi} is the native (non San Juan Chama) flow past the Otowi gage [L^3/T].
> dS_{native}^{res} is the native water storage change in reservoirs upstream of Otowi [L^3/T].
> E_{native}^{res} is evaporation of native water from reservoirs upstream of Otowi [L^3/T].

For modeling purposes, the reservoir storage change and evaporation terms are for native

water in El Vado or Abiquiu as Heron does not store native water. These definitions are

slight simplifications from the compact definitions which include more complex pre-

reservoir loss calculations than are included in the monthly model.

The OIS determines the amount of water that must be delivered to Elephant Butte,

also called the Elephant Butte Effective Index Supply (EBEIS). The relationship

between OIS and EBEIS is defined in the Rio Grande Compact and shown in Table 2-18.

Table 2-18. Elephant Butte Effective Index Supply (EBEIS)as a function of Otowi Index
Supply (OIS), both in thousands of acre feet per year. Intermediate values found by
linear interpolation. From the Rio Grande Compact (Colorado et al. 1948).

OIS [1000 AF/yr]	EBEIS [1000 AF/yr]	OIS [1000 AF/yr]	EBEIS [1000 AF/yr]	OIS [1000 AF/yr]	EBEIS [1000 AF/yr]	OIS [1000 AF/yr]	EBEIS [1000 AF/yr]	OIS [1000 AF/yr]	EBEIS [1000 AF/yr]
100	57	700	406	1300	897	1900	1495	2500	2095
200	114	800	471	1400	996	2000	1595	2600	2195
300	171	900	542	1500	1095	2100	1695	2700	2295
400	228	1000	621	1600	1195	2200	1795	2800	2395
500	286	1100	707	1700	1295	2300	1895	2900	2495
600	345	1200	800	1800	1395	2400	1995	3000	2595

The Actual Elephant Butte Effective Supply (AEBES), which represents the amount of

water actually delivered by New Mexico to Elephant Butte reservoir is modeled as

$$AEBES = dS_{native}^{EB} + Q^{EB}$$ (2-17)

where
$AEBES$ is the Actual Elephant Butte Effective Supply [L^3/T].
dS_{native}^{EB} is the native water storage change in Elephant Butte reservoir [L^3/T].
Q^{EB} is water released from Elephant Butte reservoir [L^3/T].

Annual change in New Mexico's Rio Grande Compact Balance (NMRGCB) in a given

year is calculated as the difference between EBEIS and AEBES.

$$NMRGCB^t = NMRGCB^{t-1} + (AEBES^t - EBEIS^t) \qquad (2\text{-}18)$$

where

$NMRGCB^{t-1}$ is New Mexico's previous year (t-1) compact balance [L^3].
Superscript t and $(t$-1) represent present and previous year respectively.

The balance runs from year to year, so that in any given year, New Mexico may be in a situation of credit or debit with Texas. Credit is stored as wet water in Elephant Butte, while debit water (which can be thought of as Texas credit water) if available must be held in El Vado until called for by Texas. There are limits to the cumulative credit or debit, and the maximum yearly change allowed. Credit water in Elephant Butte or debit water in El Vado are both subject to evaporative losses. In addition, if useable water is spilled from Elephant Butte or Caballo for flood control purposes, credits and debits are not calculated for that year, debits if any are erased, and credit are reduced by the spill volume. For a more detailed explanation, see the Rio Grande Compact (Colorado et al. 1938 and 1948).

2.2.3.5.4 Reservoir Calibration

A given reservoir, or more commonly a reach-reservoir combination, was calibrated so that the error inflow described in Section 2.2.3.5.3 was net zero for the 1975–1999 calibration period. Heron and Jemez reservoirs were calibrated by adding ungaged inflows to the upstream reach as described in Section 2.2.3.4.4. El Vado Reservoir was calibrated by reducing peak flows at the Rio Chama near La Puente gage. This strategy was pursued after it was observed that from 1975 through 1999, the amount of water that modeled El Vado dynamics suggested should be flowing into the reservoir

was less than the sum of gages below Heron and on the Chama at La Puente. The distribution errors at La Puente gage implied by El Vado behavior is skewed towards an overestimate of inflows as shown in Figure 2-10a, and the skew in the distribution is a strong function of flow rates observed at La Puente gage as shown in Figure 2-10b. This analysis suggests that if Equations 2-10a, 2-14, and 2-15 and associated parameters accurately represent behavior in El Vado Reservoir, the Rio Chama near La Puente gage tends to overestimate large flows. El Vado was calibrated by reducing the portion of La Puente gaged flows greater than 2,000 cfs by 35%. Abiquiu Reservoir was calibrated by adding ungaged inflows to the reservoir. The magnitude and timing of these inflows were calculated as 53% of gaged flows on the Jemez River near Jemez. The Jemez River was chosen as representative of the Jemez mountain tributaries (including the Rio Puerco and Canones drainages) assumed largely responsible for ungaged inflows to Abiquiu Reservoir. Cochiti Reservoir was calibrated with leakage to the groundwater system as described in detail in Sections 3.4.1.2.4.1 and 3.4.1.2.2.1.

2.2.3.6   Calibration and Validation Summary Information

This section serves only to summarize and aggregate information that is scattered throughout this chapter up to this point. As discussed in the previous sections, Equations 2-1 through 2-4 are used to model mass balance between surface water gages along the river, the agricultural conveyance system, and in reservoirs. The mass balances described in each of these spatial units are calibrated to match 1975–1999 observations by adding ungaged surface water inflows, adjusting riparian and agricultural ET, reducing gaged inflows, or changing reservoir leakage to the groundwater system. Table 2-19

Implied La Puente Gage Errors (estimated by El Vado behavior)
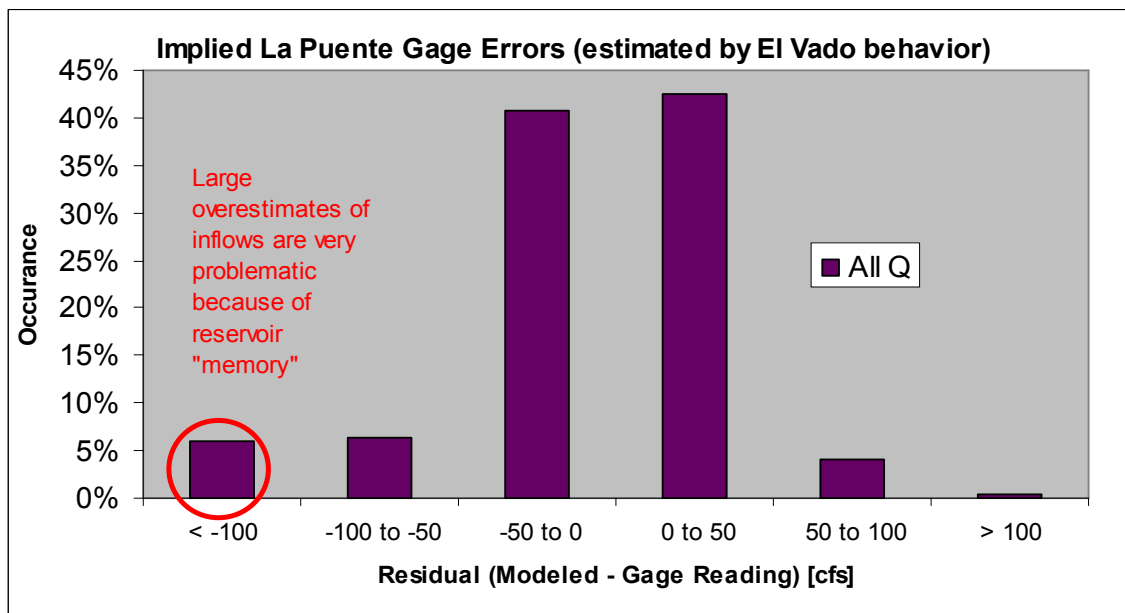
Figure 2-10a. La Puente gage errors implied by El Vado behavior. If El Vado behavior is modeled with inflows from La Puente and Heron, too much water ends up in the reservoir between 1975 and 1999. If we estimate La Puente flows with El Vado historic storage, and compare to actual La Puente flows, we can derive a distribution of gage errors as shown here. The residuals below 100 cfs stand out from an otherwise relatively normal distribution.
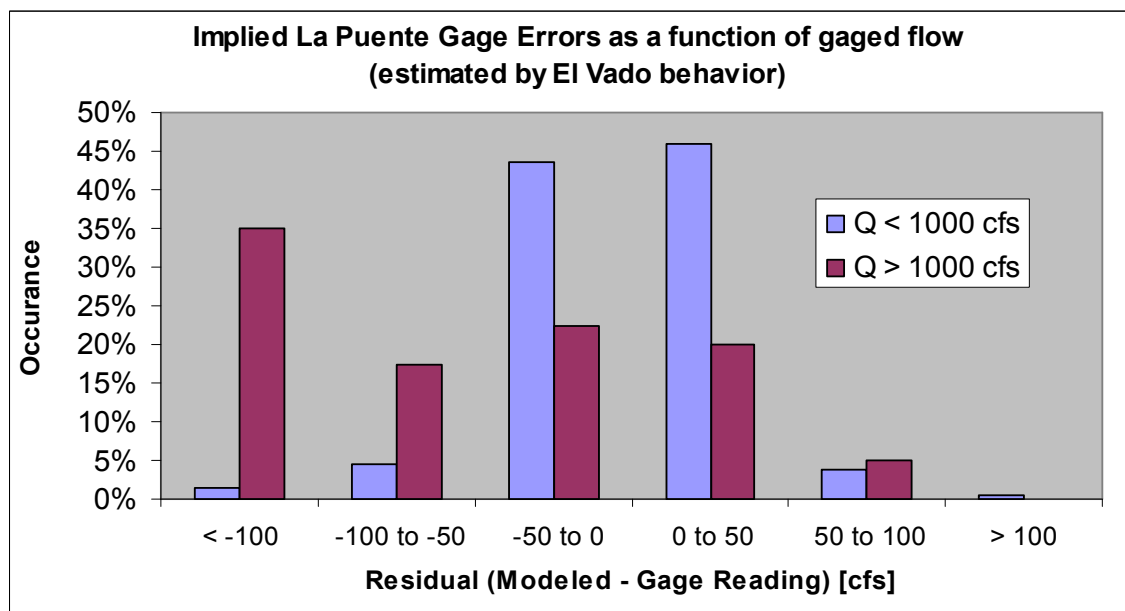
Figure 2-10b. La Puente implied gage errors as a function of gaged flow. The residuals shown in Figure 2-10a are a strong function of measured flows at La Puente. This distribution suggests that high flows at La Puente tend to be overestimated by the gage. summarizes the reach calibration method utilized for each reach and reservoir, and the 25-year average flow represented by the calibration term.

As has been mentioned previously, certain terms that are utilized or calculated in one way during the 1975–1999 calibration period are calculated differently during the 2000–2006 validation period and 2006 forward scenario evaluation period. The most important of these are calibration gages (Table 2-2), which are used to reset the model flows in each reach during calibration, but are only used for comparison purposes in validation, and are not used at all in scenario evaluation. Another major change is in the use of input gages (Table 2-1) and input climate data. These data are historical for the calibration and validation period, and from a reshuffle of historic years for the scenario evaluation period as described in Section 4.2.2.1. Reservoir releases are from historic observations for the calibration period, and based on rules for the validation and scenario evaluation periods. Table 2-20 summarizes variables in the model whose treatment changes in different model periods.

Table 2-19. Calibration summary for reaches and reservoirs in model extent. The type of calibration employed for each reach or reservoir and the total magnitude of the calibration term is included.

Reach or Reservoir	Calibration Term	Average Magnitude 1975-1999 [cfs]
Chama: Willow Creek to Heron	Ungaged SW inflow	26
Chama: Heron to El Vado	Gaged SW reduction	-17
Chama: El Vado to Abiquiu	Ungaged SW inflow	26
Abiquiu Reservoir	Ungaged SW inflow	48
Chama: Abiquiu to Chamita	Ungaged SW inflow	2
Lobatos to Cerro	none	0
Cerro to Taos Junction Bridge	Ungaged SW inflow	42
Taos Junction Bridge to Embudo	Gaged SW reduction	-7
Embudo to Otowi	Ungaged SW inflow	71
Otowi to Cochiti	Reservoir leakage	-31
Cochiti to San Felipe	Ungaged SW inflow	18
Jemez: Jemez Pueblo to Reservoir	Ungaged SW inflow	45
San Felipe to Albuquerque	Ungaged SW inflow	41
Albuquerque to Bernardo	Ungaged SW inflow	24
Bernardo to San Acacia	Riparian ET	-21
San Acacia to San Marcial	Riparian ET	-86
San Marcial to Elephant Butte	Riparian ET	-31
Elephant Butte to Caballo	Ungaged SW inflow	35

Table 2-20. Summary of variables with a change in treatment between calibration (1975–1999) and validation and scenario evaluation periods (2000 forward).

Variable	Calibration	Validation and Scenario Evaluation
Gaged inflows (Table 1)	Observed	Observed for validation, historic reshuffle for scenario evaluation.
Climate data	Observed	Observed for validation, historic reshuffle for scenario evaluation.
Mainstem SW inflow	Observed	Observed at model boundary, inflows from upstream reach outflows otherwise.
Reservoir outflows	Observed	Reservoir release rules.
Reservoir error inflows	Calculated	None.
Reservoir ice cover	Observed	Calculated based on regression to temperature.
Conveyance through flow	Observed	Percent of available.
Surface water diversions	Observed	Modeled based on demand or historic average.
Agricultural acreage	Observed	1999 data for validation, user input from 1999 defaults for scenario evaluation.
Riparian acreage	Observed	1999 data for validation, user input from 1999 defaults for scenario evaluation.
Municipal wastewater	Observed	Function of modeled human water use patterns.

2.3　Surface Water Component Results

2.3.1　Calibration and Validation Residuals

2.3.1.1　Observation Uncertainty in Theory

One way to evaluate model performance is to look at errors, or residuals, at points of historic observation. The points of observation to which we can compare surface water model performance during the calibration period include reservoir storage estimates and stream flows at gages interior to the model and not immediately below a reservoir (the reservoir is calibrated and measured reservoir releases are assumed to be without error). However, the observations themselves are not without error. As documented by the United States Geological Survey (USGS) (e.g. Miller and Stiles, 2006), the historic observations of stream flow contain errors and uncertainties from two main sources:

1.　The stability of the stage-flow relationship at the gage location. The gage measures stream stage, and uses a relationship between stage and flow, derived from field measurements of flow at various stages, to estimate stream flow. However, this relationship can change as the stream bed changes due to sediment or vegetation build up.

2.　The accuracy of the direct measurement of the flow rate. Direct measurement of stream flow is done with velocity and depth measurements, and a myriad of assumptions as to the velocity profile through the two dimensional profile through which flow occurs (e.g. Carter and Davidian, 1968).

By analogy, the historic estimates of reservoir storage contain errors associated with:

1. The stability and accuracy of the stage-storage relationship of the reservoir. This relationship is estimated based on topographic surveys and changes as sediment builds up in the reservoir.

2. The accuracy of the measurement of stage in the reservoir. This is presumably a relatively easy measurement that can be done quite accurately; however, it is a point measurement assumed to represent the entire reservoir, and the sensitivity of the volume estimate to small changes in stage is significant.

Ideally, the model residuals during calibration will be normally distributed about zero, and comparable to the distribution of uncertainty associated with the observations themselves, which should also be distributed normally about zero.

2.3.1.2   Quantification of Observation Uncertainty

The accuracy of the stream gages will be evaluated here from two perspectives, the first will be according to USGS ratings of the gages, and the second will be by comparing the predicted flow at a gage (based on stream stage) on dates when that flow was measured more directly in the field by USGS technicians.   First the USGS ratings: the USGS, in its annual water data reports (e.g. Miller and Stiles, 2006), rates each gage during a given water year as excellent, good, fair, or poor when 95% of gage estimates are thought to be within 5%, 10%, 15%, or more than 15% of the true value respectively (*ibid*). If we assume that when a gage is rated as poor, 95% of the gage estimates are within 50% of the true value, we can assign quantitative 95% confidence intervals to the calibration gages in the model during the 1975-99 historic period. Based on the USGS ratings, the best gage during the calibration period is the Rio Grande gage below Taos

Junction Bridge (see Table 2-2) which was predicted to have been within 9% of the

actual stream flow 95% of the time between 1975 and 1999. The worst gage was the Rio

Grande Floodway gage near San Acacia (see Table 2-2), which 95% of the time was

estimated to be within only 36% of the actual stream flow. Values for calibration gages

are shown in Table 2-21, along with values estimated based on field based flow

measurements as described below.

The distribution of uncertainty associated with stream gages can also be inferred

by comparison of stage based flow estimates to velocity area based flow estimates used to

calibrate the stage-flow relationship at a given gage. (A similar approach could be used

for reservoir storage estimates by comparing the stage based estimate to a more direct

measurement using gravity changes for example; however the author is not aware of any

such direct measurements associated with the reservoirs within the model extent.) Initial

gage error distribution estimates were developed for the 1975–1999 period by plotting

stage versus measured flow for all field measurements at the calibration gage locations

between 1975 and 1999. Error was assumed to be equal to the difference between the

measured values and a single best fit rating curve. This method led to very large errors,

and may have overestimated gage error by not incorporating incremental adjustments to

the rating curve made by USGS technicians through time. A second approach was

developed based on the shift adjustments made to the stage-flow relationship after each

field based flow estimate between 1975 and 1999. The shift adjustment (units of length)

was converted to a volume adjustment with the slope of the best fit stage-flow

relationship at the measured flow. The resulting volume adjustment represents the gage

error associated with that field measurement, assuming the field measurement is completely accurate. This method should represent a low end approximation of the gage error distribution at a given gage, however, as shown in Table 2-21, the resulting 95% confidence intervals implied by the "volume shift method" are far larger for most gages than those implied by the USGS ratings. The two methods agree very well for the gages

Table 2-21. 95% confidence intervals for calibration gages (See Table 2-2). 95% of the time, the gage estimate is expected to be within x% of the true stream flow. For example, the USGS reports suggest that the gage on the Rio Grande at Cerro was within 13% of the actual stream flow 95% of the time, while the volume shift method suggests 14% for the same gage.

	USGS inferred 95% confidence interval	Volume shift method estimated 95% confidence interval
Calibration Gage	1975-99	1975-99
RG Cerro	13%	14%
RG Taos Bridge	9%	10%
RG Embudo	10%	16%
Chama above Abiquiu	11%	31%
Chama Chamita	10%	100%
RG Otowi	10%	20%
RG San Felipe	12%	23%
RG Albuquerque	11%	47%
RG Bernardo	30%	63%
RG San Acacia	36%	204%
RG San Marcial	25%	100%

at Cerro and Taos Bridge, but are disparate for most of the other gage locations. If we again consider (as discussed above) that the uncertainty is a function of the stability of the flow stage relationship and the accuracy of direct measurement, and we assume that the direct measurement accuracy is similar for all stream locations within the model, then it is difficult to believe, as suggested by the USGS inferred ratings, that the gage on the Rio Grande at Albuquerque, a sometimes braided river channel characterized by a sandy,

moving bed can be more accurate than the gage at Cerro. Figure 2-11 shows flow versus

stage relationships for field measurements at each gage between 1975 and 1999 to

reinforce this point. It seems that the volume shift adjustment method may provide more

reliable (though less optimistic) estimates of gage reliability.
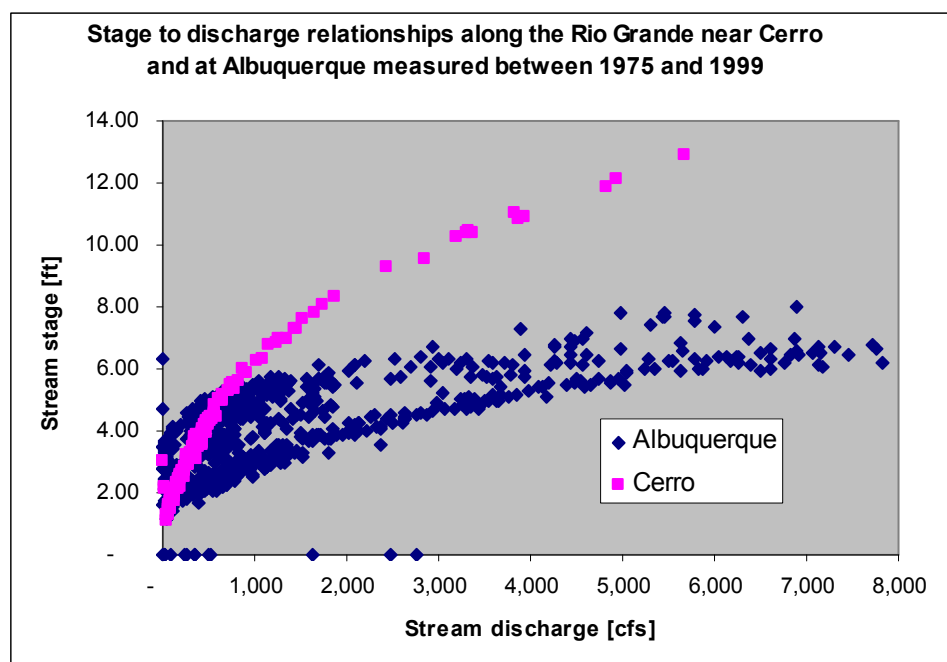
Figure 2-11. Stage and discharge relationships based on 1975-1999 field measurement at gage locations along the Rio Grande near Cerro and Albuquerque (See Table 2-2 for gage information). It is clear that the Albuquerque gage has a less stable relationship between stage and discharge through time than the Cerro gage, and thus is presumably less reliable. The volume shift adjustment method of gage uncertainty predicts this difference, while the USGS gage ratings do not (see Table 2-21).

With the exception of the gage below Taos Junction Bridge, and near Cerro,

which rate as "good" and "fair" respectively, all of the gages in Table 2-21 merit USGS

"poor" ratings for 1975-1999 based on the volume shift adjustment method. This result

is shown graphically in Figure 2-12. The USGS gage network is an impressive resource

that is invaluable to hydrologic science, and this study (among others) would not have

been possible without it. The quantitative meaning associated with the USGS ratings of

their gages may be infrequently scrutinized or relied upon in other calculations, but the

estimates of gage uncertainty published by the USGS seem optimistic. In their defense,

to consider estimates of discharge on a variable and sediment dominated stream as "poor"

if they are not within 15% of the actual value 95% of the time may not be realistic.
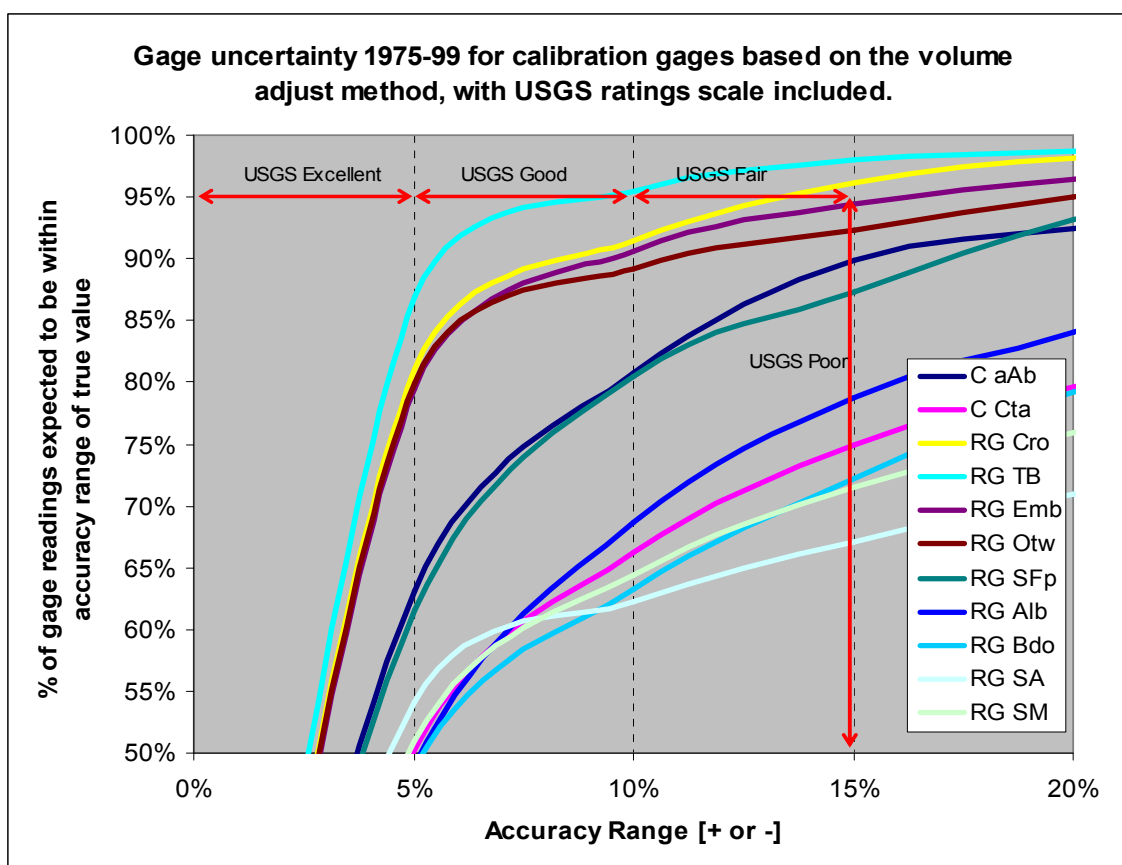
Figure 2-12. Accuracy range of a given gage 1975-99 as a function of the percentage of readings within that range (volume adjust method). The better a gage, the further left it will plot on this figure. According to USGS ratings, the gage below Taos Junction Bridge, and near Cerro, would rate as "good" and "fair" respectively, while all other gages would rate as "poor".

2.3.1.3   Calibration Residuals:

As mentioned previously, the model is calibrated from 1975 to 1999 (see Section 2.2.3.6). The calibration residuals (historic observation less model value) for calibration river gages (Table 2-2), are shown in Figures 2-13 through 2-23. In general, model performance degrades as distance downstream increases. This is a combination of increases in system complexity with distance downstream, and the decreases in gage accuracy seen in Table 2-21 and Figure 2-12 that result from shifting channel geometries associated with sand-dominated riverbeds characteristic of lower reaches. Storage residuals for the seven reservoirs within the model extent for the same time period are shown in Figures 2-24 through 2-30. Figure 2-31 shows the cumulative distribution of the reservoir residuals, and shows clearly that Elephant Butte residuals are the largest, and Jemez residuals the smallest. Figure 2-32 shows the cumulative distribution of the reservoir residuals normalized to the capacity of each reservoir. Caballo reservoir is the most poorly modeled reservoir from a percent of capacity perspective, while the other reservoirs are tightly clustered. Abiquiu residuals are small as a percent of capacity, due to a large, but typically unused, capacity.
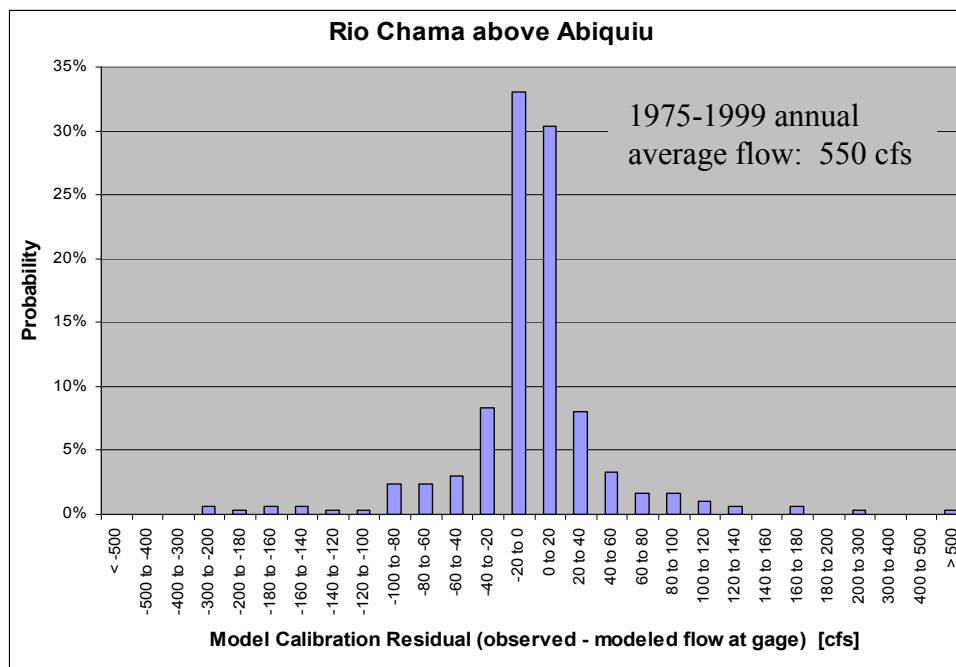
Figure 2-13. Model residual (observed – modeled) distribution for the surface water gage on the Chama above Abiquiu Reservoir (USGS Gage ID 8286500) for 1975–1999 calibration period. Ideally, modeled residuals are normally distributed tightly about zero.
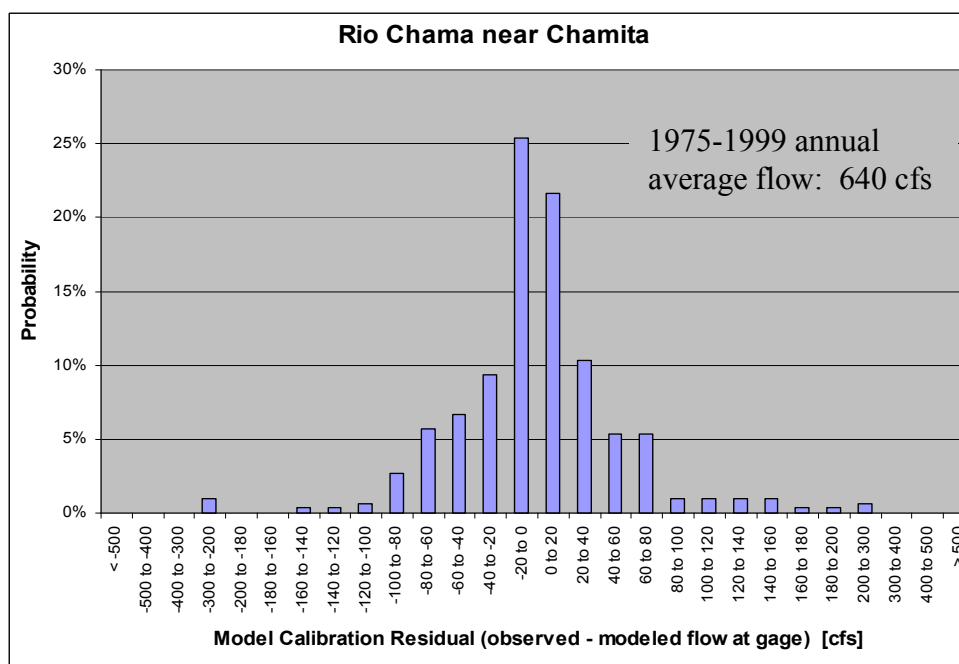
Figure 2-14. Model residual (observed – modeled) distribution for the surface water gage on the Chama near Chamita (USGS Gage ID 8290000) for the 1975–1999 calibration period. Ideally, modeled residuals are normally distributed tightly about zero.
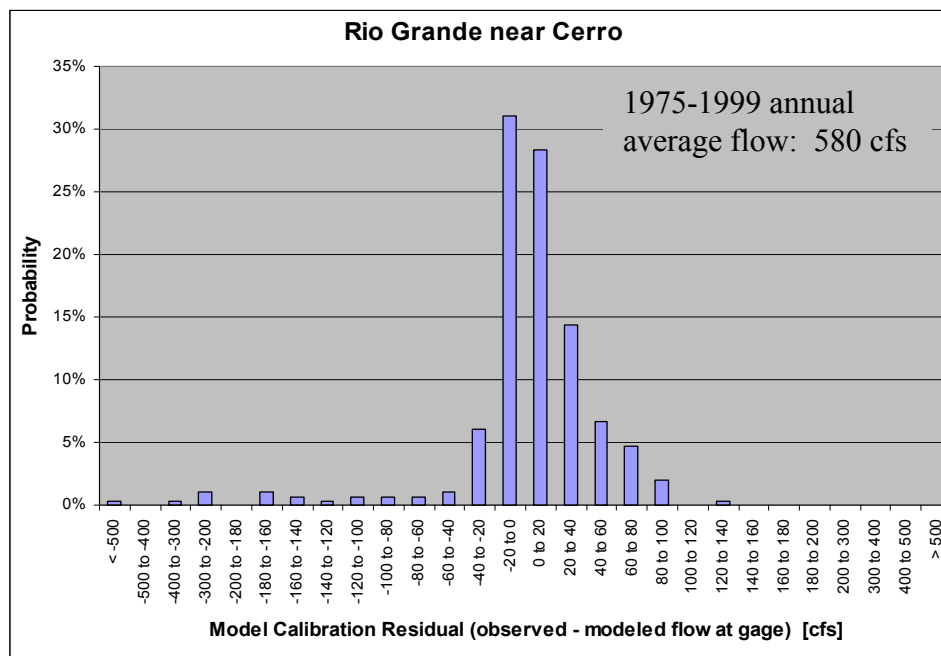
Figure 2-15. Model residual (observed – modeled) distribution for the surface water gage on the Rio Grande near Cerro (USGS Gage ID 8263500) for the 1975–1999 calibration period. Ideally, modeled residuals are normally distributed tightly about zero.
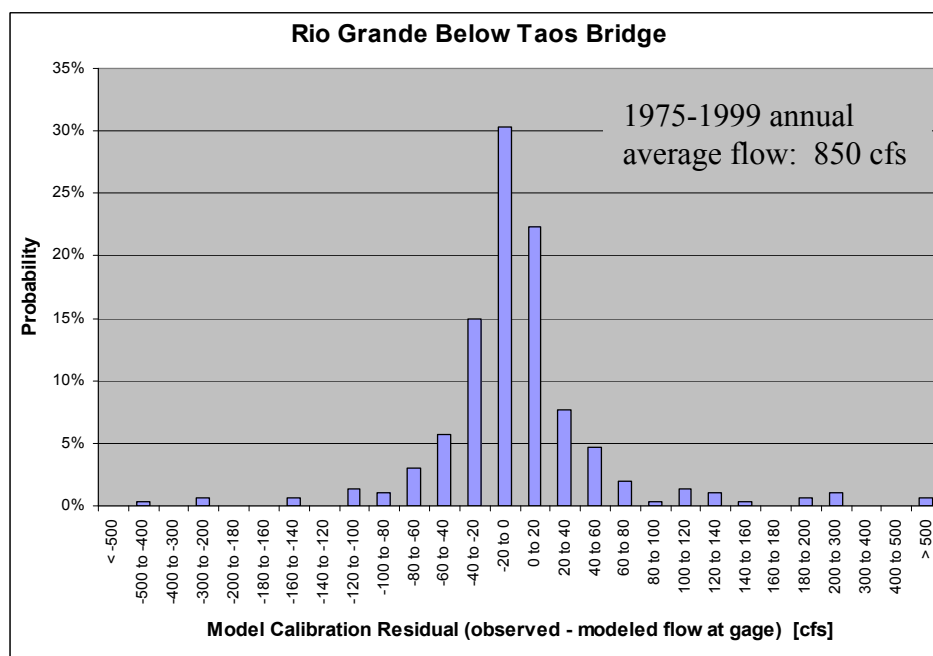
Figure 2-16. Model residual (observed – modeled) distribution for the surface water gage on the Rio Grande below Taos Bridge (USGS Gage ID 8276500) for the 1975–1999 calibration period. Ideally, modeled residuals are normally distributed tightly about zero.
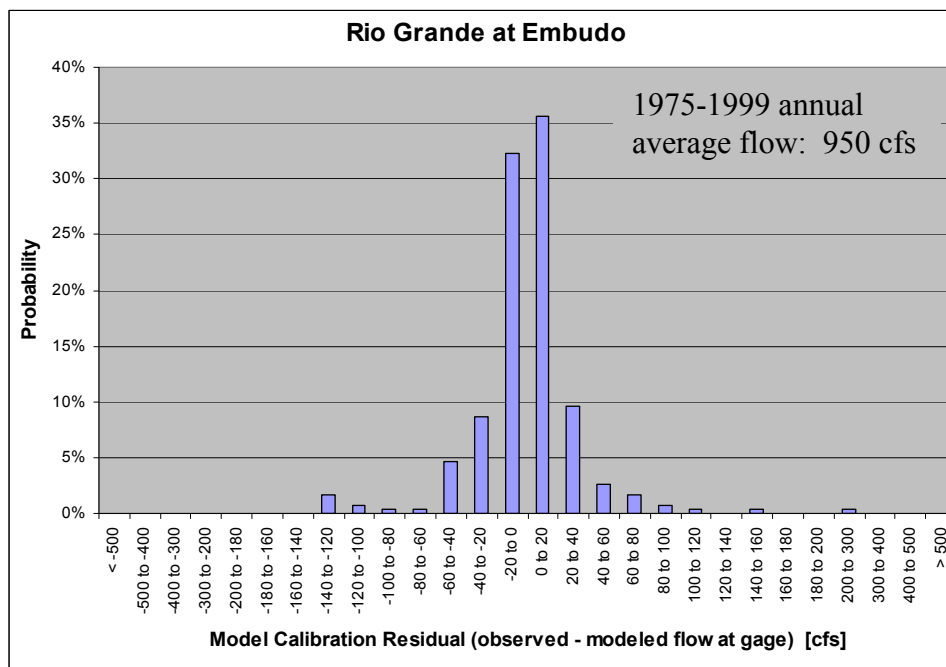
Figure 2-17. Model residual (observed – modeled) distribution for the surface water gage on the Rio Grande at Embudo (USGS Gage ID 8279500) for the 1975–1999 calibration period. Ideally, modeled residuals are normally distributed tightly about zero.
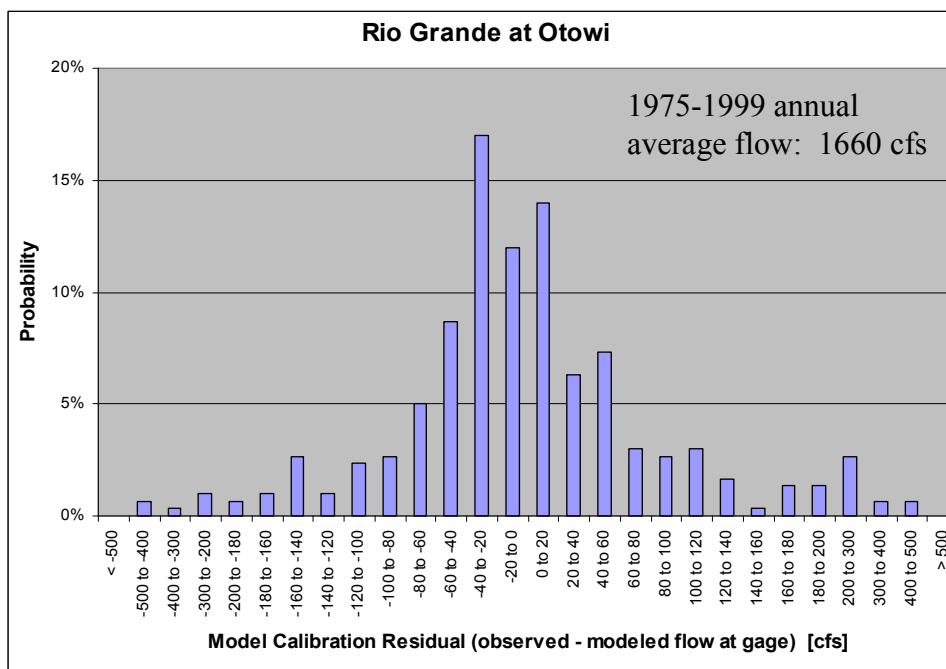
Figure 2-18. Model residual (observed – modeled) distribution for the surface water gage on the Rio Grande at Otowi (USGS Gage ID 8313000) for the 1975–1999 calibration period. Ideally, modeled residuals are normally distributed tightly about zero.
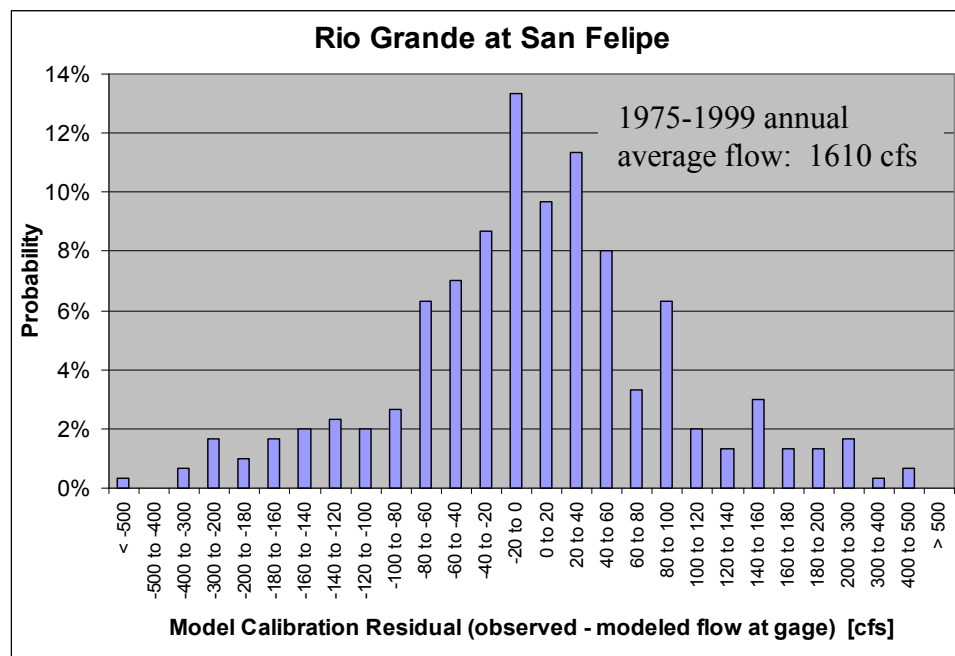
Figure 2-19. Model residual (observed – modeled) distribution for the surface water gage on the Rio Grande at San Felipe (USGS Gage ID 8319000) for the 1975–1999 calibration period. Ideally, modeled residuals are normally distributed tightly about zero.
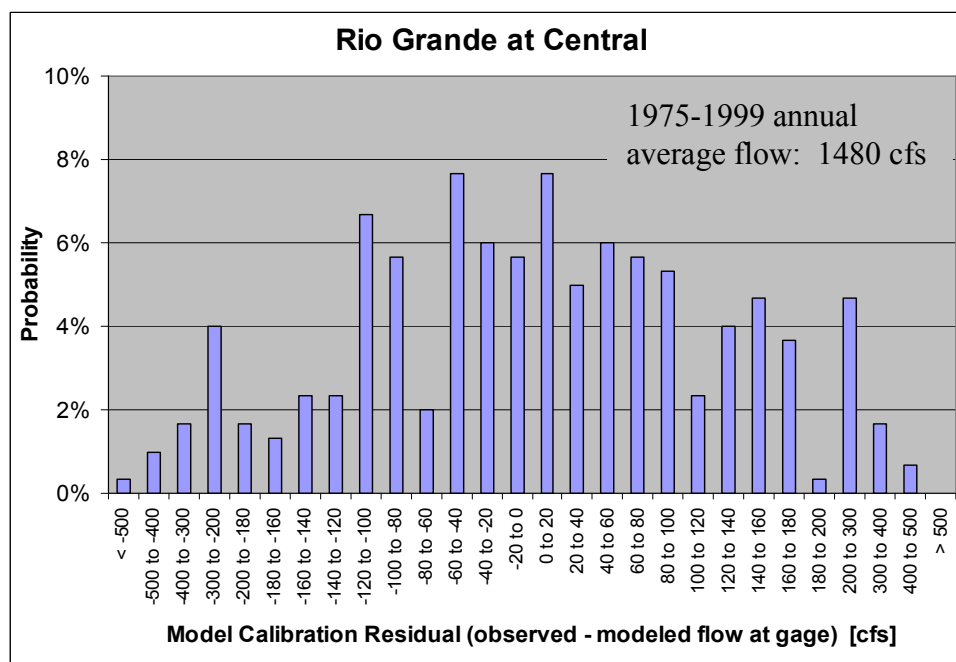
Figure 2-20. Model residual (observed – modeled) distribution for the surface water gage on the Rio Grande in Albuquerque (USGS Gage ID 8330000) for the 1975–1999 calibration period. Ideally, modeled residuals are normally distributed tightly about zero.

117
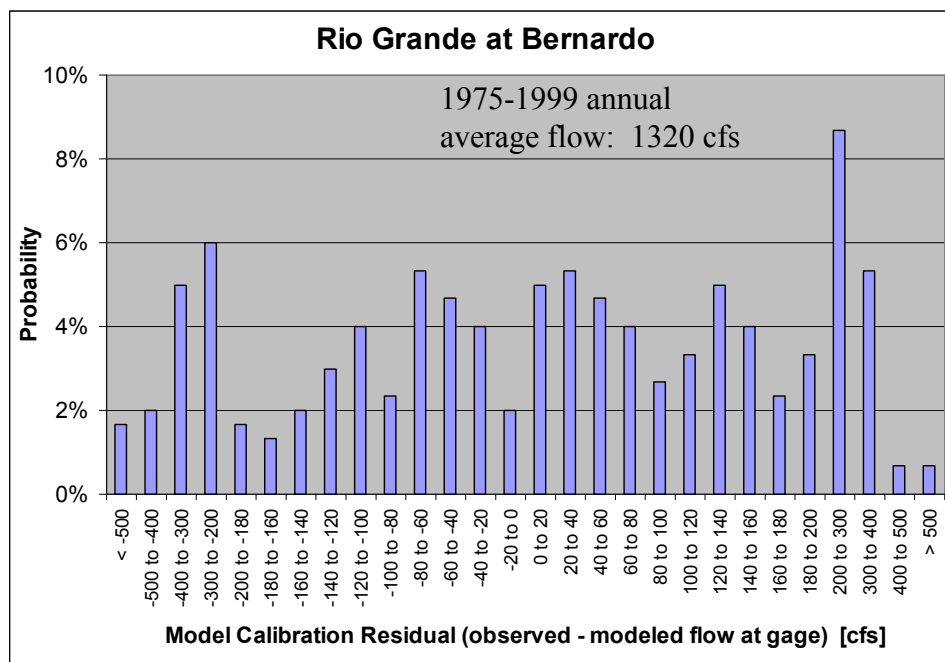
Figure 2-21. Model residual (observed – modeled) distribution for the surface water gage on the Rio Grande floodway at Bernardo (USGS Gage ID 8332010) for 1975–1999 calibration period.Ideally, modeled residuals are normally distributed tightly about zero.
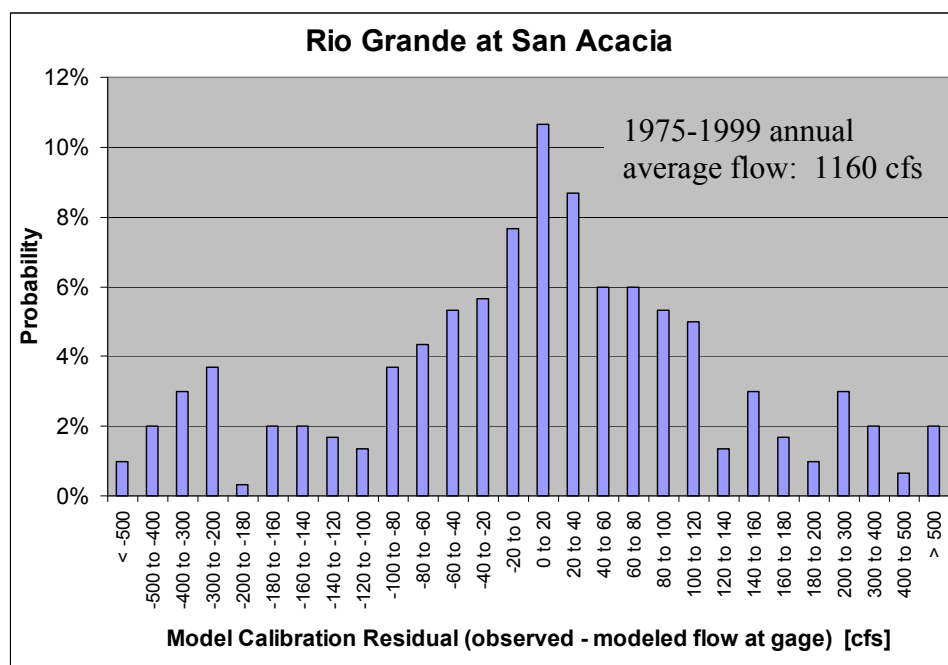
Figure 2-22. Model residual (observed – modeled) distribution for the surface water gage on the Rio Grande at San Acacia (USGS Gage ID 8354900) for the 1975–1999 calibration period. Ideally, modeled residuals are normally distributed tightly about zero.
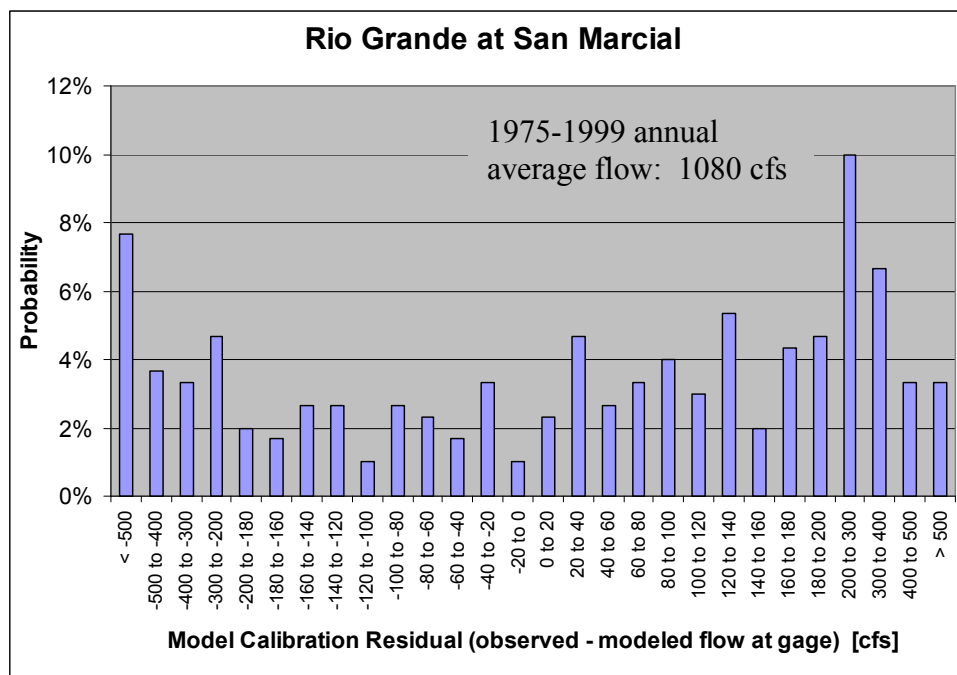
Figure 2-23. Model residual (observed – modeled) distribution for the surface water
gage on the Rio Grande at San Marcial (USGS Gage ID 8358400) for the 1975–1999
calibration period. Ideally, modeled residuals are normally distributed tightly about zero.
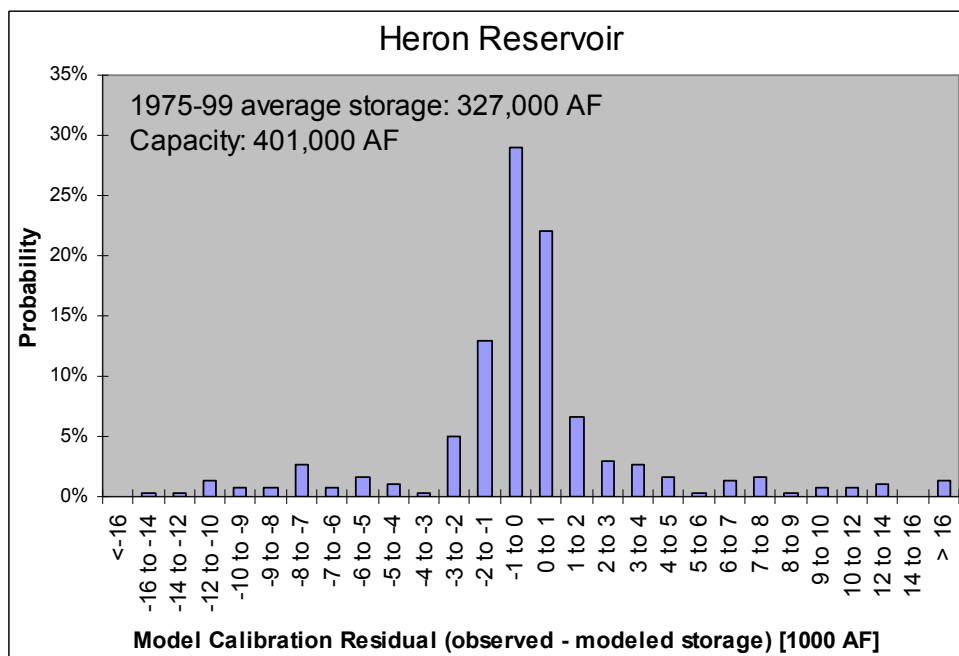
Figure 2-24. Model residual (observed – modeled) distribution
for storage in Heron Reservoir for the 1975–1999 calibration period.
Ideally, modeled residuals are normally distributed tightly about zero.
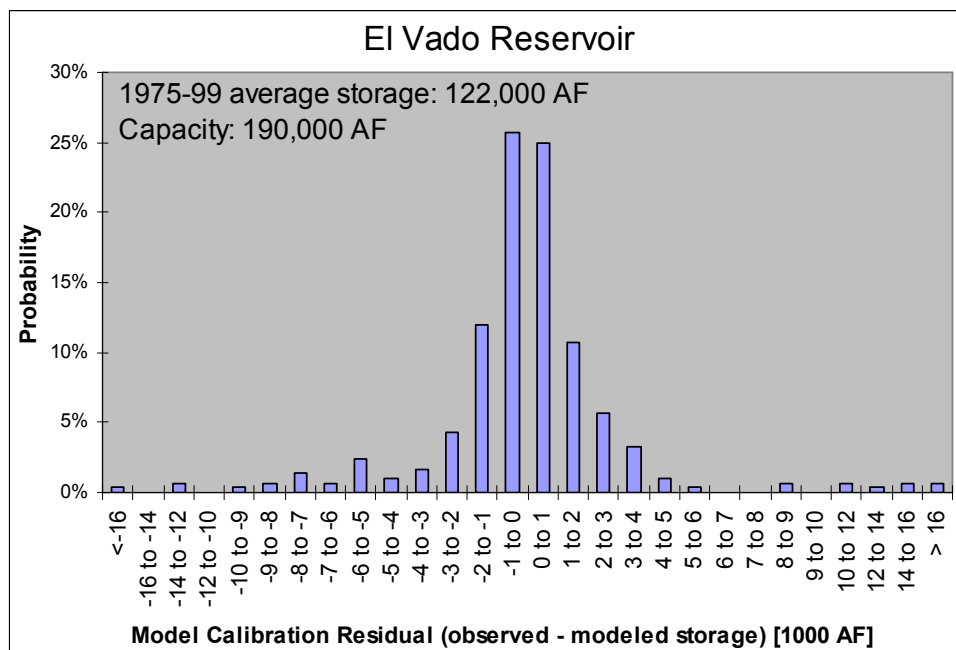
*Figure 2-25. Model residual (observed – modeled) distribution
for storage in El Vado Reservoir for the 1975–1999 calibration period.
Ideally, modeled residuals are normally distributed tightly about zero.*
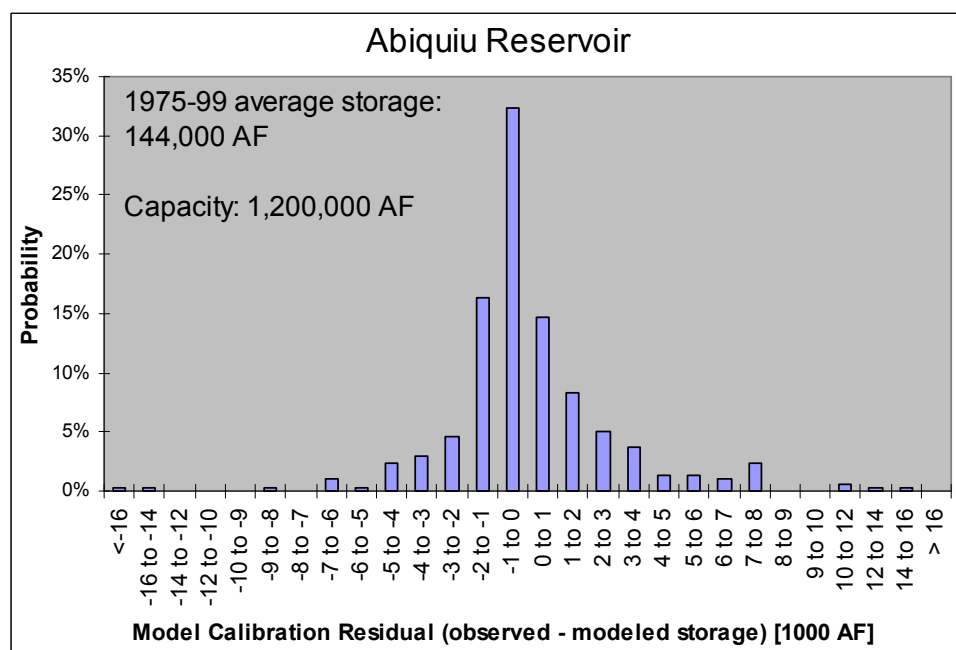
*Figure 2-26. Model residual (observed – modeled) distribution
for storage in Abiquiu Reservoir for the 1975–1999 calibration period.
Ideally, modeled residuals are normally distributed tightly about zero.*
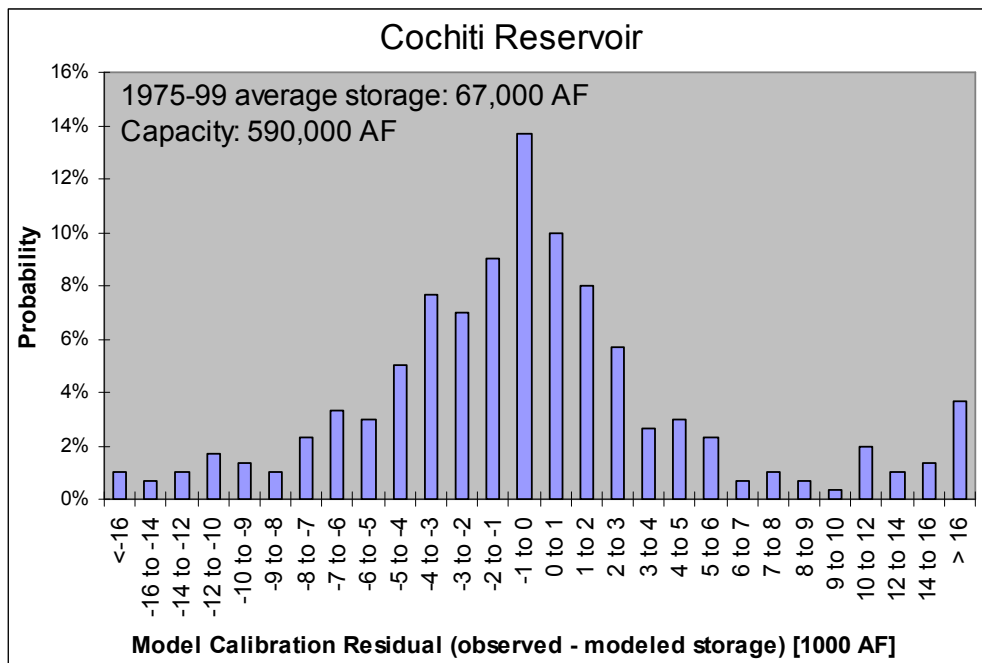
Figure 2-27. Model residual (observed – modeled) distribution
for storage in Cochiti Reservoir for the 1975–1999 calibration period.
Ideally, modeled residuals are normally distributed tightly about zero.
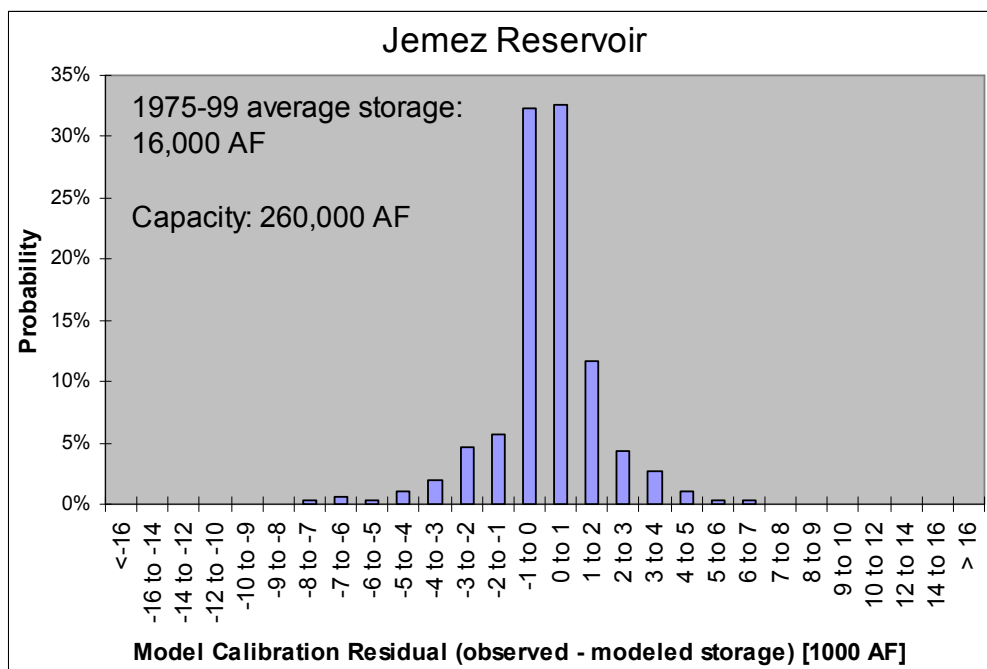
Figure 2-28. Model residual (observed – modeled) distribution for
storage in Jemez Reservoir for the 1975–1999 calibration period.
Ideally, modeled residuals are normally distributed tightly about zero.
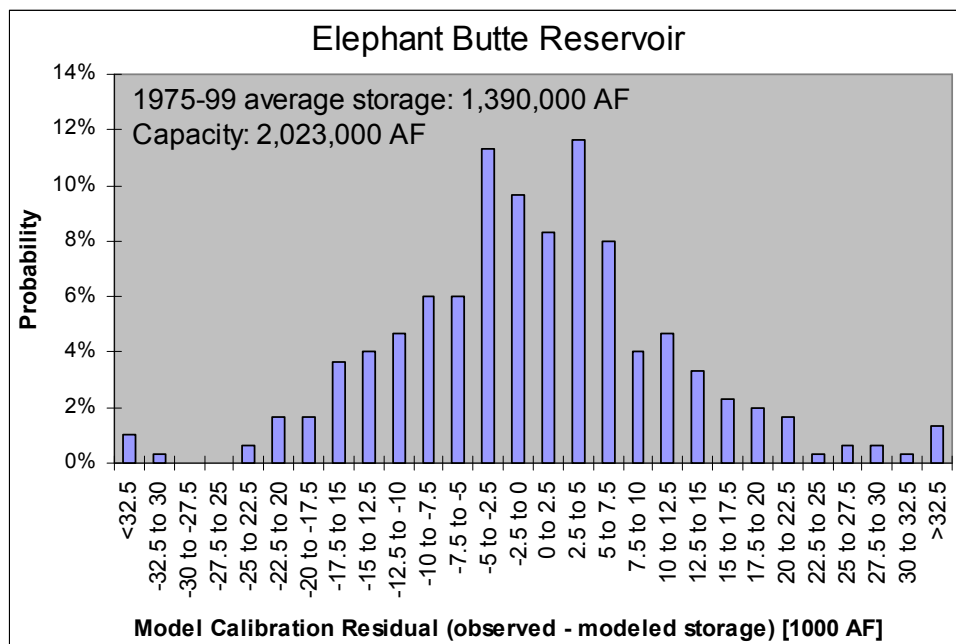
Figure 2-29. Model residual (observed – modeled) distribution for storage in Elephant Butte Reservoir during 1975-99 calibration period. Elephant Butte is a significantly larger reservoir than other modeled reservoirs, thus the different bin ranges (x-axis). Ideally, modeled residuals are normally distributed tightly about zero.
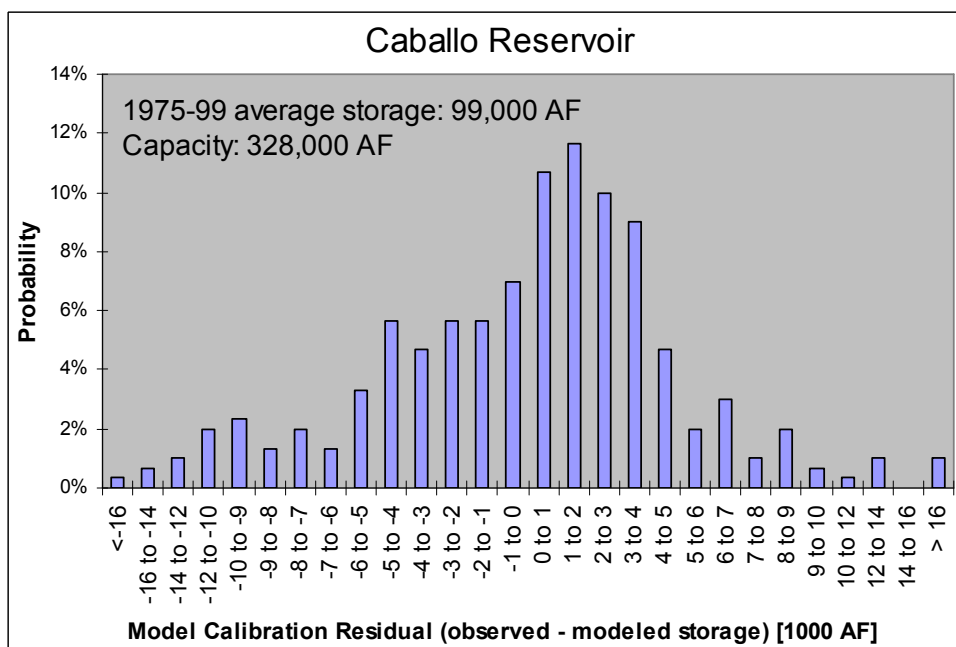
Figure 2-30. Model residual (observed – modeled) distribution for storage in Caballo Butte Reservoir during 1975-99 calibration period. Ideally, modeled residuals are normally distributed tightly about zero.
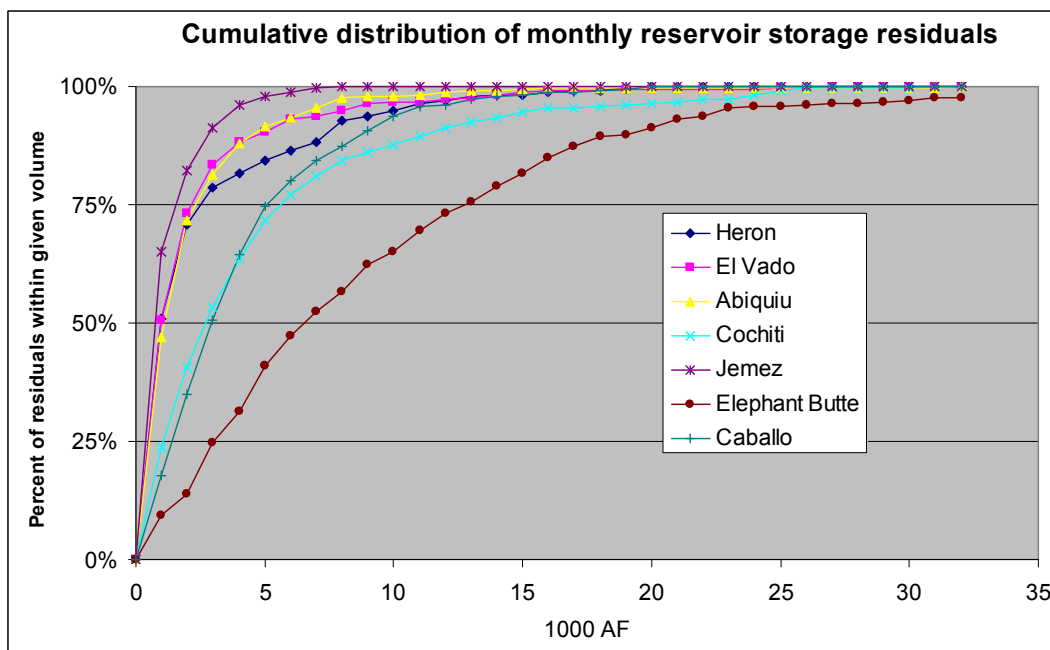
Figure 2-31. Cumulative distribution of monthly reservoir storage residuals shown in Figures 2-24 through 2-30. The graph shows the percent of monthly storage residuals (y-axis) whose absolute value is within a given volume (x-axis).
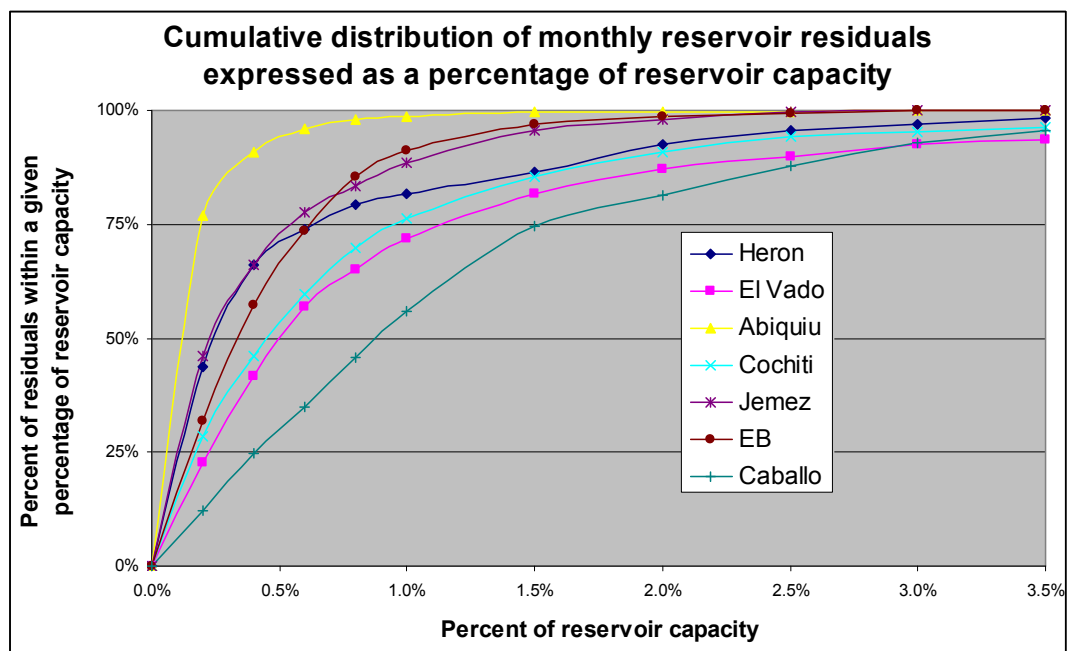
Figure 2-32. Cumulative distribution of monthly reservoir storage residuals normalized to reservoir capacity. The graph shows the percent of monthly storage residuals (y-axis) whose absolute value is within a given percent of the individual reservoir capacity (x-axis).

2.3.1.4 Calibration and Validation Residual Analysis for Stream Flow Observations:

After the 1975-99 calibration period, the model is run in validation mode from 2000 through 2004. In validation mode, input gages (Table 2-1) and climate data are fed with historic observations. Irrigated and riparian acreages are set to 1999 values. River diversions upstream of Cochiti reservoir are set to twice modeled agricultural ET demand, with half of the diversion returning to the river. River diversions downstream of Cochiti are set to monthly average values from 1975-99 up to amount available, and reservoir releases are based on either historic observations or rules, depending on the analysis. Validation results presented first are for historic reservoir releases. Validation residuals are the observed – modeled values at internal observation points during the 2000 to 2004 period. As shown in Figure 2-33, hydrologic conditions during the 2000-2004 validation period were significantly drier than those of the 1975-1999 calibration period, which may lead to worse model performance during the validation period than might be expected from a more average series of years.

Figure 2-34 compares estimated gage uncertainty with calibration and validation residuals (historic observation value less modeled value). Four important results can be drawn from Figure 2-34. First, for most gage locations, the estimated gage uncertainty (left most bar) is comparable to the calibration residuals (middle bar). This suggests, that for the reaches above these gages (recall that during calibration, the flows at interior gages (Table 2-2) are reset to match historic observations), the model is limited most significantly by the quality of the historic observations. Second, in three locations, the calibration residuals are significantly smaller than the estimated gage uncertainty. These
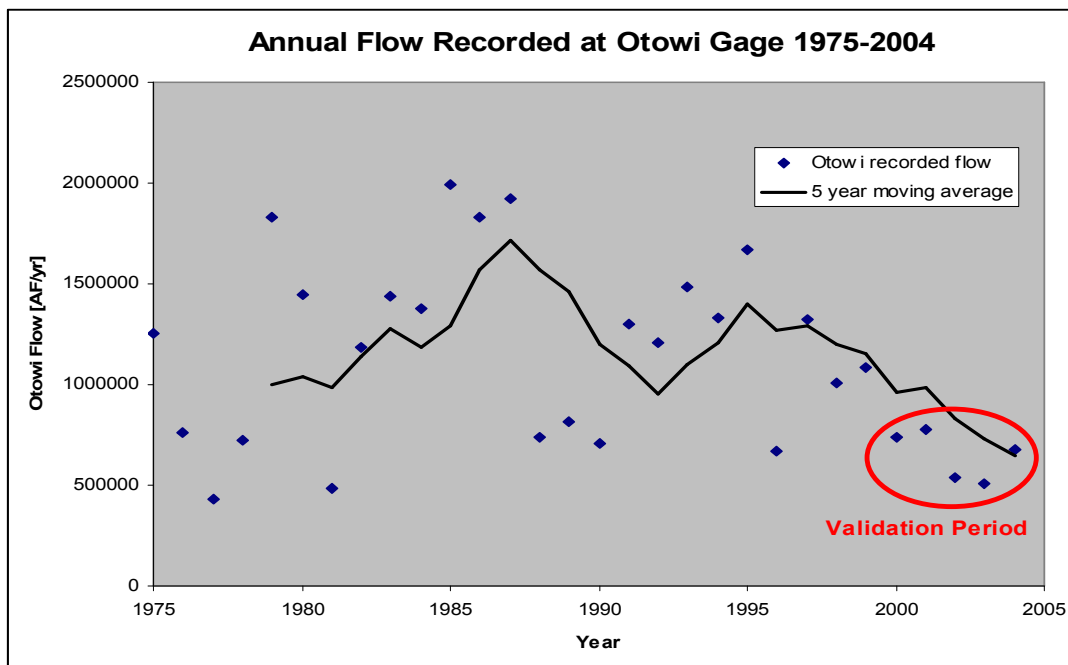
Figure 2-33. Gaged annual flows at Otowi bridge 1975-2004. Total flow during the five year calibration period is less than for any other consecutive five year sequence from 1975 forward.
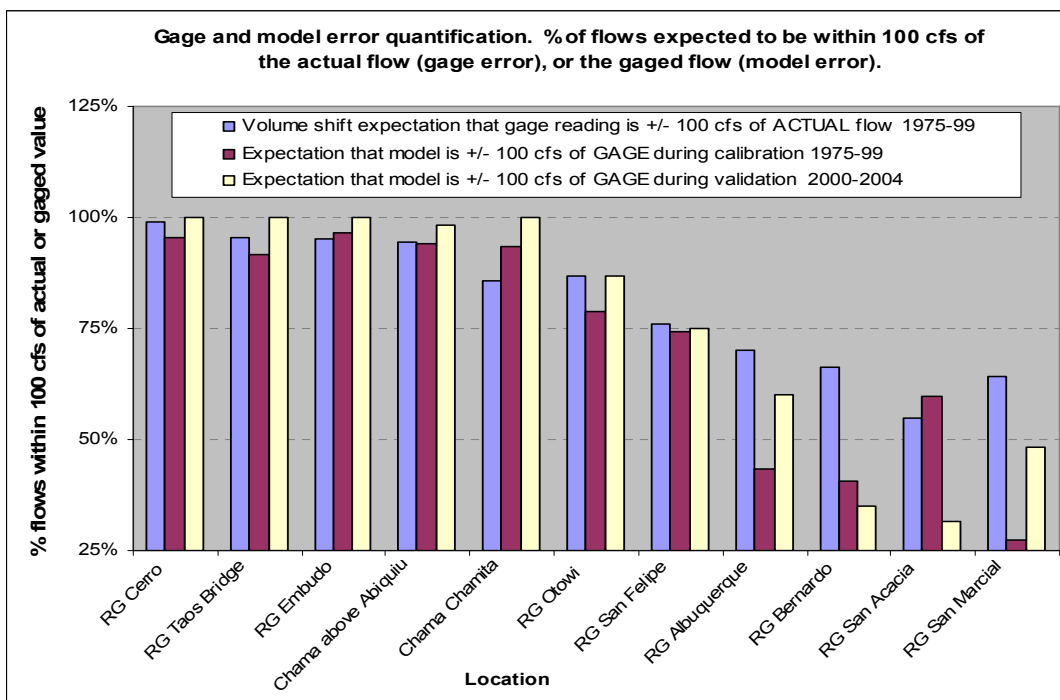
Figure 2-34. Comparison of expected gage accuracy (left bar) to calibration and validation residuals (observed – modeled) for calibration gages.

locations are along the Rio Grande in Albuquerque, near Bernardo, and near San Marcial. In the reaches above these gages, the model could likely be improved without significant improvements to gage data. The reason that the model performance is relatively poor in these reaches may be because the three reaches hold about 80% of the agricultural area and 65% of riparian area contained in the model respectively. The demand in these reaches dominates the mass balance. Future model improvements should start with the agricultural system in these reaches (see also the discussion of model sensitivity to various parameters in Section 2.3.5 below). The third significant result seen in Figure 2-34, is that for all gages above Albuquerque, validation residuals are comparable to calibration residuals and gage uncertainty estimates, suggesting a reasonable model of the physical system. Finally, with the exception of the Bernardo gage, there is significant variation between calibration and validation residuals from Albuquerque down. As described previously (Section 2.2.2 and Table 2-3), water can flow past these points in the river, or in agricultural conveyance structures. The operation of these structures, especially the Low Flow Conveyance Channel (LFCC) (see 2.2.3.4.3) has changed through time since 1975, and one might expect that the model is capturing the overall mass balance, but not the relative amounts of water in the river as compared to the agricultural conveyance system. However, Figure 2-35 shows the river only residuals from Figure 2-34 compared to the total residuals for water moving past the gage locations below Cochiti, and it can be seen that with the exception of San Marcial, the total residuals mimic the qualitative trends seen in the river only residuals. The discrepancies between calibration and validation residuals at Albuquerque, San Acacia, and San

Marcial are likely the result of a combination of gage uncertainty, model error, and an

unrepresentative validation period.
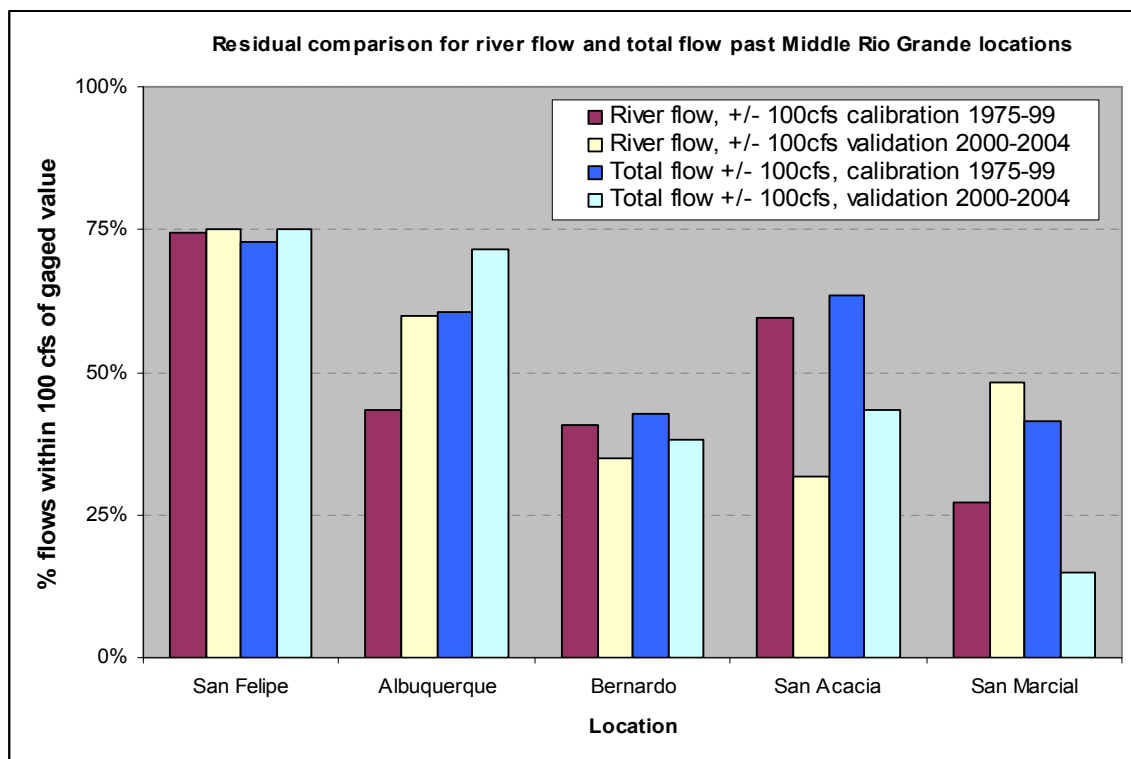
Figure 2-35. Calibration and validation residuals (observed – modeled) for the river only (left 2 bars) and the total river and conveyance system flow for locations with significant non-river flow.

The poorest model performance determined by validation residuals from Figures 2-34

and 2-35 is for total flow past San Marcial, where only 15% of total flows modeled are

within 100 cfs of total flows measured. Figure 2-36 shows the modeled flow and

observed flows at San Marcial from 2000 through 2004. The model consistently

overestimates flows, perhaps due to underestimated losses, gage errors, or significant

flow under the largely dry sandy river sediments. Agricultural diversions may be limited

Modeled and observed total flows past San Marcial during validation period.
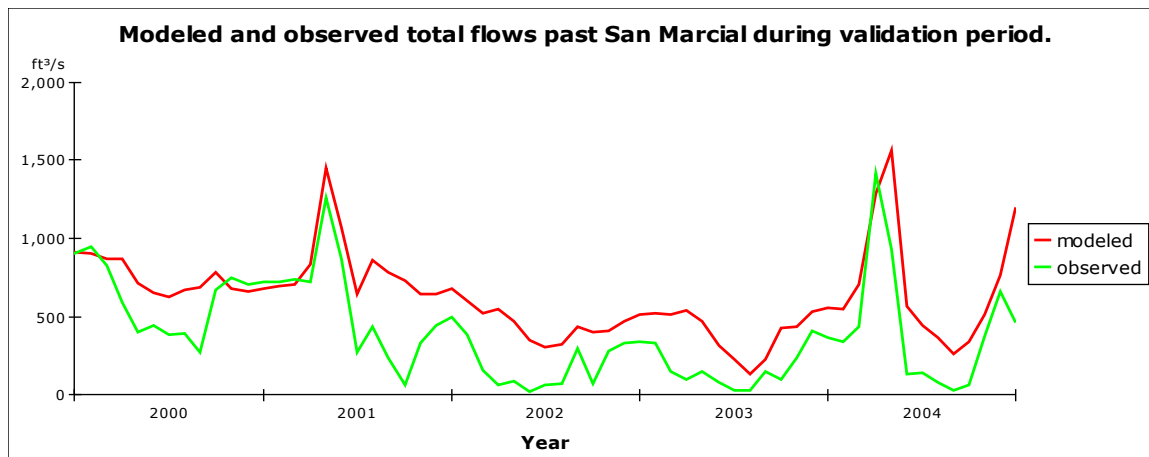
Figure 2-36. *Modeled and observed surface water flows past San Marcial 2000-2004. This is the poorest performing observation point in the validation run with modeled flows within 100 cfs of observed flows only 15% of the time. Even so, system behavior is tracked to a reasonable degree.*

more by water availability in the model than they were in practice. Regardless of the

reason however, the model still tracks the overall system behavior to a reasonable degree,

and a degree that is reasonable for basin scale multi-decadal scenario analysis.

The daily timestep URGWOM (USACE et al. 2002) model was run in validation

mode from below Cochiti reservoir to San Acacia for the 2001 to 2004 period.

URGWOM validation residuals (Wilkins 2006) for this run are compared to equivalent

residuals for the monthly model in Figure 2-37. In general, both models lose accuracy

with distance downstream as would be expected, and lose the most accuracy between

Albuquerque and Bernardo, the longest of the reaches below Cochiti, and a reach with

significant evaporative losses to agricultural and riparian vegetation. The accuracy of the

monthly model decays more rapidly with distance downstream from Cochiti than does

that of URGWOM. Considering the unrepresentative nature (Figure 2-33) of the

relatively short validation period evaluated for Figure 3-32, and gage uncertainties, the

Expectation that the model is within 100 cfs of observed Rio Grande gage flows (2001-2004 validation run with specified Cochiti releases)
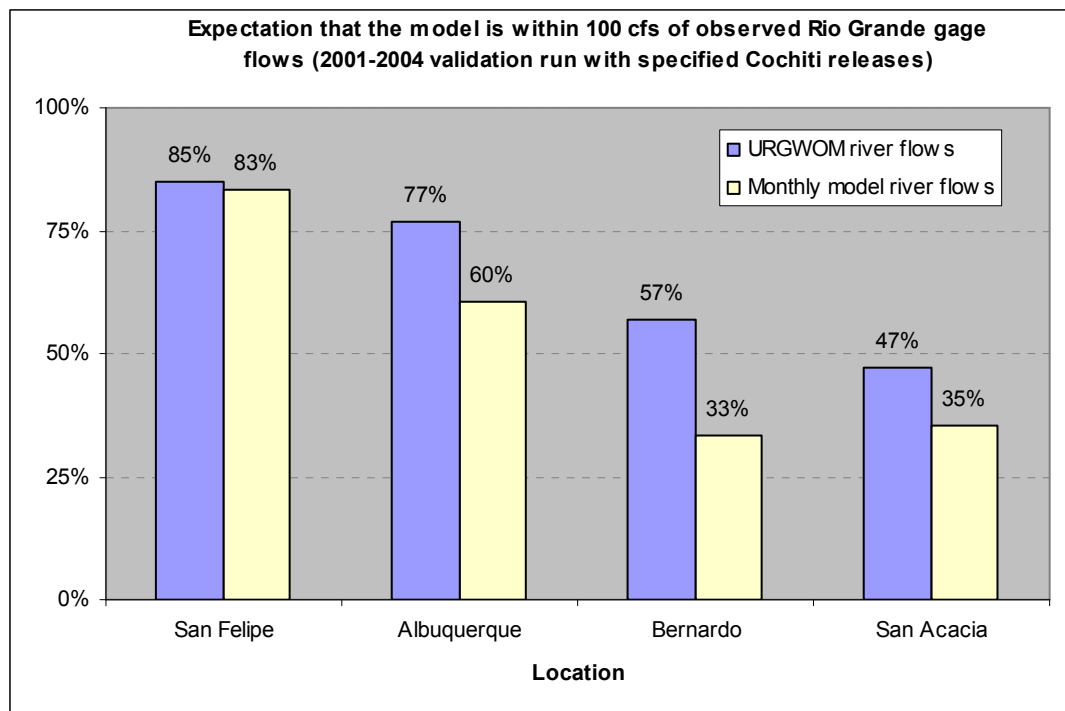
Figure 2-37. Comparison of validation residuals from downstream of Cochiti to San Acacia between 2001 and 2004 for the daily timestep URGWOM, and the monthly model described here.

difference between the monthly model and URGWOM downstream of San Felipe

probably does not constitute grounds for alarm, however the fact that the model tends to

overestimate flows at all gages below Cochiti during the validation period may suggest

that the calibration method of adding ungaged inflows as a function of nearby tributary

gages (Section 2.2.3.4.4) overestimates ungaged inflows during dry periods. The

mechanism for this overestimate is that tributary gages may be a reasonable proxy for

ungaged surface inflows during periods of average or above average precipitation, but

may be poor indicators of local inflow as flows at those gages get closer to base flow.

Alternatively, agricultural losses may be underestimated due to the way the model only

allows a fixed percentage of conveyance flows to be applied to the fields (Section

2.2.3.2.9 and Table 2-4). This possibility is also considered in Section 4.3.5.

To clarify residual discussion, and facilitate comparisons to URGWOM middle

valley residuals, discussion to this point have been for a validation run in which reservoir

releases were set to observed. A validation run more representative of scenario

conditions is one in which reservoir releases are predicted within the model by the rules

described in Section 2.2.3.5.3. In such a case, the model runs with only observed input

flows and climate conditions, representing a scenario condition with known inputs.

Figure 2-38 shows validation residuals at flow observation points for the pure validation

run, and for comparison also includes the validation residuals for the run with observed

reservoir releases (as shown previously in Figure 2-34).

Because there are no reservoirs within the model extent along the Rio Grande

above the Rio Chama, Rio Grande confluence, the residuals at the Rio Grande at Cerro

(RG Cro), Taos Junction Bridge (RG TB), and Embudo (RG Emb) are not affected by

reservoir behavior. The Chama gage above Abiquiu reservoir (C aAb) is below two

modeled reservoirs, the Chama gage near Chamita (C Cta) and Rio Grande gage at Otowi

(RG Otw) are downstream of three modeled reservoirs, and the other calibration locations

shown in Figure 2-38 are downstream of four modeled reservoirs. Clearly the Chama

gages and the Otowi and San Felipe (RG SFp) gages along the Rio Grande are the most

affected by the inability of the model to predict reservoir releases. The gages along the

Rio Grande from Albuquerque (RG Alb) down are essentially unaffected by the different

reservoir releases upstream. This may be a result of the validation period being a dry

period during which the consumptive uses in the middle valley are limited by water in

both model runs, with flows thus reduced to similar levels based on allowable use.

Model errors associated with reservoir releases are discussed in Sections 2.3.1.5 and

2.3.3.
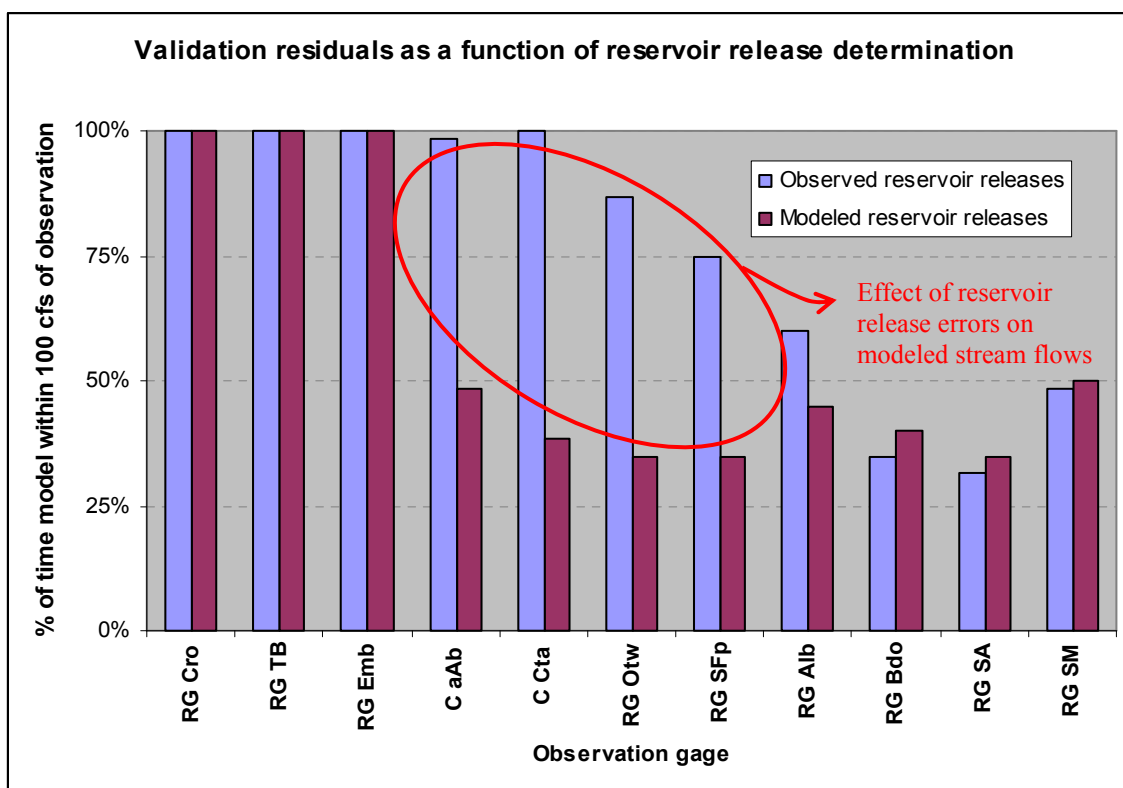
Figure 2-38. Comparison of validation residuals from the monthly model for a 2000-2004 run with observed reservoir releases, and a 2000-2004 run with modeled reservoir releases. Gages located below reservoirs but above the major consumptive use in the middle valley are most affected by errors in modeled reservoir releases.

2.3.1.5 Calibration and Validation Residual Analysis for Reservoir Storage Observations:

Stream flow residuals at a given observation point during the validation period

reflect total model error for all points upstream (to any point where flows are set to

observed) plus observation error at a given timestep. Reservoirs on the other hand are hydrologic memories for inflows and outflows, and thus accumulate upstream error associated with the model through time. For this reason, as described in Sections 2.2.3.5.3 and 2.2.3.5.4, reservoir residuals (distributions shown in Figures 2-24 through 2-30) are added to the reservoirs at each timestep during calibration, essentially as an error inflow (positive or negative) to keep the modeled reservoir storage the same as the observed. During validation however, the residuals are not added back to the reservoir, and as a result errors accumulate, and validation residuals are not a

Reservoir storage residuals
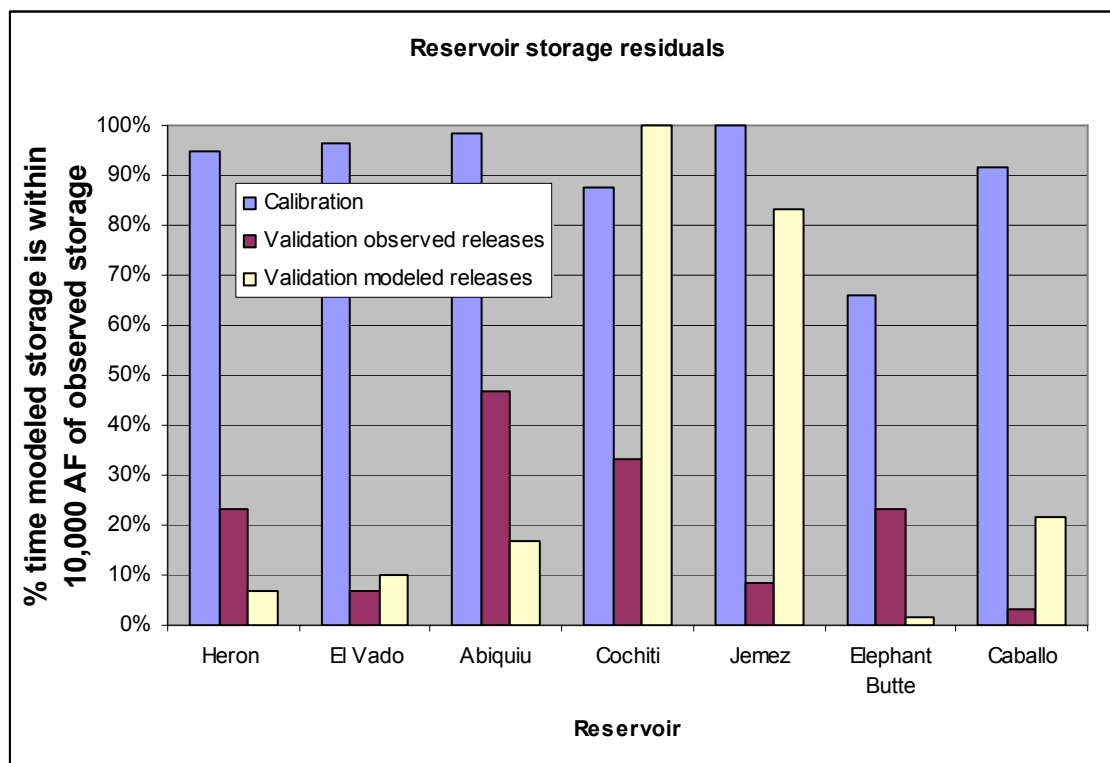
Figure 2-39. Comparison of reservoir storage residuals for the 1975-99 calibration period with those from the 2000-2004 validation run with observed or modeled reservoir releases. Error accumulation in the reservoirs during the validation run limits the usefulness of validation residuals as a quality metric for modeled reservoirs. Model reservoir performance is evaluated in a more meaningful way in Section 2.3.3.

particularly useful metric for quantifying model behavior. Because reservoir storages are arguably the most important observation metric in the system however, calibration and validation residuals for the seven modeled reservoirs are included here in Figure 2-39, but discussion of these residuals will be limited. Heron reservoir is on the model boundary, and thus reservoir inflows are the same in both validation runs resulting in better reservoir history matching when
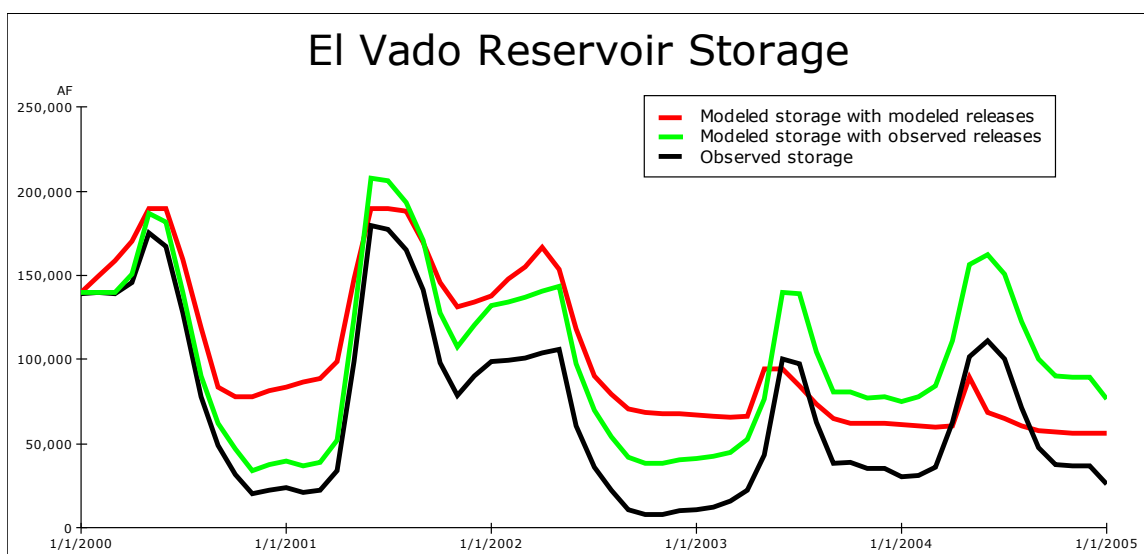
Figure 2-40. El Vado reservoir storage during the 2000-2004 validation period. The model appears to overestimate reservoir inflows or underestimate reservoir losses during validation.

reservoir releases are set to historical. El Vado validation behavior appears to be limited by overestimated inflows or underestimated reservoir losses during the validation period, as shown in Figure 2-40. Inflows are not significantly reduced by the La Puente flow reduction calibration method described in Section 2.2.3.5.4, which results in less than 2000 AF total reduction to LaPuente flows during the validation period. Abiquiu inflows are a strong function of El Vado releases resulting in better reservoir history matching

when reservoir releases are set to historical. Both Cochiti and Jemez reservoirs are

operated primarily as flood control reservoirs (Section 2.2.3.5.3) with target storages, and

thus match observed storages better when releases are modeled and reservoir volume

maintained near the target volume rather than when releases are forced to observed while

inputs determined in the model. As seen in Figure 2-41, Elephant Butte reservoir

behavior is matched well by the model during the validation period when releases are set

to observed values. This is an encouraging result because it suggests that modeled

inflows (determined by overall model behavior upstream, effectively representing overall

model performance) and reservoir dynamics are modeled fairly well. Modeled releases

from Elephant Butte are likely greater than observed releases due to errors in modeling of

the Rio Grande Compact which will be discussed in Section 2.3.4.   Finally, validation

residuals for Caballo reservoir seen in Figure 2-39 are better for modeled releases than

for observed. This is surprising considering Caballo inflows are a strong function of

Elephant Butte releases, and is a perfect example of the relative lack of value associated

with storage residuals as a measure of model quality. Figure 2-42 shows that when

reservoir releases are specified, Caballo reservoir modeled storage values track the

overall observed trend very closely, but are consistently high. This may be partially a

result of occasional but systematic overestimates of ungaged surface water inflows to the

river reach above Caballo (see Section 2.2.3.4.4 for a description of estimates of ungaged

inflows to the river reach between Elephant Butte and Caballo reservoirs). Because of

reservoir memory, the errors are propagated through time resulting in a poor reservoir
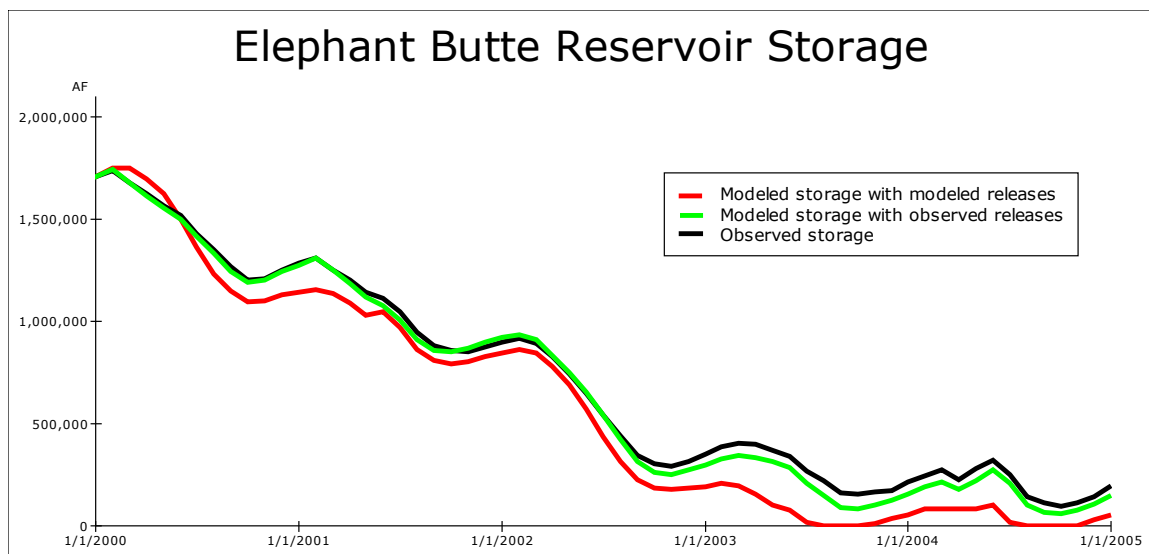
Figure 2-41. Elephant Butte reservoir storage during the 2000-2004 validation period. The model tends to overestimate reservoir releases, but modeled reservoir behavior is very close to observed when reservoir releases are set to observed values. Modeled releases are overestimated due to errors in tracking the Rio Grande compact (see Section 2.3.4).
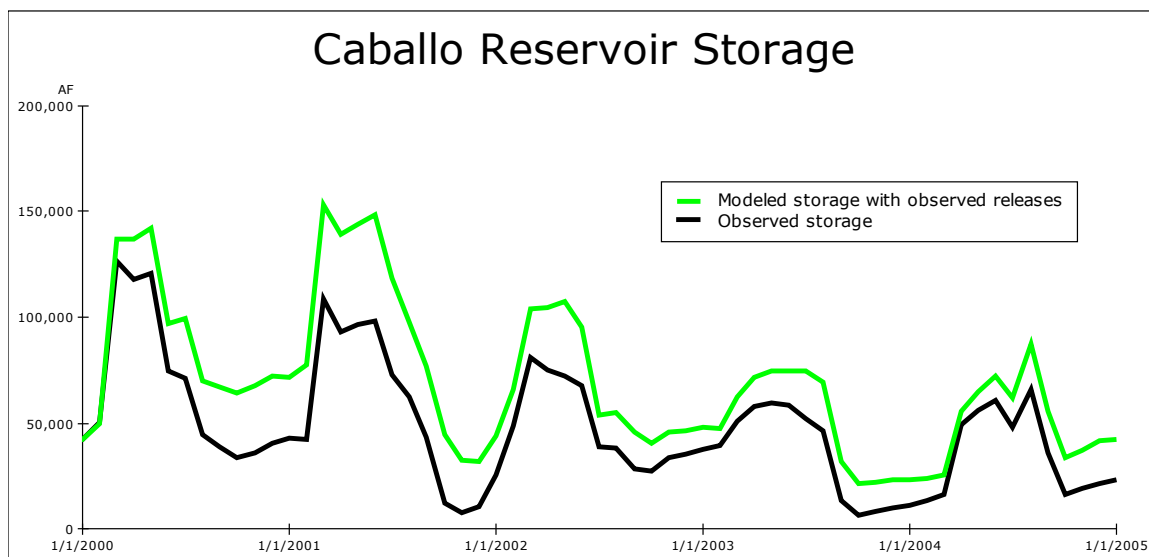
Figure 2-42. Caballo reservoir storage during the 2000-2004 validation period as observed and modeled with observed releases from Elephant Butte and Caballo. The model tends to overestimate storage as a result of errors in modeled inflows that are propagated through time.

storage residual distribution for model behavior that is actually reasonably good.

Because of the limitations associated with reservoir storage residuals discussed above, the

discussion in this section is intended as a cursory overview of modeled reservoir storage

compared to observed storage during the calibration and validation periods. A more

thorough and potentially more meaningful evaluation of reservoir performance is

included in Section 2.3.3.

2.3.2 Calibration Mass Balance Compared to URGWOM

In balance, the monthly timestep simulation model of the Rio Grande river system

in New Mexico described here, like the daily timestep URGWOM, is a mass balance

model. The main differences between URGWOM and the monthly model aside from the

timestep, are in how losses are calculated above Cochiti, how surface water groundwater

interactions are handled, and how un-gaged surface water inflows are calculated. As

described previously, above Cochiti the monthly model uses calculations of river area,

riparian vegetation area, and reference ET to estimate losses to evapotranspiration

(Section 2.2.3.2). URGWOM on the other hand uses a monthly fixed percentage loss

(USACE et al. 2002) for losses above Cochiti. In terms of surface water groundwater

interactions, the monthly model uses winter data to derive a constant groundwater input

to the river system above the Rio Grande Rio Chama confluence (Section 2.2.3.3.1),

while below this point, the groundwater system is modeled dynamically, with surface

water groundwater interactions modeled as a function of aquifer head and surface water

stage (Section 2.2.3.3.2 and Chapter 3). URGWOM does not explicitly model

groundwater interactions with the river system above Cochiti, and below Cochiti uses

data output from an in-house groundwater model for interactions below Cochiti. Finally, the monthly model predicts un-gaged inflows as a function of tributary gages close to the reach of interest (Section 2.2.3.4.4), while URGWOM specifies un-gaged inflows to close the mass balance in each reach. Groundwater surface water interactions predicted by each model are considered in detail in Chapter 3. This section will compare URGWOM and monthly model predicted overall surface water mass balance for reaches and reservoirs above and including Cochiti, and below Cochiti in light of the differences in timestep and conceptual approaches between the two models.

Figure 2-43 shows the overall mass balance above Cochiti as modeled by URGWOM and the monthly timestep model for the 1975-1999 calibration period. The main difference between the flows into the models is that the monthly formulation specifies groundwater flows (Section 2.2.3.3.1), and relies more heavily on stream gages where available, including the Chama at La Puente, Ojo Caliente at La Madera, and Costilla Creek near Garcia gages (see Table 2-1) which are not directly used by URGWOM. Despite these differences in accounting, the total inflows to the models are quite similar, with URGWOM's slightly larger to allow for larger predicted losses.

On the losses side of the equation, the two models are comparable upstream of Cochiti (Figure 2-43 right charts) for all terms with the exception of reach losses where they differ significantly. URGWOM calculates reach losses above Cochiti with monthly loss factors that are derived by filtering historic, daily flow data for days when the downstream gage reading (corrected for routing effects) is smaller than the upstream

INFLOWS

OUTFLOWS

U R G W O M

M O N T H L Y   M O D E L

Average inflows to URGWOM above and including Cochiti reservoir 1975-1999 [cfs]

20
941
1192
Total: 2153 cfs

- Gaged SW In
- Ungaged SW In
- Reservoir Precip

Average outflows from URGWOM above and including Cochiti reservoir 1975-1999 [cfs]

28
35
376
61
1660
Total: 2160 cfs

- Gaged SW Out
- Reservoir Evap
- Reach Losses
- Ag ET
- Reservoir Storage Change

Average inflows to monthly model above and including Cochiti reservoir 1975-1999 [cfs]

195
21
198
1432
Total: 1846 cfs

- Gaged SW In
- Ungaged SW In
- Reservoir Precip
- GW Inflows

Average outflows from monthly model above and including Cochiti reservoir 1975-1999 [cfs]

31
28
51
18
63
1660
Total: 1850 cfs

- Gaged SW Out
- Reservoir Evap
- Reach Losses
- Ag ET
- Reservoir Storage Change
- GW Outflows

Figure 2-43. Mass balance inflows and outflows for URGWOM and the monthly timestep model above Cochiti dam between 1975 and 1999. The left charts represent total inflows to the models, the right charts total outflows. The top charts show the URGWOM mass balance, and the bottom charts show the monthly model mass balance.

reading (USACE et al. 2002). Most of the reaches above Cochiti however, are likely

gaining reaches, so that we might expect winter flows at least (when evaporative losses

are small) to, on average, increase through the reach. Filtering the gage data for days

when the gaining flow seems to diminish would tend to skew the data heavily to periods

when the upstream gage is erring to the high and/or the downstream gage erring to the

low. (For a discussion of gage confidence, see Section 2.3.1.2.) From Lobatos to Arroyo

Hondo for example, the Rio Grande gains enough un-gaged water, that URGWOM uses

loss factors derived from data from the Arroyo Hondo to Taos Bridge data for all reaches

above Taos Bridge. In the Arroyo Hondo to Taos Bridge reach, direct flow estimates

suggest 10 to 20 cfs of gw gains for the 19 mile reach (Tetra Tech Inc. 2003). Therefore,

perhaps it is not surprising that for the period of analysis, only 9% (325/3608) of winter

days (November through February) resulted in a downstream gage reading greater than

the upstream gage reading. If, all other things being equal, the gages give a normal

distribution of readings about the true flow, and the true downstream flow is $10-20$ cfs

greater than the true upstream flow, it is not hard to imagine that the downstream reading

was smaller than the upstream reading only 10% of the time during the winter when

losses are lowest. All of which is to say that gage errors make everything more difficult,

and may be overwhelming to the selective filtering method applied by URGWOM. The

URGWOM approach does lead to a seasonal signal, which may suggest that the loss

signal is being captured, or alternatively that estimated losses are greater in spring

because flows and thus potential gage errors are greater in the spring. The URGWOM

monthly loss factors for the reaches from Lobatos to Taos Bridge are largest in April and

May. The monthly model estimates reach losses as comprised of direct evaporation from the river channel, and riparian evapotranspiration assumed to come from groundwater that would otherwise reach the river (Section 2.2.3.2). The resulting loss predictions are more than an order of magnitude less than the URGWOM estimates. As a result of larger predicted losses, URGWOM also predicts more ungaged inflows. This is the main reason for the discrepancy between total inflows or total outflows predicted by each model. Agricultural ET is another area of some discrepancy between models, and is a result of the monthly model explicitly including irrigated agriculture in the reaches from Taos Junction Bridge to Otowi, while it is lumped into reach losses in URGWOM. Finally, the groundwater outflows of 31 cfs shown for the monthly model are due to reservoir leakage from Cochiti not explicitly represented in URGWOM. Temporal comparisons of fluxes associated with reservoirs are shown in Section 2.3.3. Other temporal comparisons for the water budget terms in Figure 2-43 for the models above Cochiti are not included because of the relative differences in model approaches just described. Despite the differences in specific terms, both models predict similar overall water budgets. In addition, each model shows average inflows close to average outflows for the 25 year period. The fact that inflows and outflows don't quite balance above Cochiti dam during the calibration period for either model may be a result of storage changes in the river system between the calibration start and end times.

The majority of consumptive use in the model occurs between Cochiti and Elephant Butte (see Section 2.2.2), a stretch of river often referred to as the Middle Rio Grande or middle valley. The middle valley is arguably the most important and most
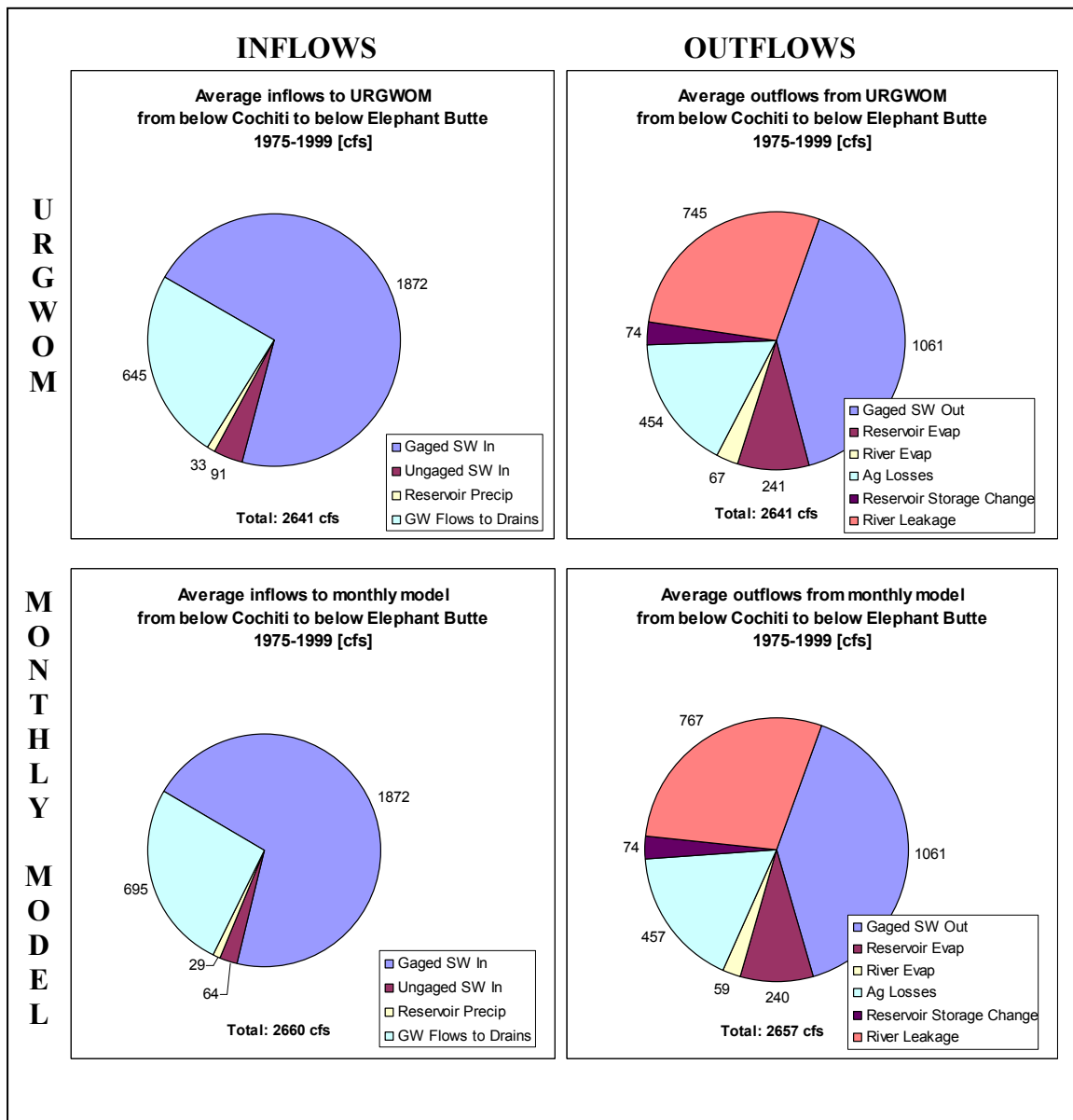
Figure 2-44. Mass balance inflows and outflows for URGWOM and the monthly timestep model from below Cochiti reservoir to below Elephant Butte between 1975 and 1999. The left charts represent total inflows to the models, the right charts total outflows. The top charts show the URGWOM mass balance, and the bottom charts show the monthly model mass balance.

complex segment of the model, and in this portion of the models, the mass balance

comparison between models is far more similar than it was for the system above Cochiti.

The model mass balance comparison is shown in Figure 2-44, and, for ease of

comparison does not include the Jemez tributary, or the reach from below Elephant Butte

to below Caballo due to differences in model approaches in those reaches[6]. The gaged

surface water shown in the left charts of Figure 2-44 includes the 1660 cfs of gaged

surface water releases from Cochiti shown as outflows in the right charts of Figure 2-43.

The 1061 cfs of gaged surface water outflows seen in the right charts of Figure 2-44

represent releases from Elephant Butte. Agricultural losses shown in Figure 2-44 include

ET as well as seepage of irrigation water from irrigation canals and agricultural fields

into the groundwater system.

Temporal comparisons of the middle valley fluxes shown in Figure 2-44, but

related to the groundwater system, including surface water groundwater interactions and

riparian ET, are shown in Sections 3.4. Temporal comparisons of reservoir evaporation

and precipitation between models are shown in Section 2.3.3. Fluxes of gaged surface

water into and out of the models, and reservoir storage change are based on observations,

and are identical for the two models in the middle valley. Temporal comparisons

between models of un-gaged surface water inflows, river evaporation, and agricultural

ET are shown in Figures 2-45 through 2-47 respectively.

---

[6] URGWOM treats the Jemez reach like reaches above Cochiti, with monthly loss factors and ungaged
inflows closing the mass balance, while the monthly model treats it like reaches below the Rio Chama
Rio Grande confluence, with specified losses to agriculture, river leakage, and riparian ET from a
connected groundwater system. URGWOM does not explicitly model evaporation from or
precipitation to Caballo reservoir.

Modeled un-gaged surface water inflows to river system between Cochiti and Elephant Butte 1975-1999
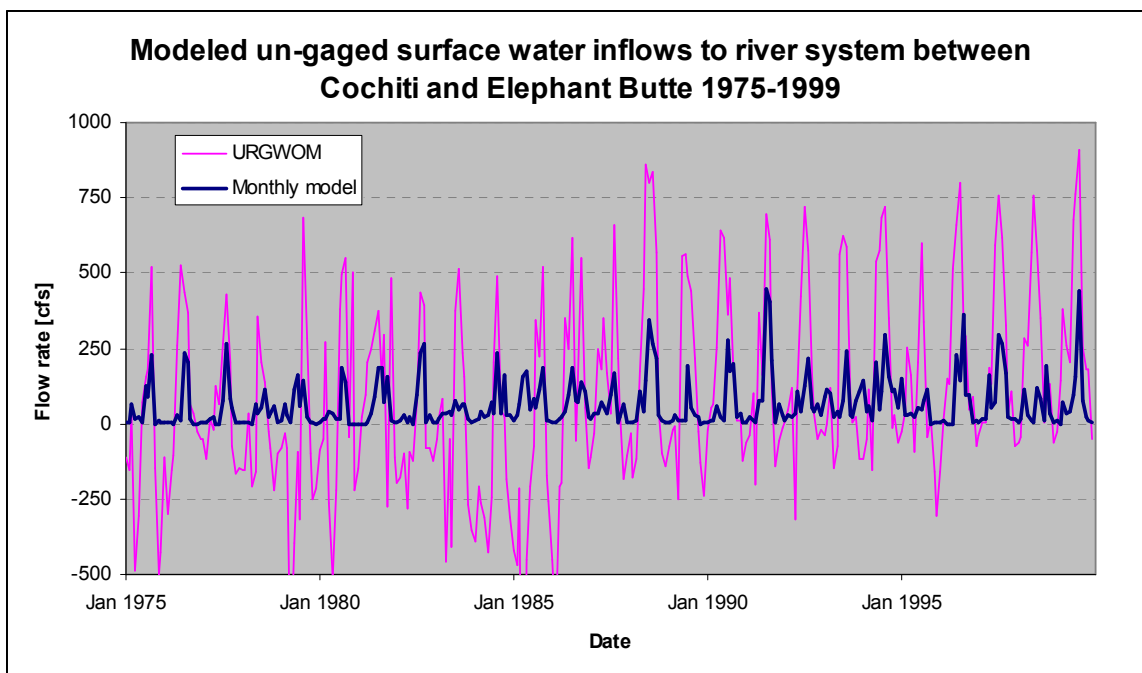
Figure 2-45. Un-gaged surface water inflows added to URGWOM and the monthly model between Cochiti and Elephant Butte 1975-99.

Modeled river evaporation from the Rio Grande between Cochiti and Elephant Butte 1975-1999
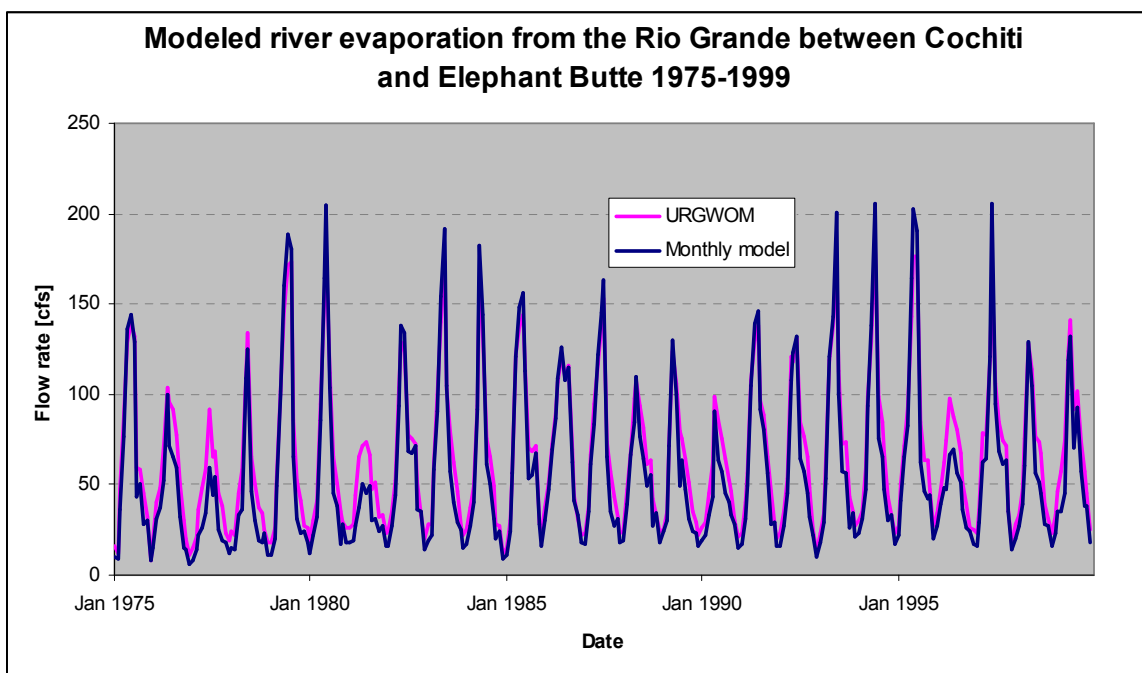
Figure 2-46. Evaporation from the Rio Grande between Cochiti and Elephant Butte 1975-99 as modeled by URGWOM and the monthly model.

The un-gaged inflows to the middle valley seen in Figure 2-45 are used to close the mass balance between gages in both models, however URGWOM closes it perfectly on a daily basis, meaning that the un-gaged inflow term is essentially a combination of ungaged inflows and error, and can be negative. As described in Section 2.2.3.4.4, the monthly model calculates these flows as a percentage of flows gaged in tributaries close to each reach, and for this reason they follow the seasonal pattern of a typical tributary hydrograph in the model extent. Unlike URGWOM, which closes the mass balance at each timestep, the monthly model uses the flows to close the mass balance for the entire 25 year calibration period, resulting in residuals at each timestep at each interior gage location as shown previously in Figures 2-13 through 2-23.

Direct evaporation from the river channel below Cochiti (Section 2.2.3.2) is modeled in similar ways by both models, with the main difference being daily versus monthly timestep, and a reference ET estimate of open water evaporation approach used by the monthly model as compared to an observed pan evaporation approach used by URGWOM. Figure 2-46 shows the predicted values during the historic period for the two models. With the exception of 1977, 1981, and 1996, the two models are very similar. During those years there may have been differences between calculated reference ET and observed pan evaporation, or non-linear effects associated with average monthly flow not being representative of daily flow for purposes of area calculations. However, overall, the fit is quite acceptable for the purposes of the monthly model.

Agricultural ET rates are compared for the two models between 1975 and 1999 in Figure 2-47. The fit between models is better after 1983 than before. Both models utilize

the same crop acreage and agricultural diversion data however, so the significant

discrepancies early in the run may suggest that calibration methods used by the monthly

model to replicate daily shortages with monthly data (see Section 2.2.3.2.9) result in

more variability in the monthly model than the daily to achieve the same 25 year volume

between models.
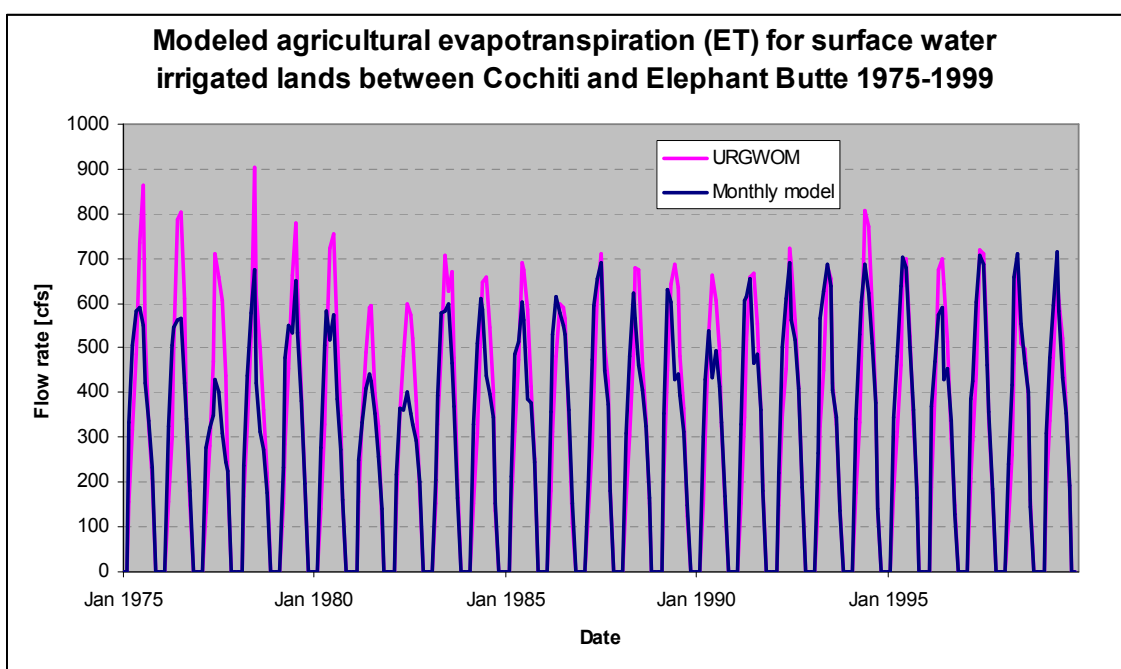
Figure 2-47. Agricultural evapotranspiration for lands irrigated with Rio Grande surface water between Cochiti and Elephant Butte 1975-99 as modeled by URGWOM and the monthly model.

2.3.3 Reservoir Specific Behavior

2.3.3.1 Surface Water and Groundwater Fluxes to Reservoirs

As outlined by Equation 2-4, the fluxes used to determine reservoir storage

through time in the model include surface water inflows, groundwater interactions,

precipitation and evaporation, and reservoir releases. Surface water inflows are

determined by upstream reaches, and in the case of Abiquiu, un-gaged inflows estimated

based on Jemez River flows near Jemez pueblo. The reliability of reservoir inflows can

be inferred from calibration and validation residuals associated with surface water gages

upstream of the reservoir (Section 2.3.1.4). Groundwater interactions for Cochiti, Jemez,

and Elephant Butte are covered in Sections 3.4.1 and 3.4.3. All groundwater seepage

from Heron is assumed to end up in the river below the reservoir, and thus is effectively

an uncontrolled release with little effect on overall model behavior. No groundwater

surface water interaction is modeled for El Vado, Abiquiu, or Caballo reservoirs.

2.3.3.2 Reservoir Evaporation and Precipitation

Both the daily timestep URGWOM, and the monthly model predict reservoir

evaporation and precipitation by calculating reservoir surface area based on modeled

storage, and reducing it by observed ice covered area if any (USACE et al. 2002 and

Section 2.2.3.2.5). This area is then multiplied by rainfall or evaporation rate to get

volumetric flux values. URGWOM and the monthly model use the same rainfall data

and climatic data driving the evaporation rate calculation. The difference between the

models in terms of reservoir precipitation and evaporation then is strictly limited to a

difference in the timestep of the input data and the calculations for the two models. By

comparing these reservoir fluxes, the loss of information associated with a monthly

timestep versus a daily timestep can be evaluated. As seen in Figure 2-48, reservoir

evaporation can be predicted at a monthly timestep with no significant information loss

compared to a daily timestep. This is because evaporation occurs constantly, and daily

rates are distributed relatively uniformly during a given month. As shown by Figure 2-49

however, precipitation cannot be as accurately modeled at a monthly timestep as it can be

at a daily timestep. This is likely because precipitation is highly variable at a daily

timestep, with many days with no precipitation, and a single day or two often responsible

for an entire month's precipitation. The reservoir storage when these sparse events arrive

is then critical for prediction of precipitation actually landing on the reservoir. The

monthly model simply cannot resolve this effect, and for this reason the predicted

reservoir precipitation shown in Figure 2-49 varies far more significantly between models

than does the reservoir evaporation.
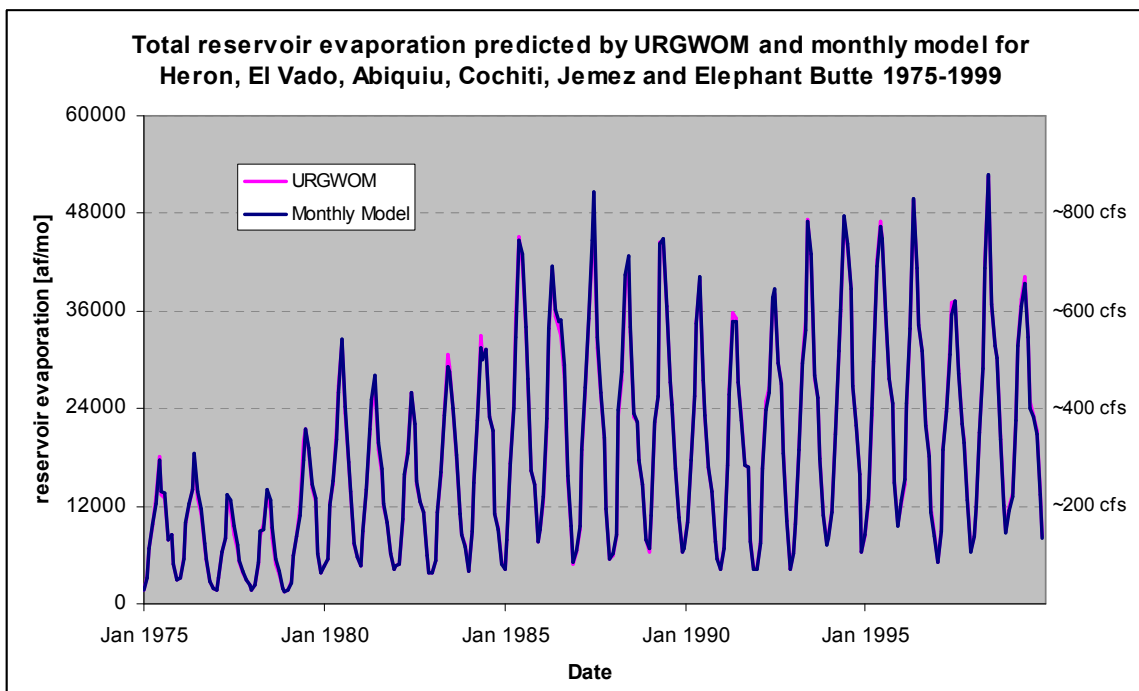
Figure 2-48. Total volume of evaporation from 6 modeled reservoirs predicted by URGWOM and the monthly model for the calibration period 1975-1999. Caballo reservoir is not included as URGWOM does not explicitly model evaporation or precipitation from that reservoir.

Total reservoir precipitation predicted by URGWOM and monthly model for Heron, El Vado, Abiquiu, Cochiti, Jemez and Elephant Butte 1975-1999
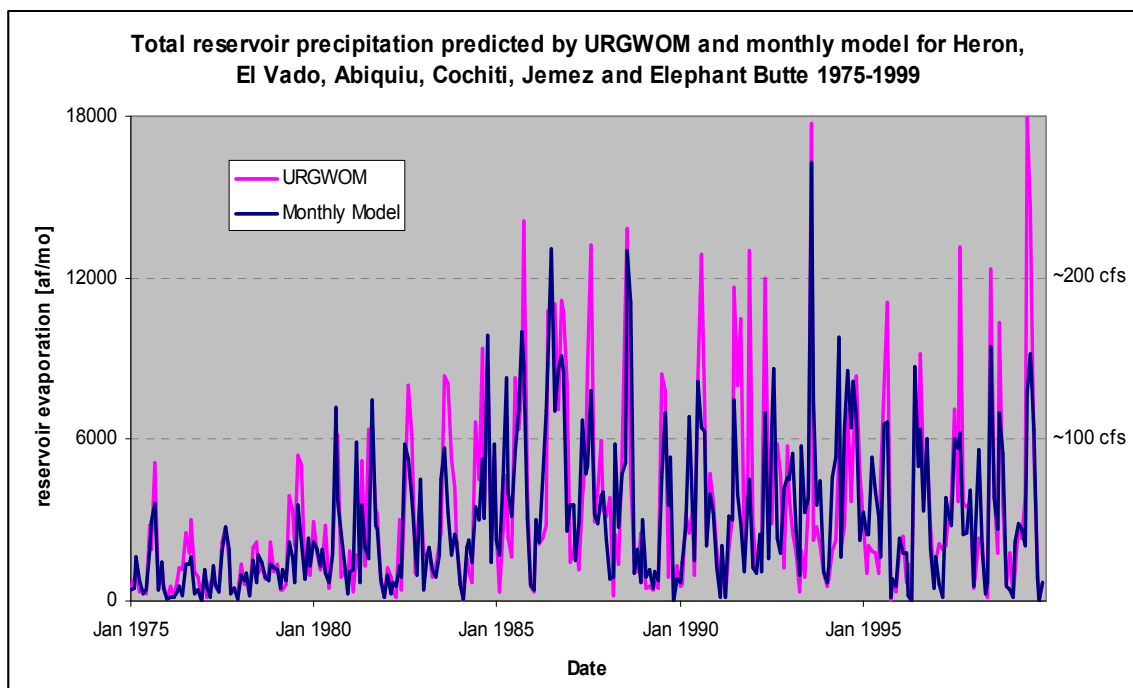
Figure 2-49. Total volume of precipitation to 6 modeled reservoirs predicted by URGWOM and the monthly model for the calibration period 1975-1999. Caballo reservoir is not included as URGWOM does not explicitly model evaporation or precipitation from that reservoir.

2.3.3.3 Reservoir Releases

As outlined in Section 2.2.3.5.3, reservoir operations are guided by a complex set of institutional and physical constraints. There is also room for human operators to exercise a significant amount of flexibility in determining reservoir releases as unforeseen circumstances or opportunities for efficiencies arise. As a result of these flexibilities and changing operations, historic reservoir behavior cannot be completely captured by a general set of reservoir rules based on current operations. Figure 2-50 shows how observed reservoir releases summed for all seven modeled reservoirs compare to model predicted releases for the same from 1975 through 2004. The modeled release targets follow overall patterns of observed releases fairly closely, with notable exceptions

occurring during high flow years in the late 1980's and mid 1990's. Visual comparison of model release targets to observed actual releases during calibration and validation shown in Figure 2-50 suggests that the ability of the rule set to predict actual releases is not considerably different during calibration than it is during validation.

2.3.3.4 Overall Reservoir Behavior

Calibration storage residuals (Section 2.3.1.3) can be used to estimate the model's ability to simulate reservoir behavior when inflows and releases are known. However, as discussed in Section 2.3.1.5, because reservoir storage propagates error through time, reservoir storage residuals can be a misleading metric for quantification of model performance when storage errors are not corrected at each timestep as they are during calibration. One way to evaluate the performance of the monthly model reservoirs is to compare their behavior during a given scenario to reservoir behavior in URGWOM under the same set of hydrologic conditions.

The URGWOM model is the best available model of reservoir operations within the model extent, so that if the monthly model can capture the dominant operations behavior represented in URGWOM, it can be considered a valid representation of those rules. URGWOM has set up a base case planning run ten years long using hydrologic and climatic input from the historic years 1982, 1988, 1992, 1976, 1989, 1996, 1977, 1989, 1989, and 1981 respectively, which is the first 10 years of a 40 year general sequence developed for use in scenario analysis by the Upper Rio Grande Water Operations Review (USACE et al. 2006, Chapter 2). The overall climate sequence is discussed in more detail in Section 4.2.2.1. Using this climate sequence to derive
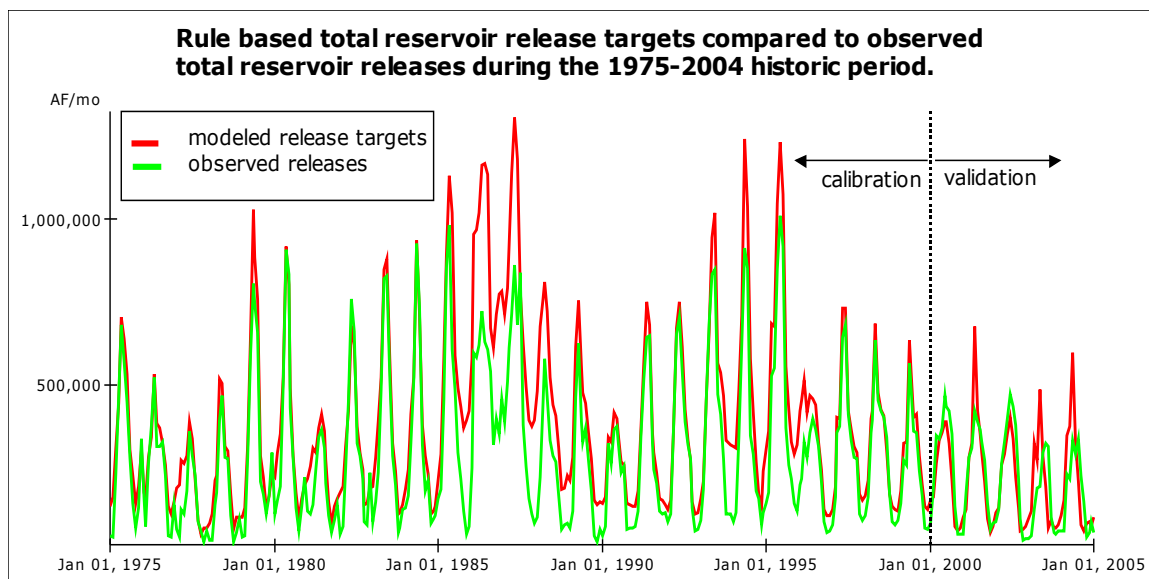
Figure 2-50. Total volume of releases from all seven modeled reservoirs predicted and observed during the period from 1975 through 2004.

hydrologic and climatic model inputs, reservoir behavior at the seven modeled reservoirs

was compared between models. Figure 2-51 shows the reservoir storage predicted by

each model at six of the reservoirs. Jemez reservoir is empty for the entire ten year cycle

in both models, and so is not included in Figure 2-51. Storage at all reservoirs is plotted

on the same scale with the exception of Elephant Butte where the scale is doubled. To

simplify the El Vado comparison, Article VII of the Rio Grande compact (see Section

2.2.3.5.3.2) is specified based on Elephant Butte and Caballo reservoir storage predicted

by URGWOM. This allows El Vado to add native water to storage during the same

months when URGWOM does. In general, the monthly model captures the overall

behavior of the reservoirs, with the most systematic discrepancy at Elephant Butte where

the monthly model predicts smaller storages than those predicted by URGWOM. The

total inflows to Elephant Butte modeled by URGWOM and the monthly model for the ten

Heron Reservoir Storage

El Vado Reservoir Storage

Abiquiu Reservoir Storage

Cochiti Reservoir Storage

Elephant Butte Res Storage

Caballo Reservoir Storage
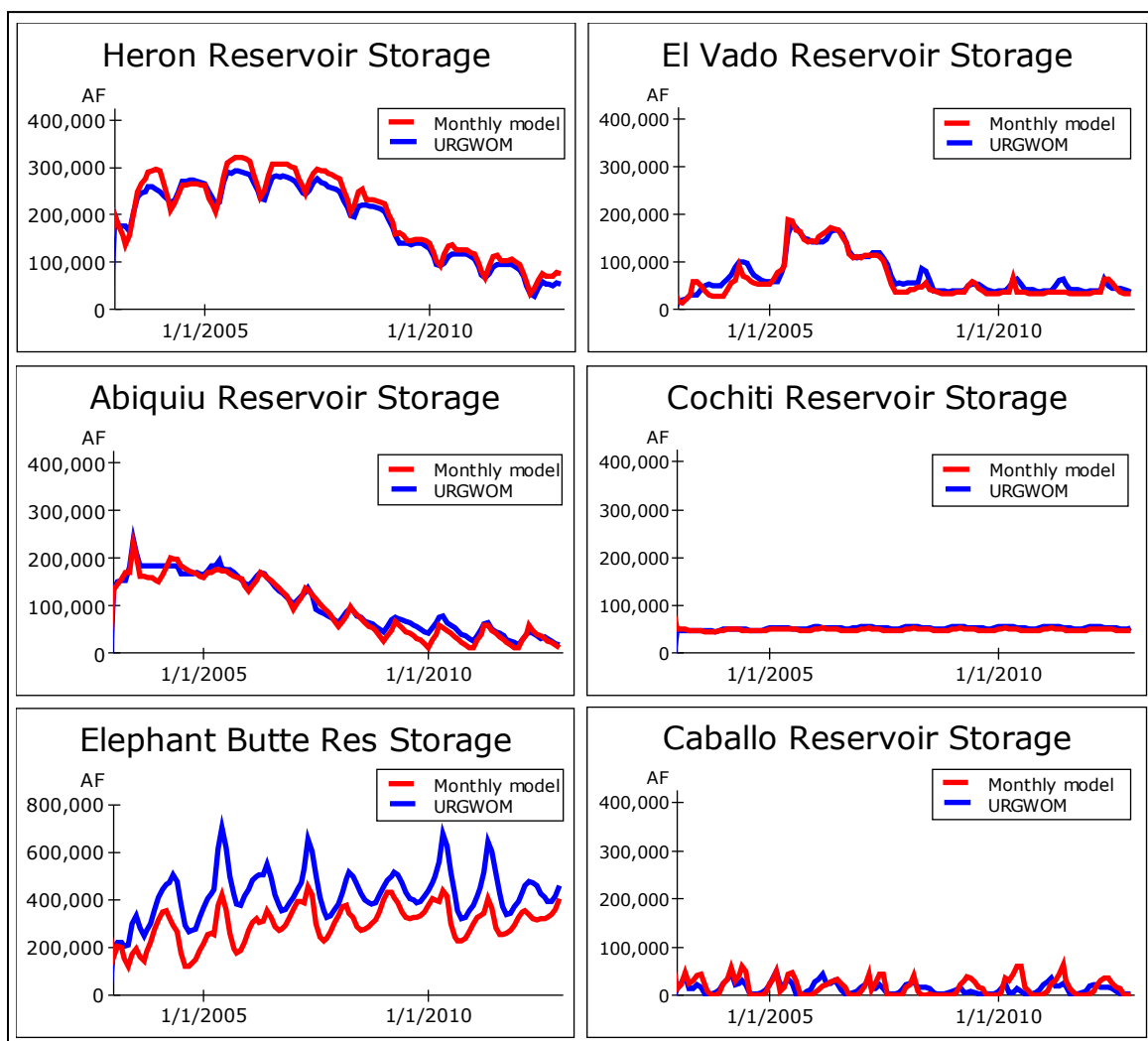
Figure 2-51. Reservoir storage modeled by monthly model and URGWOM for the same 10 year historical climate sequence, run as a scenario from 2003 through 2012. All reservoir storages are shown on the same scale except Elephant Butte which is shown on a scale twice as large.

year run are 5.78 and 5.94 million acre feet respectively, while the ten year total releases are 4.8 and 5.1 million acre feet respectively. The annual releases predicted by each model are shown in Figure 2-52, and explain the consistent discrepancy in modeled Elephant Butte storages seen in Figure 2-51, while differences from month to month explain the seasonal variations. The ten year sequence used for climatic inputs represents

a relatively dry period during which target releases from Elephant Butte are limited by availability. It is difficult to predict how releases will be curtailed during dry periods, and the methodologies differ slightly between models with URGWOM reducing deliveries each month by a fixed percentage based on predicted total annual supply, and the monthly model, which does not employ predictive methods to as a great an extent as URGWOM, delivering what is available each month. During wetter periods, the two models would predict similar annual total releases.
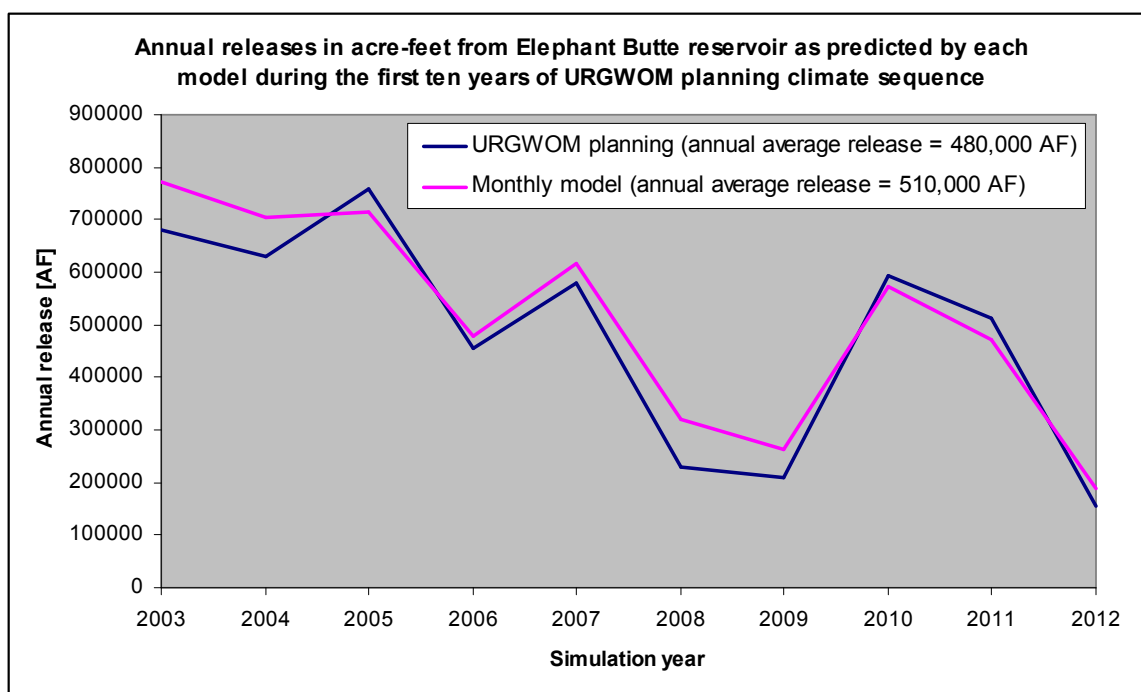
Figure 2-52. Annual releases from Elephant Butte modeled by monthly model and URGWOM for the same 10 year historical climate sequence, run as a scenario from 2003 through 2012.

2.3.4 Rio Grande Compact

New Mexico's Rio Grande Compact Balance (NMRGCB) (Colorado et al. 1938 and 1948) was calculated with equations 2-16, 2-17, and 2-18, and Table 2-18. Results are shown in Figure 2-53. Rio Grande Compact calculations are only made at the end of a given year, thus the stairstep pattern seen in the monthly representation of Figure 2-53. The green line represents historic values as calculated by the Rio Grande Compact Commission. The red line represents modeled values. The model captures the relative change in NMRGCB within 10% of the actual change every year until 1993 when spill related errors begin. The spill accounting is too complex to be fully captured by the current model. Indeed, in some years such as 1996 where the largest difference between the green and red lines occur, even the states did not agree on whether or not a spill of useable water actually occurred! To begin the 2000-2004 validation period, NMRGCB is reset to avoid cumulative errors during the validation period. As seen in Figure 2-53, the validation period match between modeled and historical New Mexico compact balance is poor.   However, as seen in Figure 2-54, the major components used to calculate the compact balance are modeled reasonably well; it is compounding errors that throw off the overall modeled compact change. The overall compact balance change is too sensitive to reservoir behavior to model well without almost perfect reservoir behavior as was forced during the calibration period.
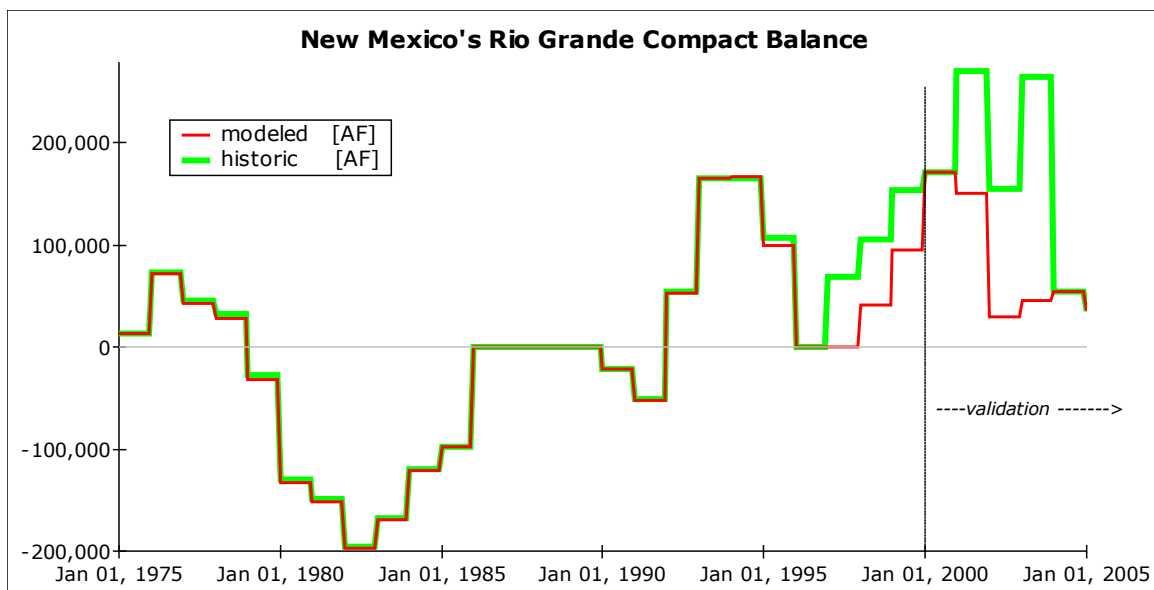
Figure 2-53. New Mexico's Rio Grande Compact Balance 1975-2000, modeled and historic. Model errors late in the calibration run are a result of spill accounting errors.
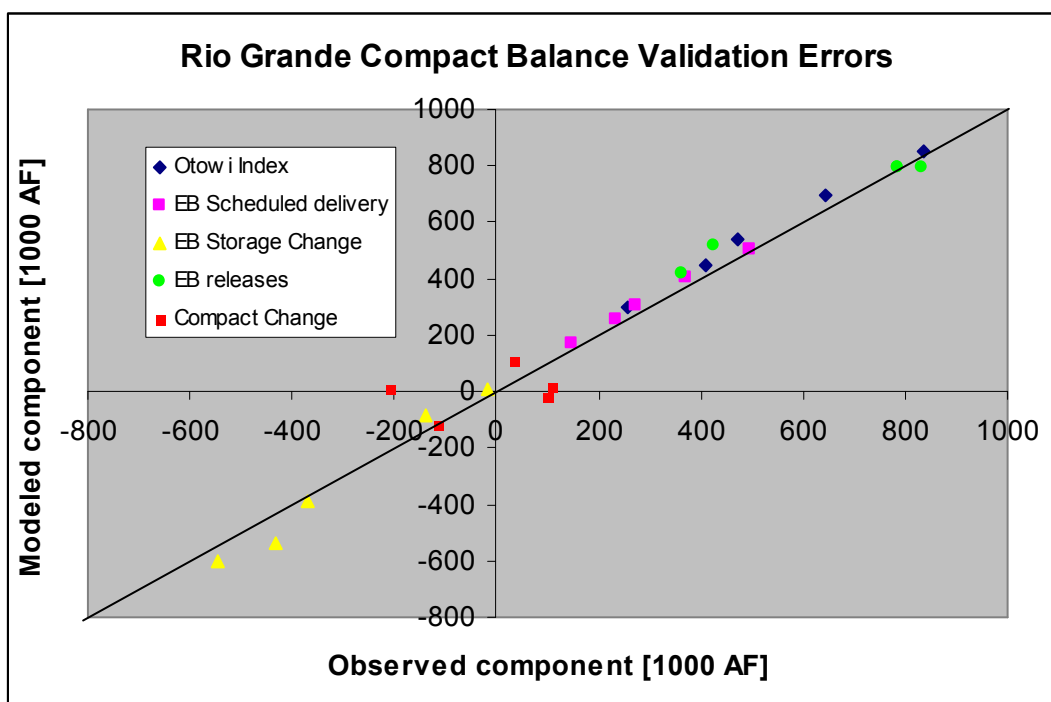
Figure 2-54. New Mexico's Rio Grande Compact balance component errors during validation.

2.3.5 *Physical Model Sensitivity Analysis (scenario mode)*

Model sensitivity to major physical input and water use related parameters was tested by systematic variation of the input parameters during a forty year scenario run. The forty year climate sequence was developed by the Upper Rio Grande Basin Water Operations Review (URGWOPS) to be a sequence representative of long term climate averages in the basin based on direct measurements and paleoclimate analysis (USACE et al. 2006, Section 2.2.2). The forty year sequence is derived from a sampling of historic years between 1975 and 1999, however, because the twenty five year calibration sequence was wetter than long term averages, certain years are used more often than others, and some years are not used at all. For additional information on the 40 year sequence, as well as sensitivity analysis for human behavioral related parameters, see Sections 4.2.2.1 and 4.3.7 in this dissertation.

The model output metric evaluated for sensitivity to parameter changes is the sum of modeled reservoir storage change between the start and finish of the scenario, and the total reservoir releases from Caballo reservoir, which represent surface water flows out of the southern model boundary. This metric was chosen because it is representative of overall surface water behavior in the model during the scenario run. Groundwater storage change could have also been included, but for simplicity, and because the groundwater and surface water systems are connected, only the major surface water indicators are considered here. Because the sensitivity analysis run is used to explore relative changes to the model under different forcings, the specifics of the base case run are not relevant, however, for context, Table 2-22 shows initial and final reservoir storage

conditions for the base case run. The total reservoir storage change of 209,900 AF for the

40 year period represents an average flow into storage of about 7 cfs. The forty year base

case scenario releases from Caballo reservoir are 25,482,800 AF (880 cfs). In other

words, in the base case scenario run, on average, approximately 887 cfs of surface water

are being added to storage, or leaving the model at any given point. Compare this to

1140 cfs during the 1975-1999 calibration period. From the base case forty year

scenario, inputs and parameters were adjusted up and down 10% and 20% to derive

relative sensitivities of model output to variations in inputs. Figure 2-55 shows these

sensitivities graphically. Mainstem inflows for the purpose of Figure 2-55 include the

Rio Grande gage near Lobatos, and the Jemez River gage near Jemez pueblo. Tributaries

include the Chama near La Puente, and the Azotea tunnel flows, as well as all smaller

tributaries to reaches shown in Table 2-1.

Table 2-22. Initial and final reservoir storage for the base case scenario run used to evaluate model sensitivity to major input and consumption related parameters.

Reservoir	Heron	El Vado	Abiquiu	Cochiti	Jemez	Elephant Butte	Caballo	Total
Initial storage [1000 AF]	271.4	56.3	153.2	49	0	49.8	36.3	616
Final storage [1000 AF]	356	79.7	22.2	49	0	264.2	54.8	825.9
Change [1000 AF/40yrs]	84.6	23.4	-131	0	0	214.4	18.5	209.9

The model output increases by 13% for a 20% increase in tributary flows. The model is

most sensitive to changes in tributary values because of the relative magnitude of flows

from tributary gages, as well as the fact that ungaged inflows are calculated based on

flows at the tributary gages. The model output decreases by 6% on the other hand as a
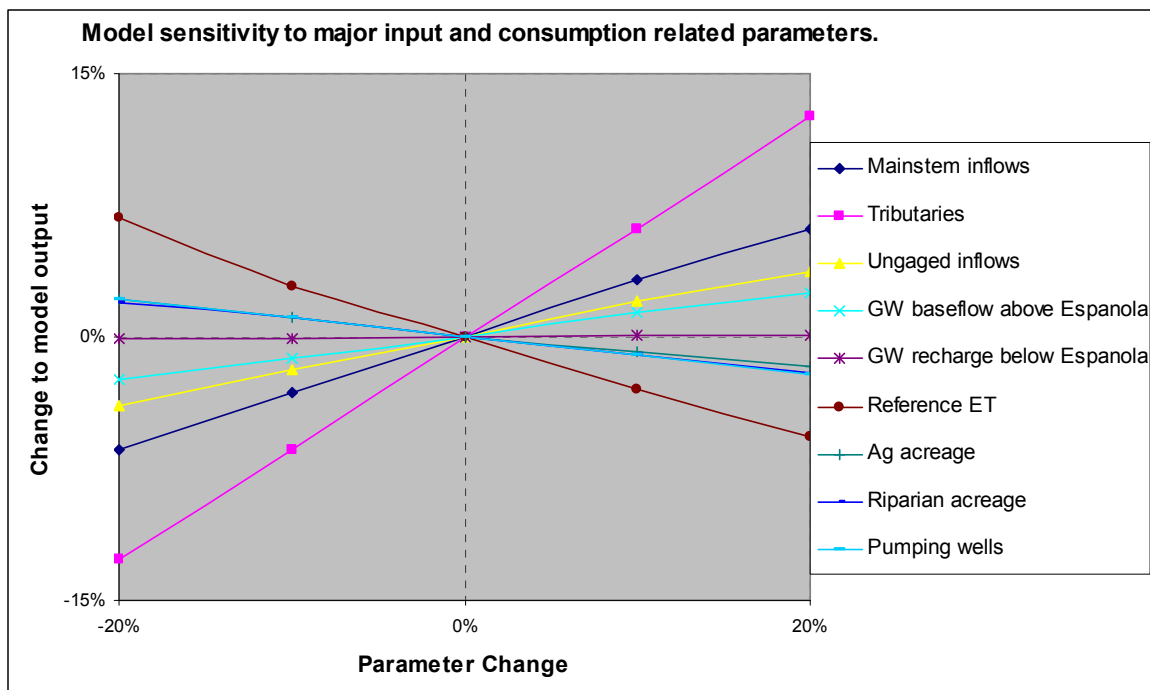
Figure 2-55. Model sensitivity to major input and water consumption related parameters. The Y axis shows the model response to parameter changes on the X axis.

result of a 20% increase in reference ET calculations. This relatively large sensitivity is important given the uncertainty associated with reference ET due to climatic data observation error, climatic data measured at a point used to estimate reference ET for an entire reach or reaches, and errors associated with the semi-empical nature of the modified Penman-Monteith equation (see Section 2.2.3.2.2). Future model improvements may come from improved spatial representation of reference ET.

Agricultural acreage changes, riparian acreage changes, and well pumping changes of similar relative sizes have similar effects on the model, which is interesting because these terms represent the majority of water use by the agricultural, environmental, and municipal sectors respectively. Improvements in efficiency or reductions in overall use by these sectors are considered in Chapter 4.

2.4 Surface Water Component Conclusions

Initial work suggests that a monthly timestep mass balance model is able to capture salient surface water dynamics of the Rio Grande river system in New Mexico between 1975 and 1999. Validation using 2000–2005 data suggests that a system dynamics approach to the surface water system provides a useful foundation for a fast, multidisciplinary, and basin scale model of the myriad of systems whose interactions through time affect how water moves through the Rio Grande. The largest gap in the current surface water model is the lack of a land surface model to transfer atmospheric precipitation to the surface water gages, ungaged tributaries, and groundwater system. Current work by Aragon and Vivoni is addressing this gap (Tidwell et al. 2006, Chapter 4). Future analysis might also explore different methods for calibration of the agricultural ET loss estimates discussed in Section 2.2.3.2.9. The next chapter will explore in greater detail the groundwater model that underlies the Rio Grande system from the Rio Chama, Rio Grande confluence to Elephant Butte reservoir.

CHAPTER 3: GROUNDWATER COMPONENT

3.1 Introduction

A common goal of system dynamics modeling is a high-level model that can capture the salient behavior of a system without sacrificing computational speed. To model groundwater flow, the majority of numerical model schemes rely on a fixed-grid finite difference approximation to the governing groundwater flow equations (e.g., MODFLOW, McDonald and Harbaugh 1998). The fixed-grid approach allows for a very systematic and thus numerically efficient approach to development and solution of the driving finite difference equations, but can be cumbersome for modeling large, heterogeneous basins, because the most detailed spatial resolution required in any one part of the model is carried throughout the spatial extent of the model. If runtime is not an issue, a groundwater model can likely be created most easily and quickly with an off-the-shelf fixed-grid approach. However, where runtime is important and fixed-grid inefficiencies are significant, finite element, variable-grid finite difference, and compartmental approaches may reduce model size significantly by utilizing spatial units of varying size.

This chapter will explore the use of a compartmental modeling approach for rapid, reduced resolution groundwater modeling. Compartmental models have been used extensively in the literature to model steady state groundwater flow as a function of hydrochemical data when hydrologic parameter data are sparse (e.g., Campana and Simpson 1984; Adar and Neuman 1986; Adar et al. 1988), but not to model groundwater flow as a function of head. A close exception to this rule appears in Adar and Sorek

(1989) where hydrochemical data are used to solve for quasi steady state flows between compartments, which are then combined with available head data to estimate transmissivities based on Darcy's law. In this chapter similar concepts are used to create a head-based groundwater flow model between zones of irregular size and shape.

3.2   Compartmental Groundwater Modeling

Compartmental groundwater models are referred to interchangeably in the

literature as compartmental, cell, or mixing-cell models, and are used most commonly to

constrain bulk groundwater movement using available groundwater chemistry data

(Campana et al. 2001). Compartmental models can also be thought of as a spatially

distributed and communicating set of "lumped-parameter" models (models that do not

use spatial coordinates (Gelhar and Wilson 1974)), and compartmental models with

explicit development of hydrologic parameters have been referred to as distributed

parameter models (e.g., Adar and Sorek 1989). The irregular shapes common to a

compartmental approach can be convenient for describing areas of hydrologic uniformity,

but render a rigorous finite difference approximation to the governing flow equations

tedious. Thus, the distributed parameters are typically not derived mathematically from

hydrolgeologic data, but rather empirically as an inverse modeling exercise. Flow and

head values must be independently obtained in order to solve for transmissivities. Model

quality is limited by the choice of representative groundwater compartments, especially

as spatial resolution is reduced.

3.2.1 Groundwater Compartment Delineation

An effective compartmental groundwater model should capture the first-order behavior of

a groundwater system with relatively low complexity. Such a model provides the ability

to capture basic system behavior with minimal runtime. The amount of complexity that

should be built into a compartmental model depends on the balance between model

requirements and the runtime that can be afforded. The advantage of a simplified

approach is strengthened if the relationship between model complexity and the ability of

the model to describe the physical system is strongly nonlinear as diagrammed

theoretically in Figure 3-1. In these situations, once the first order behavior has been

captured, relatively modest model improvements require significant increases in

complexity. When this is true and runtime is important (as it is in systems models

designed for interactive use), complexity should be limited to the point at which salient

system behavior is captured in the model.
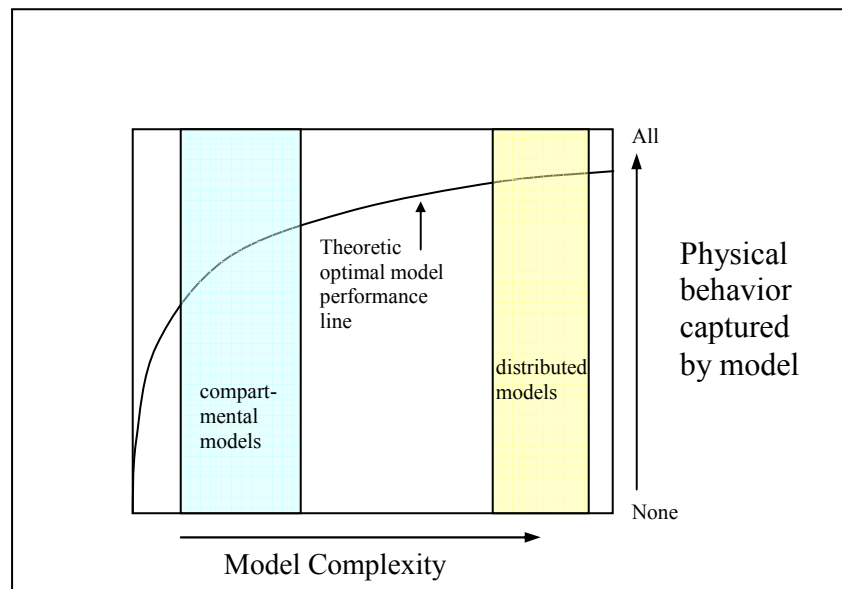
*Figure 3-1. Theoretical relationship between model complexity
and physical behavior captured by the model.*

In the context of a compartmental groundwater model, the choice of appropriate

compartments to capture system behavior is the key to development of a meaningful

model. Physically meaningful compartments will represent areas of relatively

homogenous aquifer properties and groundwater behavior. According to Campana et al.

(2001, p. 37), compartment differentiation depends on "hydrogeological uniformity, the availability of data, the degree of resolution desired, and constraints imposed by numerical solutions" (e.g., stability criteria as mentioned above). The resolution desired will depend on the questions being addressed by the model, as well as spatial resolution required to meaningfully couple to other modeled systems. Choosing the spatial resolution requires, as with any modeling effort, a good conceptual model of the groundwater system, especially for basins with limited data availability. If reliable spatially distributed models of the basin in question exist, they can be used to help choose representative groundwater compartments and calibrate a simplified model. As implied above, even with an excellent spatially distributed model available for a given basin, run time and dynamic input and output considerations can make a compartmental model more appropriate than a large spatially distributed model for certain applications.

3.2.2 Groundwater Compartment Numeric Mass Balance

Assuming that they have been well chosen, consider the irregular spatial groundwater compartments shown in Figure 3-2. Applying conservation of mass to compartment a, the change in storage in compartment a is equal to the sum of flows into a less the sum of flows out of a. Mathematically,

$$\frac{dS_a}{dt} = Q_{ab} + Q_{ac} + Q_{ad} + Q_{aS} \qquad (3\text{-}1)$$

where

$\dfrac{dS_a}{dt}$ =   change in storage through time in compartment a [L^3/T]

Q_{ab}, Q_{ac}, Q_{ad} =   net flows into a from b, c, and d respectively [L^3/T]

Q_{aS} = sum of interior source and boundary flows into compartment a [L^3/T]
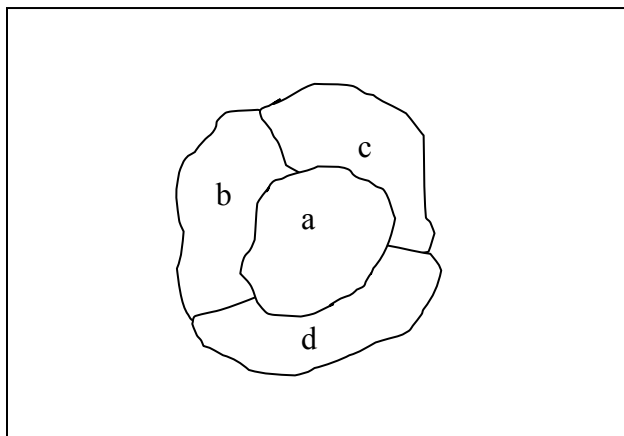
Figure 3-2. Example groundwater compartments.

Boundary flows include all flows from external sources including, for example,

evapotranspiration, well extraction or injection, recharge, stream leakage, and drain

capture. Q terms in Equation 3-1 are positive for flow into compartment a, and negative

for flow out. Applying Darcy's law for flow between compartments,

$$Q_{ab} \cong \frac{-K_{ab} A_{ab}}{L_{ab}} (h_a - h_b) \qquad (3\text{-}2)$$

where

K_{ab} = effective saturated hydraulic conductivity between compartments a and b [L/T]

A_{ab} = effective cross-sectional area between a and b normal to net flow [L^2]

L_{ab} = effective distance between compartments a and b [L]

h_a, h_b = representative heads in compartment a and b respectively [L]

A key assumption in compartmental modeling when dealing with hydrochemical data is

that a given compartment is fully mixed, such that a singe concentration represents the

concentration throughout the compartment. The analogous assumption implicit in Equation 3-2 is that a single head value is representative of head throughout the compartment. This approximation improves as compartment size and heterogeneity decrease.

In an unconfined aquifer, the cross-sectional area between compartments will change as head changes in either compartment, making flow between compartments a nonlinear function of head. For compartmental model applications, spatial scale is usually relatively large compared to head changes, meaning that the variation of A_{ab} through time will be very small. In these cases, it is reasonable to assume that A_{ab} is constant, particularly given the overall accuracy loss accepted with reduced resolution groundwater modeling. The remainder of this development employs this assumption; however, it is important to point out that the development of the model without this assumption would be analogous though slightly more complex.

With the assumption that A_{ab} is constant with respect to head, Equation 3-2 can be simplified to a linear description of flow as a function of head:

$$Q_{ab} \cong \alpha_{ab}(h_b - h_a) \qquad (3\text{-}3)$$

where

$$\alpha_{ab} \equiv \frac{Keff_{ab} A_{ab}}{L_{ab}} \qquad (3\text{-}4)$$

Substituting Equation 3-3, and analogous terms for compartments c and d, Equation 3-1 can be rewritten as

$$\frac{dS_a}{dt} = \alpha_{ab}(h_b - h_a) + \alpha_{ac}(h_c - h_a) + \alpha_{ad}(h_d - h_a) + Q_{aS} \qquad (3\text{-}5)$$

Using a finite timestep approximation for storage change, and adding superscript notation

to specify time, Equation 3-5 can be rewritten to solve for storage in aquifer compartment

a at time $t+1$ as a function of storage and head values at time t

$$S_a^{t+1} = S_a^t + \Delta t \left[\alpha_{ab} \Delta h_{ab}^t + \alpha_{ac} \Delta h_{ac}^t + \alpha_{ad} \Delta h_{ad}^t + Q_{aS} \right] \qquad (3\text{-}6)$$

where

S^t = aquifer storage at time t [L^3]
Δt = timestep duration [T]
Δh_{ab}^t = the head in compartment b minus the head in compartment a at time t [L]

Equation 3-6 approximates a forward difference explicit solution to the Darcy-based,

compartmental groundwater flow equation.

In matrix form for all groundwater compartments

$$\underline{S}_i^{t+1} = \underline{S}_i^t + \Delta t \left[\sum_{i=1}^{n} \left(\underline{\underline{Q}}_{ij}^t \right) + \underline{Q}_{iS}^t \right] \qquad (3\text{-}7)$$

where

n = total number of groundwater compartments
$\underline{S}_i^{t+1}$ $\underline{S}_i^t$ = storage vectors for n groundwater compartments at times $t+1$ and t [L^3]
$\underline{Q}_{iS}^t$ = source flow vector for n groundwater compartments at time t [L^3/T]
$\underline{\underline{Q}}_{ij}^t$ = n by n matrix representing flow to i from j at time t for all i and j [L^3/T]

The n by n flow matrix $\underline{\underline{Q}}_{ij}^t$ is developed with compartmental heads and conductance

values:

$$\underline{\underline{Q}}_{ij}^t = \sum_{i=1}^{n} \sum_{j=1}^{n} \left(\alpha_{ij} * \Delta h_{ij}^t \right) \qquad (3\text{-}8)$$

where

α_{ij} =   conductance value (Equation 3-4) between compartment i and j [L^2/T]

Δh_{ij}^t = $h_j - h_i$ at time t [L].

Note that the conductance value for compartments that are not hydrologically connected is zero, thus if stored as a matrix ($\underset{=}{\alpha_{ij}}$) serves the purpose of connectivity matrix as well.

Note also in Equation 3-7 that the flow matrix $\underset{=}{Q_{ij}^t}$ is summed across all i to result in vector of total internal flows to each of n compartments.

If all source flows ($\underline{Q_{iS}^t}$) are either known or a function of aquifer heads, the alpha matrix ($\underset{=}{\alpha_{ij}}$) is known, and storage and head conditions at the beginning of the timestep are known, we end up with a system of n equations and n unknowns whose solution describes groundwater movement at a given model timestep (Equation 3-8) and aquifer storage at the beginning of the next timestep (Equation 3-7). The new aquifer storage is used to calculate a new aquifer head using the following relationship between storage and head in an unconfined aquifer:

$$S_i = (h_i - zbot_i) * F_i * sy_i \tag{3-9}$$

where

F_i =   the horizontal area (footprint) of compartment i [L^2]

sy_i =   specific yield of compartment i [-]

Equation 3-9 is used to update the heads so that Equation 3-7 may be solved for at the next timestep, thereby modeling groundwater movement and storage through time.

3.2.3 Stability Criteria

Because the forward difference explicit formulation predicts the future state of a

system based on the present state of that system, the system of equations can be unstable

if the timestep is too long relative to the spatial scale and rate of movement of water

between compartments. Conditional stability for Equation 3-6 (and by analogy the set of

equations represented by Equation 3-7) is satisfied for an unconfined aquifer if the

following stability criterion is met.

$$\Delta t \sum_{j=1}^{n} \alpha_{ij} \leq F_i sy_i \qquad (3\text{-}10)$$

The term on the left side of the equation is equal to the maximum amount of water

that could move into compartment i in one timestep if the head in i is one unit less than

the head in all other connected compartments. The term on the right side of the equation

is the storage capacity available in compartment i for the same head differences before

flow would switch directions. This is analogous to the well-known unconditional

stability criteria for a forward difference explicit 2d square grid solution:

$\Delta t \left[2T_x + 2T_y \right] \leq F * sy$ where T_x, T_y are transmissivities in the x and y direction, and are

doubled because there are two faces in each direction through which water can reach the

square cell of interest (modified from Bear and Verruijt (1987), eq. 9.3.5).

3.2.4 Boundary and Source Terms

Having characterized groundwater flow between compartments with the $\underset{=}{Q_{ij}^t}$

matrix of Equation 3-7, we must describe the boundary and source fluxes to each

groundwater compartment through time (Q_{iS}^t). In a dynamic systems framework, the

source fluxes and boundary terms are coupling points between systems, in particular the

surface water system, atmospheric system, land surface system, socio-economic system,

and other groundwater basins. The source and boundary fluxes can be prescribed head

(Dirichlet or Type 1), prescribed flux (Neumann or Type 2), or mixed (Cuachy or Type

3) boundary conditions. For boundary or source flows described by prescribed flow, the

appropriate boundary flow rate (Q_{iS}^t) is substituted into Equation 3-7. Mathematically,

$$Q_{iS}^t = Q_p \qquad \text{(3-11a)}$$

where

$\quad Q_p \quad = \quad$ prescribed flow rate [L^3/T]

For boundary or source flow described by prescribed head on the boundary, with or

without a leaky membrane condition, flow across the boundary of zone i can be modeled

as

$$Q_{iS}^t = \alpha_{iB}(h_B^t - h_i^t) \qquad \text{(3-11b)}$$

where

$\quad \alpha_{iB} \quad = \quad$ conductance across boundary of compartment i [L^2/T]
$\quad h_B^t \quad = \quad$ boundary head at time t [L]

The α_{iB} coefficient may be head dependent. If there are data to warrant it, and the

boundary flux can be described with Darcy's law, the α_{iB} coefficient can be resolved into

component parts

$$\alpha_{iB} \cong \frac{K_{iB} A_{iB}}{b_{iB}} \tag{3-11c}$$

where

K_{iB} = effective conductivity across the boundary [L/T]

A_{iB} = effective area normal to flow through which that flow occurs [L^2]

b_{iB} = representative distance across which the driving head change occurs [L].

The following section outlines a method for compartment selection and model calibration when a reliable MODFLOW model of the basin already exists.

3.3   Compartmental Model Development Using a MODFLOW Model

If a reliable, spatially distributed MODFLOW model exists, fixed Cartesian grid inefficiencies make it likely that a spatially aggregated, compartmental, groundwater model of the type described above can be developed that will capture a large amount of the MODFLOW model behavior with a fraction of the complexity. A trial-and-error iterative process using the software package ZONEBUDGET for model development is described below. Future research into automation and optimization of compartment delineation holds promise for streamlining this otherwise tedious step.

3.3.1 Define Groundwater Compartments

As discussed above, groundwater compartments should be chosen based on hydrogeologic uniformity, data availability, and resolution desired, which within the context of systems modeling will depend on model purpose as well as on resolution of linked systems. When using a MODFLOW model to develop and calibrate a compartmental model, we are essentially modeling a model. The simplified model can only be as good as the spatially distributed model, with the implicit assumption being that the more complex model represents reality. This is a key assumption to keep in mind when validating and running the simplified model, because even a well-developed MODFLOW model based on an accurate conceptual model is an imperfect and non-unique representation of reality. With that weakness in mind, the strength of the approach lies in the rich dataset provided by the MODFLOW model input and output files. MODFLOW input files can be used to define areas of uniform hydrologic

parameters, as well as areas of acute forcings (e.g., recharge and well pumping).

MODFLOW output files can be used to define areas of uniform head values, steep head

gradients, and large transient drawdown. Using these fields and an overall understanding

of the conceptual groundwater model they describe, compartments should be chosen that

are representative of uniform groundwater behavior. The goal is to choose the number,

size, and shape of the compartments so that at steady state, or on average through the

transient run, MODFLOW flows between the compartments are from compartments of

higher average head to compartments of lower average head. This step sounds trivial, but

depending on the degree of simplification desired can be both challenging and tedious

because flow at a relatively small compartmental interface is being predicted based on the

head average for the entire two compartments sharing that interface. Future work on

automating and optimizing the selection of zone sizes and shapes might help streamline

what is now the most time-intensive step in creation of a spatially aggregated

groundwater model from an existing distributed model. The process for checking the

behavior of the flow between compartments once the compartments have been defined is

outlined below.

3.3.2 Describe Head-Dependent Groundwater Flow Between Compartments

MODFLOW modeled groundwater flow between spatially lumped compartments

can be tracked using the United States Geological Survey (USGS) computer program

ZONEBUDGET (Harbaugh 1990). To start, a cell-by-cell water budget output file for

the calibration period of interest must be generated with the MODFLOW model. This

cell-by-cell budget is specific to the MODFLOW model, and will serve as input to the

ZONEBUDGET routine for all aggregation trials. Once spatially aggregated

compartments have been defined, the average head in each compartment at each timestep

in the MODFLOW model must be calculated. This can be done either by defining the

initial compartment storage, tracking storage changes through time with ZONEBUDGET

storage change output, and relating storage at each timestep to average compartment

head, or by using MODFLOW head fields from each timestep to define average

compartment head. Next, ZONEBUDGET is used to find the groundwater flow between

compartments at each timestep. Finally, rearranging Equation 3-3 and adding explicit

timestep notation, we obtain an equation for the linear flow parameter that equates

differences in head between compartments to flow between those compartments.

$$\alpha_{ij}^t \cong \frac{Q_{ij}^t}{(h_j^t - h_i^t)} \qquad (3\text{-}12\text{a})$$

Physically meaningful flow occurs from compartments of higher head to compartments

of lower head meaning that the linear flow parameter α_{ij} cannot be negative.

$$\alpha_{ij}^t \geq 0 \qquad (3\text{-}12\text{b})$$

Recall that Q_{ij}^t is groundwater flow from compartment j into compartment i at timestep t

such that a negative Q value means flow is into j from i. h_j^t and h_i^t represent average

head in compartment j and compartment i at timestep t. It is important to note that poor

spatial aggregation can lead to situations where a compartment of average higher head

flows to a compartment of lower average head because the average head is not

representative of the contact area between compartments. For this reason we evaluate

Equation 3-12 through time. Solving Equation 3-12a at each timestep for each

compartment and checking the distribution of α_{ab}^{t} for all compartment pairs through

time, including frequency of violation of Equation 3-12b provides metrics that can be

used to evaluate the quality of compartment delineation. For example, one criteria for

acceptable compartment delineation would be that for all compartment pairs, the

arithmetic average of the α_{ab}^{t} values for all timesteps is greater than or equal to zero. In

other words, on average groundwater moves from compartments of higher head to

compartments of lower head. If the acceptability criterion is not met, compartment size,

shape, and/or number must be manipulated appropriately, and the process repeated until a

satisfactory compartment delineation is achieved. This iterative process is diagramed in

Figure 3-3. The acceptable spatial aggregation is used to derive the alpha matrix ($\underline{\underline{\alpha_{ij}}}$) of

Equation 3-8, either by simply taking the temporal averages of each compartment pair

flow parameter array ($\overline{\alpha_{ab}^{t}}$ for all t), or by optimization to match flows in the

compartmental model to flows in the MODFLOW model, constrained by Equation 3-12b.

3.3.3 Calibrate Boundary and Source Flows

With the alpha matrix defining groundwater connectivity and head-dependent

flow, the boundary and source flow terms can be added. The MODFLOW packages

typically used to model source and boundary terms include the recharge package, the well

package, the evaportranspiration (ET) package, the river package, the stream-aquifer

package, and the drain package, of which the recharge and well package model specified

flux terms, while the others model head-dependent fluxes. Because of the

1. Define groundwater compartments

2. Describe head-dependent groundwater flow between compartments

MODFLOW model

Cell by cell storage or head fields

Groundwater compartments

Cell by cell budget

Matlab or other script

ZONEBUDGET routine

Average compartment head at each timestep: h^t

Flow from compartment to compartment at each

Matlab or other script

No

Acceptable α_{ab}^t distribution?

Linear flow parameter for each compartment pair at each timestep: α_{ab}^t

Yes

Take temporal average of linear flow parameter arrays, or use an optimization scheme to get a single α_{ab} value for each compartment pair. This parameter is NOT time dependent, so need a single value for each compartment pair to describe groundwater flow in the compartmental modeling scheme.

3. Calibrate boundary and source flows

4. Compare spatially aggregated model with spatially explicit MODFLOW model

Figure 3-3. Visual representation of compartmental model development from a more spatially distributed MODFLOW model. Emphasis given to description of head-dependent groundwater flow parameters.

interdependence of fluxes, especially head-dependent fluxes, as a general rule, the constant or specified boundary and source flows should be calibrated or added first, followed by groundwater head-dependent fluxes, followed by groundwater head- and surface-water-dependent fluxes as applicable. In practice this usually means starting with recharge and well fluxes, then moving to ET, and finally to the more complex river and drain interactions, with iterations through the more complex calibrations until the overall calibration is satisfactory.

3.3.3.1 Specified Flux Terms

If the relevant atmospheric and land surface systems are being modeled, natural recharge can be linked dynamically to the appropriate groundwater compartments. If human behavior and demand systems are being modeled, artificial and crop recharge, and well use can also be linked dynamically to the appropriate groundwater compartments. If these systems are not being modeled to a sufficient degree to estimate recharge or well demand, these terms can be specified with values from the associated MODFLOW input files. In all cases, the trivial equation 11a is used to populate the specified flux terms.

3.3.3.2 Head-Dependent Flux Terms

Head- and/or stage-dependent flux terms describing interaction between surface and groundwater systems including river leakage/gain and drain capture can be calculated using Equation 3-11b when the systems are hydrologically connected and Equation 3-11a otherwise. Calibration of head-dependent flux terms as modeled by the compartmental model to the same flux terms modeled by MODFLOW can be done by manipulation of

the alpha term as a lumped parameter, or, where appropriate, by calibration of the most

poorly understood or measured portions of the constant term (Equation 3-11c). For

example, if we are using Equation 3-11b to model river leakage, and the river area (A) is

well characterized, we might choose to calibrate the flux by adjusting the sediment

conductivity divided by sediment thickness term ($\frac{K}{b}$). If the sediment thickness is well

characterized also, we may decide to adjust the bed sediment conductivity value only.

Mathematically it makes no difference, but keeping track of the individual components of

the constant term and adjusting those that are less well understood has advantages in

comparison of calibrated parameters between the spatially aggregated model and the

MODFLOW model, as well as in connectivity to other systems that may use the same

constants in other calculations. If the lumped calibration approach is used, a new

constant should be created in the model structure with no association to the component

constants.

Once calibration is complete, the spatially aggregated compartmental model is a

stand-alone model of reduced complexity imitating to some degree the groundwater

system behavior as represented by the MODFLOW model. The next step in model

development is evaluation to determine if the model is sufficient for its designed purpose,

or if it should be refined further.

3.3.4 Evaluate Spatially Aggregated Model

Because spatially distributed groundwater models require three-dimensional parameter and initial condition fields that are rarely if ever experimentally available, calibration of groundwater models is a famously non-unique exercise (e.g., Neuman and Wierenga 2003, pp. 35-36). This problem has led some researchers to argue that complex groundwater models cannot be validated at all (Konikow and Bredehoeft 1992). Validation of the MODFLOW model, and the associated debate, though important, are beyond the scope of this discussion. Clearly the MODFLOW model being spatially aggregated must be meaningful before any attempt is made to reproduce it at a different spatial scale. Insofar as a reliable MODFLOW model exists that is used and trusted by decision makers, a spatially simplified version can be a very useful part of systems-level interactive modeling. In the case of spatial aggregation of a reliable MODFLOW model, the evaluation is an exercise to see how well the spatially simplified model can capture the behavior of the MODFLOW model for the calibration period, and what will be called a robustness analysis period where the magnitudes of forcings (source and boundary fluxes) are different from those of the calibration period. Useful comparison metrics include the magnitude of groundwater flows between compartments through time, drawdown through time, and magnitude of head-dependent source fluxes through time. A root mean square error (RMSE) or other error function can be used to evaluate goodness of fit. These validation metrics can be summarized in table form as shown in Table 3-1.

Table 3-1. *Example evaluation table for spatially aggregated model comparison to MODFLOW model.*

Comparison Metric	Calibration Period	Robustness Analysis Period
Groundwater Flows (Q_{ab}^{t})	RMSE or other error function	RMSE or other error function
Drawdown	RMSE or other error function	RMSE or other error function
Head-Dependent Flux i: e.g., ET	RMSE or other error function	RMSE or other error function

Typically if a MODFLOW model has a historic calibration and future prediction period, model output from these can be used as the calibration and robustness analysis periods respectively for the spatially aggregated model. The robustness analysis may involve changing a single stress systematically and watching the effect on model comparison. For example, pumping from a single well or all wells in a certain area could be multiplied by 0.7, 0.85, 1.15, and 1.30, and for each change the behavior of the MODFLOW and spatially aggregated models compared. The idea of these metrics is to get a sense of to what degree and under what circumstances the spatially aggregated groundwater model can be considered a good representation of the source MODFLOW model.

3.4   Case Studies in the Rio Grande River-Aquifer System

The remainder of this chapter will discuss application of the spatially aggregated modeling theory described above to three contiguous groundwater basins along the Rio Grande river system in New Mexico. The three basins of interest, the Albuquerque Basin, the Espanola Basin, and the Socorro Basin, underlie the Rio Grande river system from the Rio Chama confluence in the north to Elephant Butte Reservoir in the south. Figure 3-4 shows the spatial relationship of the three basins of interest.

3.4.1   The Albuquerque Groundwater Basin

3.4.1.1   Albuquerque Basin Model Development

Using the techniques described in Section 3.3, a compartmental model with 51 compartments (zones) was developed as a spatially simplified representation of a large (over 100,000 cells) MODFLOW model used to describe groundwater flow in the Albuquerque Basin in New Mexico (McAda and Barroll 2002). The McAda and Barroll MODFLOW model extent is shown in Figure 3-5, and underlies the Rio Grande from above Cochiti Reservoir to San Acacia. The development of a spatially aggregated version of the McAda and Barroll model is described below.

3.4.1.1.1 Define Albuquerque Basin Groundwater Compartments (zones)

The sequence of steps necessary for compartmental model development from a MODFLOW model, as shown in Figure 3-3 and discussed previously, begins with delineation of groundwater compartments or zones. Because a driving goal for the reduced spatial resolution groundwater model for Albuquerque Basin was to create
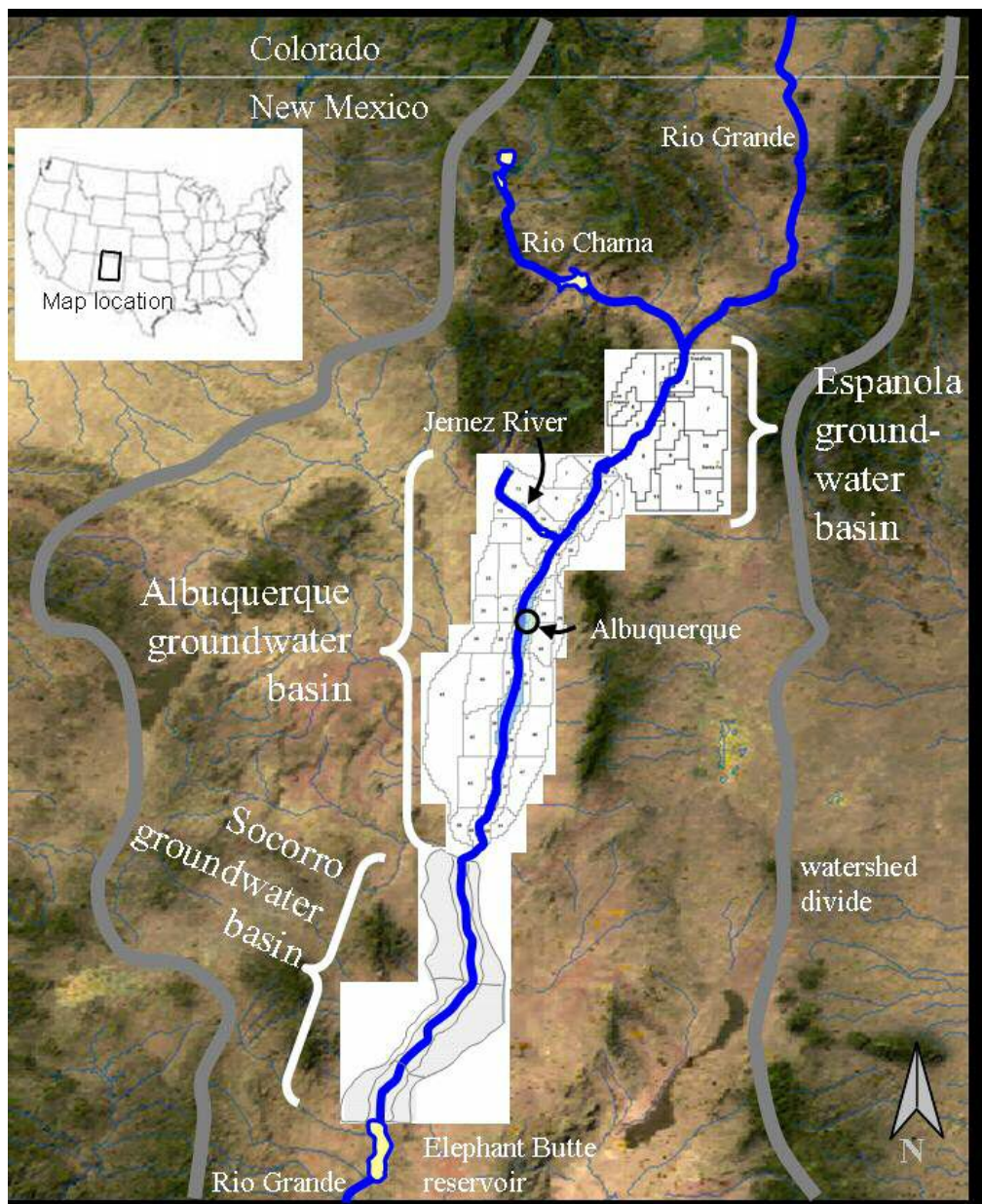
Figure 3-4. Geographic locations and model extent of the spatially aggregated groundwater models of the Espanola, Albuquerque, and Socorro groundwater basins in New Mexico.

dynamic groundwater surface water linkages, groundwater zones were chosen to be

coincident with surface water gages. Specifically, the gages of interest for the

Albuquerque Basin include the USGS gages located on the Rio Grande below Cochiti

Dam (USGS Gage number 08317400), near San Felipe (08319000), in Albuquerque

(08330000), near Bernardo (0832010), and near San Acacia (08354900), and the gages

located on the Jemez River near Jemez Springs (08324000), and below Jemez Canyon

Dam (08329000). Together these gages define five river reaches in which calculated

mass balance changes can be compared to gage readings. A second factor used in initial

zone demarcation is the presence of high-conductivity sediments located in close

proximity to the river. These alluvial sediments are relatively dynamic from a

groundwater perspective, with a strong seasonal signal as water is gained from river,

canal, and crop seepage, and lost to agricultural drain capture and riparian vegetation ET.

These hydrologically active alluvial sediments act differently enough from the rest of the

aquifer that they can be conceptualized as a shallow alluvial aquifer on top of a more

stable regional aquifer. The first two layers of the MODFLOW model near the river were

set up to be coincident with these high-conductivity sediments (McAda and Barroll 2002,

p. 20), and spatial aggregation efforts defined the shallow aquifer to include only the top

two MODFLOW layers. Initial efforts to create a compartmental model for description

of the groundwater flow system broke the basin into four zones per river reach, a shallow

alluvial zone, and three regional zones, for a total of 20 zones. Once these zones were

chosen (step 1 in Figure 3-3), the alpha matrix ($\underline{\underline{\alpha_{ij}}}$) was calculated for the zones as

follows.

3.4.1.1.2 Albuquerque basin alpha matrix determination

Using Equation 3-12a, at each model timestep the ratio of flows to head

difference can be calculated for each zone pair.
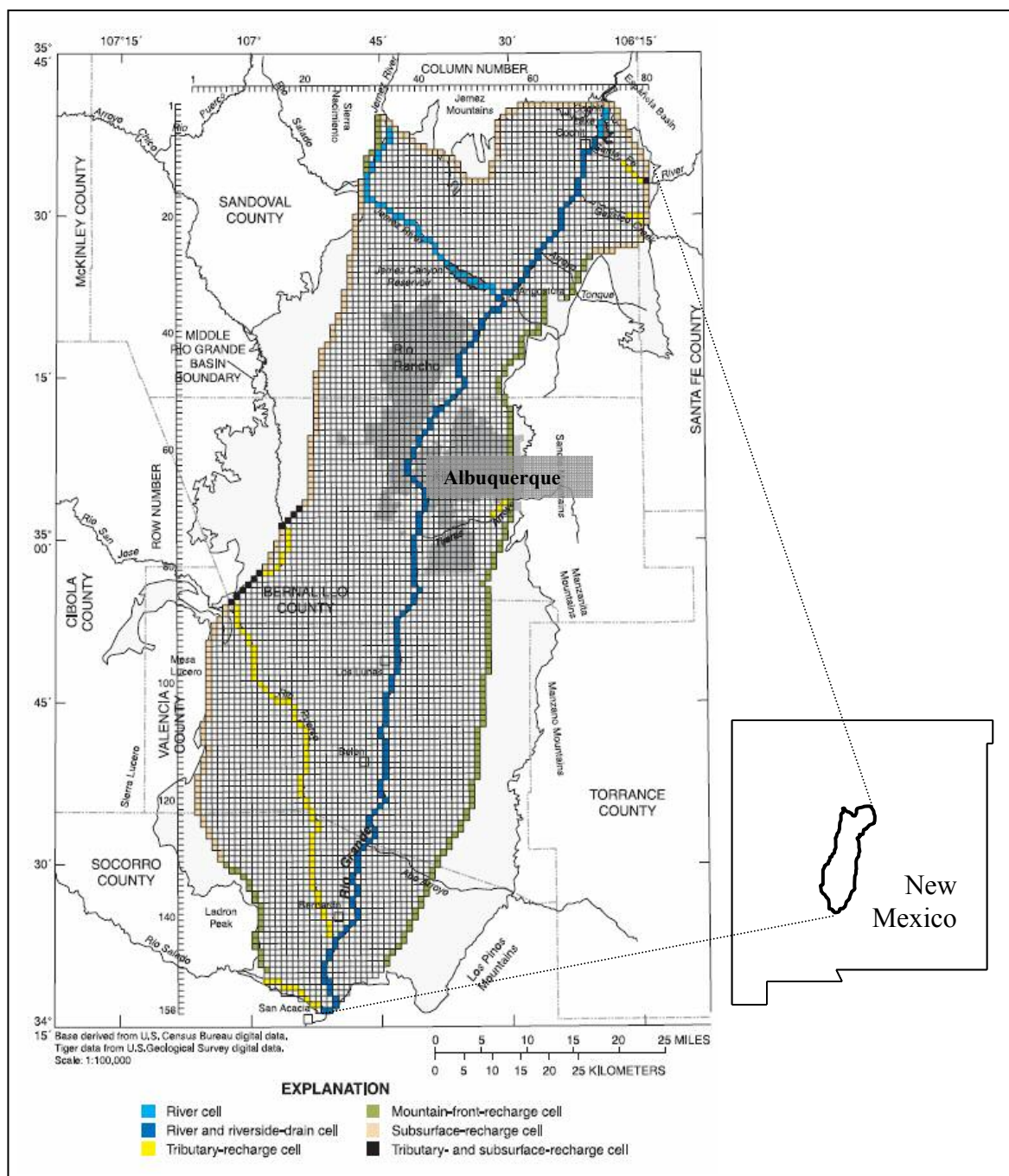
Figure 3-5. Albuquerque Basin MODFLOW model extent.
Modified from McAda and Barroll (2002), Figure 7.

$$Q_{ij} = \alpha_{ij}(h_j - h_i) \Rightarrow \alpha_{ij} = \frac{Q_{ij}}{h_j - h_i} \qquad [L^2/T] \qquad\qquad (3\text{-}13)$$

A non-negative time averaged value suggests that on average, MODFLOW flow is from a zone of higher average head to a zone of lower average head (see previous discussion associated with derivation of Equation 3-12). The zonal geometry was altered in search of a zone geometry that would result in non-negative average alpha values over all timesteps for all zone pairs. When the initial 20 zone delineation did not prove satisfactory, additional zones were added using hydrogeological and source flux data to reduce the number of negative time averaged alpha values. This process was accomplished through trial and error, with a 51-zone model finally satisfying the non-negative alpha requirement for all zone pairs except one. The one negative average alpha value was for flow between shallow aquifers north and south of Central Bridge in Albuquerque (near a significant pumping-induced cone of depression), and was set to a positive value based on alpha values and contact areas for other shallow aquifer to shallow aquifer contacts. The final zone geometries for the 51-zone compartmental model are shown in Figure 3-6. The alpha matrix, zone bottom elevations, and January 1975 initial zone heads for the 51-zone model can be found in Appendix A, Tables A-1 and A-2. A specific yield value of 0.2 is used in all compartments, consistent with the McAda and Barroll model.

3.4.1.1.3 Albuquerque Basin Source and Boundary Fluxes; Definition and Calibration

It is important to note that within a systems context, nearly all of the boundary and source terms may be functions of the operation of other interdependent systems. In a fully integrated systems model, systems affecting groundwater source terms include the land surface system (mountain front and tributary recharge), other groundwater basins (subflow), the surface water system (canal recharge, river leakage, drain capture), and the human behavioral system (canal, septic, and crop recharge). A significant advantage to systems-level modeling is that linked systems add constraints to make model realizations less non-unique. The amount of water that moves out of the surface water system into the groundwater system must be considered in both systems. A key purpose of the spatial aggregation described here is to facilitate dynamic linkages to other systems, specifically a previously existing monthly timestep surface water model. For this reason, the spatially aggregated groundwater model was set up to run on a monthly timestep, and fluxes between the surface water and groundwater system were set up to take advantage of monthly surface water information. The integration of the surface water system to the groundwater system necessitated some departures from the McAda and Barroll estimated fluxes between surface water and groundwater, and is discussed later in this chapter. The immediate discussion will focus on initial calibration of the spatially aggregated groundwater model to fluxes from the McAda and Barroll model for purposes of evaluating the performance of the compartmental groundwater model.

3.4.1.1.3.1 Fluxes Independent of Groundwater Head (specified flux boundary conditions)

Albuquerque basin fluxes treated as independent of groundwater head by McAda and Barroll and the initial calibration of the compartmental model include well extraction, specified flux groundwater flow along model margins, and recharge from surface sources that are not connected hydrologically to the aquifer, including recharge from the mountain front, ephemeral and tributary channels, disconnected streams, irrigation canals, irrigated crops, and septic tanks. These terms are applied as appropriate in the compartmental model using Equation 3-11a.

3.4.1.1.3.2 Fluxes Dependent on Groundwater Head

Source or boundary fluxes modeled as groundwater head dependent by McAda and Barroll include aquifer interaction with hydrologically connected surface water including the Jemez and Rio Grande rivers and the Jemez Canyon and Cochiti Reservoirs, agricultural drains, and ET. These fluxes as well as irrigation canal leakage are modeled as groundwater head dependent in the compartmental model.

3.4.1.1.3.2.1 River and Reservoir Leakage

In the 51-zone compartmental model, Jemez and Rio Grande river-aquifer interactions, irrigation canal leakage, and reservoir-aquifer interactions were modeled by combining Equations 3-11b and 3-11c as follows:
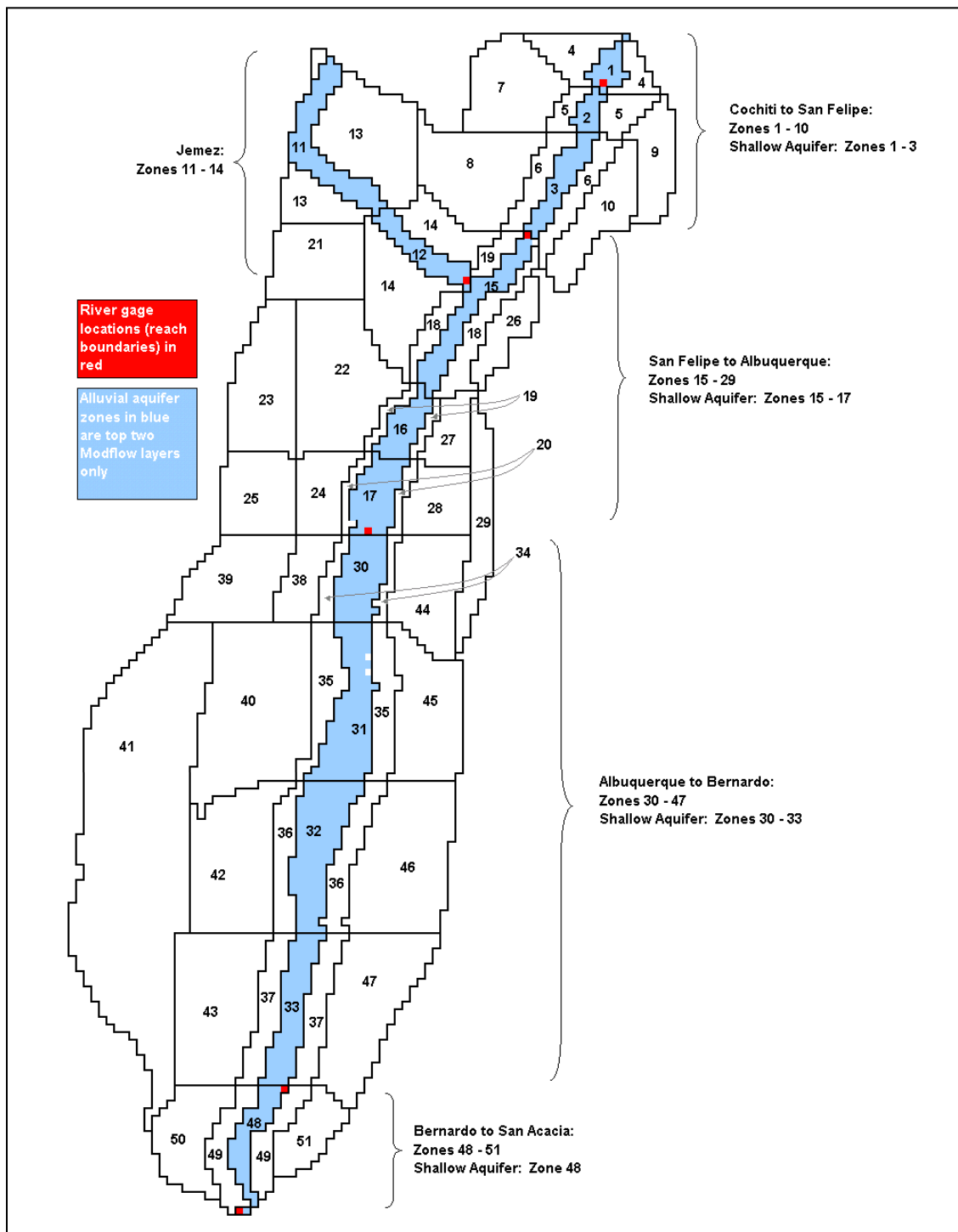
*Figure 3-6. Groundwater zones for the spatially aggregated
compartmental flow model of the Albuquerque groundwater basin.
Zones filled with blue are alluvial aquifer zones, and include only the
top two MODFLOW layers. Other zones include all MODFLOW layers.*

$$Q_{i-SWGW} = \frac{K_{i-bed}F_{i-bed}}{b_{i-bed}}(z_{i-sw} - \beta)\begin{cases} \beta = z_{i-bed} & if \quad z_{i-bed} - b_{i-bed} \geq h_i \\ \\ \beta = h_i & if \quad z_{i-bed} - b_{i-bed} < h_i \end{cases} \qquad (3\text{-}14)$$

where z_{i-sw} is the surface water elevation; z_{i-bed} is the elevation of the top of the bed

sediments; b_{i-bed} is thickness of the flow limiting bed sediments; K_{i-bed} is the saturated

hydraulic conductivity of the flow limiting bed sediments; h_i is the groundwater head; all

terms are specific to compartment i; and all head and elevation terms are defined based

on a common datum. Equation 3-14 describes hydrologically separate flow when

groundwater head is below the flow-limiting sediments, and head-dependent flow to or

from the surface water system otherwise, and is consistent with the conceptual approach

used by MODFLOW in the river package (McDonald and Harbaugh 1988). For the Rio

Grande, bed thickness (b_{i-bed}) and bed conductivity (K_{i-bed}) were set to 5 feet and 0.5

feet/day respectively consistent with a value of 0.1 day^{-1} for $\dfrac{K_{i-bed}}{b_{i-bed}}$ used by McAda and

Barroll (2002). For river leakage in the Rio Grande, Equation 3-14 was calibrated by

modifying the river bed elevation of each shallow aquifer compartment within an

acceptable range. River bed conductivity K_{i-bed} was also adjusted during calibration of

the shallow aquifer north of Albuquerque, where spatial aggregation seems to result in

larger leakage near the cones of depression than is predicted by the MODFLOW model.

For the Jemez River, bed thickness was set to 1 foot consistent with McAda and Barroll,

and both bed elevation and river bed conductivity adjusted during calibration. For

reservoir leakage, values of river bed thickness and river bed conductivity were adjusted

during calibration. Jemez Reservoir was assumed hydrologically separate from the

groundwater system. For irrigation canals, canal conductivity was set to 0.15 feet per day

consistent with estimates cited by McAda and Barroll (2002), and canal bed thickness to

two feet consistent with McAda and Barroll (2002) values after calibration. Calibrated

parameters for river and reservoir leakage are shown in Appendix A, Table A-3.

Determination of surface water elevations will be described after consideration of drain

flows.

3.4.1.1.3.2.2 Drain Capture

In unconfined aquifers where groundwater flow to a surface water sink is

predominantly horizontal, and there is no significant seepage face, a Dupuit-

Forchheimer-based approach may be used to model flux (e.g., Fetter 1980, eq. 5-59).

This approach was used to model groundwater flow to the agricultural drains:

$$Q_{DUP} = \frac{K_{i-a}L_i}{x_i}(h_i{}^2 - z_{i-sw}{}^2) \qquad (3\text{-}15)$$

where K_{i-a} is the hydraulic conductivity of the aquifer compartment, L_i is the length of

the drain, x_i is a characteristic distance beyond which the drain has negligible effect on

groundwater head, and all terms are specific to compartment i. All other terms are as

defined previously. Equation 3-15 is expressed as double the typical Dupuit-Forchheimer

equation to represent flow to a drain from two sides. Drain elevations were set to 5 feet

below the corresponding river bed elevation, and flow to the drains was calibrated by

adjusting aquifer conductivity (K_{i-a}) and characteristic length values (x_i). Calibrated

parameter values for the drains are shown in Appendix A.

Surface water stage (z_{sw}) for reservoirs was taken from historic data, while

surface water stage for rivers and drains was found at each timestep by iterative solution

of Manning's equation for open channel flow:

$$Q_{MAN} = \frac{1.49 \; A \; R^{2/3} S^{1/2}}{n} \qquad \text{(3-16a)}$$

where Q_{MAN} is discharge in cubic feet per second, S is the dimensionless drain slope, n is

the dimensionless Manning coefficient of roughness, A is the cross-sectional area of flow

in square feet, and R is the hydraulic radius in feet (e.g., Grant and Dawson 1997, p. 130).

For a channel with vertical sides,

$$A = (z_{sw} - z_{bed}) * W \qquad \text{(3-16b)}$$

$$R = \frac{A}{2(z_{sw} - z_{bed}) + W} \qquad \text{(3-16c)}$$

where W is the channel width. Groundwater fluxes from the river are small compared to

surface water fluxes, and thus have negligible effect on surface water discharge and

stage. In the case of drains, however, groundwater movement is the primary source of

any surface water flow in the drains. The amount of water that will move to the drain

depends on the stage in the drain, which itself determines how much water will move

through the drain as surface flow. For this situation, an iterative solution was necessary

to find the surface water stage that resulted in surface flow in the drain equivalent to flow

to the drain from the groundwater system. In the Albuquerque basin model, an iterative

solution was used to find a drain stage (z_{sw}) that would result in a Dupuit-Forchheimer

predicted groundwater flow to the drain (Equation 3-15) equal to a Manning-based

surface water flow out of the drain (Equation 3-16a). A Manning coefficient of 0.028

was used for the river and drain channels. Average drain width was assumed to be 10

feet. River width was calculated by dividing river area (Table 2-12) by reach length

(Table 2-4). River and drain slope were assumed equal (drains only work by having a

slope slightly less than the river slope, however this difference was assumed negligible),

and were calculated by dividing the elevation difference of the reach defining gages

(Table 2-2) by the reach length (Table 2-4). Reach slopes are included in Table A-3 of

Appendix A. River discharge values come from the surface water model, which is

calibrated to USGS historic gaged flows.

3.4.1.1.3.2.3 Evapotranspiration

ET is modeled as a head-dependent flux based on McAda and Barroll (2002). ET

is 5 feet/year when water level is at or above the land surface, and decreases linearly to

2 feet/year when depth to groundwater is 9 feet, then decreases linearly from there to

0.75 feet per year when depth to groundwater is 16 feet, then decreases linearly from

there to 0 feet/year when depth to groundwater is 30 feet, and is 0 feet/year for all

groundwater depths greater than 30 feet below the surface (McAda and Barroll 2002, p.

38). This same relationship is used in the compartmental model. In mathematical form:

$$Q_{iET} = ET_{i-ref} F_{i-ET} * \theta \begin{cases} \theta = 1 \quad if \quad (z_{i-surf} - h_i) < 0\,ft \hfill (3\text{-}17) \\[2mm] \theta = 1 - \dfrac{2(z_{i-surf} - h_i)}{30} \quad if \quad 0\,ft \le (z_{i-surf} - h_i) \le 9\,ft \\[2mm] \theta = 0.4 - \dfrac{(z_{i-surf} - h_i) - 9}{28} \quad if \quad 9\,ft \le (z_{i-surf} - h_i) \le 16\,ft \\[2mm] \theta = 0.15 - \dfrac{3(z_{i-surf} - h_i) - 48}{280} \quad if \quad 16\,ft \le (z_{i-surf} - h_i) \le 30\,ft \\[2mm] \theta = 0 \quad if \quad (z_{i-surf} - h_i) > 30\,ft \end{cases}$$

where ET_{i-ref} is -5 feet/year for all i, F_{i-ET} is the area of vegetation using groundwater

in compartment i, h_i is groundwater head in compartment i, and z_{i-surf} is the surface

elevation of compartment i, with all elevations defined from the same datum used to

define groundwater head. Equation 3-17 was calibrated to McAda and Barroll estimated

ET fluxes by adjusting the representative surface elevation (z_{i-surf}) of shallow aquifer

compartments containing riparian vegetation (all except the shallow aquifer underlying

Cochiti Reservoir). Calibrated surface elevations are listed in Appendix A, Table A-5.

3.4.1.1.4 Evaluation of Albuquerque Basin Spatially Aggregated Model

Within the context of this discussion, evaluation refers to ascertaining the extent

to which the spatially aggregated model can capture the salient behavior of the spatially

distributed McAda and Barroll model in both calibration and predictive periods. For

general discussion of this step, see Section 3.3.4. The evaluation of the Albuquerque

Basin spatially aggregated groundwater model makes up the bulk of Section 3.4.1.2.

3.4.1.2 Albuquerque Basin Results

With the initial goal of replicating the McAda and Barroll (2002) MODFLOW model of the Albuquerque Basin as closely as possible with 51 zones, the reduced resolution Albuquerque basin groundwater model was implemented using Equations 3-7 through 3-9 to describe flow between groundwater zones.

3.4.1.2.1 Internal Groundwater Movement

Spatial aggregation leads to a loss of spatial head distribution information, which affects the ability to predict both internal groundwater flows and head-dependent source and boundary flows. To see the effect on predicted internal groundwater flows alone, the spatially aggregated model was implemented with source terms ($\underline{Q}_{iS}^{t}$ in Equation 3-7) from the McAda and Barroll model, meaning both models are being forced by the same source terms. Figures 3-7a and 3-7b compare modeled groundwater flows between zones under these conditions. Figure 3-7a shows the absolute value of all predicted flows between zones for the 51-zone model compared to the absolute value of all flows between the same zones in the McAda and Barroll model. The average difference between total groundwater flows between zones predicted by the two models is less than 1%. Transient high reservoir storage episodes account for the increased movement "hump" seen between 1985 and 1988, and reservoir-induced recharge and groundwater pumping both lead to the trend of increased overall groundwater movement. Seasonal oscillations are seen beginning in 1990 when the MODFLOW model goes from an annual timestep to a biannual timestep based on a 7.5-month growing season, and a
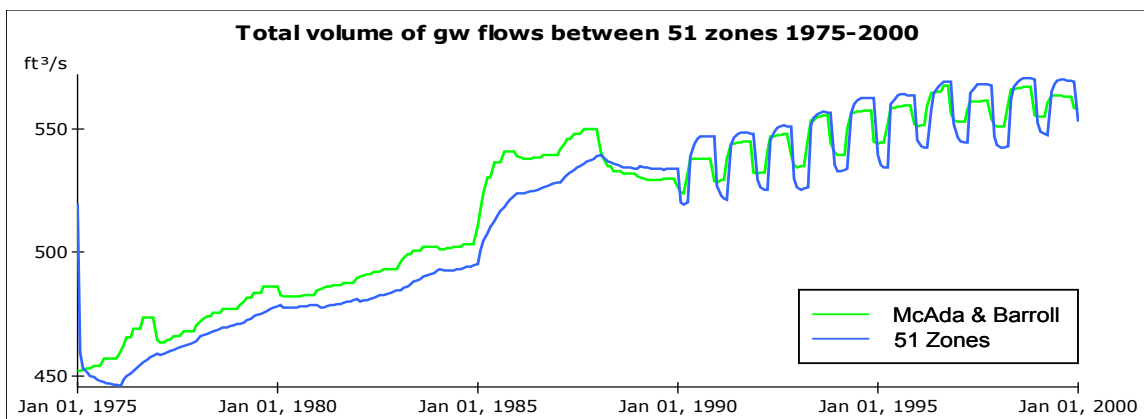
Figure 3-7a. Absolute value of predicted flow between 51 zones compared to McAda and Barroll values. The y-axis shows the summed absolute value of flows between any two zones.

4.5-month nongrowing season. The lower left plot in Figure 3-7b shows flows from the shallow aquifer north of Central Bridge in Albuquerque (zone 17) to the shallow aquifer to the south (zone 30). The 51 zone model predicts southward flow only, while the McAda Barroll flow switches to northward around 1985. (See Section 3.4.1.1.2 for additional discussion of this particular zone to zone flow.) In general, though lacking spatial resolution, the 51-zone compartmental model captures the overall patterns of groundwater movement predicted by McAda and Barroll under the same set of forcings.

Figure 3-8 shows 1975 to 2000 groundwater drawdown as predicted by the two models. The 51 zone model is able to capture the spatial nature of the driving changes to the Albuquerque groundwater system between 1975 and 2000, namely mounding under the leaky and young (closed in 1975[7]) Cochiti Reservoir in the north, and groundwater pumping induced drawdown under Albuquerque and Rio Rancho in the center of the basin.

---

[7]   http://www.fws.gov/southwest/mrgbi/Resources/Dams/#cochiti
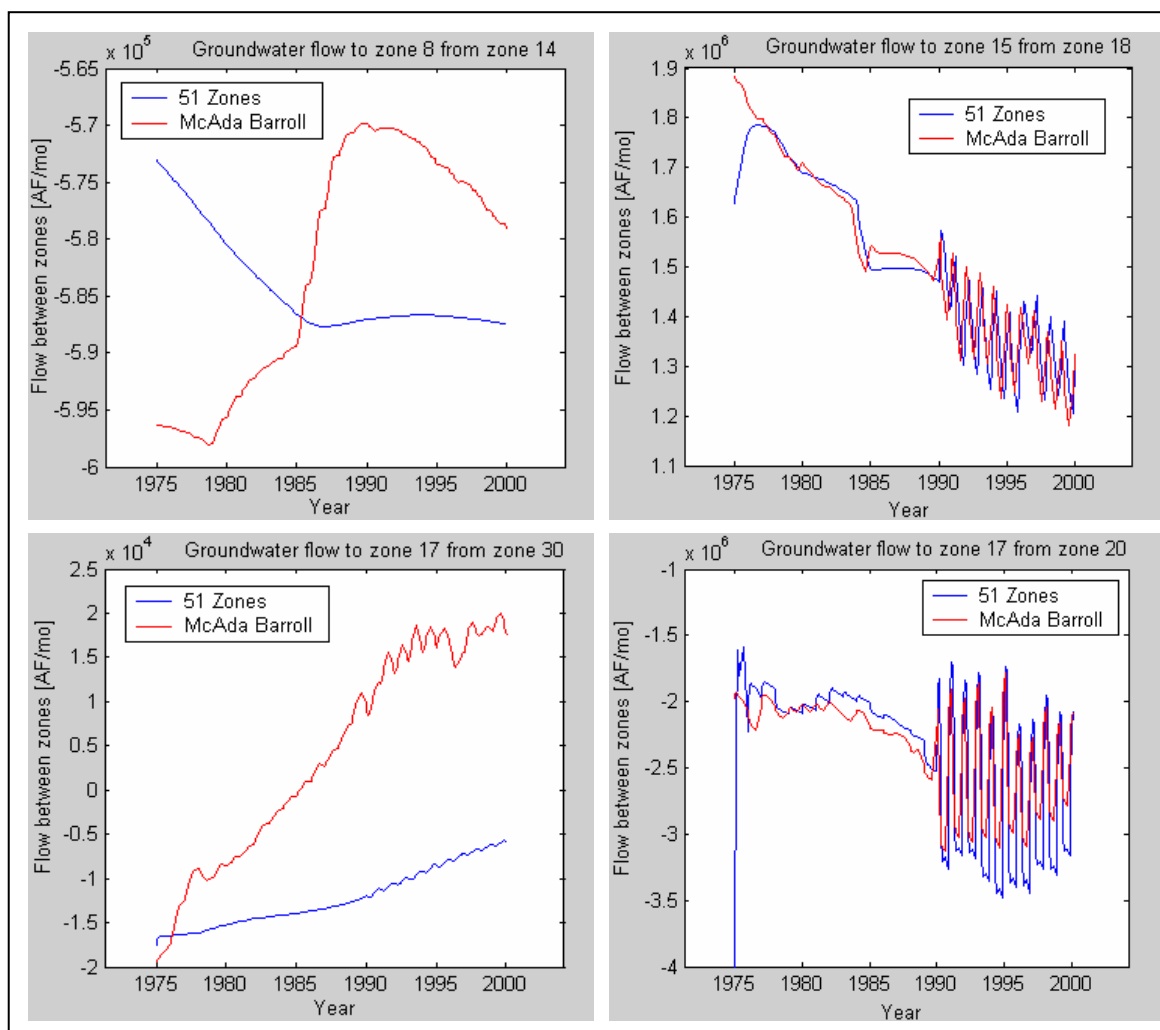
Figure 3-7b. Groundwater flow between selected zones in the Albuquerque basin model. The zones selected represent extremes of poor (left) and good (right) fits to McAda Barroll (2002).

3.4.1.2.2 Boundary Fluxes

Specified flux terms in the two models are the same. Head-dependent flux terms include river and reservoir leakage, drain capture, and ET, modeled in the 51-zone model with Equations 3-14, 3-15, and 3-17 respectively, with surface stage from Equation 3-16.
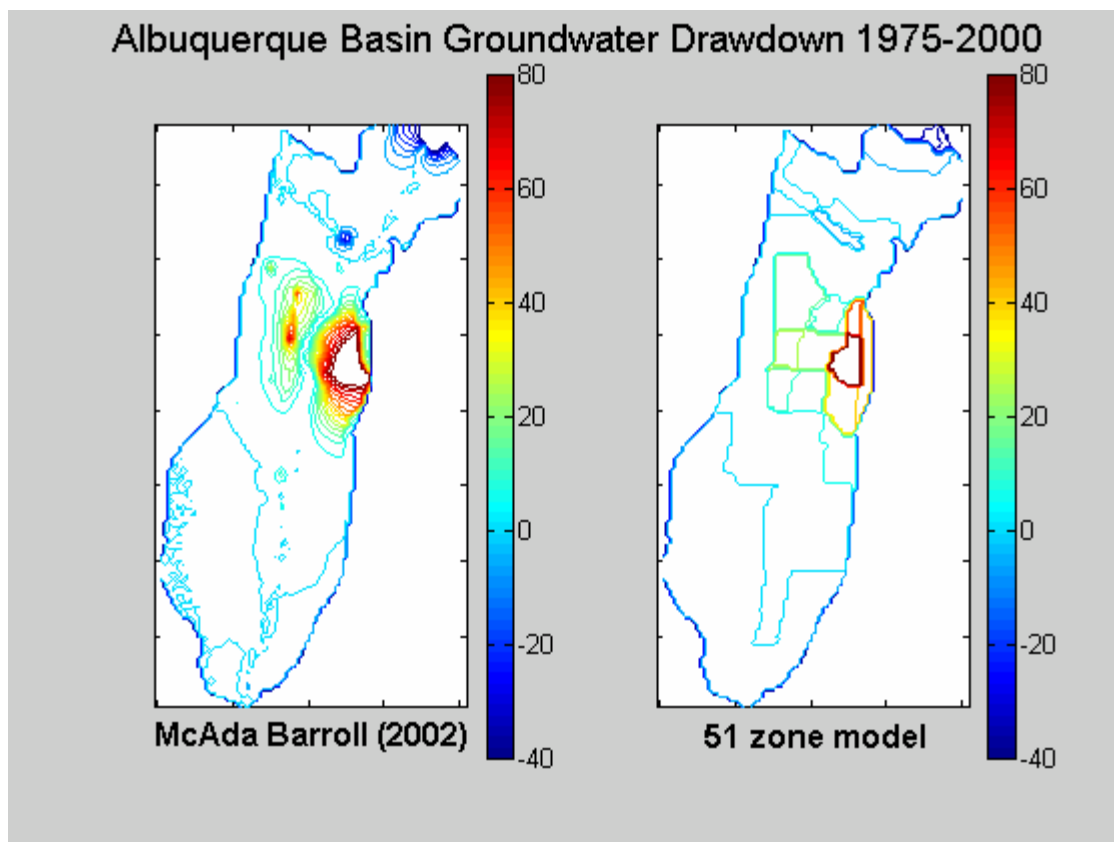
Figure 3-8. Drawdown in the Albuquerque Basin from 1975 to 2000 as modeled by McAda and Barroll (2002), and with the 51-zone compartmental groundwater model. Both models show the dominant patterns of mounding in the north from Cochiti Reservoir, and drawdown in the center due to municipal groundwater use.

3.4.1.2.2.1 River, Irrigation Canal, and Reservoir Leakage

Figure 3-9 shows the head-dependent river leakage simulated by each model from 1975–2000 for the Jemez and Rio Grande rivers. Cumulative leakage for the 25-year period served as the calibration target, and is approximately 8 million acre feet (MAF) for both models. The difference in magnitude of fluctuations is a result of temporal resolution differences between the models, with the compartmental model using monthly data and the MODFLOW model using annual data until 1990, and biannual (growing and nongrowing seasons) data from 1990–2000. River leakage is driven in large part by river

stage, which varies significantly at a monthly timestep, to a lesser degree in a biannual timestep, and negligibly when averaged across an entire year.

Simulated Cochiti and Jemez Reservoir leakages are shown in Figures 3-10 and 3-11. Again, the cumulative leakages for the 25-year period (400,000 AF for Cochiti and 60,000 AF for Jemez) served as the calibration targets, and are the same for both models. Differences in temporal resolution are evident; however, the compartmental model does replicate the basic system behavior represented by the McAda and Barroll model.
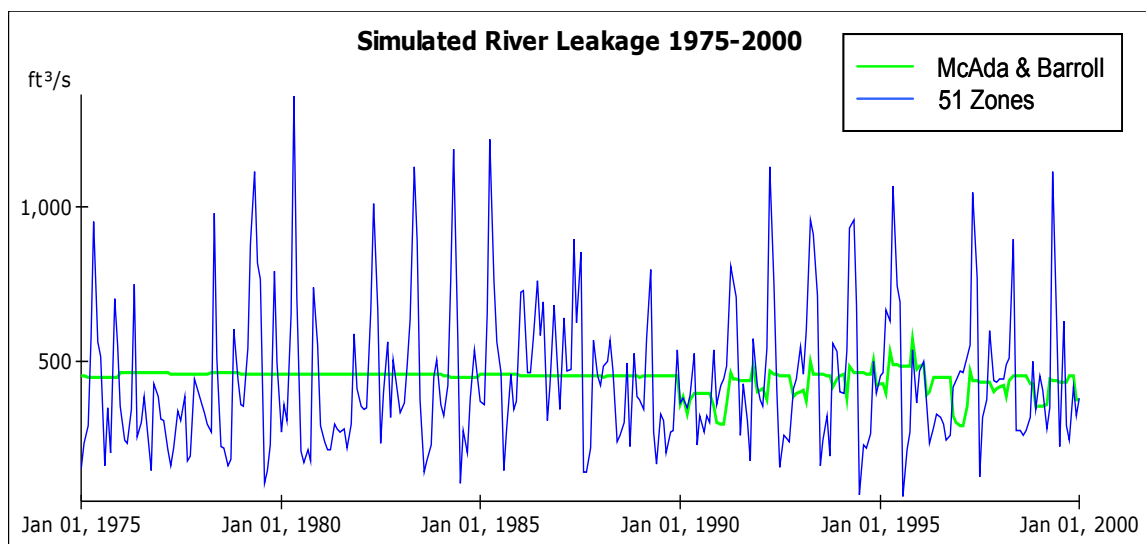
Figure 3-9. *Head-dependent river leakage in Jemez River and Rio Grande from below Cochiti Reservoir to San Acacia, as modeled by McAda and Barroll (2002), and the 51-zone spatially aggregated model for the period from 1975 to 2000.*

Simulated Cochiti Reservoir Leakage 1975-2000
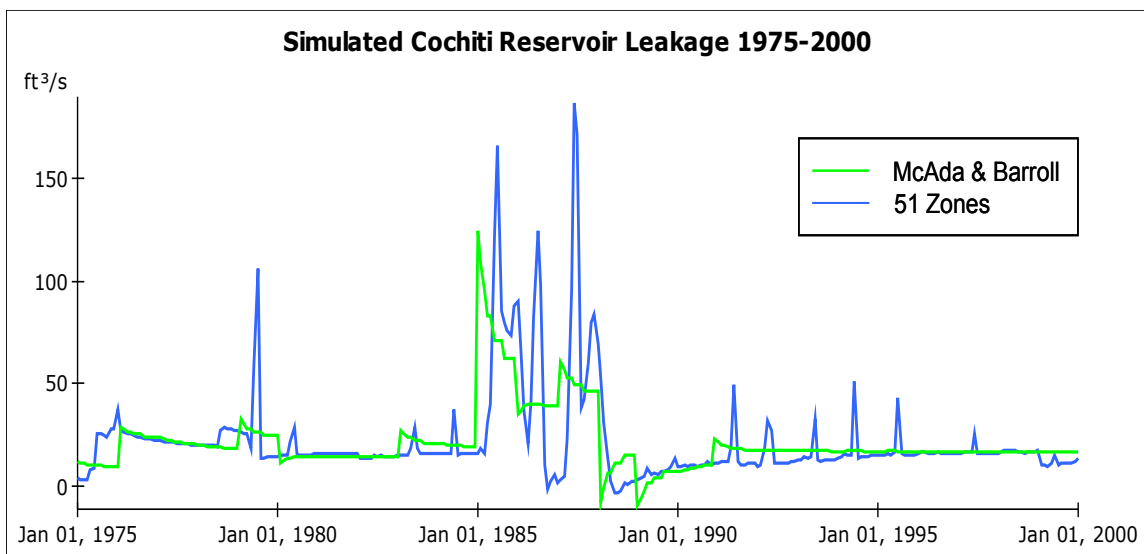
Figure 3-10. *Head-dependent reservoir leakage in Cochiti Reservoir, as modeled by McAda and Barroll (2002), and 51-zone spatially aggregated model for the period from 1975 to 2000.*

Simulated Jemez Reservoir Leakage 1975-2000
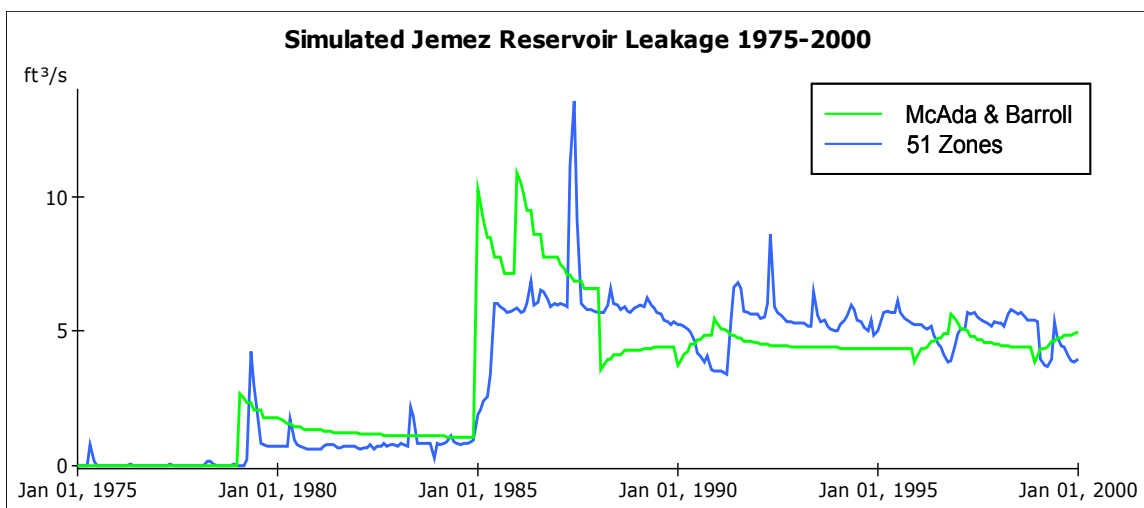
Figure 3-11. *Head-dependent reservoir leakage in Jemez Reservoir, as modeled by McAda and Barroll (2002), and 51-zone spatially aggregated model for the period from 1975 to 2000.*

3.4.1.2.2.2 Drain Flow

Groundwater flow to the drains is modeled in the spatially aggregated model with

the Dupuit-Forchheimer approach shown in Equation 3-15, while it is modeled with a

flow-limiting bed approach similar to Equation 3-14 in the McAda and Barroll model.

Table A-4 in Appendix A lists specific parameters used to model drain capture in the

Albuquerque basin with Equation 3-15. As shown in Figure 3-12, the Dupuit-

Forchheimer approach captures the overall behavior of the groundwater system, with

cumulative drain capture in the compartmental model calibrated to match the McAda and

Barroll estimate of 9 MAF in 25 years. Seasonal fluctuations again are due to a finer

temporal resolution and the shallow aquifer responding to significant seasonal river

leakage fluctuations. As is the case in the McAda and Barroll model (2002, p. 62), the

drains capture a significant amount of the river leakage, and thus seasonal variations in

river leakage are reflected in seasonal variations in drain flow.
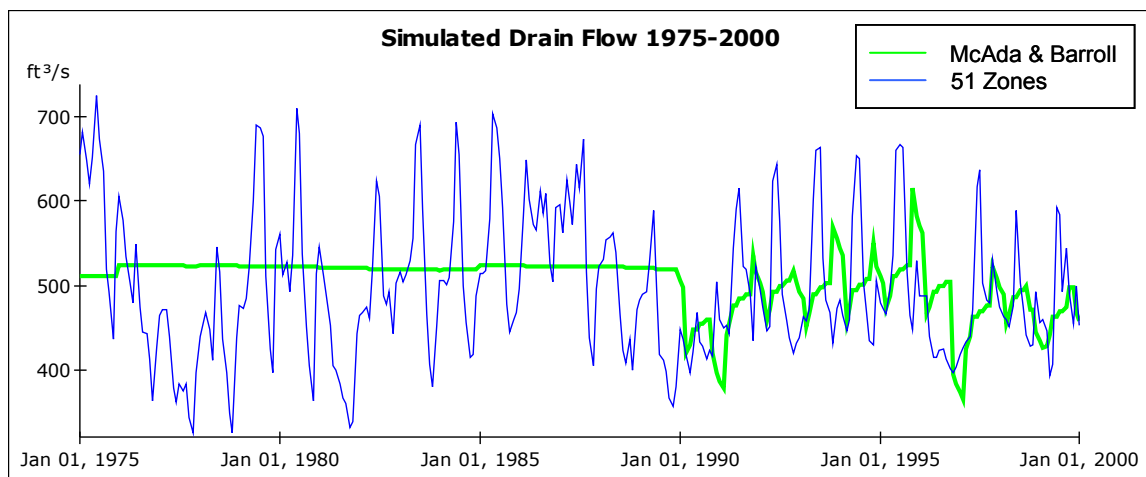
Figure 3-12. Head-dependent flow to drains, as modeled by McAda and Barroll (2002), and the 51-zone spatially aggregated model for the period from 1975 to 2000.

3.4.1.2.2.3 Riparian ET

Figure 3-13 shows simulated riparian ET in the two models for the 1975 to 2000

calibration period. Surface elevations resulting in the model behavior shown in Figure 3-

13 are shown in Table A-5 in Appendix A. ET drops slightly beginning in 1984 because total riparian area before 1984 is estimated with a 1975 United States Bureau of Reclamation (BoR) spatial dataset (~145 km^2), and after 1984 with a 1992 BoR spatial dataset (~126 km^2) (McAda and Barroll 2002, p. 38). The visible match between models is easiest to see after 1990 when the MODFLOW model begins using seasonal data.
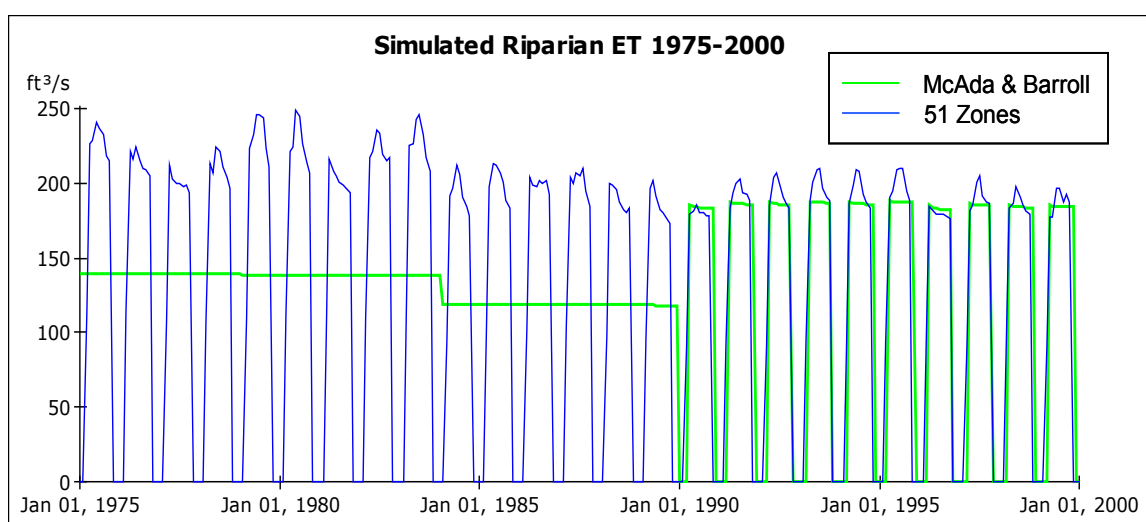
Figure 3-13. Head-dependent riparian ET as modeled by McAda and Barroll (2002), and 51-zone spatially aggregated model for the period from 1975 to 2000.

With head-dependent fluxes calculated based on average compartmental head, the 51-zone model is a stand-alone representation of the Albuquerque basin groundwater system. Figure 3-14, a corollary to Figure 3-7a, shows the total groundwater fluxes predicted between zones for the stand-alone model and McAda and Barroll's model. Although the average error between predicted flows is still less than 1%, there is a visible drop-off in how closely the compartmental model tracks the MODFLOW model. Part of that is due to lack of spatial resolution, and part is also due to the increased seasonality of boundary fluxes that can be represented with a monthly timestep. Incorporation of

dynamic head-dependent fluxes to the compartmental model does not result in significant

changes to the drawdown patterns shown in Figure 3-8 (Figure A-1, Appendix A).

Overall, considering the level of spatial aggregation associated with the 51-zone

model, it is able to capture salient groundwater system behavior during the calibration

period, and thus provides a reasonable approximation to groundwater system behavior

when system forcings are within the range of those seen in the past. The next section

describes the behavior of the stand-alone compartmental model compared to the McAda

and Barroll (2002) model for model forcings outside of the historic range.
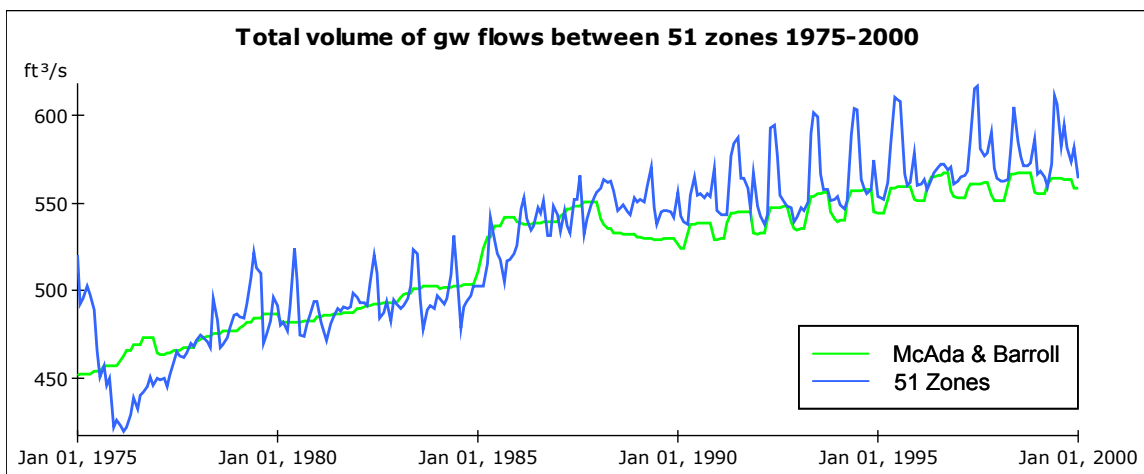
Figure 3-14. Total groundwater fluxes predicted between zones for the stand-alone model and McAda and Barroll model. At each timestep, the absolute value of all flows between any two zones is summed as a comparison metric to help evaluate the ability of the 51-zone compartmental model to capture the overall groundwater movement patterns. The average difference between the modeled total flows is less than 1%. As compared to Figure 3-7a, Figure 3-14 tracks simulated flows for the compartmental model with internally calculated head-dependent boundary flux terms.

3.4.1.2.3 Robustness Analysis

The results shown so far in this section suggest that the 51-zone, spatially

aggregated compartmental groundwater model is able to capture the salient behavior of

McAda and Barroll's more highly spatially resolved MODFLOW groundwater model during the calibration period. The next step is a "robustness analysis"[8], in which the results of the two models are compared for groundwater use scenarios that differ from conditions observed during the 1975-99 calibration period. In the case of the Albuquerque Basin, this comparison is facilitated by existing analysis of the McAda and Barroll (2002) model for three different groundwater use scenarios for the city of Albuquerque from 2001-2040 (Bexfield and McAda, 2003). For their analysis, Bexfield and McAda used three different pumping scenarios for the city of Albuquerque. The high pumping scenario assumed all projected Albuquerque demand between 2001 and 2040 would be satisfied by groundwater pumping. The medium pumping scenario froze Albuquerque groundwater pumping at 2000 levels for the 2001 to 2040 period. The low pumping scenario assumed that Albuquerque would use direct diversion of surface water from the river as a primary source of water, with groundwater pumping used to augment the surface supply. Projected demand and projected available surface water supply were based on calculations and a synthetic climate sequence used by the City of Albuquerque (Bexfield and McAda 2003 p.9). For simplicity, only the low and high pumping scenarios are considered here. Figure 3-15 shows the pumping in the Albuquerque area assumed for the two simulations.

---

[8] The word "validation" is consciously avoided here to make it clear that the 51 zone model is an abstraction from a more spatially resolved model, which is itself a non-unique abstraction of a very complex physical system. If the 51 zone model is able to capture the salient behavior of the McAda and Barroll MODFLOW not only during calibration, but under forcings significantly different from calibration forcings, it may be considered a reasonable representation of the groundwater system for the purpose of rapid, first level, basin scale scenario analysis.
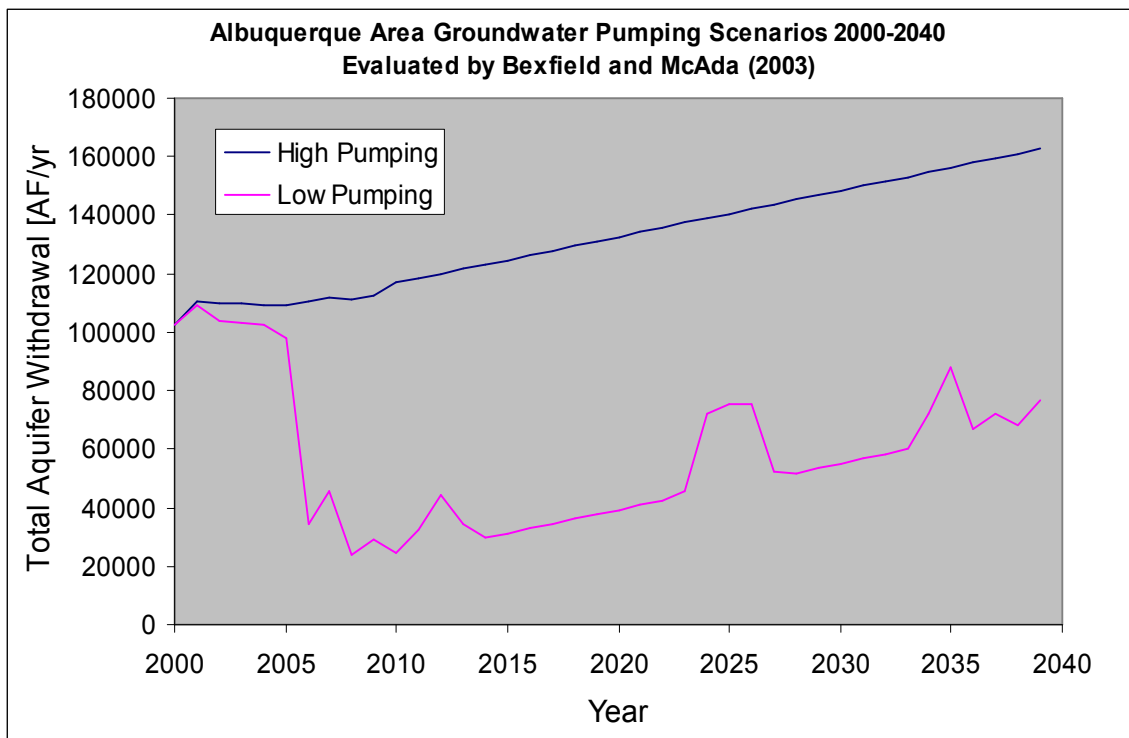
Figure 3-15. Albuquerque area scenario groundwater pumping. "High Pumping" assumes projected Albuquerque demand met with groundwater only. "Low Pumping" assumes a combination of surface water as available, augmented with groundwater.

As was the case in the calibration period, to match specified model forcings, the spatially aggregated model was forced with MODFLOW specified recharge and well extraction terms for the robustness analysis. Riparian ET, drain flow, and river and reservoir leakage were calculated within the spatially aggregated model. For consistency with MODFLOW, Cochiti reservoir stage and area were set to 5340 feet amsl and 1120 acres respectively for the entire 2000 to 2040 model run. Jemez reservoir stage and area were set to 5190 feet amsl and 1000 acres respectively, also constant for the entire robustness analysis period. Bexfield and McAda (2003) divided a synthetic series of historic streamflow data into three divisions: below the 25th percentile of streamflow, between the 25th and 75th percentile, and above the 75th percentile. Each of these groups

was averaged to come up with a characteristic river stage and area associated with dry, average, and wet conditions during the irrigation and non-irrigation stress periods (semi-annual temporal resolution). The spatially aggregated model calculates river stage and area on a monthly basis based on river flows. To roughly reproduce the MODFLOW climate sequence, annual total Cochiti reservoir releases from 1975-1999 were sorted from smallest (driest) to largest (wettest). The monthly values from the six driest years (1977,1981,1990,1996,1978,1976) were averaged to represent the monthly flows for the driest 25% of years. The six wettest years (1993,1987,1995,1985,1979,1986) and middle 13 years were similarly treated to represent the monthly flows for the wettest 25% of years, and average 50% of years respectively. Finally, each year of the 2001-2040 scenario run was classified as dry, average, or wet based on the irrigation stress period in river package input file of the MODFLOW model. Years specified as dry are: 2007, 2009, 2012, 2016, 2024-26, 2035, 2040. Years specified as wet are: 2008, 2014, 2018, 2020-22, 2028, 2030, 2036. Remaining years are specified as average. Gaged tributary inflows and waste water discharge 2000 to 2040 were set to average values for the 1975-1999 period. Albuquerque diversions from the river were set to the difference between the high pumping and low pumping scenarios, and Albuquerque waste water returns were set to average for 90-99 period, plus ½ of the difference in pumping between 1999 values and the high pumping scenario values.

Figure 3-16 shows annual net surface water contribution to the aquifer from the combined river and drain system. The spatially aggregated model is able to track overall water movement patterns predicted by the Bexfield and McAda model for both pumping

scenarios, however the year to year variability is significantly dampened. Recall from

discussions of figure 3-9 and 3-12, that use of a monthly timestep results in greater

variability in river stage and thus river leakage and resulting drain flow within a given

year for the 51 zone groundwater model than the biannual MODFLOW model.

However, despite greater intra-annual variability in river leakage and drain flow, the

spatial aggregation of the 51 zone model leads to a dampening of response in the

groundwater system to inter-annual changes in overall magnitude of river leakage. The

MODFLOW lines in Figure 3-16 show climate variability from year to year that is

dampened in the 51 zone model. Both models suggest that under the high pumping

scenario, around 2015, the net contribution of the river leakage less drain capture goes

from net gains to the surface water system to net gains to the groundwater system. This

type of consistency between models suggests that the 51 zone model can be used with

relative confidence for first order scenario analysis.

Figure 3-17 shows the change in ET in each model as a result of pumping

changes. Note that the range of Figure 3-17 is 16,000 AF/yr as compared to 100,000

AF/yr in Figure 3-16. Clearly both models suggest that river leakage and drain capture

will be far more influenced by changes in pumping regime than will riparian ET. In both

models, the majority of the ET response to reduced pumping occurs between 2010 and

2020 after the dramatic drop in pumping which begins in 2006 in the reduced pumping

scenario (see Figure 3-15).
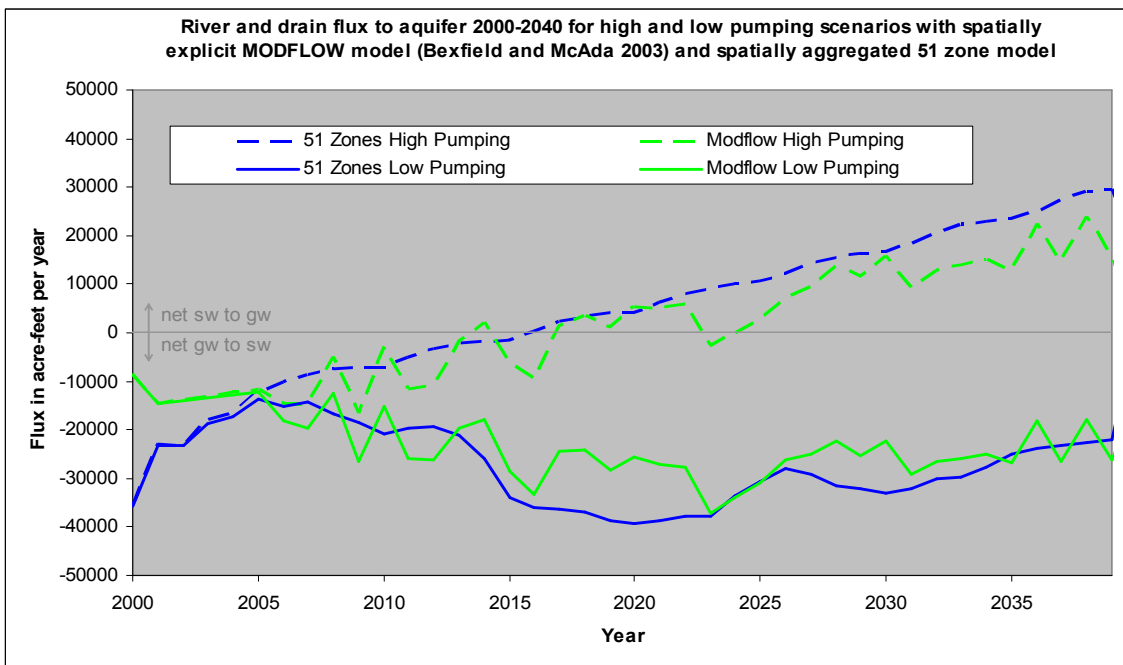
Figure 3-16. Robustness analysis combined river leakage and drain capture flux to aquifer. The magnitude of fluxes is well represented by the 51 zone model, though year to year variability is dampened as a result of the spatial aggregation.
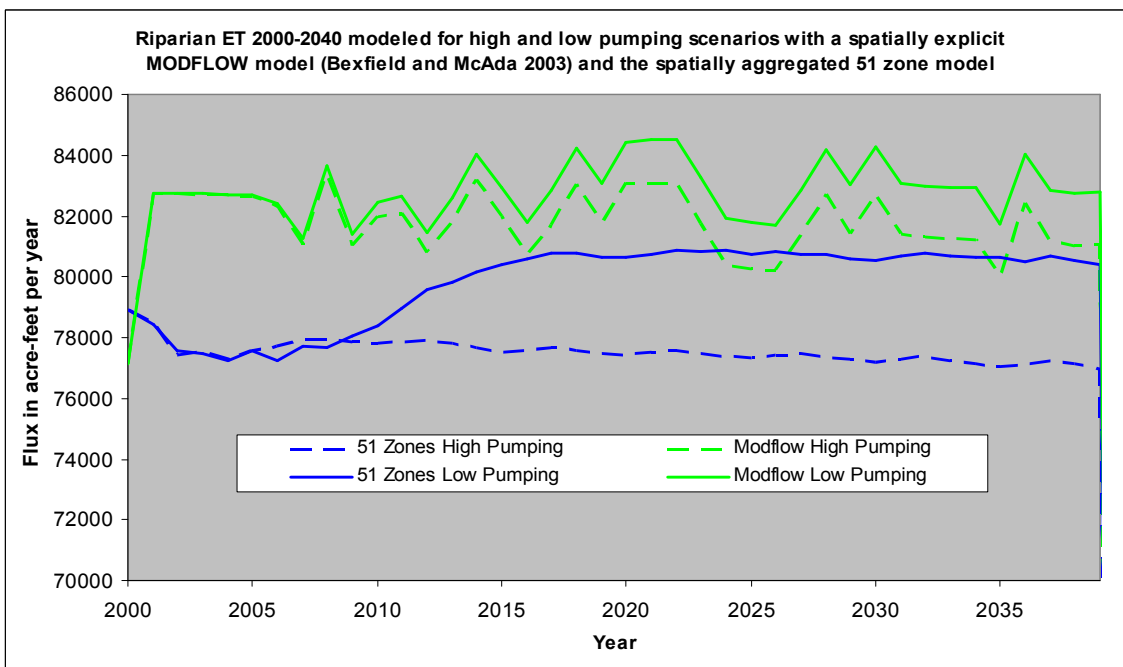
Figure 3-17. Riparian ET flux from Albuquerque basin during robustness analysis. Note the scale. ET in the 51 zone model is more sensitive to pumping, though the difference between the high and low pumping ET at year 40 is less than 5% of the annual ET flux.

Figure 3-18 shows aquifer storage change predicted by each model for the two pumping scenarios. Because storage change in the entire aquifer is essentially a function of specified and head dependent fluxes, the specified fluxes are equal, and as seen in Figures 3-16 and 3-17, the head dependent fluxes match reasonably, it is not suprising to see that storage change predicted by the 51 zone model follows that predicted by the Bexfield and McAda (2003) model to a reasonable degree. Overall, the spatially aggregated 51 zone model appears to be a reasonable proxy of the spatially resolved MODFLOW model, even outside the range of calibration conditions.
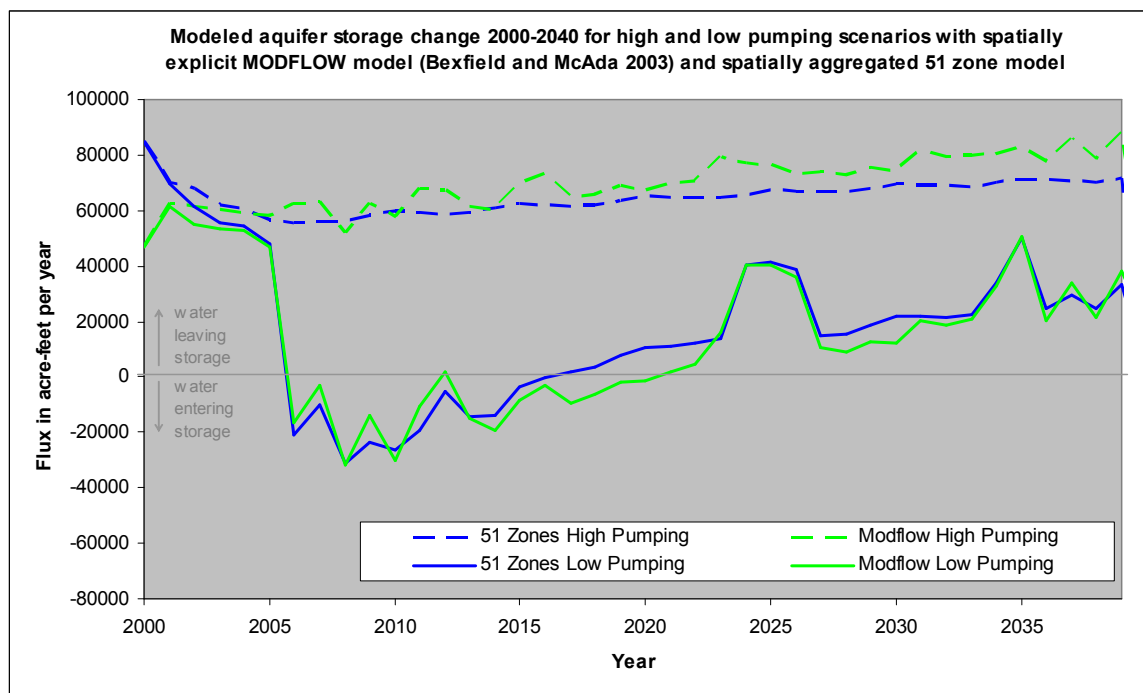
Figure 3-18. Aquifer storage change during robustness analysis.
The spatially aggregated model tracks overall modeled storage changes.

The ability of the spatially aggregated model to capture the behavior of the MODFLOW model during the robustness analysis period can be compared to the same

ability during the calibration period by using the root mean squared error (RMSE) of model outputs as the comparison metric. The comparison metrics are derived on an annual basis for the groundwater zones in and around Albuquerque only. This temporal and spatial resolution is chosen for comparison purposes because the McAda and Barroll (2002) model uses an annual stress period before 1990, and a semi-annual stress period based on irrigation season from 1990 forward, and the Bexfield and

McAda (2003) model is based on changing pumping regimes for the municipal pumps serving the greater Albuquerque area only. In general, the spatially aggregated model would be expected to match the behavior of the spatially explicit model more closely during calibration than during robustness analysis, however as seen in Table 3-2, this is only true for ET. The same comparisons made at a monthly basis for the Albuquerque area, or at a monthly or annual basis for the entire model extent, yield a better match to the MODFLOW model(s) during the robustness analysis than the calibration period for all metrics. This unexpected improvedperformance during future conditions is likely a result of two factors. First, McAda and Barroll (2002) use constant river stage for the 1975 to 1990 period resulting in constant estimates of river leakage, while the monthly model uses historic flows, resulting in large inter-annual variability in the surface water stage dependent river leakage term. The result is large differences between the models' predictions of annual river drain flux and thus aquifer storage change during the calibration period, as seen in Table 3-2. Second, during the scenario analysis period, all model drivers are held constant, with the exception of three hydrologic year types, and Albuquerque pumping. The historic period on the other hand

is driven by constantly changing pumping regimes and river and reservoir conditions. The relatively stable future conditions assumed in the groundwater basin outside of Albuquerque allow both models to approach a dynamic equilibrium in the majority of the basin, resulting in similar model performance in these areas. Though unexpected, this result suggests that our ability to predict future groundwater conditions is limited more by our inability to predict future model stresses, than by the errors associated with spatial aggregation of the groundwater model. Given that the future is inherently unknown, the spatially aggregated model provides a legitimate proxy to the more complex MODFLOW models for rapid scenario evaluation of a wide range of alternative futures.

Table 3-2. Evaluation table for spatially aggregated 51 zone model compared to McAda-Barroll Bexfield-McAda MODFLOW models.

Comparison Metric	1975-1999 Calibration Period (McAda and Barroll MODFLOW model)	2000-2040 Robustness Analysis Periods (Bexfield and McAda MODFLOW model)
RMSE Aquifer Storage Change [AF/yr]	80000	5900
RMSE River-Drain Flux to GW [AF/yr]	23000	4600
RMSE ET Flux from GW [AF/yr]	700	1800

3.4.1.2.4 Integration of Groundwater System and Surface Water System

Several major changes were made to the calibrated groundwater model described above to allow for connection to the surface water model described in Chapter 2. It was necessary to increase Cochiti Reservoir leakage to the groundwater system for consistency with the reservoir mass balance. It was also necessary to combine the atmospheric and head dependent constraints on riparian evapotranspiration represented in the surface water and groundwater models respectively, and finally adjustments were

made to calibration parameters to balance both the surface water and groundwater systems within the constraints of historic surface water flow data.

3.4.1.2.4.1 Cochiti Reservoir Recalibration

When the groundwater leakage for Cochiti Reservoir shown in Figure 3-10 was incorporated into a surface water model of Cochiti storage, the modeled reservoir storage exceeded the historic stage-based estimates, as shown in Figure 3-19. The surface water reservoir mass balance includes estimates of precipitation gains and evaporative losses, and inflows from an upstream gage, modified by modeled losses and groundwater gains from the Espanola Basin (see Section 3.4.2.2) in the reach between the gage and the reservoir. The excess modeled reservoir storage suggests an underestimate of losses or an overestimate of gains to the reservoir. There are no direct measurements of reservoir leakage; McAda and Barroll (2002) estimated Cochiti leakage with a surface water mass balance (p. 37), but that water balance may not have included groundwater gains from the Espanola Basin of approximately 12 cubic feet per second (cfs) between the Otowi gage and Cochiti Reservoir (see Section 3.4.2.2) that are included in the surface water model used here. The relative leakiness of Cochiti is supported by anecdotal evidence of waterlogging of fields downstream of Cochiti Reservoir after its completion that necessitated expensive drainage projects and mandates limiting the target storage pool in the reservoir (Smith 2001, p. 98). Of the flows into and out of the reservoir, groundwater leakage and ungaged runoff into the reservoir are the most difficult to quantify. Without

Cochiti Reservoir Modeled and Historic Storage with MODFLOW Magnitude Leakage
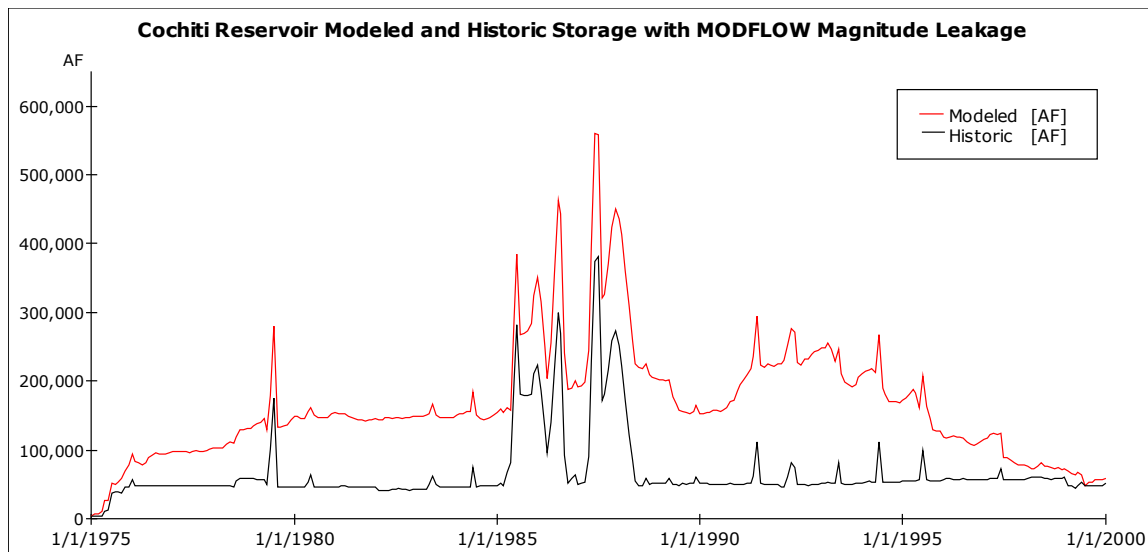
Figure 3-19. Cochiti Reservoir modeled with McAda and Barroll MODFLOW magnitude leakage. Reservoir leakage is likely underestimated, resulting in a model with too much water in the reservoir.

Cochiti Leakage Compared to McAda Barroll 2002 MODFLOW Model
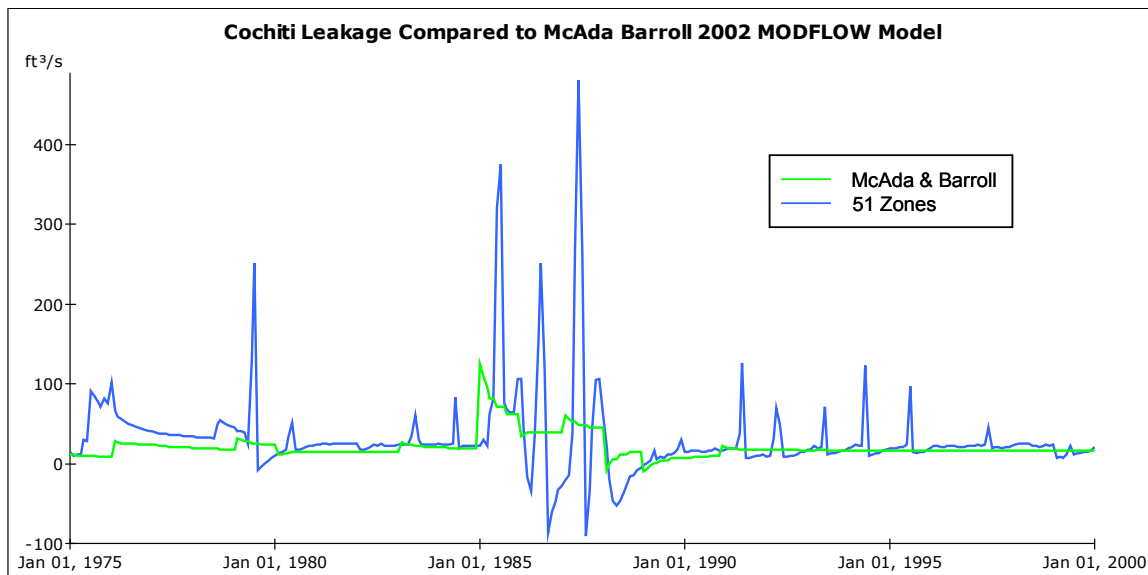
Figure 3-20. Cochiti Reservoir modified (increased) leakage (compare to Figure 3-10) to improve mass balance in the reservoir.

considering ungaged runoff, the model has too much water in the reservoir, and so increased groundwater leakage is the most plausible adjustment to be made within the constraints of the surface water balance. Leakage in the reservoir was increased on

average by approximately 7,700 AF per year (11 cfs) for the historic period to attain mass

balance in the reservoir. The historic calibrated leakage is shown in Figure 3-20. The

increased leakage in high-storage events results in drainage of groundwater back to the

reservoir when the reservoir volume is rapidly reduced. This is physically plausible, and

happens in the MODFLOW model as well.

Interestingly, during calibration of the Albuquerque basin MODFLOW model,

McAda and Barroll increased tributary recharge from the nearby Santa Fe River and

Galisteo Creek by 1,500 AF per year over initial estimates. It is plausible that

underestimates of Cochiti Reservoir leakage in the MODFLOW model led modelers to

increase nearby stream recharge. The increased leakage in Cochiti also made calibration

of the surface water reach downstream easier.

3.4.1.2.4.2 Evapotranspiration as a Function of Groundwater Head and Atmospheric Variables

Recall Equation 3-17, rewritten in a simplified form below for convenience:

$$Q_{iET} = ET_{i-ref} F_{i-ET} * \theta \tag{3-17}$$

ET_{i-ref} is the maximum ET rate possible, F_{i-ET} is the spatial area over which that

evaporation occurs, and θ is a groundwater-dependent function that goes from unity

when depth to groundwater is zero, to zero when depth to groundwater is greater than the

rootzone, which in the McAda and Barroll (2002) MODFLOW model is 30 feet. In the

McAda and Barroll model, as in most groundwater models, ET_{i-ref} is a constant,

independent of atmospheric conditions or plant type. On the other hand, surface water

models often estimate phreatophytic ET based on atmospheric conditions and plant type information, with no regard to groundwater availability. The monthly surface water model to which the 51-zone groundwater model is coupled uses a modified Penman Monteith reference ET equation based on atmospheric conditions, and a plant coefficient based on vegetative properties. This approach is consistent with that of a daily timestep operations model known as the Upper Rio Grande Water Operations Model (URGWOM) (USACE et al. 2002), which makes use of an ET engine called the ET Toolbox (ETTB) (Brower 2004). To make phreatophytic evapotranspiration a function of atmospheric demand, vegetative properties, and groundwater availability, the approaches were combined as described below.

In the surface water model, the maximum predicted riparian (phreatophytic) evaporation for the 1975–1999 monthly average climate conditions averages approximately 3.5 feet per year. In the McAda and Barroll model, ET of 5 ft/yr occurs when depth to the groundwater is zero, and this rate drops linearly to 2 ft/yr when depth to groundwater is 9 feet. Thus the surface water approach is consistent with the MODFLOW approach for an average depth to groundwater of 4.5 feet. This suggests that the surface water model riparian vegetation crop factors may have been developed for riparian vegetation that on average had a depth to water of about 5 feet. The implication of this hypothesis is that when both atmospheric potential and depth to groundwater are constraints to riparian ET, the atmospheric potential rates must be adjusted upward to be consistent with a situation where groundwater levels are not limiting at all to ET rates. For purposes of this modeling effort, a correction factor of 1.3

was found by trial and error, and applied to bosque, cottonwood, and salt cedar riparian plant coefficients (see Section 2.2.3.2.3) in the surface model to account for this effect. Grass and marsh crop coefficients were not changed as it was assumed that these species can only use groundwater resources when depth to groundwater is essentially zero. The ET_{i-ref} term became the maximum potential ET rate for the species in question as calculated in the surface water model, including the calibration adjustment of 1.3 to woody phyreatophte species. Riparian ET volumes predicted by the McAda and Barroll groundwater model, the URGWOM surface water model, and the coupled approach for the Rio Grande corridor from Cochiti to San Acacia are shown in Figure 3-21.
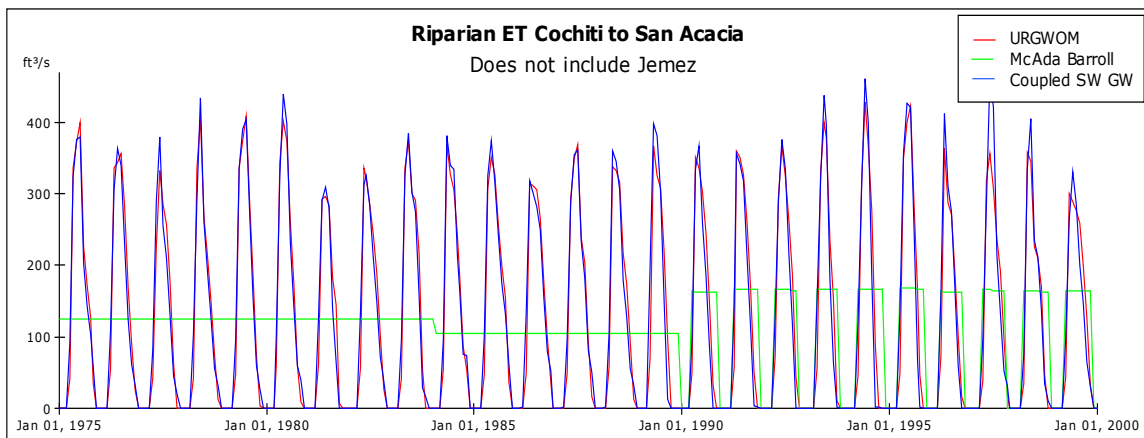
Figure 3-21. Riparian ET 1975–1999 for Rio Grande reaches from Cochiti to San Acacia as modeled by the coupled monthly timestep model, the URGWOM surface water model, and the McAda and Barroll (2002) regional groundwater model. Jemez ET is not included in the graph because it is not represented explicitly in URGWOM.

3.4.1.2.4.3 Connection To Dynamic Espanola Basin Groundwater Model

The Albuquerque groundwater basin is hydrologically connected to the Espanola groundwater basin to the northeast. McAda and Barroll (2002) assume a constant inflow

of 10,000 AF per year from the Espanola Basin. As will be described in the next section,

a spatially aggregated groundwater model of the Espanola Basin has also been developed.

The Espanola and Albuquerque models were connected, allowing dynamic, head-

dependent flow between the basins. Details of this connection are presented in Section

3.4.2.

3.4.1.2.4.4 Other Adjustments to GW Fluxes Made During Calibration of Coupled Model

Three other changes were made to the groundwater model to bring the fully

coupled surface water/groundwater model into calibration with historic stream gage data

between 1975 and 1999. First, for consistency with URGWOM, a value of 8 inches/year

was used as a crop seepage constant (compared to 6 inches/year used by McAda and

Barroll), depending on water actually delivered to the field. Crop acreages from

URGWOM were also used instead of crop acreages used by McAda and Barroll. The

approximate average acreages and seepage rates for crop recharge are summarized in

Table 3-3; however, the URGWOM values for crop acreage vary with time from 1975–

1999 and are broken down by crop type. For more information, see the URGWOM

Physical Model Documentation (USACE et al. 2002). Agricultural water actually

delivered to the fields was also reduced for consistency between the surface water model

and URGWOM. This reduction of water applied to the fields resulted in a decrease in

crop seepage recharge (see Appendix A, Figure A-2); however, this change in flux was

relatively minor compared to overall fluxes from the surface water to the groundwater.

*Table 3-3. Approximate irrigated acreages and crop seepage rates used
by the URGWOM surface water model, the McAda and Barroll regional
groundwater model, and the coupled model described here.*

	Middle Valley Ag (acres)	Seepage Rate (inches/yr)	Potential Seepage (AF/yr)
URGWOM	46,000	8	31,000
Coupled	46,000	8	31,000
McAda & Barroll	67,000	6	34,000

Second, irrigation canals were changed from a constant specified flux in the groundwater model alone to a surface water stage and groundwater head-dependent flux, modeled with Equation 3-14. Surface stage estimates were derived with Manning's equation (Equation 3-16). Canal bed conductivity was set to 0.15 feet per day consistent with estimates cited by McAda and Barroll (2002), and canal bed thickness to two feet consistent with McAda and Barroll (2002) calibrated values. Canal bed elevation values were set to 5 feet above river channel elevation, effectively eliminating groundwater head dependence. Figure 3-22 shows canal leakage values estimated by the coupled surface water groundwater model as compared to URGWOM and McAda and Barroll (2002) models. The spatially aggregated and coupled model estimates are comparable in overall magnitude to the McAda and Barroll estimates to which they were calibrated; however, they do not drop to zero in the winter because drain capture results in water flowing in the conveyance system year round, with water captured in the drains in one surface water reach assumed to return to the river or flow into the irrigation canals in the next reach.

The final change made to the groundwater parameters associated with coupling to the surface water model was to reduce the effective surface elevation for the shallow aquifer zone between Bernardo and San Acacia (zone 48) from 4,716.5 feet above mean

sea level (amsl) to 4712 feet amsl to increase riparian ET in that reach for consistency

with San Acacia stream and agricultural conveyance gage data between 1975 and 1999.

(See also Section 2.2.3.6.)
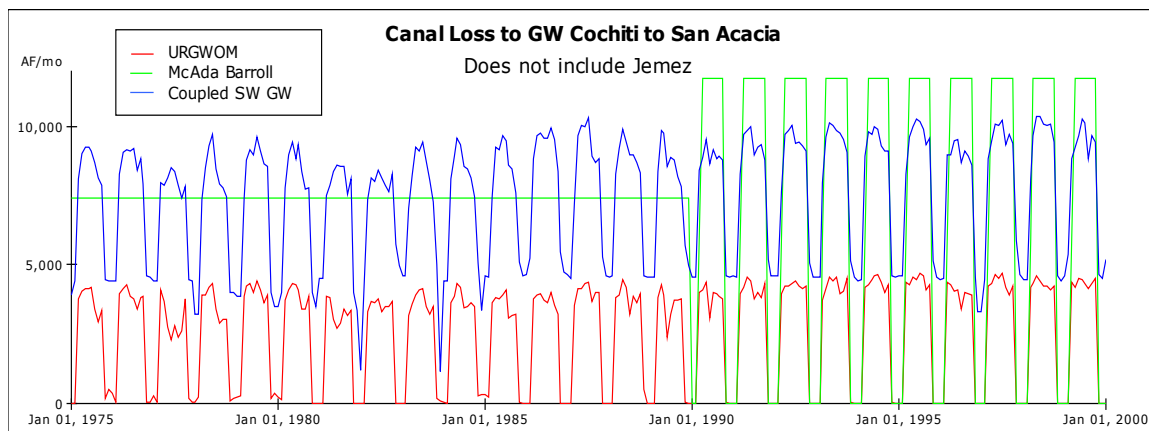
Figure 3-22. Irrigation canal seepage losses to the groundwater aquifer 1975–1999 for Rio Grande reaches from Cochiti to San Acacia as modeled by the coupled monthly timestep model, URGWOM, and McAda and Barroll (2002). Jemez canals are not included in the graph because they are not represented in URGWOM.

Figures 3-23 and 3-24 show the overall fluxes from the surface water to the

groundwater systems, and out of the groundwater system as modeled by the URGWOM

model, the McAda and Barroll model, and the coupled model described here. Though

component terms vary in space and time between the models, the overall fluxes to and

from the groundwater system are very consistent for the 1975 to 1999 calibration period.

For more information, see the cumulative and timestep-specific component fluxes and

summary fluxes compared for the three models shown in Figures A-2 through A-8 in

Appendix A.
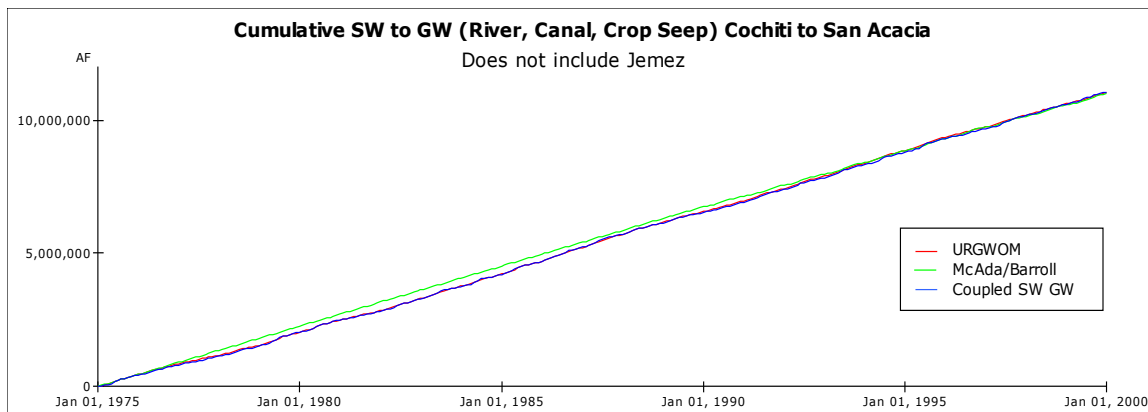
Figure 3-23. Cumulative fluxes to the groundwater system from the surface water system for the Rio Grande reaches from Cochiti to San Acacia as modeled by the coupled monthly timestep model, URGWOM, and McAda and Barroll (2002). Jemez is not included because surface water/groundwater fluxes in the Jemez reach are not represented in URGWOM.
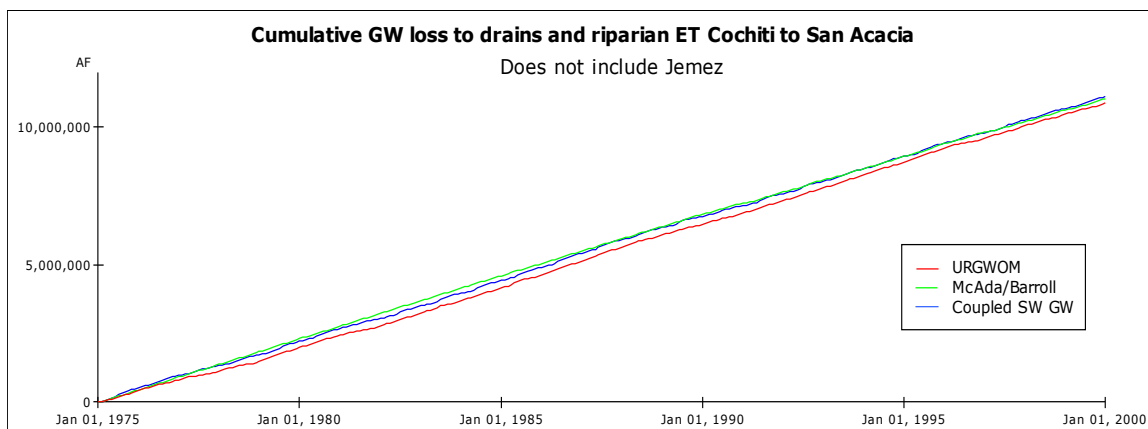
Figure 3-24. Cumulative fluxes out of the groundwater system via drains and riparian ET for the Rio Grande reaches from Cochiti to San Acacia as modeled by the coupled monthly timestep model, URGWOM, and McAda and Barroll (2002). Jemez is not included because surface water/groundwater fluxes in the Jemez reach are not represented in URGWOM.

3.4.2 The Espanola Groundwater Basin

3.4.2.1   Espanola Basin Model Development

The Espanola groundwater basin lies to the north of the Albuquerque Basin (see

Figure 3-4), and for the purposes of this analysis interacts with the Rio Grande river

system from the Rio Chama/Rio Grande confluence in the north to the beginning of the

Cochiti Reservoir maximum pool extent in the south. This spatial extent is based on a

MODFLOW regional groundwater model of the area created by Peter Frenzel (1995) as

an enhanced version of a MODFLOW model created by McAda and Wasiolek (1988).

The spatial extent of the Frenzel model is shown in Figure 3-25.

3.4.2.1.1 Define Espanola Basin Groundwater Compartments (zones)

Using the methodology outlined in Figure 3-3 and discussed above, 16 zones

were spatially aggregated from the Frenzel grid. The trial-and-error procedure was

analogous to the approach taken in the Albuquerque basin, and proceeded until, on

average, MODFLOW estimated flows between the zones chosen traveled from higher

average head to lower average head. The 16 zones are shown in Figure 3-26. Three

shallow aquifer zones (14–16) were defined to represent the alluvial aquifer sediments

associated with the Rio Grande and Pojoaque River. The shallow aquifer zones contain

only the top layer of the Frenzel MODFLOW grid. All other aquifer zones contain all

eight Frenzel model layers. Zone bottom elevations were assumed to be 200 feet beneath

1975 heads for alluvial zones, and 5,600 feet beneath the 1975 heads for all other zones,

based on Frenzel model layer thicknesses for layer 1 and 1-8 respectively. Zone
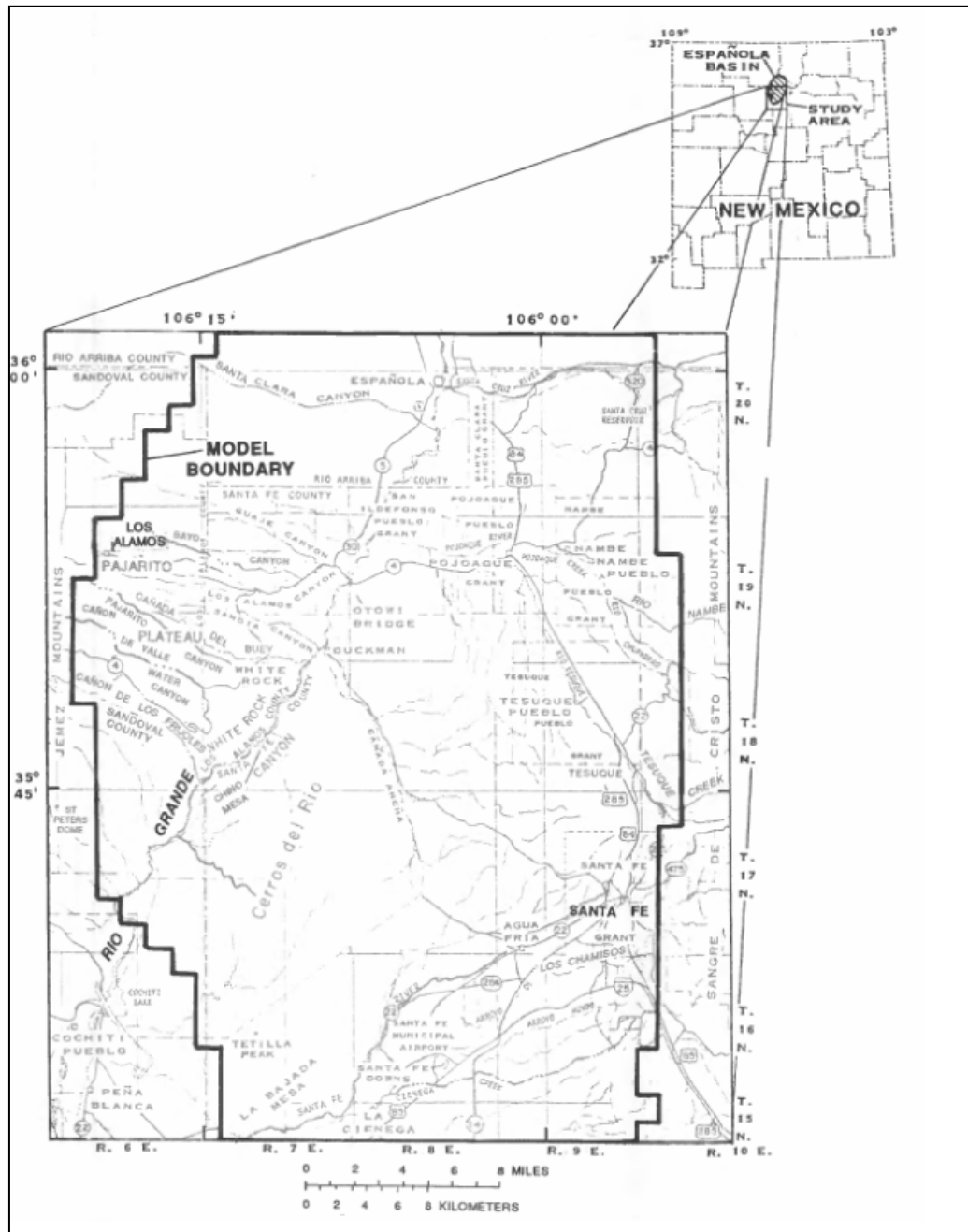
Figure 3-25. Spatial extent of Frenzel (1995) regional groundwater model of the Espanola Basin. Taken from Frenzel (1995), Figure 1.
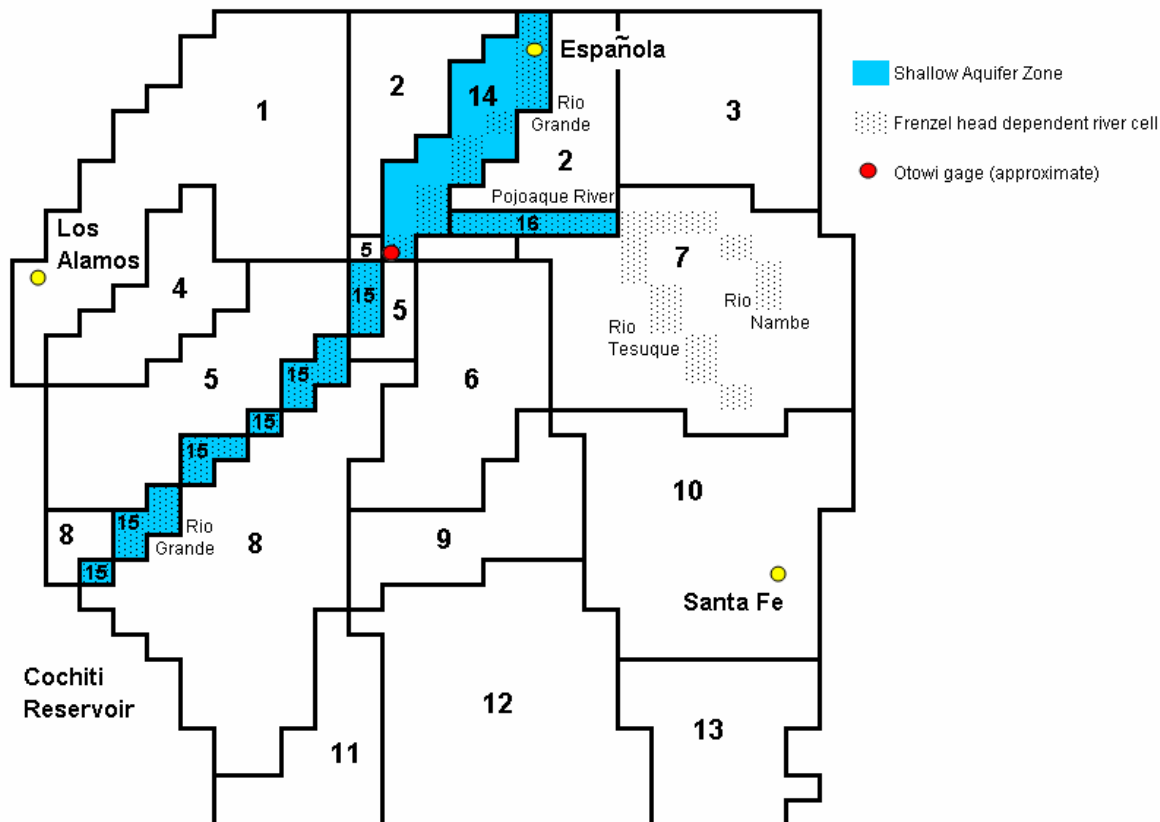
*Figure 3-26. Spatially aggregated zones used for
simulation of Espanola Basin groundwater system.
Shallow aquifer zones (14 through 16) are associated
with top two layers of Frenzel (1995) model.*

geometry information and 1975 initial head values are shown in Table A-6 of Appendix

A. A specific yield of 0.15 is used for all zones, consistent with the Frenzel model.

3.4.2.1.2 Espanola Basin Alpha Matrix Determination

As was done with the 51-zone Albuquerque basin model described in Section

3.4.1, head values through time from the MODFLOW groundwater model were used to

find flow between zones and average head values for the 16 zones for the calibration

period 1975–1992 (end of Frenzel historic period) from which average alpha values for

each zone pair were calculated by rearranging Equation 3-11b to solve for alpha. The alpha matrix for the 16-zone model is shown in Table A-7 of Appendix A.

3.4.2.1.3 Espanola Basin Source and Boundary Flux Definition and Calibration

Modeled groundwater dynamics are less complex in the Espanola basin than the Albuquerque basin. Irrigated agriculture within the Espanola basin model extent is not explicitly connected to the groundwater system by Frenzel or the spatially aggregated model, nor is there a head-dependent ET term modeled.

3.4.2.1.3.1 Specified Fluxes

Specified flux terms in the Frenzel model were used as specified terms in the 16-zone model as well. Spatial distribution of terms was taken from Frenzel input files. Specified flux terms for the Espanola Basin model are summarized in Table 3-4. The specified channel recharge includes input from losing stretches of the Rio Nambe, Rio Tesuque, and Arroyo Hondo. The minor disparity in the southern boundary flows seen in Table 3-4 may be the result of misinterpretation of the MODFLOW input files, though all other terms reported in Table 3-4 were extracted from those same input files, and are consistent with the overall Frenzel (1995) budget.

Sewer recharge from the Los Alamos area is not included in the Frenzel model or the 16-zone model due to lack of information; sewer recharge from the Espanola area is assumed to return to the surface water system and is not included in either groundwater model. Sewer recharge from the Santa Fe area recharges the lower Santa Fe river channel, and is treated as a specified time variant flux by Frenzel. Frenzel values are

used in the 16-zone model from 1975 to 1992, and thereafter by assuming Santa Fe

indoor water use ends up as effluent, ½ of which is assumed to recharge the groundwater

system. Calculations of Santa Fe indoor water use are discussed in Section 4.2.2.2.2.

Estimated Santa Fe sewage recharge input values for the 1975–1999 period are shown in

Figure 3-27.

Table 3-4. Specified fluxes to the 16-zone spatially aggregated Espanola Basin groundwater model. Unit of flows is cubic feet per second (cfs) for consistency with Frenzel (1995) report.

Zone	Areal Recharge [cfs]	Mountain Front Recharge [cfs]	Channel Recharge [cfs]	Santa Fe River Recharge [cfs]	La Cienaga Springs [cfs]	South Boundary Flow [cfs]
1	0.0812	8.02				
2	0.0884					
3	0.0449	4.2				
4	0.0333					
5	0.0870	2.06				
6	0.0812					
7	0.1000	6.1	4.3			
8	0.2392					
9	0.0645					
10	0.5393	8.3	5.1	2.2		
11	0.0689					0.28
12	1.7309				-6.5	-1.74
13	0.9785	2.25	0.7			-0.17
14	0.5813					
15	0.0507					
16	0.0072					
Total	4.8	30.9	10.1	2.2	-6.5	-1.6
Frenzel Total	4.8	31	10.1	2.2	-6.5	-2.3

Well data for Los Alamos and Santa Fe well fields were specified based on

Frenzel values for the 1975–1992 period, and based on the Jemez y Sangre Water

Estimated recharge from Santa Fe Sewage returns 1975-1999

ft³/s
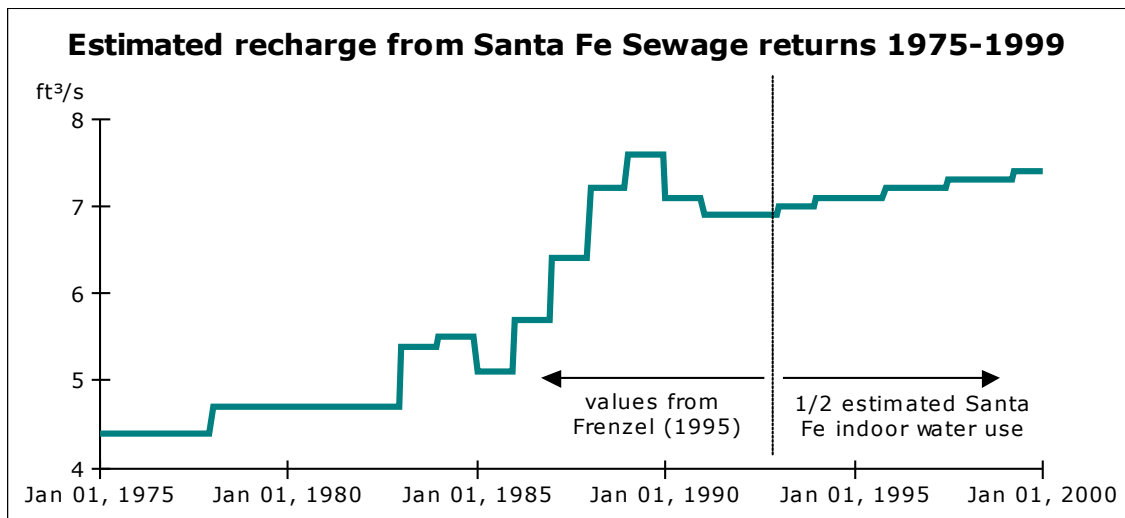
Figure 3-27. *Estimated Santa Fe sewage return values 1975–1999.*
Used as specified flux recharge input data in the Espanola basin groundwater model.

Planning Council's Regional Water Plan (2003) for the 1993–1999 period. Espanola

well field pumping is not represented in the Frenzel model, and was taken from the Jemez

y Sangre Water Plan as available from 1975 forward for use in the 16-zone model.

Private and domestic well data are used from Frenzel for 1975–1992, and increased by

2.4% per year from 1992 values for the 1993–1999 period. Adopted well extraction

values for the major well fields in the Espanola basin are shown

in Figure 3-28.

3.4.2.1.3.2 Head-Dependent Fluxes

Consistent with the Frenzel approach, head-dependent terms incorporated into the

16-zone model include a constant head boundary to the north, and river-aquifer

interactions for the Rio Grande, Pojoaque River, Rio Tesuque and Rio Nambe.   For

simplicity and consistency with Frenzel, stream-aquifer interactions were calculated

using stream conductance
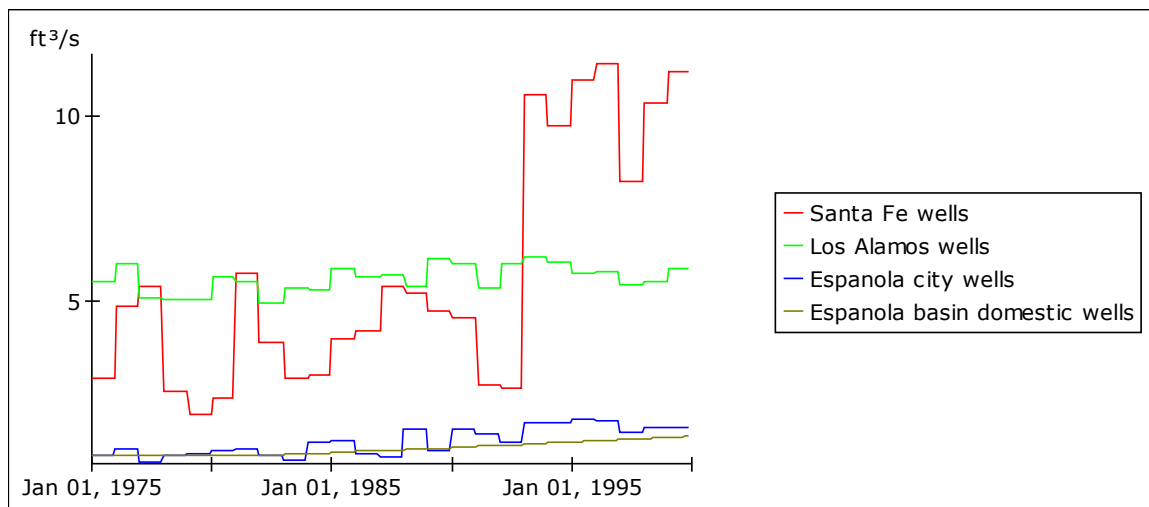
Figure 3-28. Well extraction input data for the Espanola Basin 1975–1999.

$$Q_{aq2str} = C_{str}(h_{aq} - z_{str}) \qquad (3\text{-}18)$$

where Q_{aq2str} is volumetric flow from the aquifer to the stream, h_{aq} and z_{str} are the

aquifer head and stream stage respectively, and C_{str} is the stream bed conductance, a

constant with units of length squared per time, which lumps hydrologic and geometric

properties of the stream bed through which flow occurs. Stream stage for the Rio Grande

is calculated as a function of flow rate using flow-stage relationships for Embudo and

Otowi gages (Table 2-11). Stream stages above Otowi are calculated with an average of

Embudo and Otowi predicted stages, and stream stages below Otowi with the Otowi

predicted stage. Flows come from the surface water model, which is calibrated to USGS

historic gaged flows (see Chapter 2). Stream stage for the other streams is a spatial

average of the values used by Frenzel, and is time invariant. Parameters associated with

stream-aquifer interactions are summarized in Appendix A, Table A-8.

The spatially aggregated model incorporates a head-dependent flow from the 16-zone Espanola basin model to the 51-zone Albuquerque basin model to the southwest, which connects the models, replacing a constant head boundary in the Frenzel (1995) model, and a constant flux boundary in the McAda and Barroll (2002) model. Alpha values used for boundary flow to the north and southwest are shown in Appendix A, Table A-9.

3.4.2.2 Espanola Basin Results

Head-dependent stream-aquifer interactions for the Rio Grande are compared to the Frenzel values in Figure 3-29. The Frenzel values, which end in 1992, were the overall calibration target, and do not show seasonality because of the annual timestep of the Frenzel model. Seasonality in the spatially aggregated model comes from a monthly stream stage calculated in the coupled surface water model. The seasonality is far greater in the system south of Otowi because the river in this section is within a canyon, and subject to large stage variations as flows change. As described above, stream aquifer interactions for the Pojoaque River and Rio Nambe/Rio Tesuque combination are modeled with fixed stream stage. These interactions are essentially constant at 4.3 and 4.6 cfs flow to the streams respectively, as a result of calibration to associated values in the Frenzel model.

Head-dependent flows modeled from the 16-zone Espanola basin model to the 51-zone Albuquerque basin model are compared to the associated specified flows used by Frenzel (1995) as an outflow from the Espanola basin, and McAda and Barroll (2002) as an inflow to the Albuquerque basin in Figure 3-30. The head-dependent flow between

Simulated Rio Grande surface water gains from groundwater system 1975-99
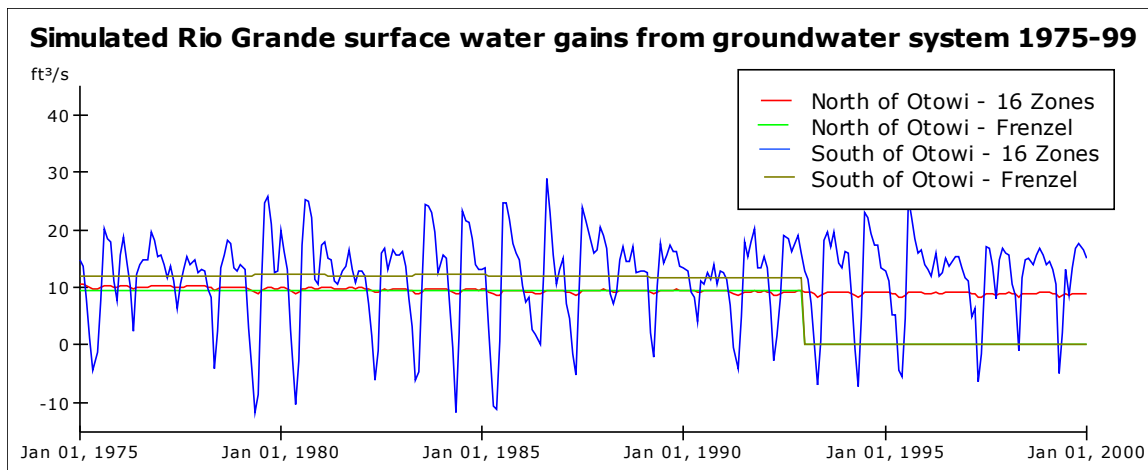
Figure 3-29. Stream-aquifer interactions for the Rio Grande–Espanola Basin groundwater system north of Otowi gage.

Flows from Espanola groundwater basin to Albuquerque groundwater basin.
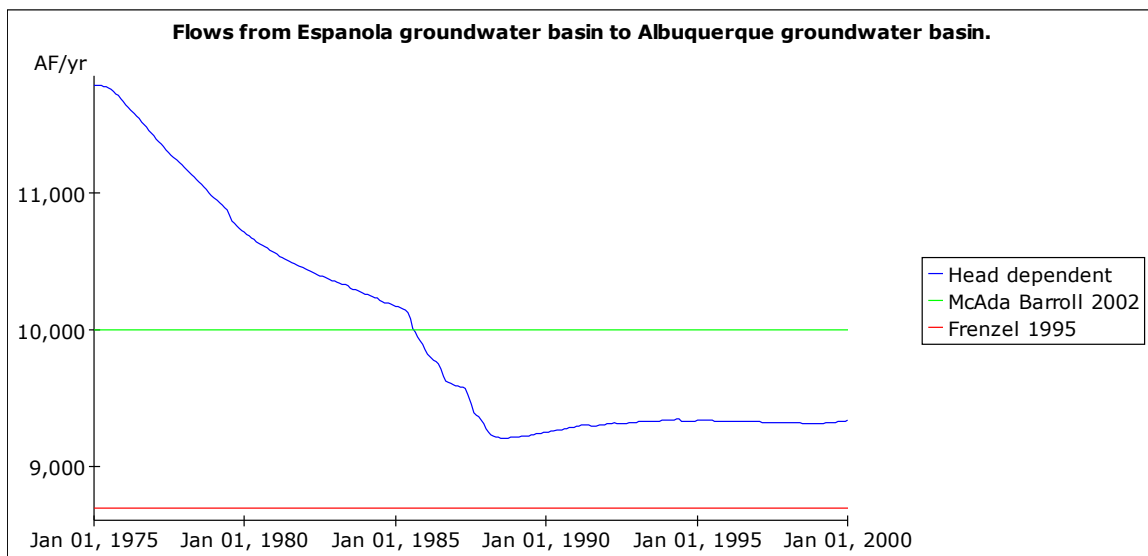
Figure 3-30. Simulated groundwater flows from the Espanola Basin to the Albuquerque Basin from 1975–1999. Combination of the Espanola Basin and Albuquerque Basin spatially aggregated groundwater models compared to fixed boundary flows estimated by Frenzel (1995) and McAda and Barroll (2002). Combined model decreases initially due to groundwater mounding beneath Cochiti reservoir (See Figure 3-21).

basins was calibrated to end up between the Frenzel and McAda and Barroll estimate, and

declines initially as leakage from Cochiti Reservoir associated with reservoir operations

beginning around 1975 slows groundwater flow from Albuquerque basin to the Espanola basin (see mounding under Cochiti Reservoir in Figure 3-8).

Drawdown in the basin between 1975 and 1999 as simulated by Frenzel and the 16-zone model are shown in Figure 3-31. Another way to compare relative model performance is to look at each timestep at net subsurface flow between any two zones, and then sum all of these flows for all zones. The resulting metric is a measure of how much groundwater movement there is in each model at each timestep. Figure 3-32 shows the net groundwater movement between zones for both models.

Figures 3-31 and 3-32 demonstrate that the spatially aggregated Espanola basin model is able to capture the salient behavior of Frenzel's spatially distributed model. In addition, the spatially aggregated model runs rapidly on a desktop computer, and facilitates dynamic connection to the Albuquerque basin spatially aggregated groundwater model and overlying surface water model.
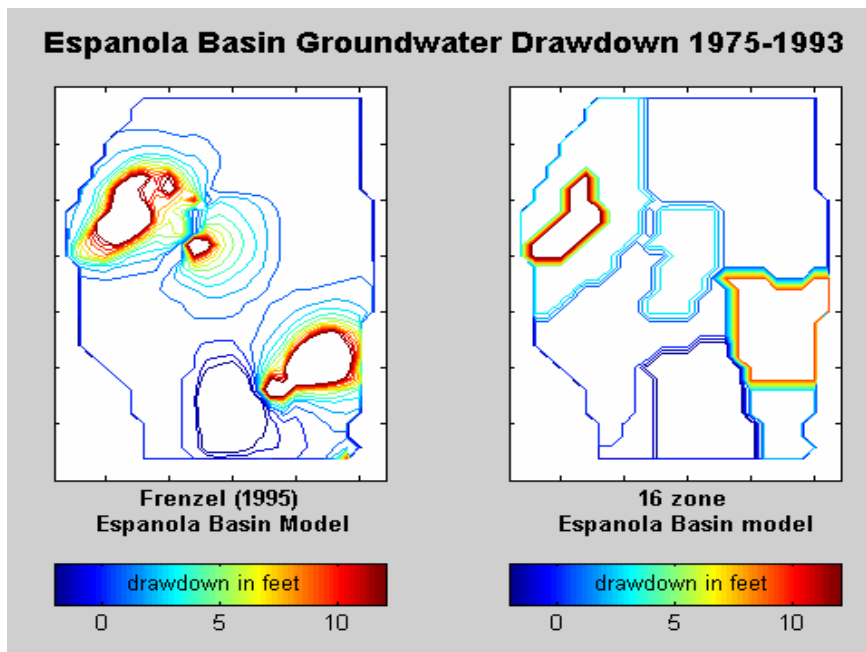
Figure 3-31. Drawdown in the Espanola Basin from 1975 to 1992 as modeled by Frenzel (1995) and the 16-zone compartmental groundwater model. Both models show the dominant patterns of drawdown from Santa Fe and Los Alamos well fields, and mounding from Santa Fe sewage recharge in the southwest.
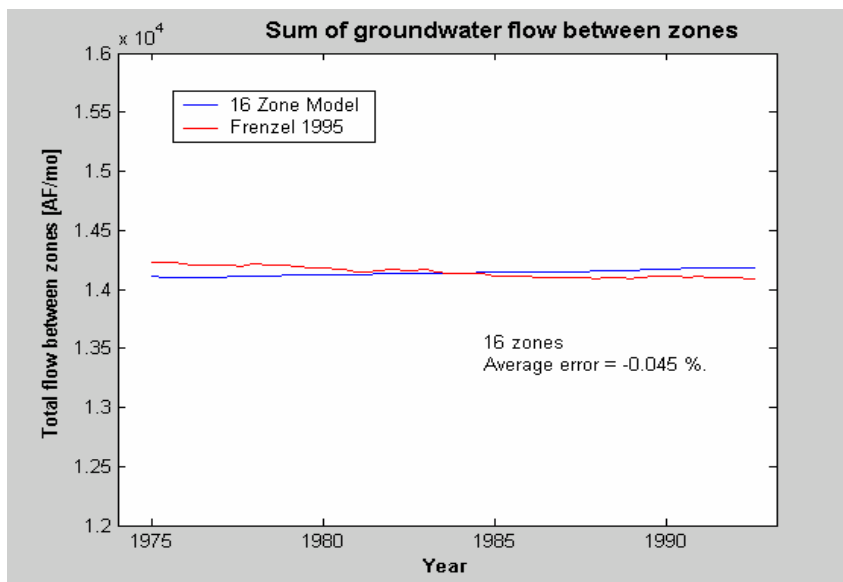
Figure 3-32. Net groundwater movement between Espanola basin groundwater zones. At each timestep, the absolute value of all flows between any two zones is summed as a comparison metric to help evaluate the ability of the 16-zone compartmental model to capture the overall groundwater movement patterns.

3.4.3 The Socorro Groundwater Basin

3.4.3.1   Socorro Basin Model Development

As seen in Figure 3-4, the Socorro groundwater basin is associated with the Rio Grande river system south of San Acacia. The Albuquerque and Socorro groundwater basins are separated by a basin uplift known as the San Acacia constriction, which effectively separates the two groundwater systems (Shafike 2005). Groundwater pumping in the Socorro basin serves domestic, municipal, and industrial use in sparsely populated Socorro county, (2005 population of 18,000 according to the U.S. Census Bureau (2007)), as well as supplemental irrigation demand if surface irrigation supplies are short (Shafike 2005). The relatively small groundwater use associated with these demands compared to overall basin fluxes suggests that the groundwater system can be reasonably approximated assuming steady state (Nabil Shafike, personal communication October 2006). Following this reasoning, Shafike calibrated a spatially explicit model of the basin using steady state flow estimates, and used that parameterization for a one-year transient run using surface water conditions observed in 2001. Figure 3-33 shows the spatial extent of the Shafike model. Because of the limited timeframe of the transient run and the relative equilibrium of the overall groundwater system, a different approach was used to develop a spatially aggregated groundwater model for the Socorro basin than was used in the Albuquerque and Espanola basins described above. A spatially aggregated groundwater model containing 12 zones was calibrated to the steady state fluxes reported by Shafike for the basin to develop the alpha matrix ($\underline{\underline{\alpha_{ij}}}$) needed to solve Equation

3-11b. The groundwater model was then run for the 1975–1999 calibration period with

dynamic surface water exchanges modeled using Equations 3-14 through 3-17 as in the

Albuquerque and Espanola basin models described above. The source fluxes (crop

seepage, canal leakage, river leakage, drain capture, and riparian ET) were modified as

necessary from the steady state estimates during calibration to result in mass balance for

the coupled surface water groundwater system between 1975 and 1999. The remainder

of this section describes this procedure in more detail.

3.4.3.1.1 Define Socorro Basin Groundwater Compartments (zones)

In the 48-mile (USACE et al. 2002) surface water reach from the Rio Grande

gage near San Acacia to the Rio Grande gage near San Marcial, surface water diversions

largely support irrigated agriculture demands in the top 30 miles (approximate), and

wildlife habitat conservation for the Bosque del Apache National Wildlife Refuge in the

bottom 18 miles (approximate). For this reason, the spatially aggregated groundwater

system model was divided into three major longitudinal sections, the first covering the

river system from San Acacia to the northern boundary of Bosque del Apache, the second

covering the river system from the northern boundary of Bosque del Apache to San

Marcial, and the third covering the river system from San Marcial to the southern extent

of the Shafike model in Elephant Butte Reservoir. In each of these sections, the

groundwater system is partitioned into four compartments, a narrow and thin shallow

aquifer compartment representing high-conductivity alluvial sediments, a central regional

aquifer compartment surrounding and underlying the shallow aquifer compartment, and a

regional aquifer compartment on each side of the central regional compartment. The

groundwater compartments are shown in Figure 3-33.

3.4.3.1.2 Socorro Basin Alpha Matrix Determination

To estimate the alpha parameters (α_{ij} from Equation 3-8) for the spatially

aggregated model, steady state groundwater flows between the 12 zones were estimated

as follows. First, flow along the river axis from shallow aquifer zone to shallow aquifer

zone (1 to 2, 2 to 3, and 3 to south boundary) and from central regional to central regional

zone (5 to 8, 8 to 11, and 11 to south boundary) was estimated with Darcy's law using

visual inspection of steady state hydraulic gradients from a file of steady state heads

provided by Nabil Shafike (personal communication 2005) and average aquifer geometry

and hydrologic properties from the Shafike (2005) report. Results of those calculations

are shown in Table 3-5.

Table 3-5. Darcy-based calculations to estimate steady state flow in north-south direction for Socorro groundwater basin shallow and central regional aquifer zones.

	Sub-Reach	Zone	Ksat [ft/da]	Ave Zone Width [ft]	Ave Zone Depth [ft]	SS Hydraulic Gradient [-]	North South SS Flow through Zone [AF/yr]
Shallow Aquifer Zone	San Acacia to Bosque del Apache	1	100	10000	100	0.0008	690
	Bosque del Apache to San Marcial	2	100	10000	100	0.0006	510
	San Marcial to Elephant Butte	3	100	10000	100	0.0006	480
Center Regional Aquifer Zone	San Acacia to Bosque del Apache	5	0.3	20000	4000	0.0008	170
	Bosque del Apache to San Marcial	8	0.3	20000	4000	0.0006	130
	San Marcial to Elephant Butte	11	0.3	20000	4000	0.0006	120

Second, visual inspection of steady state heads led to the rough assumption that of mountain front recharge occurring between San Acacia and Bosque del Apache, 10% flowed south to neighboring regional zones (4 to 7 and 6 to 9), and 90% flowed to zone 5. Groundwater flow between regional aquifer zones on the margins of the model north and south of San Marcial (7 to 10 and 9 to 12) was assumed negligible. Finally, it was assumed that at steady state, flow across the southern boundary of the model from the regional aquifer east of the river (12) was also negligible. With these assumptions, flow between each zone could be specified. For example, the central regional aquifer between San Acacia and Bosque del Apache (zone 5) receives 90% of mountain front recharge from the regional aquifers to the east (zone 6) and west (zone 4) totaling 4,806 AF/yr. As seen in Table 3-5, 170 AF/yr moves to the next central regional aquifer south (zone 8). Thus 4,806 – 170, or 4,636, AF/yr must flow to the overlying shallow aquifer zone (zone 1). The same logic was applied to each zone, resulting in the flow matrix shown in Table 3-6.

Average steady state head values for each zone were estimated by visual inspection of the steady state head distribution file generated by the Shafike model. The steady state average heads adopted for each zone are shown in Table 3-7. With the head values, head differences between all zones were calculated, and Equation 3-11b rearranged to solve for alpha by dividing flows between zones by the head difference between the same zones. The alpha value for 11 to 12 could not be set this way because there is no assumed steady state gradient. $\alpha_{11,12}$ was set at 1 acre/mo by analogy to $\alpha_{8,9}$. The resulting alpha matrix for the 12-zone model is listed in Table A-10 of Appendix A.
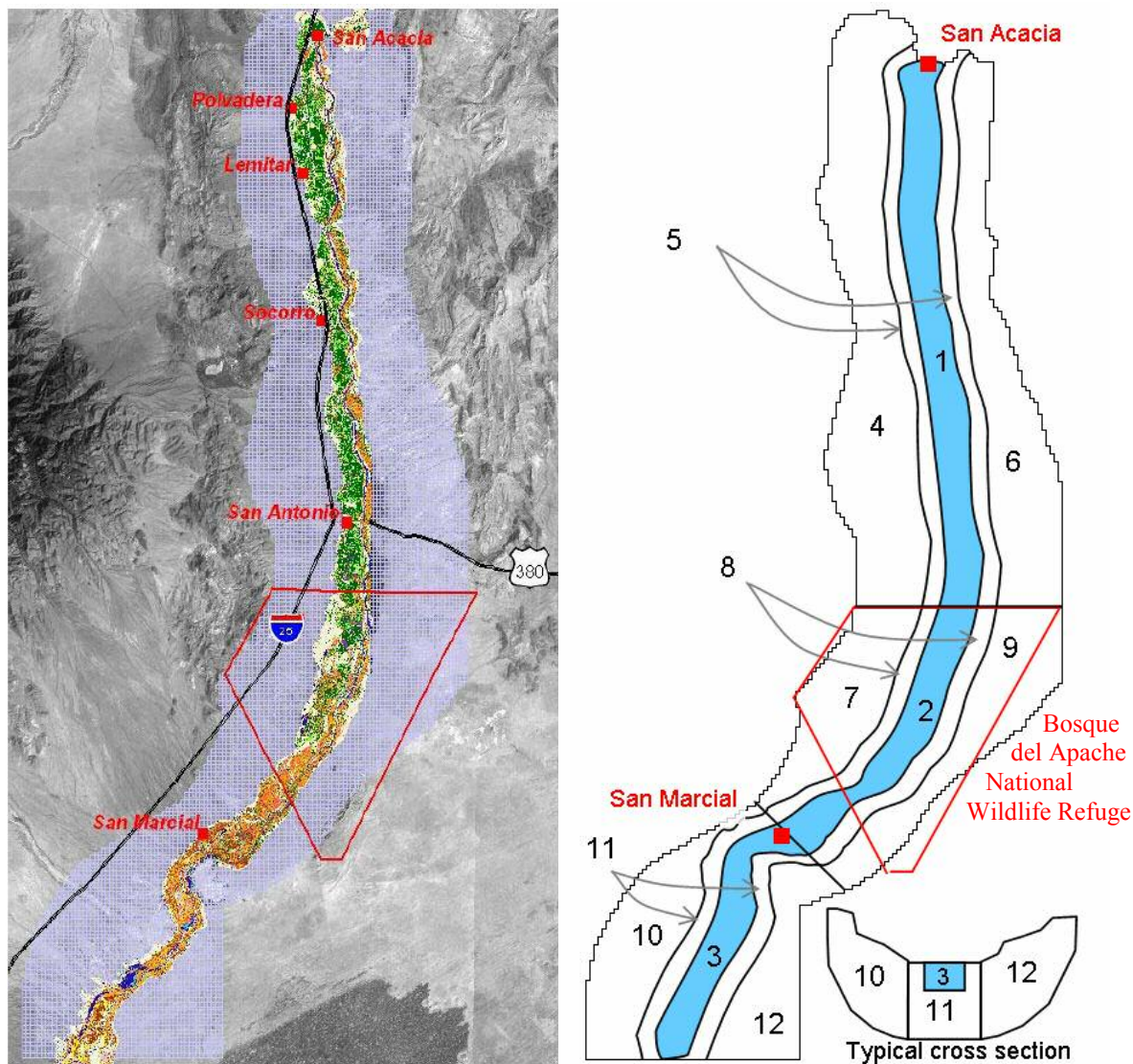
Figure 3-33. Active model grid for Shafike (2005) groundwater model of Socorro Basin (left), and zone delineation for the spatially aggregated model (right). The spatially aggregated model contains shallow aquifer zones (1–3) that roughly coincide with the top layer of the Shafike model within the inner valley. The models extend from San Acacia in the north to Elephant Butte Reservoir in the south. The red outline delineates the Bosque del Apache National Wildlife Refuge. For reference, San Acacia can be seen at the south end of the McAda and Barroll Albuquerque basin grid (Figure 3-5). Left image from Shafike (2005, Figure 11a).

Table 3-6. Estimated steady state groundwater flows between Socorro groundwater basin zones, and to south boundary (SB) for 12-zone spatially aggregated model.

		Socorro Basin Estimated SS GW Flows [100 af/yr]											
		To Zone:											
		1	2	3	4	5	6	7	8	9	10	11	12	SB
From Zone:	1		6.9			-46.4								
	2	-6.9		5.1					-40					
	3		-5.1									-16.2		4.8
	4					36.5		4.1						
	5	46.4			-36.5		-11.6		1.7					
	6					11.6				1.3				
	7				-4.1				38.4		0			
	8		40			-1.7		-38.4		-1.3		1.3		
	9						-1.3		1.3				0	
	10							0				16.1		48.3
	11			16.2					-1.3		-16.1		0	1.2
	12									0		0		0
	SB			-4.8							-48.3	-1.2	0	
	Sum	39.5	41.8	16.5	-40.5	0	-12.9	-34.3	0	0	-64.4	0	0	54.3

Table 3-7. Adopted zonal heads for Socorro Basin spatially aggregated model. EB is steady state reservoir stage at Elephant Butte.

Zone:	1	2	3	4	5	6	7	8	9	10	11	12	EB
Adopted SS Head:	4580	4500	4460	4640	4590	4600	4560	4510	4520	4850	4440	4440	4430

3.4.3.1.3 Socorro Basin Source and Boundary Flux Definition and Calibration

Steady state source terms to and from each of the zones were also estimated. The steady state run evaluated by Shafike (2005) does not include crop irrigation and associated conveyance canal and crop seepage recharge terms, nor does it include well pumping. The steady state run does include flow from the groundwater system into a low-elevation conveyance channel called the Low Flow Conveyance Channel (LFCC), which serves as a drain for the system. To estimate steady state flows between the 12

groundwater zones, steady state basin fluxes reported by Shafike (2005) were distributed to each of the zones.

3.4.3.1.3.1 <u>Socorro Basin Steady State Groundwater Gains</u>

Mountain front recharge was assigned to zones 4, 6, 7, and 10 with locations based on estimated mountain front spatial distributions in the area from Roybal (1991), summing to the 15,210 AF/yr used by Shafike (2005). Values are shown in Table 3-8. Shafike (2005, Figure 14) reports the results of Rio Grande seepage runs, suggesting weighted average river leakage ranging from 224.5 cfs to 500 cfs between San Acacia and Fort Craig, with 61% to 71% of the leakage occurring between San Acacia and the north boundary of Bosque del Apache, 27% to 37% occurring between the north boundary of Bosque del Apache and San Marcial, and 2% between San Marcial and Fort Craig. For the approximately 6 miles from Fort Craig to Elephant Butte, river leakage was assumed to be the same as from San Marcial to Fort Craig: 1 to 2 cfs/mile. Using these distributions, the total steady state estimated river leakage of 205,020 AF/yr (~280 cfs) used by Shafike was partitioned into groundwater zones 1-3 as shown in Table 3-8.

3.4.3.1.3.2 <u>Socorro Basin Steady State Groundwater Losses</u>

Groundwater leaves the Socorro basin groundwater system by drainage to the LFCC (drain flow), by riparian ET, and via subflow out the southern boundary of the model. Visual inspection of Shafike (2005, Figure 15) suggests that about 75% of steady state groundwater flows to the LFCC occur north of Bosque del Apache, and essentially 100% occur north of San Marcial. Shafike reports total steady state groundwater flow to

the LFCC of 152,140 AF/yr. In the spatially aggregated model 75% of this amount is lost

from shallow aquifer zone 1, and the remainder from shallow aquifer zone 2. Values are

shown in Table 3-8. Having identified all other steady state flux terms associated with

the shallow aquifer zones, riparian ET was solved for using mass balance. For example,

in the shallow aquifer zone from San Acacia to Bosque del Apache (zone 1), river

leakage adds 135,500 AF/yr to the groundwater system, LFCC losses remove 117,100,

and net flows from adjacent aquifer zones add 3,950, leaving 135,500 + 3,950 − 117,100

= 22,350 AF/yr available for removal by ET. Values are summarized in Table 3-8.

Table 3-8. Steady state fluxes adopted for 12-zone Socorro Basin model.
The net groundwater flow of -5,410 AF/yr represents groundwater flow out the
southern boundary of the model, as calculated by Shafike (2005).
Shafike totals listed are from Table 2 of the 2005 report.

GW Zone	GW Gain [AF/yr]		GW Loss [AF/yr]		Implied Subsurface Flows [AF/yr]
	MtnFrnt	Rvr Leak	LFCC	ET	
1	0	135500	117100	22350	3950
2	0	61000	35000	30200	4200
3	0	8600	0	10250	1650
4	4050	0	0	0	-4050
5	0	0	0	0	0
6	1290	0	0	0	-1290
7	3430	0	0	0	-3430
8	0	0	0	0	0
9	0	0	0	0	0
10	6440	0	0	0	-6440
11	0	0	0	0	0
12	0	0	0	0	0
Total	15210	205100	152100	62800	-5410
Shafike SS Totals	15210	205020	152140	63030	-5430

The groundwater model was coupled to the surface water model for the 1975–1999 calibration period in stages. Fluxes across the southern boundary from zones 3 and 11 were modeled as head-dependent on Elephant Butte Reservoir, and fluxes across the southern boundary from zone 10 were modeled as constant flux. Fluxes across the southern boundary from zone 12 were assumed negligible.

Initially, river leakage was held constant and LFCC capture and riparian ET implemented as a function of relevant aquifer and surface characteristics using Equations 3-15 through 3-17 as described previously for the Albuquerque basin. A Manning's roughness of 0.028 was assumed for the LFCC, consistent with the Albuquerque basin assumed value. A width of 28 feet and a slope of 0.00097 were assumed for the LFCC based on data from a USDoI report on LFCC operations (USDoI 2002). Reference ET (1975–1999) from the surface water model modified for use with depth to groundwater as an additional constraint (described previously in Section 3.4.1.2.4.2) was used to drive atmospheric ET demand. LFCC fluxes were calibrated to steady state by manipulation of bed elevation values. ET fluxes were calibrated to steady state by manipulation of average surface elevation of the shallow aquifer zones. Once the LFCC and riparian ET parameters were set, river leakage was implemented using Equation 3-14. Initially, all 1975–1999 flows at San Acacia (floodway and conveyance) were set as flows in the river channel. The river bed conductivity and thickness values were set to 0.5 feet/day and 5 feet respectively, consistent with values used in the Albuquerque basin. A Manning's roughness of 0.028 was assumed for the river. River bed slopes were estimated based on relevant gage elevations (Table 2-2) and reach lengths (Table 2-4), and are shown in

Table A-11 of Appendix A. River bed elevation values were manipulated to bring average 1975–1999 river leakage close to steady state estimated values (Table 3-8).
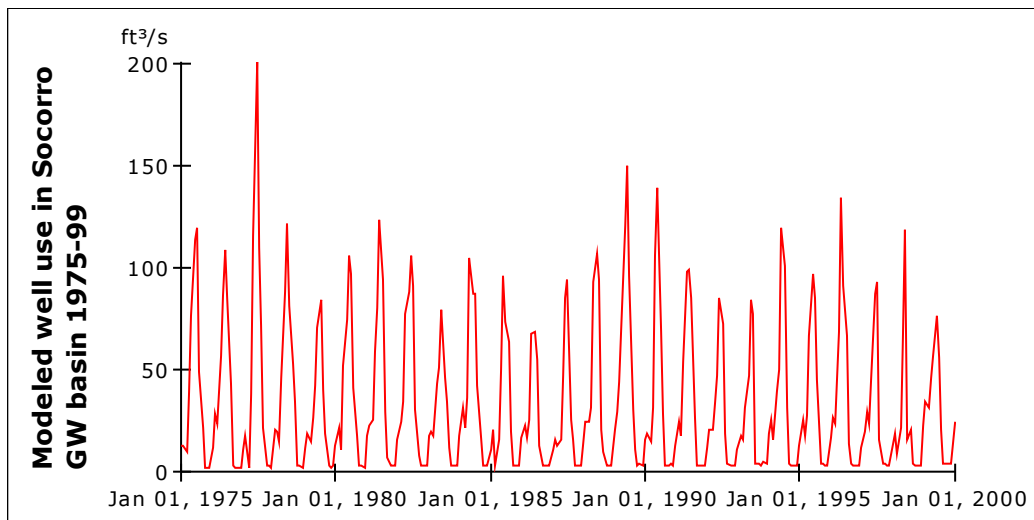
Figure 3-34. Well pumping assumed for Socorro Basin 1975–1999.
Based on estimates of municipal and industrial use and supplemental irrigation demand.

Finally, historic diversions into the LFCC and agricultural conveyance system were restored, and canal leakage (non-LFCC), crop seepage, well pumping, and historic Elephant Butte stage incorporated into the surface water groundwater interaction. Well pumping is calculated based on simple estimates of the small municipal and industrial demand in the area, and estimates of supplemental water needs when agricultural demand exceeds available water in the irrigation conveyance system. Well pumping values assumed for the Socorro Basin spatially aggregated model are shown in Figure 3-34. Seventy-five percent of the extraction is assumed to occur from the shallow aquifer between San Acacia and the northern boundary of Bosque del Apache (groundwater zone 1), and the remaining 25% from the underlying regional aquifer (groundwater zone 5). Septic recharge is a minor term, but for consistency with the Albuquerque basin

groundwater model is included. Septic recharge is assumed to be 50% of indoor water use in the basin, and is added in equal amounts to zones one, four, and five. It is indeed minor at just 40 AF/mo in 1990 for example. For a description of indoor water use calculations, see Section 4.2.2.2.2 in Chapter 4.

Canal bed conductivities were set to 0.2 feet per day consistent with values reported in the URGWOM physical model documentation for canal bed conductivities below San Acacia (USACE et al. 2002). Canal bed thickness values were set to 2 feet based on values used in the Albuquerque basin (see Step 3 in Section 3.4.1.1), and canal bed elevations were set 2 feet above the river channel elevation. Irrigation canals are only included in the model between San Acacia and Bosque del Apache. Steady state parameters were adjusted as necessary to achieve 1975–1999 mass balance between the San Acacia and San Marcial gages, and between the San Marcial and Elephant Butte Reservoir, as estimated by Elephant Butte behavior (see Chapter 2). The major adjustments associated with calibration of the coupled model were an increase in riparian acreage in the San Acacia to San Marcial reach as described in Chapter 2, an adjustment of the shallow aquifer effective surface elevation (controlling depth to groundwater and thus riparian ET) between San Marcial and Elephant Butte, and a limit to the leakage of the LFCC. The LFCC was modeled as a drain according to the Dupuit-Forchheimer approach using Equation 3-15 as described previously. However, unlike drains in the Albuquerque basin, the LFCC can carry thousands of cubic feet per second. When the LFCC is carrying thousands of cubic feet per second, the stage of the water in the LFCC may be greater than that of the surrounding aquifer, leading to leakage to the aquifer.

Equation 3-13 seems to do a reasonable job of predicting this leakage as long as the stage in the canal does not get too much larger than the aquifer head, but when this occurs, Equation 3-13 seems to result in excessively large flows from the canal back to the groundwater. This may be a problem inherent to the approach. The problem has been addressed by limiting the amount of water that can move from the LFCC back to the aquifer to 300 cfs in each groundwater zone. Table A-11 in Appendix A summarizes calibrated parameters used to model interactions between the aquifer and the LFCC, river, irrigation canals, and riparian vegetation.

3.4.3.2   Socorro Basin Results

As explained above, the spatially aggregated Socorro Basin groundwater model was developed from a spatially explicit but steady state groundwater model developed by Nabil Shafike (2005), and run in a transient mode. Figure 3-35 shows the groundwater heads in the 12 aquifer zones from 1975–1999. There is no trend in any of the zones, suggesting that despite temporal fluctuations in stream aquifer exchanges due to temporally varying surface water conditions the groundwater system is in a quasi-steady state. Zones 1-3 are the shallow aquifer zones, and show noise about a steady average.

LFCC gains from the groundwater system modeled with the coupled model as compared to URGWOM and steady state values from the Shafike (2005) model are shown in Figure 3-36. The LFCC was used significantly until around 1986 (Shafike 2005), and the groundwater gains to the canal are clearly greater after that time in both transient models. The cumulative 25-year groundwater flow to the LFCC modeled by the

coupled model falls between the URGWOM prediction, and the steady state prediction,

as seen in Figure A-9 in Appendix A.
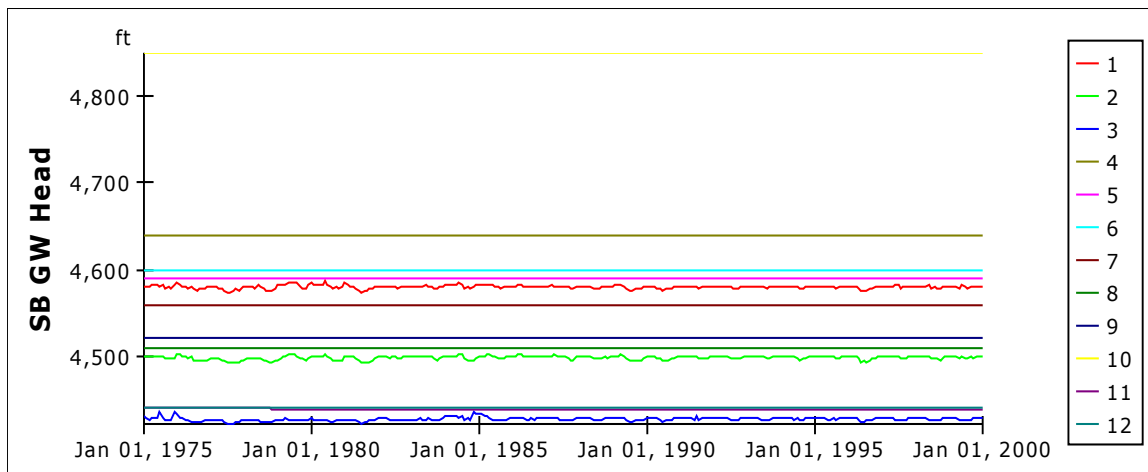
Figure 3-35. Modeled groundwater heads in Socorro Basin by groundwater zone between 1975–1999. Flat trend justifies the steady state assumptions used to develop the groundwater model parameters.
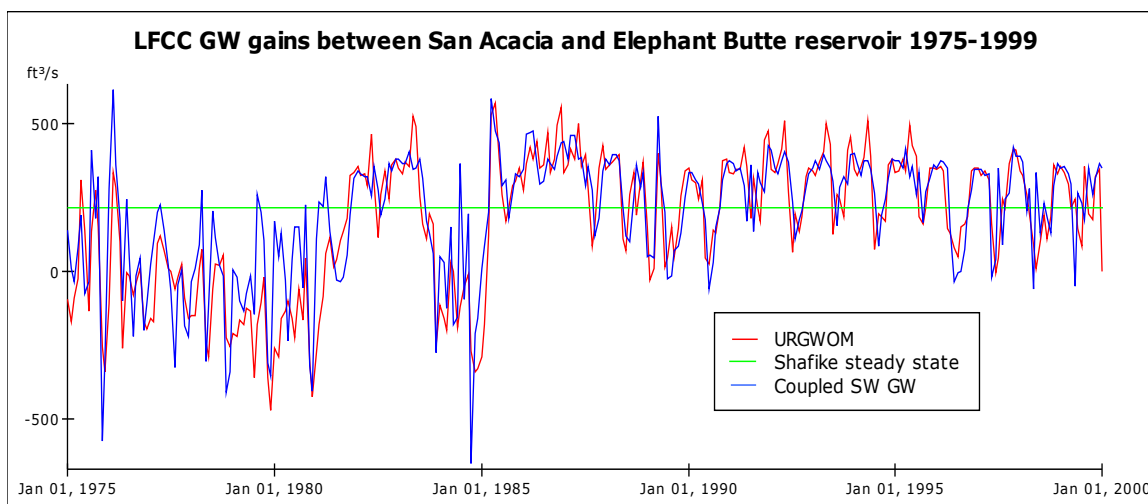
Figure 3-36. Flows from the groundwater system to the LFCC for Rio Grande reaches from San Acacia to Elephant Butte as modeled by the coupled monthly timestep model, the URGWOM surface water model, and steady state values reported by Shafike (2005).

River leakage values from the different models are shown in Figure 3-37. The

coupled values and URGWOM values agree well from 1985 on, but not before. The

River leakage between San Acacia and Elephant Butte reservoir 1975-1999
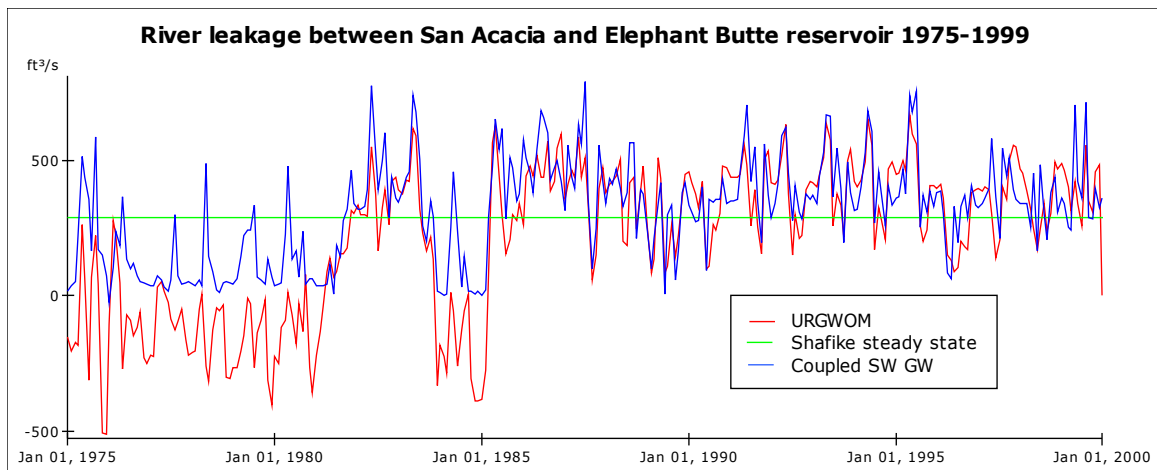
*Figure 3-37. Rio Grande river leakage San Acacia to Elephant Butte
as modeled by the coupled monthly timestep model, the URGWOM surface
water model, and steady state values reported by Shafike (2005).*

URGWOM reaches below San Acacia have recently been reworked, in part because

modelers were skeptical of URGWOM results suggesting any gaining segments between

San Acacia and Elephant Butte[9]. From a cumulative river leakage perspective, the

25-year total river leakage predicted by the coupled model is similar to the steady state

cumulative. The URGWOM cumulative value is less, again largely because of the

gaining reach tendencies estimated by URGWOM between 1975 and 1985. The

cumulative river leakage values are shown in Figure A-10 in Appendix A.

Riparian ET values predicted by the different models are shown in Figure 3-38,

and cumulatively in Figure A-11 in Appendix A. As discussed in Chapter 2, the

seemingly overly large losses observed between San Acacia and San Marcial may be a

result of gage errors, particularly between 1985 and 1988; however, analysis of

systematic gage error is beyond the scope of this effort, and so gage error is assumed to

be normally distributed about zero, and other methods are used to obtain mass balance at

[9] Personal communication with URGWOM technical team, February 2007.

each gage between 1975 and 1999. In the case of the San Acacia to San Marcial reach,

calibration of the coupled model was achieved by increasing riparian vegetation area in

the reach by 33%. See Chapter 2 for further discussion. As a result of this calibration,

the coupled values shown in Figure 3-38 are significantly higher than the URGWOM

values. The surface water balance between San Acacia and San Marcial appears to be

closed in URGWOM with large crop seepage rates as seen in Figure 3-39. In the coupled

model, large seepage rates end up back in the drain system (LFCC), and so cannot be

used to close the surface mass balance.

The last head-dependent flux of consideration for the historic period in the

Socorro Basin groundwater system is canal leakage, which is modeled from San Acacia

to San Marcial in the coupled model. It is not modeled explicitly in URGWOM, and not

included in the steady state mass balance done by Shafike (2005). This is a relatively

small flux in the coupled model, averaging a fairly steady 8 cfs, as shown in Figure A-12

in Appendix A.

The spatially aggregated and coupled surfacewater/groundwater model of

Socorro Basin is able to capture many of the temporal signals of the surface water system

modeled by URGWOM as seen in Figures 3-36 and 3-37, while maintaining a quasi-

steady state groundwater mass balance as shown in Figure 3-35 and predicted by Shafike

(2005). The combination of the surface and groundwater mass balance constraints

suggest that either gage error led to significant overestimates of reach losses between

1985 and 1988 (see also Chapter 2), or the ET losses in that reach are larger than

suggested by either URGWOM or Shafike's (2005) steady state analysis. These

conclusions support the value of basin scale multi-decadal analysis of coupled surface water groundwater systems that is made rapid and accessible by the spatial aggregation techniques for groundwater modeling described in this chapter.
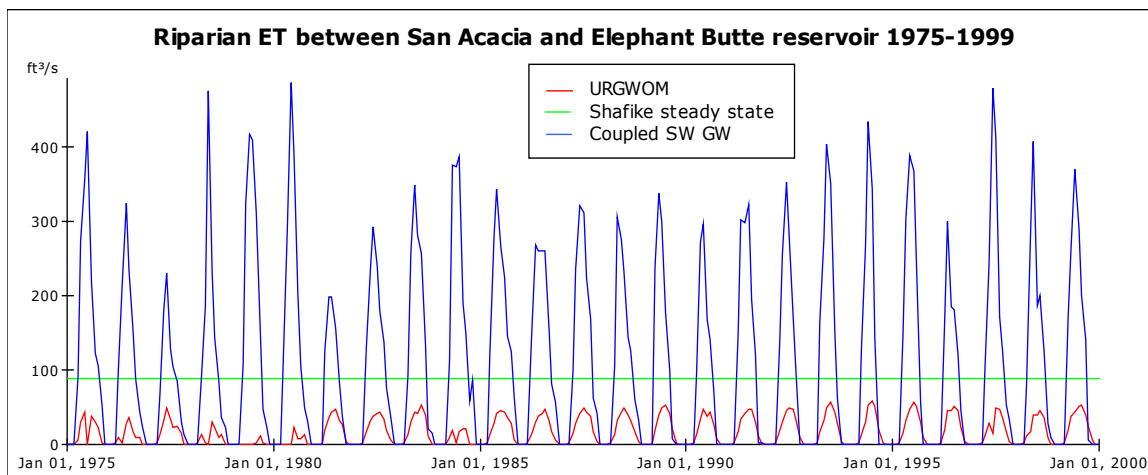
Figure 3-38. Riparian ET between San Acacia and Elephant Butte as modeled by the coupled monthly timestep model, the URGWOM surface water model, and steady state values reported by Shafike (2005).
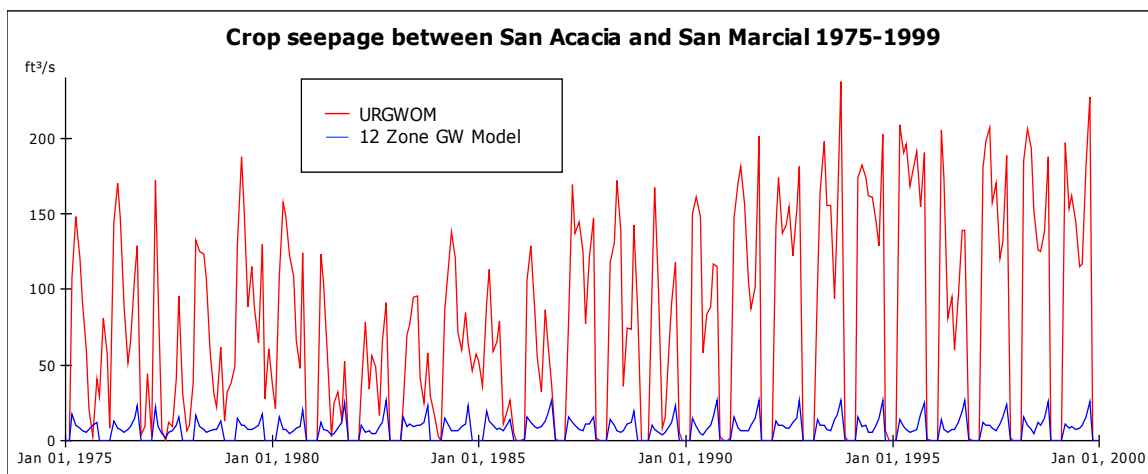
Figure 3-39. Crop seepage between San Acacia and Elephant Butte as modeled by the coupled monthly timestep model and the URGWOM surface water model.

3.5 Groundwater component conclusions

Numerical modeling of groundwater behavior for policy analysis is currently

dominated by finite difference solutions using MODFLOW models. Such models

typically incorporate the best available spatial data and conceptual understanding of a

groundwater system, and are calibrated to point data at observation wells. When they are

done well, they also represent the best available numerical representation of complex

groundwater systems. However, for real time, interactive scenario analysis, MODFLOW

models can be limiting for three main reasons. First, the text based input files of

MODFLOW models cannot be easily understood or manipulated by non-expert users

without expensive third party software. Second, and closely related, in cases where

surface water system behavior may change through time, the ability to change

MODFLOW input files dynamically with changing surface water conditions and human

demands poses a significant software challenge. Finally, the minutes or several minutes

required for spatially complex groundwater model run times can be too long for effective,

group based, real time model interaction. For all of these reasons, the available

MODFLOW models describing groundwater behavior along the Rio Grande between the

Chama confluence and Elephant Butte reservoir were spatially simplified and combined

on a software platform amenable to surface water modeling and the creation of graphical

user interfaces. The result is a basin scale groundwater model linked dynamically to an

overlying basin scale surface water model, which can run 40 year scenarios in tens of

seconds on a laptop computer, and can accept any allowed range of changeable user

inputs. Such a model is a potentially powerful tool for use in public education and

preliminary policy discussions and decisions, the outcomes of which may then be tested further with the higher resolution MODFLOW models.

The most important, and also most time consuming step in developing spatially aggregated groundwater models from more resolved models, is the selection of groundwater zones. This process is currently a time intensive fuzzy effort relying heavily on trial and error. If the model developed for this study does indeed gain traction and is successful as a public awareness or a policy scoping tool, some attempt to automate the zone selection may prove worthwhile to streamline future spatially aggregated model development.

CHAPTER 4: SCENARIO ANALYSIS

4.1 Introduction

The ultimate goal of the model development documented in this dissertation is a basin scale model of the Rio Grande system in New Mexico that captures the salient physical behavior of a system, and runs rapidly on a personal computer. The previous two chapters have focused on model development for the surface and groundwater systems that together dictate the physical behavior of water in the river system. These techniques have resulted in a basin scale, integrated surface water groundwater model that runs through the 25 year (1975-1999) calibration period in about 10 seconds on a 2.13 gigahertz laptop computer. This relative speed and portability makes the model ideally suited for planning scale scenario analysis in real time by decision makers, stakeholders, and the interested public, either alone or in groups. The ability to analyze alternative futures in real time allows users to evaluate an essentially infinite continuum of scenarios based on user changed inputs, rather than a specific set of pre-run scenarios as is necessary with slower models. This chapter will focus on additional model developments necessary for scenario mode runs, and model results from scenario mode.

4.2 Scenario Development

4.2.1 Scenario Mode Disclaimer

The idea of a "scenario mode" has been mentioned previously in this dissertation, but never adequately defined. Once calibration and validation are complete, a model can in theory be run into the future with overall physical behavior consistent with historic due to calibration, and some idea of the relative uncertainty of the model due to validation. As pointed out by Michael Lyons (2004), as a model moves into the future, it serves a purpose somewhere on a continuum between predictive and exploratory, depending on the nature and accuracy of the model, the timeframe being considered, and the level of certainty of future inputs. The model developed here is more exploratory than predictive for three main reasons. First, the monthly timestep model represents an abstraction from more temporally or spatially explicit surface water and groundwater models respectively, which are themselves imperfect representations of the physical system. Second, the future inputs to the physical model described here include hydrologic flows at gages, atmospheric climate data, and groundwater boundary recharge, whose future distributions are of tremendous uncertainty. Finally, the integrated model has been developed to run quickly so that runs on the order of 40 or 50 years can be evaluated in tens of seconds. Due to the exploratory nature of the model, general patterns and trends maybe predicted with some degree of confidence, and results that at first look seem counterintuitive may be understood by closer inspection of model output. However, the absolute value of a given stream flow or reservoir storage or groundwater head given by the model for some future date will almost certainly not be observed on that date in the future. The model is

suited for relative comparison of a variety of potential future scenarios, and that, not prediction is the purpose of the scenario mode.

4.2.2 Scenario Mode Model Inputs

As discussed in Chapter 1, the impetus for scenario analysis in the Rio Grande basin is new and growing demands to a finite, over allocated and variable supply of water. The underlying question driving this research might be summarized as: "What are the likely or possible outcomes of continued growth in demand?". To address this question, the model runs from 2005 (the end of the validation period) to 2045 with a specific set of inputs that can be modified by the user. The model inputs that are a result of observations during the historic period but must be specified in some way during scenario mode include inputs to the physical model just mentioned, and human behavior related inputs. As is typical of simulation models (e.g.Tidwell et al. 2004), the physical model input used for scenario inputs are sampled from observed historic inputs. On the human behavior side of things however, growing human demands are being driven primarily by growing human population, so that meaningful scenario development must include some connection between human population and human demand for water. This relationship constitutes a human behavioral model. The sampling of observed historic model inputs and the development of a simple human behavioral model to generate model input during scenario mode are described in the next two subsections.

4.2.2.1 Physical Inputs During Scenario Mode

Specified fluxes to the groundwater model during scenario evaluation, including mountain front recharge, specified flux from tributary recharge, and constant head or specified flux subflow from adjoining groundwater basins remain unchanged from calibration and validation modes. The rule of thumb for the groundwater model is that if the flux is constant during the historic period, it remains the same during scenario evaluation. The most important surface water model inputs are the gaged surface water flows at the model boundary (which also determine ungaged surface water flows), and the climate data used to calculate reference ET (see Figure 2-55). These climate based inputs are specified in scenario mode as a selection of historic observations. Specifically, the integrated model is set up to allow the user to choose between three main climate based input distributions during scenario evaluation. The first option is to use 1975-99 monthly average gage and climate data, meaning every January during the scenario period will have the same forcing data, an average of the 25 Januarys from 1975 through 1999. The second option is to loop through historic 1975-2004 gage and climate data. The user can decide which historic year to begin with, and the model will proceed sequentially to 2004, and then return to 1975 and continue the sequential advance. If for example, the user chooses this option beginning in 2004, the first year of the scenario period will be driven by climate and gage data observed in 2004, the second by observations from 1975, the third by observations from 1976 and so forth. Finally, the third option for climate based inputs is to loop through a specific 40 year climate sequence developed by the Upper Rio Grande Basin Water Operations Review

(URGWOPS). The forty year climate sequence was developed by URGWOPS as representative of long term climate averages in the basin, based on direct measurements and paleoclimate analysis (USACE et al. 2006, Section 2.2.2). The forty year sequence is derived from a sampling of historic years between 1975 and 1999, however, because the twenty five year calibration sequence was wetter than long term averages, certain years are used more often than others, and some years are not used at all. The historic years used to create the representative 40 year sequence are shown in Table 4-1, along with the annual average river flow observed at Otowi during that year.

Sequence years 4-14 represent a sustained drought period, while years 23-29 represent a sustained wet period. Figure 4-1 shows the annual Otowi index flow for each of the historic years used in the 40 year URGWOPS sequence. The Otowi index flow, as discussed in Section 2.2.3.5.3.8 is the estimated flow that would have passed the Rio Grande gage at Otowi without transmountain diversions or reservoir storage. The average Otowi index for the 40 year URGWOPS sequence is 934,000 acre feet per year, more representative of long term climate cycles in the basin, and almost 20% lower than the 1975-1999 calibration period average of 1,150,000 acre feet per year.

Table 4-1. Historic years used to generate the 40 year URGWOPS climate sequence.
The first ten scenario years are the historic years shown in the top row, read left to right.

		Historic years used for climate inputs									
Scenario Year	1 - 10	1982	1988	1992	1976	1989	1996	1977	1989	1989	1981
	11-20	1996	1996	1977	1988	1987	1975	1998	1976	1975	1978
	21-30	1978	1998	1999	1986	1999	1991	1980	1992	1985	1998
	31-40	1978	1998	1976	1991	1989	1984	1992	1988	1982	1991

Otowi Index Supply for 40 year URGWOPS climate sequence
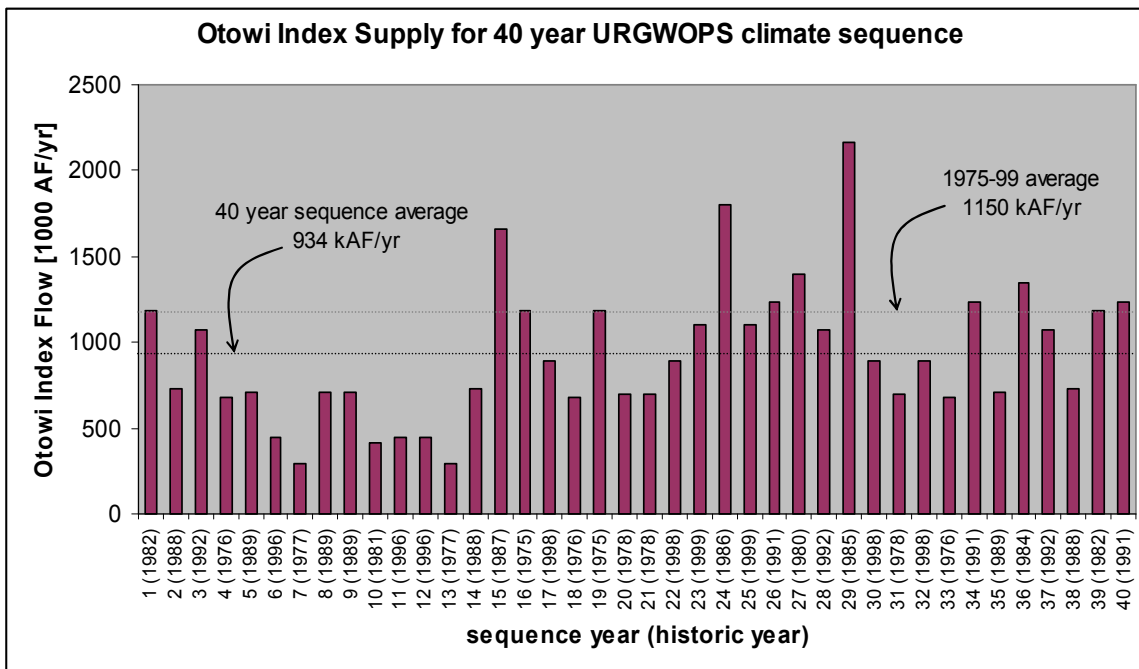
Figure 4-1. Otowi index supply for the 40 year URGWOPS sequence, showing an overall average flow below the 1975-1999 average. Note the period of drought in sequence years 4-14, and the period of sustained high flows in sequence years 23-29.

The user selects between the three climate scenario options with a set of radio buttons and sliders as shown in figure 4-2.
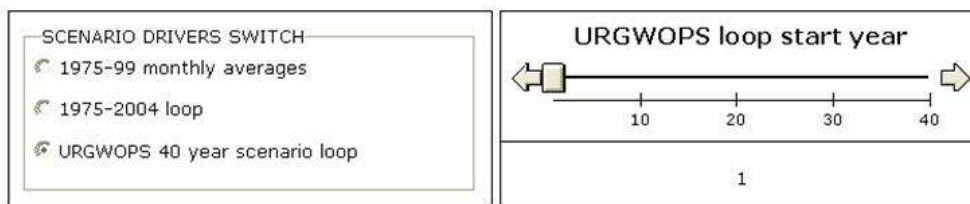
Figure 4-2. Screenshot from the model interface showing how a user selects the climate sequence to be used to drive scenario input.

4.2.2.2 Human Behavioral Related Inputs Used for Scenario Analysis

The future distribution of climate related inputs to the Rio Grande river system discussed above, apart from being uncertain, are also mostly beyond the intentional

control of human actions. Human behavior in the future is likely a bit more constrained,

and also arguably something that can be influenced by policy makers and political and

economic leaders. This section will summarize the human behavior related inputs used in

the base case scenario model run, including human population growth, municipal and

industrial demand and returns, direct diversions of water from the Rio Grande for

municipal use, and irrigated agricultural area.

4.2.2.2.1 *Human Population Estimates and Scenario Projections.*

Conceptually, urban populations are typically served by a central water supply

network, and return waste water to a central sewer and waste water treatment facility.

Rural populations on the other hand are typically served by domestic wells, and treat

waste water returns with septic tanks. Because of the difference between method of

capture from, and return of water to the river or aquifer system for urban and rural

dwellers, the two populations are accounted for separately. The populations of the cities

of Espanola, Santa Fe, Bernalillo, Rio Rancho, Albuquerque, Los Lunas, Belen, Socorro,

and Truth or Consequences, and the county of Los Alamos are modeled as urban.

Populations outside of the cities are considered rural, and lumped by surface water reach.

United States Census Bureau (2007) estimates of city populations in 1990 and

2000 were used to derive the average annual growth rate by urban area during that period.

Table 4-2 summarizes that information. To estimate reach based populations, tract based

population densities from 1990 and 2000 census data (ibid) were intersected with

approximate surface areas associated with each modeled river reach using a Geographical

Information System (GIS) environment. The resulting areas were then multiplied by

their population density and summed by reach to yield reach based population levels in 1990 and 2000. Figure 4-3 shows this process graphically. Finally, the urban population numbers from Table 4-2 were subtracted from the overall reach populations to give rural populations by reach. With the exception of Albuquerque, each modeled urban area was attributed to a single surface water reach as shown in Table 4-2. Albuquerque was assumed to have 2/3 of its population in the reach from San Felipe to Albuquerque, and 1/3 in the reach from Albuquerque to Bernardo. The resulting estimates of rural population by reach in 1990 and 2000, and the implied growth rate during that time are shown in Table 4-3. Human domestic demand is not modeled along the Rio Grande north of Embudo, nor along the Chama due to the lack of a dynamic groundwater model under those river reaches (See Chapter 2). As will be discussed in Section 4.2.2.2.2 below, reach based urban and rural population levels are used to estimate reach based human demand, and groundwater extraction is distributed spatially within the reach based on historic pumping locations.

Table 4-2. Population data for modeled urban areas.

City	Urban Population		Growth [%/yr]	Attributed reach
	1990	2000	1990-2000	
Espanola	8389	9688	1.55%	EMB2OTW
Los Alamos County	18115	18343	0.13%	OTW2CTI
Santa Fe	55859	62203	1.14%	OTW2CTI
Bernalillo	5960	6611	1.09%	SFP2ALB
Rio Rancho	32505	51765	5.93%	SFP2ALB
Albuquerque	384915	448607	1.65%	2/3 SFP2ALB, 1/3 ALB2BDO
Los Lunas	6013	10034	6.69%	ALB2BDO
Belen	6547	6901	0.54%	ALB2BDO
Socorro	8159	8877	0.88%	SA2SM
T or C	6221	7289	1.72%	EB2CBLO
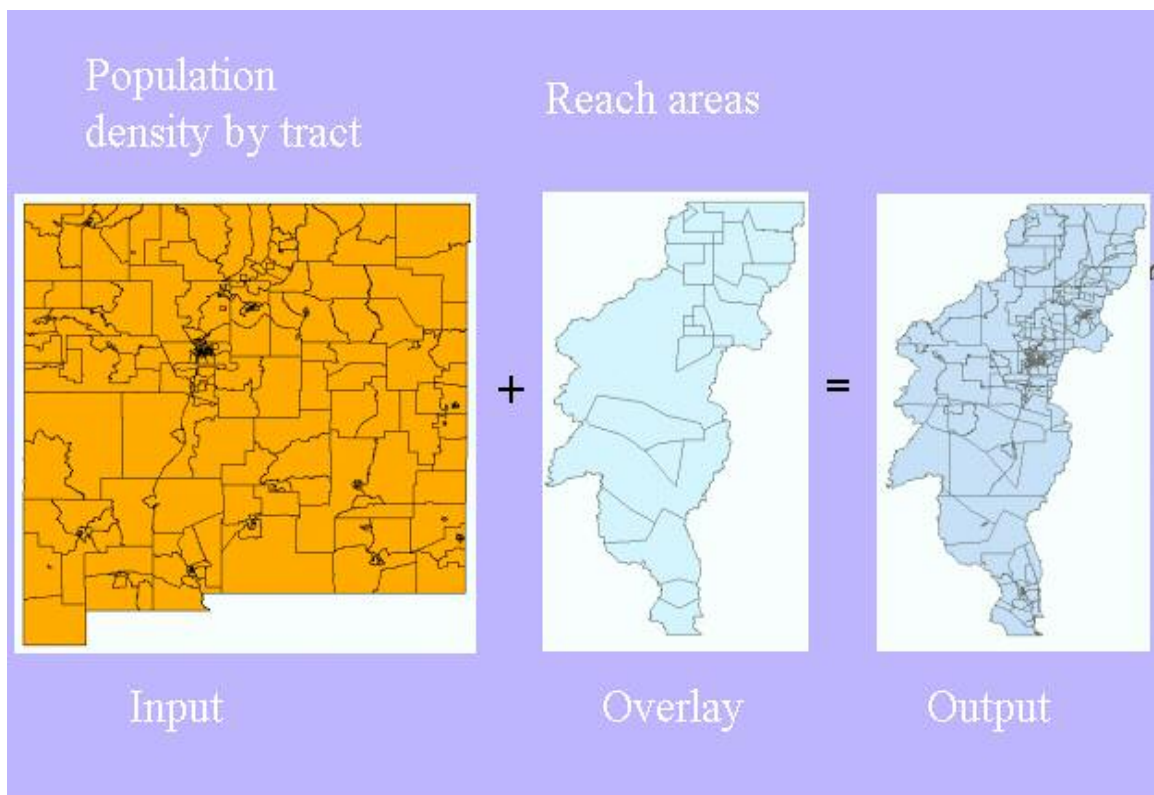
Figure 4-3. Graphical diagram demonstrating spatial data manipulations used to approximate population by reach from 1990 and 2000 census data.

Table 4-3. Human population 1990 and 2000 by modeled river reach exclusive of cities shown in Table 4-2.

Reach	Rural population [persons]		Growth rate [%/yr]
	1990	**2000**	**1990-2000**
Embudo to Otowi	25907	26137	0.1%
Otowi to Cochiti	27009	45499	6.8%
Cochiti to San Felipe	3660	5961	6.3%
Jemez River	1101	842	-2.4%
San Felipe to Albuquerque	34311	60196	7.5%
Albuquerque to Bernardo	133720	140169	0.5%
Bernardo to San Acacia	2285	3454	5.1%
San Acacia to San Marcial	1389	1397	0.1%
San Marcial to Elephant Butte	3371	5721	7.0%
Elephant Butte to Caballo	1604	2023	2.6%

4.2.2.2.2 Scenario Municipal and Industrial Demand and Returns Calculations.

The physical hydrology described in Chapters 2 and 3 is relatively well developed and provides a solid foundation upon which to incorporate human behavior. The human behavior component is on the other hand very basic at this point in the model development. Significant improvements to the model will come from a more complex description of human behavior. Human demand is broken into indoor and outdoor uses, which are modeled with a per capita indoor use rate, and a per capita effective outdoor use area respectively. The effective outdoor use area is multiplied by the reference evapotranspiration rate to give a seasonally varying volume representing outdoor water use. Within modeled cities, the human demand calculated in this way includes municipal and industrial demands, while outside of modeled cities, the demand is more representative of domestic use only. The population dependent human demand relationships for a given urban area or reach are shown mathematically in equations 4-1 and 4-2.

$$D_{hi}^t = pc_h * P^t \qquad\qquad (4\text{-}1)$$
$$D_{ho}^t = ET_{ref}^t * pc_{eoa} * P^t \qquad\qquad (4\text{-}2)$$

where

D_{hi}^t	$=$	human indoor demand at timestep t. [L^3/T]
D_{ho}^t	$=$	human outdoor demand at timestep t. [L^3/T]
pc_h	$=$	per capita human indoor use. [L^3/person/T]
pc_{eoa}	$=$	per capita effective outdoor area. [L^2/person]
ET_{ref}^t	$=$	reference evapotranspiration at timestep t (see equation 2-7). [L/T]
P^t	$=$	human population at timestep t in the city or reach of interest. [persons]

As discussed in Section 4.2.2.2.1, population is tracked within the modeled urban areas, and for rural populations by river reach.

The URGWOM data set (USACE et al. 2002) provides municipal wastewater return data for Espanola, Los Alamos, Santa Fe, Bernalillo, Rio Rancho, Albuquerque, Los Lunas, Belen, Socorro, and Truth or Consequences that is most complete and reliable from 1990 to 1999. This data was used to estimate indoor water use. By assuming indoor use between 100 and 200 gallons per day (gpd) per person, and assuming 30% - 90% of city indoor water use ends up as wastewater depending on the city, we can calculate reasonable approximations of 1990-1999 wastewater returns. These comparisons are shown in Figures 4-4a through 4-4c. The parameters assumed for each urban or rural population type are listed in Table 4-4.
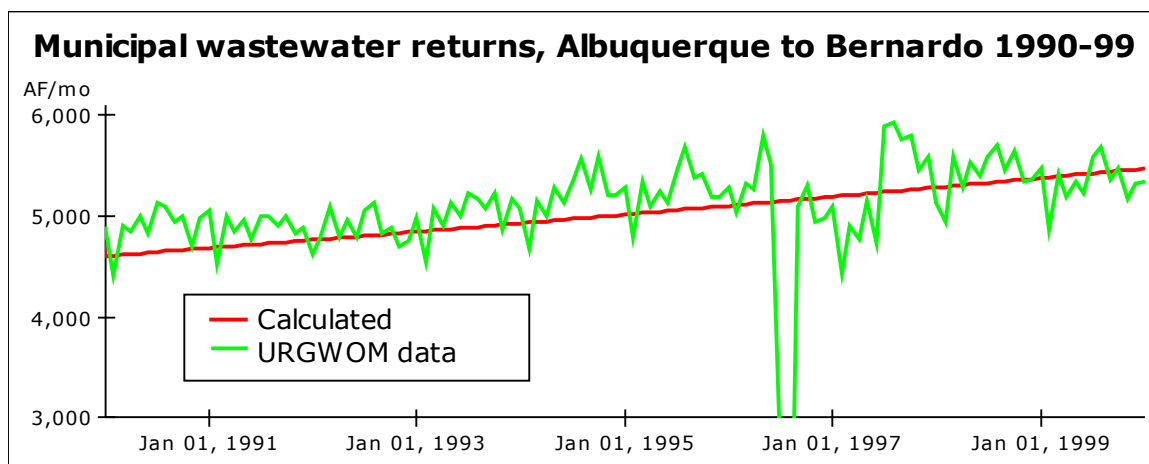
Figure 4-4a. Calculated and observed wastewater returns for Albuquerque, Belen, and Los Lunas 1990 to 1999. Calculated returns are based on the city populations and growth rates shown in Table 4-2, and indoor use and return parameters shown in Table 4-4.
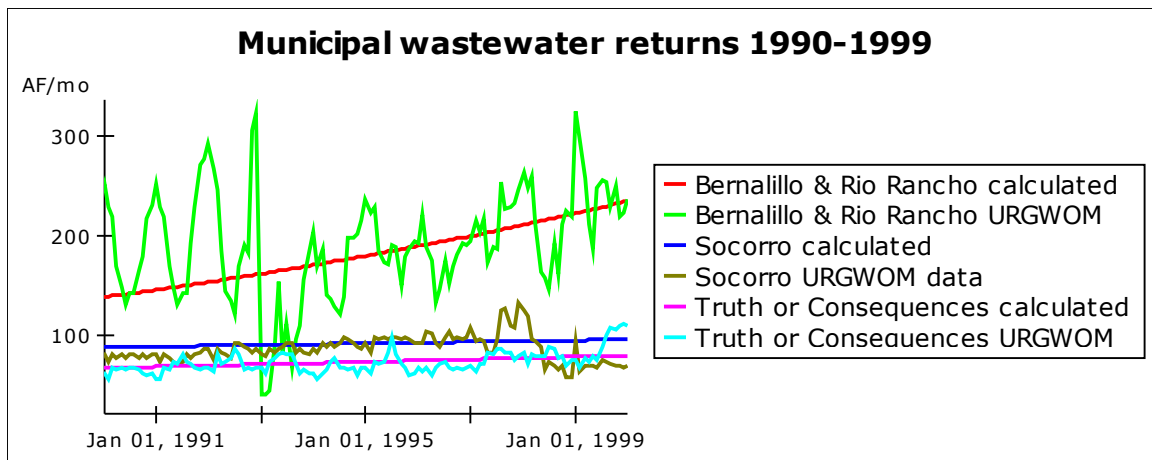
Figure 4-4b. Calculated and observed wastewater returns for Bernalillo, Rio Rancho, Socorro, and Truth or Consequences from 1990 to 1999. Calculated returns are based on city population growth rates shown in Table 4-2, and indoor use parameters shown in Table 4-4.
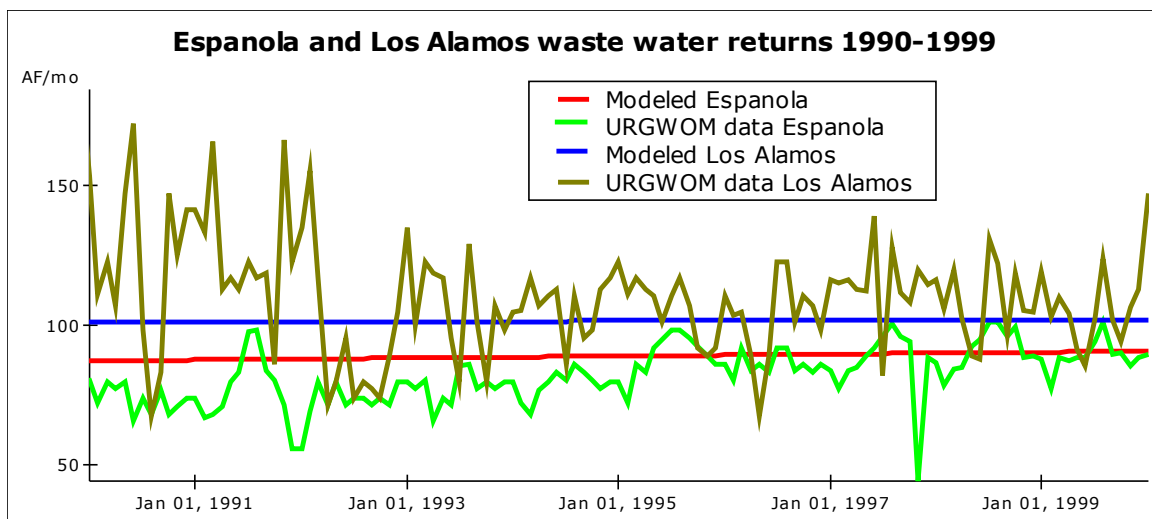
Figure 4-4c. Calculated and observed wastewater returns for Espanola and Los Alamos from 1990 to 1999. Calculated returns are based on the city populations and growth rates shown in Table 4-2, and indoor use and return parameters shown in Table 4-4.

Once indoor demand is calculated, the per capita effective outdoor area (pc_{eoa} equation 4-2) is manipulated to result in overall calculated demand between 1990 and 2000 similar to urban area groundwater pumping records. With the exception of Santa Fe, which has a local surface water resource and will be discussed below, all urban areas

are assumed to have served one hundred percent of demand with groundwater extraction.
The resulting per capita effective outdoor areas are shown in Table 4-4, and the
comparison between modeled and observed groundwater use is shown in Figures 4-5a
through 4-5d. The observed data in Figures 4-5a and 4-5b is from the Albuquerque basin
regional groundwater model (McAda and Barroll 2002), and thus has only two values per
year. The observed data in Figures 4-5c and 4-5d represents annual average values.

Table 4-4. Demand related parameters assumed for base case scenario evaluation.
Per capita human indoor use (pc$_h$) and per capita effective outdoor area (pc$_{eoa}$)
are defined in Equations 4-1 and 4-2.

Urban or rural area	pc$_h$ [gpd/person]	indoor use to ww [%]	pc$_{eoa}$ [ft^2/person]
Espanola	100	90%	50
Los Alamos county	200	30%	50
Santa Fe	150	100%	50
Bernalillo	130	30%	400
Rio Rancho	130	30%	400
Albuquerque	140	90%	400
Los Lunas	130	90%	400
Belen	130	90%	400
Socorro	130	90%	400
T or C	130	90%	400
Rural north of Cochiti	50	100%	50
Rural south of Cochiti	80	100%	250

Spatial patterns of groundwater pumping for future scenarios are based on spatial
patterns of pumping in the calibration period. The volume pumped may change, but the
relative location of that pumping is assumed to stay the same in all modeled groundwater
basins. An improved conceptual approach would be to track human populations by

groundwater model zone. Such an approach is beyond the scope of this analysis, and left

to future work.
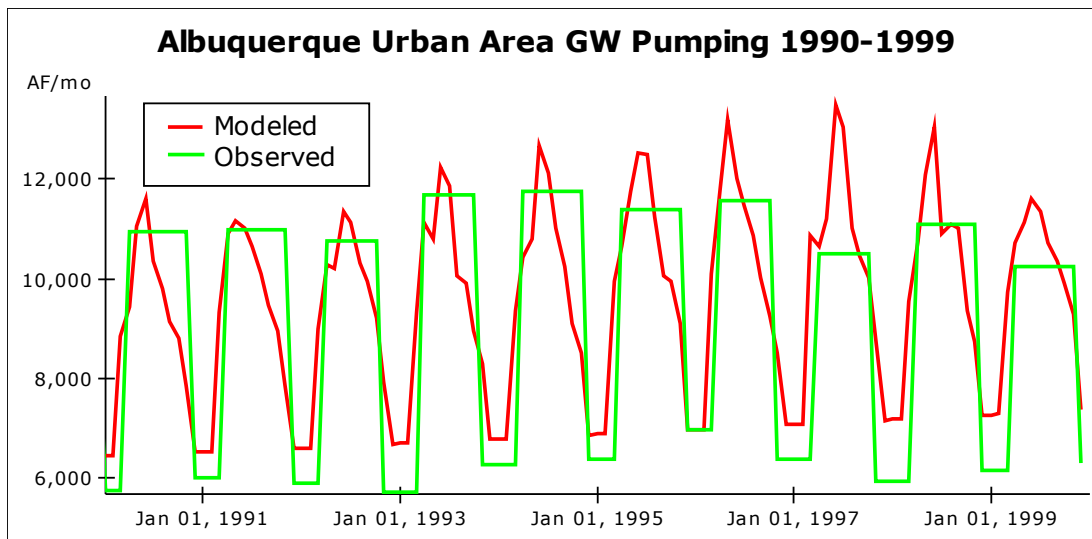
Figure 4-5a. Albuquerque urban area groundwater pumping calculated with Equations 4-1 and 4-2 with parameters from Tables 4-2 and 4-4 compared to observed data (from McAda and Barroll 2002) averaged for irrigation and non-irrigation season.
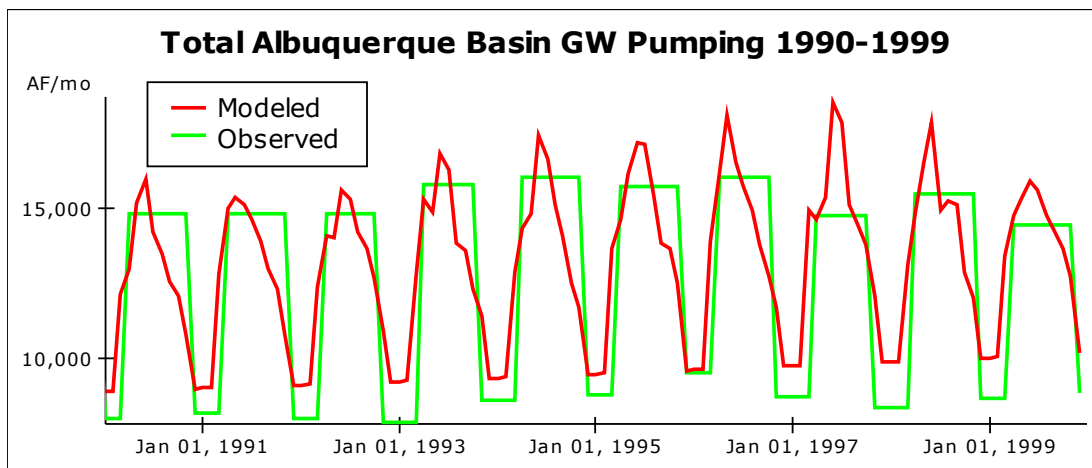
Figure 4-5b. Albuquerque basin total groundwater pumping calculated with Equations 4-1 and 4-2 with parameters from Tables 4-2, 4-3, and 4-4 compared to observed data (from McAda and Barroll 2002) averaged for irrigation and non-irrigation season.

County of Los Alamos and city of Espanola groundwater use 1975-1999

AF/mo
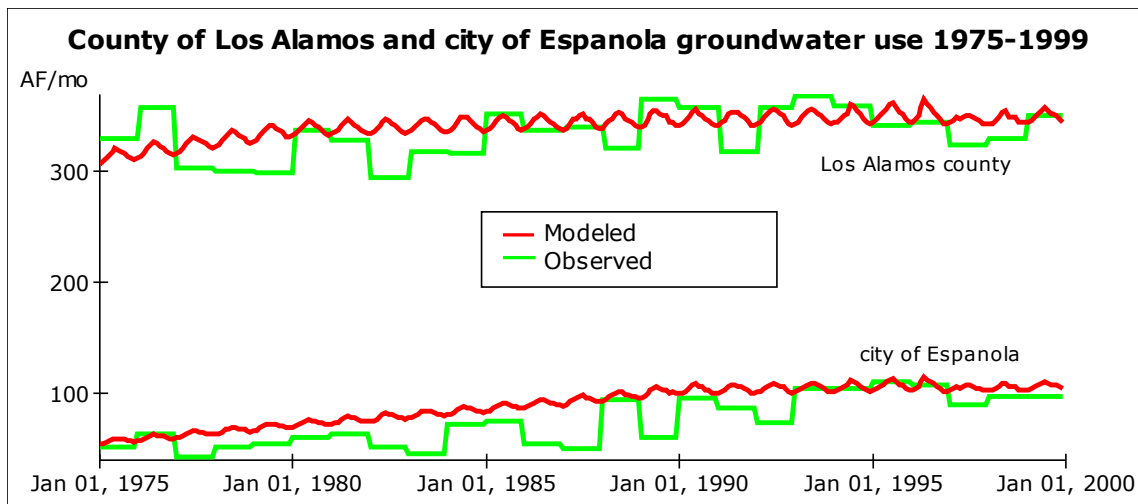
Figure 4-5c. County of Los Alamos and city of Espanola groundwater pumping calculated with Equations 4-1 and 4-2 with parameters from Tables 4-2 and 4-4 compared to observed annual average data.

Espanola basin domestic groundwater use 1975-1992

AF/mo
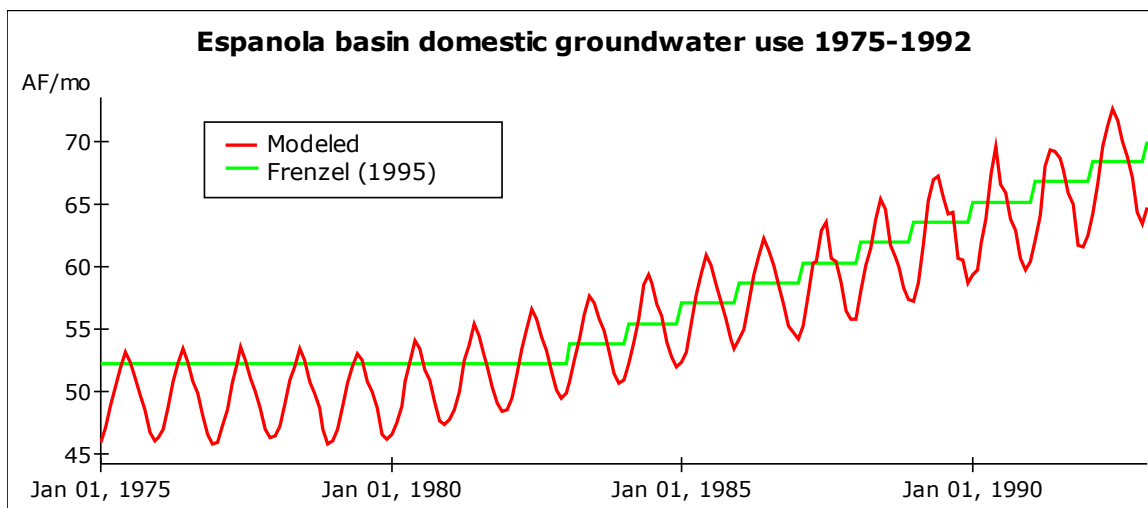
Figure 4-5d. Espanola basin domestic well groundwater pumping, calculated with Equations 4-1 and 4-2 with parameters from Tables 4-3 and 4-4, compared to estimated annual average values from Frenzel (1995).

The city of Santa Fe serves its municipal and industrial demand with Santa Fe river surface water stored in reservoirs above the town. To model groundwater use by the city of Santa Fe, surface water resources must be estimated. Annual surface water availability for the city of Santa Fe is estimated with Equation 4-3; a linear function of

snow water equivalent (SWE) measured in February, March, and April at Elk Cabin in

the upper Santa Fe watershed (USDA 2007).

$$SW_{sf}^{j} = SWE_{ec}^{j} * 0.8818[\text{ft}^3/\text{s}/\text{inch}] + 4.97[\text{ft}^3/\text{s}] \qquad (4\text{-}3)$$

where

SW_{sf}^{j} = City of Santa Fe available surface water resources in year j. $[L^3/T]$

SWE_{ec}^{j} = Average of February, March, and April snow water equivalent measurements at Elk Cabin in the upper Santa Fe river watershed. $[L]$

Using this coarse approximation of surface water resources, Santa Fe groundwater

use can be modeled with Equations 4-1 through 4-3, and parameters from Tables 4-2 and

4-4 as shown in Figure 4-6. The pencil type pattern is the result of calendar year

estimates of surface water resources leading to instantaneous changes in groundwater

demand at the beginning of each new year, coupled with seasonal demands that peak

during the summer. With the exception of some very bad years (e.g. 1986), Santa Fe

groundwater use is predicted to a reasonable degree. There is certainly room for

improvement in the modeling of Santa Fe surface water resources and their relationship

to groundwater pumping, however such analysis is beyond the scope of this study. As

mentioned in Chapter 3 and shown in Figure 3-27, 50% of Santa Fe wastewater is

assumed to recharge the regional groundwater system. 1975-99 estimated groundwater

recharge from Santa Fe wastewater is shown in Figure 4-7.

Espanola waste water returns are added to the Rio Grande in the Embudo to

Otowi reach. Consistent with Frenzel (1995), who does not account for Los Alamos

waste water recharge in the regional groundwater model due to lack of information, this

City of Santa Fe Groundwater Use 1975-99
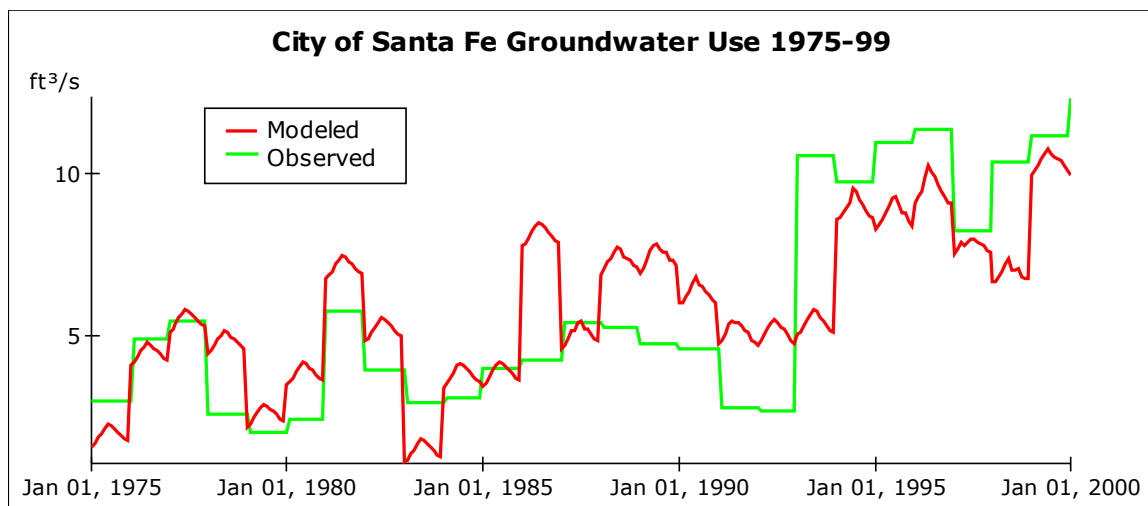
Figure 4-6. City of Santa Fe groundwater use calculated with Equations 4-1, 4-2, and 4-3 with parameters from Tables 4-2 and 4-4, compared to observed annual average values.

Groundwater recharge from Santa Fe wastewater 1975-99
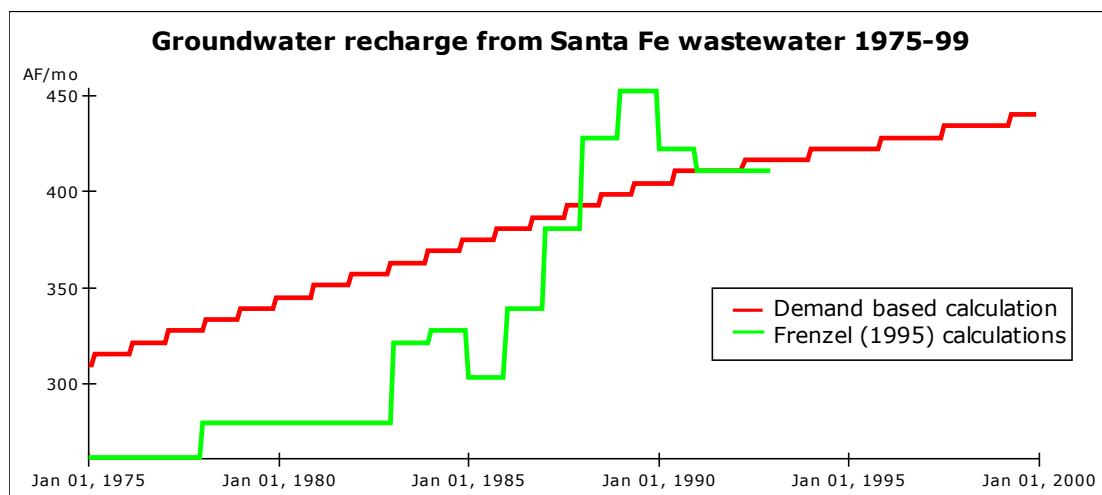
Figure 4-7. City of Santa Fe groundwater recharge calculated with Equation 4-1 with parameters from Tables 4-2 and 4-4, compared to estimates from Frenzel (1995). See also Figure 3-27.

flux is not added to the surface water or groundwater systems. This assumption might be improved in the future to allow some return of water removed from the system by Los Alamos users. Santa Fe wastewater is discharged to the Santa Fe river channel, where ½ of it is assumed to recharge the groundwater system as discussed above. Wastewater

returns from the cities of Bernalillo and Rio Rancho are returned to the Rio Grande in the San Felipe to Albuquerque reach. Wastewater returns from Albuquerque, Los Lunas, and Belen are returned to the Rio Grande in the Albuquerque to Bernardo reach. Socorro wastewater returns to the Rio Grande between San Acacia and San Marcial, and Truth or Consequences wastewater returns to the Rio Grande between Elephant Butte and Caballo.

Espanola basin septic recharge is not considered by Frenzel (1995), and is also assumed negligible here. Albuquerque basin septic recharge is estimated as 10% of all indoor water use not accounted for in wastewater returns. 10% is a calibration factor chosen to make the 1990 volume of septic returns estimated with this method (360 AF/mo) comparable to the value of 350 AF/mo used by McAda and Barroll (2002). Socorro basin septic recharge is estimated as 50% of all indoor water use between San Acacia and San Marcial not accounted for in wastewater returns, and is a minor and potentially negligible flux (40 AF/mo in 1990) included for completeness and consistency with the Albuquerque basin groundwater model.

4.2.2.2.3 *Municipal Use of Main-Stem Surface Water During the Scenario Period.*

The city of Albuquerque has begun construction on infrastructure necessary to divert San Juan Chama (Colorado river basin water transferred to the Rio Grande system, see Section 2.2.2) water directly from the Rio Grande in Albuquerque for treatment and direct household use (Albuquerque Bernalillo County Water Utility Authority, 2007). The city of Albuquerque has rights to 48,200 AF/yr of San Juan Chama water from Heron reservoir, and beginning in 2008 plans to divert double this amount (less transmission and storage losses between Heron and Albuquerque), and return ½ via the

waste water treatment plant (ibid). The base case scenario has Albuquerque beginning to

utilize this surface water resource in 2008. The city and county of Santa Fe also plan to

eventually divert 8730 AF/yr of San Juan Chama water directly from the Rio Grande in

the future, and have initiated steps towards that goal including completion of a draft

environmental impact statement (USDA and USDoI, 2004). The city of Espanola and

San Juan Pueblo are also laying plans to divert between 2000 and 4000 AF/yr of San Juan

Chama water directly from the Rio Grande in the future (Santa Fe New Mexican 2005).

Both of these diversions are in the planning stages and not currently included in the

model.

4.2.2.2.4   *Irrigated Agricultural Area During the Scenario Period.*

Irrigated agriculture is assumed to stay at 1999 levels throughout the scenario

period. This base case assumption can be changed however, with the user choosing an

annual percent change of irrigated agricultural acreage to be applied through the scenario

run. As discussed in Section 2.2.3.2.6, 1999 vegetation areas for irrigated agricultural

crops are taken from three different sources. Crop acreages along the Rio Chama are

taken from the Watermaster's Report for the Rio Chama Mainstream 2002, with crop

type percentages from the Rio Chama Watermaster (Stermon M. Wells, personal

communication July 2003). For acreages above Cochiti along the Rio Grande,

approximate acreages of 200 and 5,000 acres for the reaches Taos Junction Bridge to

Embudo and Embudo to Otowi respectively are taken from the URGWOM Physical

Model Documentation (USACE et al. 2002). The same crop distribution as used for the

Chama is assumed for the Rio Grande above Cochiti. Irrigated crop acreages for the

reaches south of Cochiti, with the exception of the Jemez river reach, are taken from

URGWOM Physical Model Documentation (*ibid*), which tabulated the data from Middle

Rio Grande Conservancy District (MRGCD) sources, and broke it into river reach based

units. Jemez river total acreage of almost 5400 acres is from McAda and Barroll (2002)

model input files, while the crop distribution is an average of URGWOM (USACE et al.

2002) crop distributions reported between Cochiti and Elephant Butte from 1975-1999.

Irrigated acreages assumed in the base case condition are summarized by reach in Table

4-5.

4.2.2.2.5   *Scenario Period Human Behavioral Drivers Summarized.*

The human behavioral inputs described in this section are a non-unique, highly

lumped estimate of rough human behavioral parameters. There is significant room for

improvement in the formulation of human demands, however as described in the previous

sections, the user is given the ability to change any of these input assumptions based on

his or her own knowledge or interest. In summary then, the base case scenario assumes a

human population between Embudo and Caballo reservoir growing from 1.4 million to

2.9 million between 2005 and 2043, based on 1990-2000 rates. Per capita indoor use of

100 to 200 gpd per person, and effective per capita outdoor use area of 50 to 400 square

feet per person depending on location (see Table 4-4) are assumed. 75,000 acres of

irrigated agriculture including 9,000 acres of irrigated riparian habitat in the Bosque del

Apache National Wildlife Refuge are assumed based on 1999 levels. The city of Santa

Fe population is served by water from local surface water resources supplemented by

groundwater extraction. The city of Albuquerque population is served by direct diversion

of San Juan Chama surface water beginning in 2008 supplemented with groundwater

extraction. All other cities are served exclusively by groundwater resources. Results of

the base case scenario run, and a run with all parameters the same except zero population

growth are summarized in Section 4-3.

Table 4-5. Irrigated area assumed for the base case scenario (based on 1999 estimates). Crop abbreviations for purposes of space include MF, MV, NS, PG, Sorgh, SB, and TF for miscellaneous fruit, miscellaneous vegetables, nursery stock, pasture grass, sorghum, spring barley, and tree fruit respectively. Reach abbreviations can be inferred by comparison to full reach names shown in Table 2-4. Jemez crops are based on McAda and Barroll (2002) for totals, and URGWOM (USACE et al. 2002) 1975-1999 Cochiti to Elephant Butte average proportions for the crop mixture.

Reach Crop	ELV ABQ	ABQ CTA	TJBE MB	EMB OTW	CTI SFP	JMZ	SFP ALB	ALB BDO	BDO SA	SA SM	Total
Alfalfa	71	1094	45	1125	1201	2870	4582	16110	138	4806	**32042**
Chile	0	0	0	0	23	56	87	305	3	91	**565**
Corn	34	522	21	537	173	224	660	2322	11	693	**5197**
Grape	0	0	0	0	1	6	5	17	0	5	**34**
Melon	0	0	0	0	2	5	8	29	0	9	**53**
MF	0	0	0	0	10	27	38	132	1	39	**247**
MV	13	193	8	199	18	104	69	243	5	72	**924**
NS	0	0	0	0	14	24	55	192	1	57	**343**
Oats	0	0	0	0	45	76	172	605	4	180	**1082**
PG	124	1903	78	1957	763	1851	2911	10234	89	3053	**22963**
Sorgh	0	0	0	0	8	33	30	104	2	31	**208**
SB	0	0	0	0	0	30	0	0	1	0	**31**
TF	34	519	21	534	1	1	4	14	0	4	**1132**
Wheat	20	311	13	320	21	65	82	287	3	86	**1208**
Total	**296**	**4542**	**186**	**4672**	**2280**	**5372**	**8703**	**30594**	**258**	**9126**	**66029**

4.3   Scenario Results

The base case scenario described above, and a scenario the same in all ways except without population growth ("no growth" scenario) are evaluated within the context of six model output metrics. These metrics are reservoir storage, Caballo reservoir releases, groundwater mass balance, critical river flows, agricultural ET shortfalls, and Rio Grande compact balance. The sensitivity of each metric to changes in agricultural acreage, human per capita indoor and outdoor use, and population growth rates is included in the analysis.

4.3.1 Reservoir Storage

Reservoir storage in six of the seven modeled reservoirs is shown in Figure 4-8. With the exception of five transient storage events lasting no more than two months each, storage in Jemez reservoir is zero throughout the scenario period, and identical for the base case and no growth cases. For a summary of reservoir operation rules, see Section 2.2.3.5.3 in Chapter 2. The effect of the series of dry years from 2008 through 2018 is visible in all reservoirs except Cochiti. The effect of wet years from 2027 through 2033 is visible to some extent in all reservoirs, and most noticeable in Elephant Butte. Population growth has a significant effect on groundwater mass balance (see Section 4.3.3), but for the 40 year scenario period the groundwater changes result in offsetting and relatively small surface water effects, which are buffered slightly by changes in agricultural consumptive use (see Section 4.3.5). As a result, reservoir behavior in the scenario period is essentially unaffected by human population growth, with minor storage differences in Elephant Butte (see Section 4.3.6) and resulting impacts on how water can
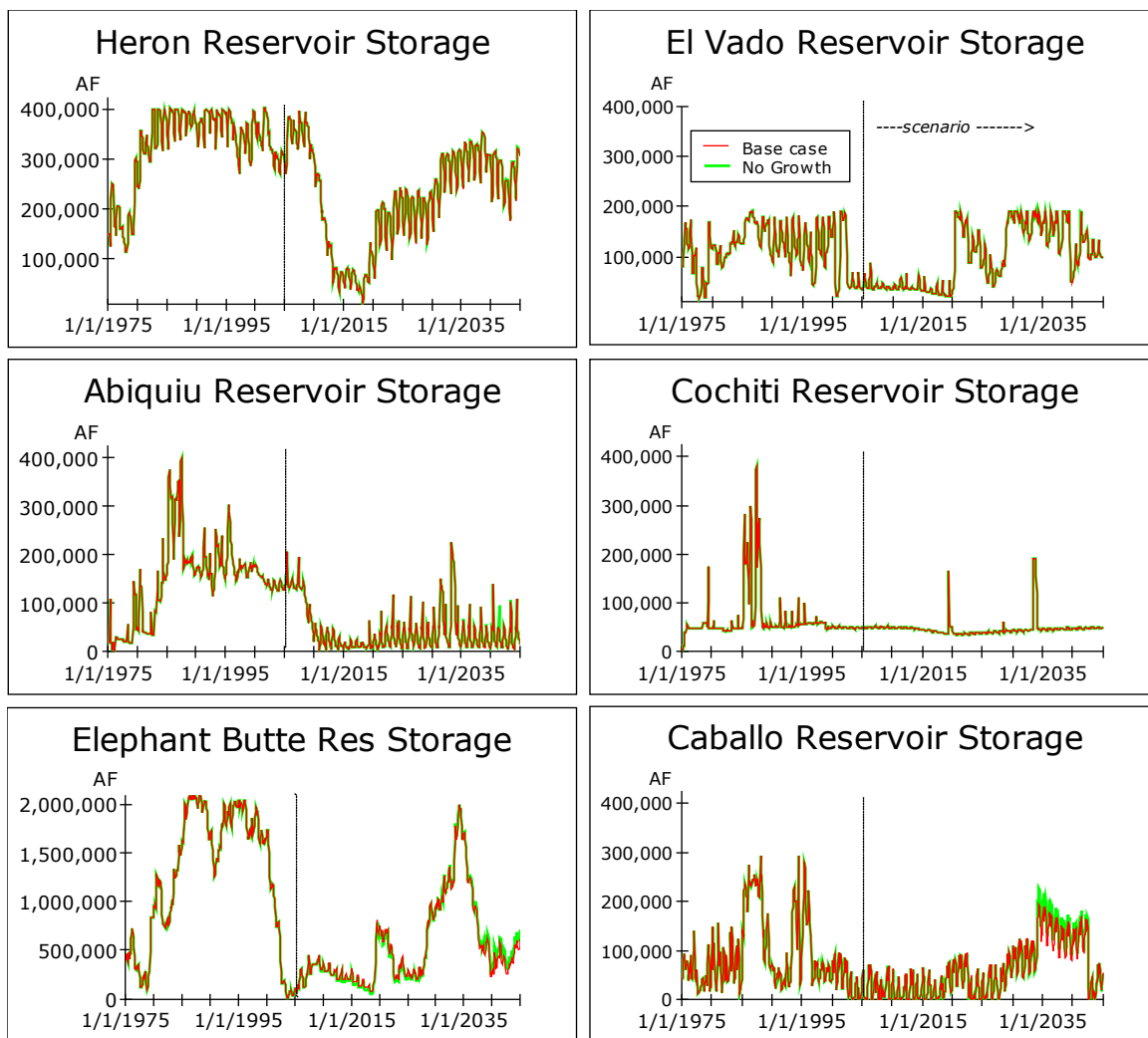
Figure 4-8. Reservoir storage between 1975 and 2045 for the base case (red) and no growth (green) scenarios. 1975-2000 storage values are equal to historic observations.

be stored upstream. Heron storage drops dramatically beginning in 2009 as a result of climate dependent reduced transmountain diversions of San Juan Chama water and an increase in availability of storage space in Abiquiu. Abiquiu storage drops significantly beginning in 2008 when the city of Albuquerque drinking water project goes online (see Section4.2.2.2.3), and water is released for direct diversion and offset of pumping induced river leakage. El Vado native storage is limited when Article VII of the Rio

Grande Compact is in effect (see Section 2.2.3.5.3.2), resulting in the low storage observed in El Vado from the beginning of the scenario in 2005 to 2019, and the reductions in storage between 2021 and 2028 and again during the final five years of the scenario. Cochiti maintains a San Juan Chama based recreation pool throughout the scenario period, with three transient flood control spikes. Elephant Butte is a strong function of the climate sequence (see Figure 4-1), releasing up to 790,000 AF/yr as available, and storing any excess. Caballo serves as a modulator of Elephant Butte releases in average or below average conditions, and builds up storage in the wetter years as Elephant Butte storage rises.

4.3.2 Caballo Releases

Cumulative Caballo outflows, which represent surface water flows out the south boundary of the model, are shown for the 1975-1999 calibration period, the 2000-2004 validation period, and the 2005-2044 scenario period in Figure 4-9. Caballo outflows are significantly reduced during the initial 15 years of the scenario period (2005-2019), which is a sustained dry period. From 2020 forward however, target deliveries of 790,000 AF/yr from Caballo are essentially met. Population growth in New Mexico has a negligable impact on Caballo outflows for the reasons discussed in Section 4.3.1.

4.3.3 Groundwater Mass Balance

Major groundwater mass balance terms for Espanola, Albuquerque, and Socorro groundwater basins during the 2005-2044 scenario period under base case and no growth scenarios are shown in Figure 4-10 a-c. The fluxes tracked include groundwater
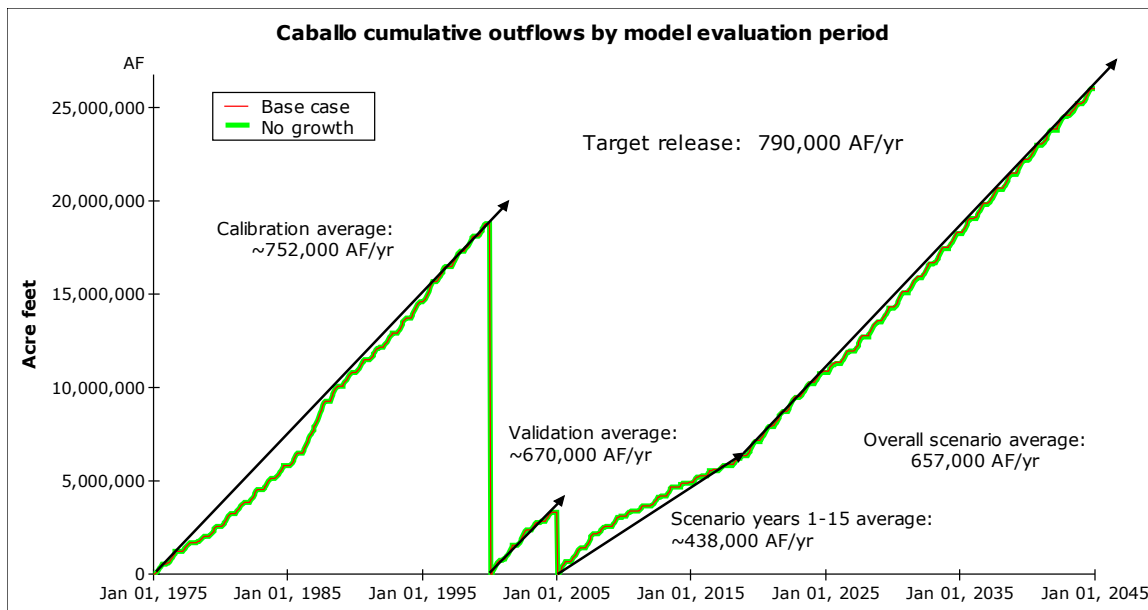
Figure 4-9. Caballo cumulative releases during calibration, validation, and scenario analysis for the base case (red) and no growth (green) scenarios. Population growth in New Mexico has no impact on Caballo releases during the scenario period.
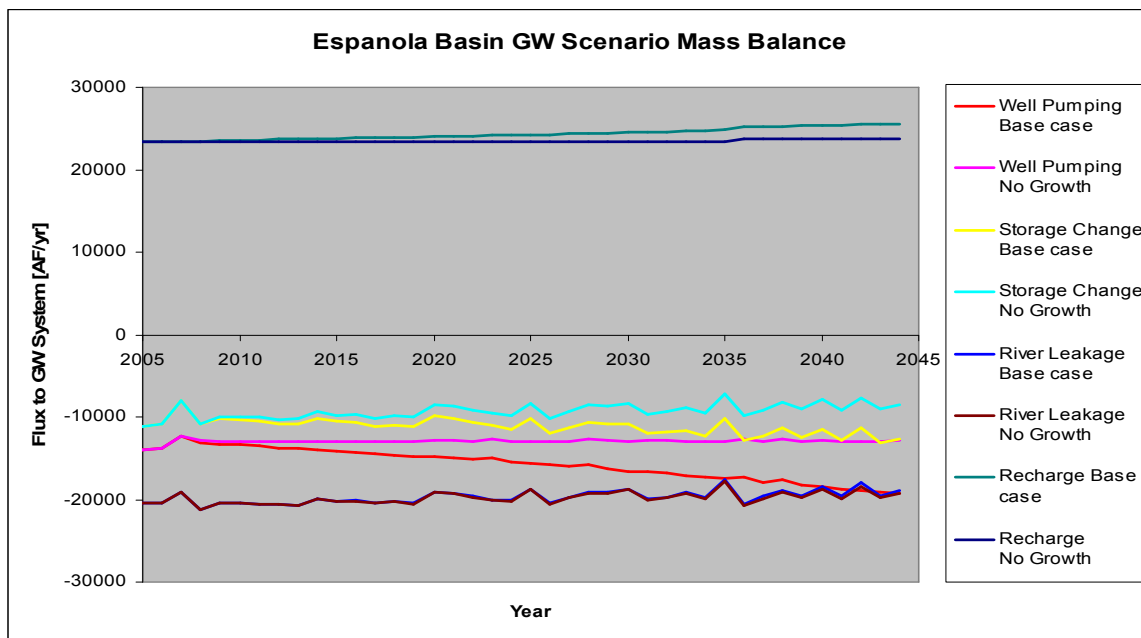
Figure 4-10a. Espanola groundwater basin major mass balance terms under base case and no growth scenario conditions. Population growth increases well pumping and wastewater recharge, but has negligible effect on river leakage.
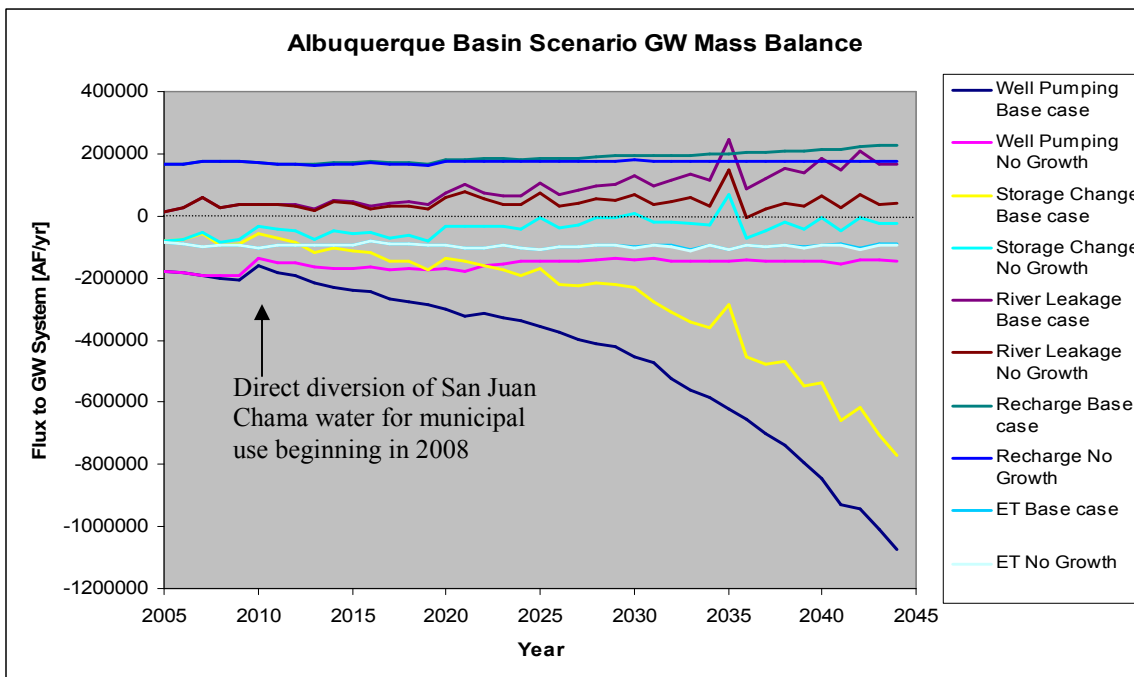
Figure 4-10b. Albuquerque groundwater basin major mass balance terms under base case and no growth scenario conditions. Population growth increases well pumping and septic tank recharge, as well as river leakage.
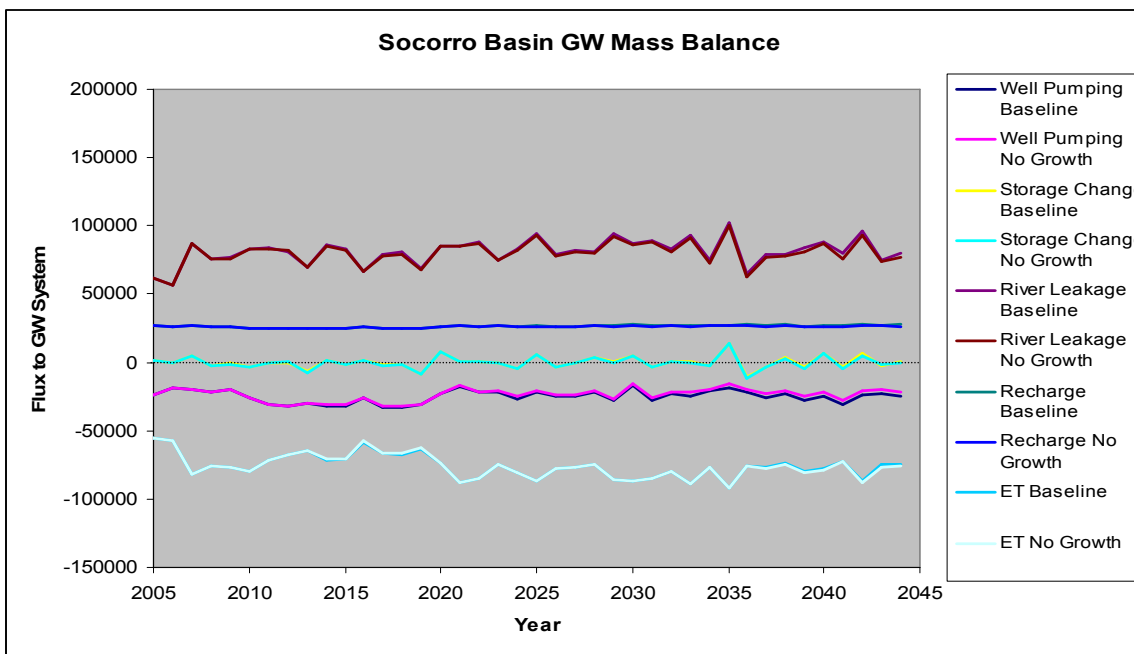
Figure 4-10c. Socorro groundwater basin mass balance terms under base case and no growth scenario conditions. Population growth has negligible effect on the groundwater basin which is effectively in steady state, even with the groundwater extraction.

recharge, river leakage to the groundwater, well pumping, and riparian ET. The recharge term includes mountain front, areal, irrigation seepage, canal leakage, tributary recharge, and net groundwater inflows along the model boundary. The river leakage term is a net term including the effect of drains. Within Espanola groundwater basin, population growth results in increased well pumping and as a result, increased wastewater recharge. The overall Espanola basin groundwater system loses about 10,000 AF of stored water per year, a value that increases with base case population growth. Rio Grande river leakage (gain) is affected only negligibly by population growth.

Albuquerque groundwater basin bears the brunt of the regional population growth under base case conditions, and even with a reduction in pumping due to direct use of San Juan Chama water by the City of Albuquerque in 2008, base case population growth results in significant groundwater extraction and resulting increases in septic recharge and river leakage. Under no growth conditions however, the basin as a whole is close to sustained yield (zero storage change) by the end of the scenario period.

Socorro groundwater basin is in a dynamic steady state, with no significant long term storage change despite annual variability in river leakage. The Socorro basin is essentially unaffected by the minor amounts of population growth projected in the area in the base case scenario.

4.3.4 Critical Flows

Due to ample reservoir storage available for flood control at Jemez, Cochiti, and Abiquiu reservoirs during the scenario period as seen in Section 4.3.1, high flow flooding

events are not evaluated as a scenario metric. While localized, and short lived flooding

may occur despite abundant flood control storage upstream, a monthly timestep model

without a rainfall runoff component is not the appropriate model in which to evaluate this

sort of risk. Much more likely is that the river will dry up in given locations with

potentially devastating ecological consequences to the aquatic fauna (USDoI, FWS,

2003a). Based on the presence of a federally endangered fish species in the river, and

associated legal consequences, providing minimum river flows has become an important

part of system management (USDoI, FWS, 2003b). Target flows at critical locations are

a part of the reservoir rules that govern reservoir behavior during the scenario period. To

estimate low flow extremes in the river channel with a monthly timestep, historical daily

data at Bernardo, San Acacia, and San Marcial was evaluated to determine the historical

relationship between a given monthly average flow, and the occurrence of at least one

day of zero flow at the gage. Results of this analysis are shown in Table 4-6, and total

zero flow days per month for the recorded history of all three gages is compared to

monthly Otowi flows in Figure 4-11.

Minimum modeled flows at each gage location are tracked during the scenario

period, and the likelihood of a zero flow day ($E(Qd=0)$) estimated based on the historical

relationship between monthly flow (Q_m) and observed zero flow days shown in Table 4-

6. As seen in Figure 4-12, the likelihood of a zero flow day in a given year decreases

during the scenario period as compared to the historic period suggesting that the way

reservoirs and diversions are operated during the scenario period differs from the way

they were operated historically. This change is quantified in Table 4-7, and is most likely

Table 4-6. *Historic relationship between monthly average gaged flow (Q_m) and the likelihood of observing at least one zero flow day at the same gage (E(Q_d=0)), including the logarithmic best fit relationship and R^2 measurement of goodness of fit for each gage location.*

Monthly average flow [cfs]	Percent of historic months in given monthly flow range recording at least one day of zero flow		
	Bernardo gage	San Acacia gage	San Marcial gage
0 to 10	90%	25%	100%
10 to 30	82%	20%	81%
30 to 100	50%	13%	49%
100 to 500	49%	2%	38%
500 to 1000	24%	1%	10%
Period of Record	1957 - 2005	1958 - 2006	1949 - 2006
E(Q_d=0) =	$-0.1337Ln(Q_m) + 1.2164$	$-0.0654Ln(Q_m) + 0.4068$	$-0.1819Ln(Q_m) + 1.4083$
R^2 =	0.91	0.95	0.96
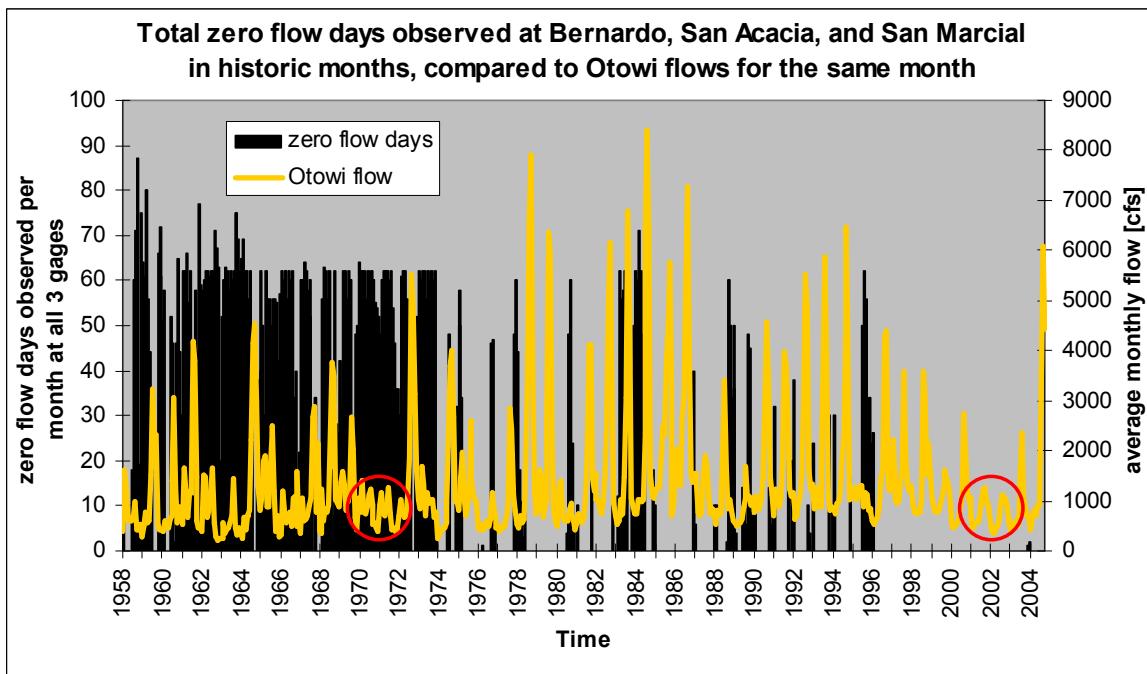
Figure 4-11. *Observed zero flow days per month along the Rio Grande at Bernardo, San Acacia, and San Marcial between October 1958 and June 2005 compared to average monthly flows at Otowi. Note the similarities in 1970-1972 and 2001-2003 Otowi flows with significant differences in occurance of zero flow days at the gages south of Albuquerque.*

a result of water operations changes intended to maintain river habitat for the endangered

Rio Grande silvery minnow (USDoI, FWS 2003b). Indeed, although 2000-2004 were

very dry years in the system (see Figure 2-33); no zero flow days were observed at

Bernardo or San Marcial, and only 3 at San Acacia during that period, far less than any

other 5 year period with observations at all three gages, as seen in Figure 4-11. Of

particular interest are the periods 1970-1972 and 2001-2003 when Otowi flows are

relatively similar, but zero flow events at the downstream gages are common in the 1970-

1972 period and unseen in the 2001-2003 period. As minimum stream flow has become

a factor in water operations, zero flow events have become less common, even in low

flow years. With scenario water operations based on current rules, it seems reasonable

that zero flow events occur less in the scenario period than they did in the historic period.

Figure 4-12 and Table 4-7 show base case only, as these results do not change

appreciably in the no growth scenario for a variety of reasons discussed in Section 4.3.1.

The chance of zero flow events is increased during the first 15 years of the scenario

period, consistent with the below average hydrological inputs seen early in the base case

scenario.

These results should be considered approximate for 3 main reasons. A more exact

calculation of the expectation of at least one zero flow day occurring in a year would be

done by multiplying the twelve monthly probabilities of no zero flow days to get the

probability of no zero flow days in the year, and then subtracting the result from one.

The method shown here uses the probability of a zero flow event based only on the

lowest flow month in a given year, and so should tend to underestimate the probability by
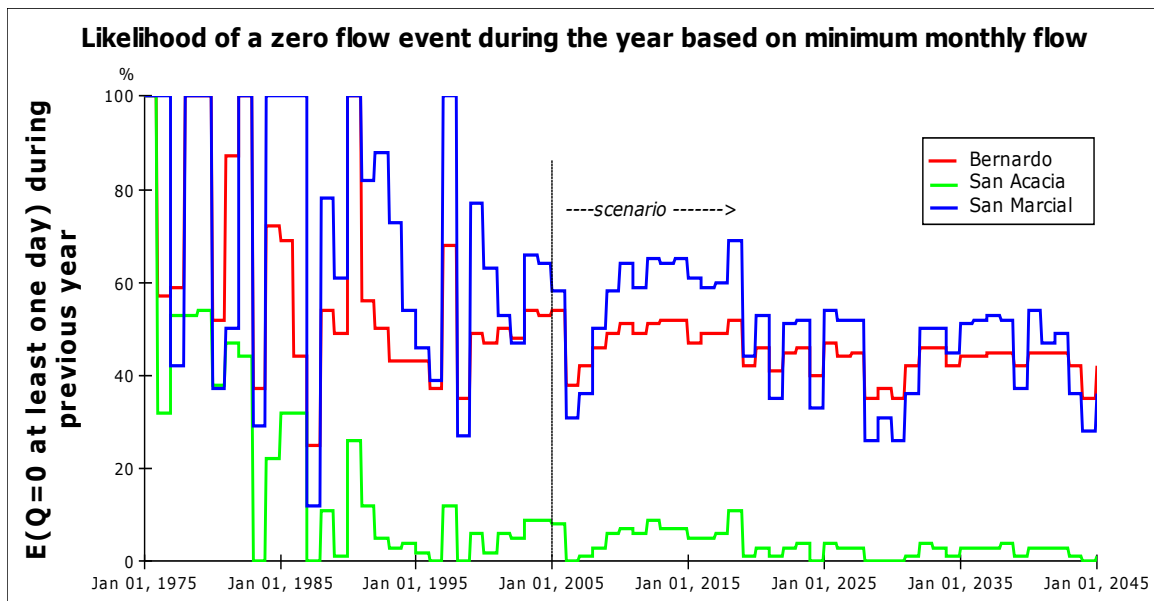
Figure 4-12. Likelihood of at least one zero flow day in the Rio Grande at Bernardo, San Acacia, and San Marcial in a given year based on the minimum monthly flow for that year.

Table 4-7. The modeled likelihood of zero flow days decreases at each gage location from Bernardo to San Marcial during the scenario as compared to the historic period (modeled or observed). This change is likely the result of endangered species motivated water operations.

Gage Location	% years with observed zero flow		Modeled likelihood of zero flow event	
	Historic observed		Historic modeled	Scenario modeled
Bernardo	59%		60%	45%
San Acacia	18%		20%	5%
San Marcial	58%		70%	50%

ignoring other low flow months in the same year. Second, the relationship between a

given monthly flow at a gage, and the observation of zero flow days at that same gage

can change with time as seen in Figure 4-11. Finally, using a monthly model to estimate

zero flow events of much shorter timescale is a risky proposition in general, and,

estimates of zero flows at point locations do not explicitly consider the relationship

between the point location zero flow, and the sections of river upstream and downstream of the gage. For all of these reasons, the estimates of likelihood of zero flow events are approximate from an absolute standpoint, however they are a useful proxy for how wet the river will be in the future under a specific set of climatic conditions. Specifically, the water operations rules used to run the reservoirs and diversions during the scenario period should result in fewer low flow days in the future than have been observed historically.

4.3.5 Agricultural ET Shortfalls

Agricultural consumptive demand is calculated based on potential ET (PET) volume as described in Section 2.2.3.2. This potential is limited by actual water availability to actual ET (AET) as discussed in Section 2.2.3.2.9. Comparison of AET to PET is one way to measure reduced surface water availability for irrigation purposes. Figure 4-13 shows the ratio of AET (volume) divided by PET (volume) between Cochiti and Elephant Butte between 1975 and 2045. (Due to lack of return flow data, AET is modeled as equal to PET for irrigation above Cochiti.) The ratio of AET/PET is low during the early dry years of the scenario, recovering to more historically average values later in the scenario run. Interestingly, unlike other surface water metrics considered in the previous sections, the AET/PET ratio for agriculture between Cochiti and Elephant Butte is visibly reduced by population growth. To figure out why, consider that the total water available for agricultural use in a given reach is the sum of diversions from the river into the conveyance system in the reach, and the amount of water remaining in the conveyance system from the reach immediately upstream (see equation 2-3). These two terms will be called the agricultural inflows and throughflows respectively, and are
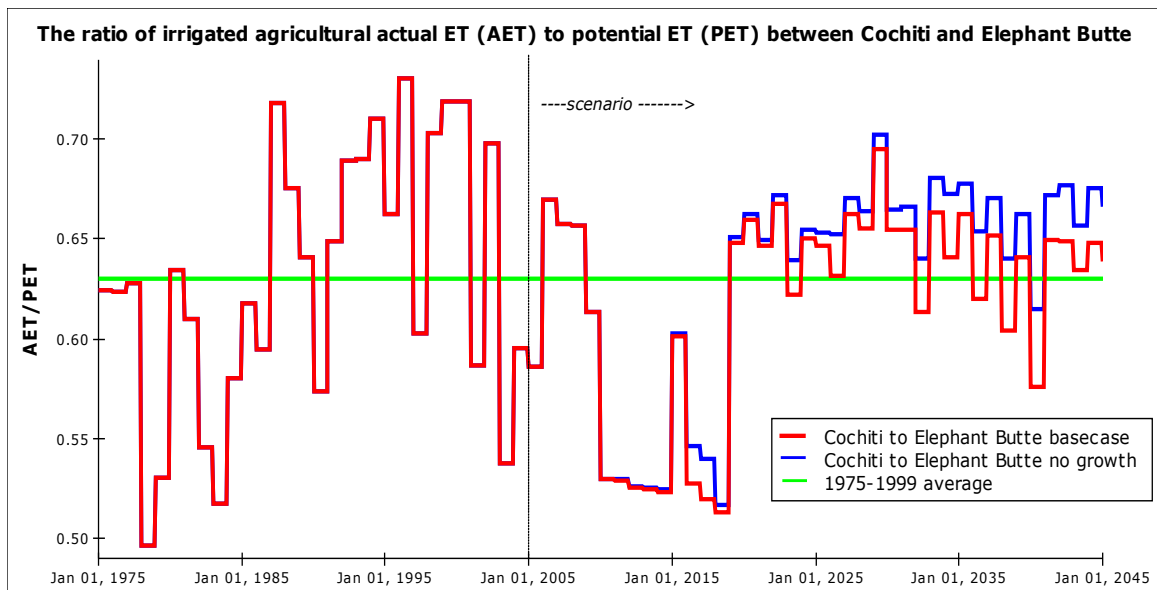
Figure 4-13. Actual ET (AET) volume divided by potential ET (PET) volume for irrigated agriculture between Cochiti and Elephant Butte reservoirs for the base case and no growth scenarios. Population growth reduces the ratio suggesting reduced water delivered to ag.

shown as cumulative sums for the reaches from Albuquerque to San Marcial during the scenario period for basecase and no growth conditions in Figure 4-14. Essentially all variations in inflows are a result of variations in throughflows, meaning that agricultural consumptive use is reduced during the base case scenario as compared to the no growth scenario because there is less water in the conveyance system from one reach to the next. Importantly, water in the conveyance system is made up to large degree of return flows from agricultural drains which drain the shallow groundwater system to prevent water logging in fields. As seen in Figure 4-15, the drain flows between San Felipe and Bernardo decrease as population grows in the greater Albuquerque metro area. Increased population growth drives increased well pumping which reduces groundwater heads and leads to decreased drain flows and thus decreased water availability for agriculture. With
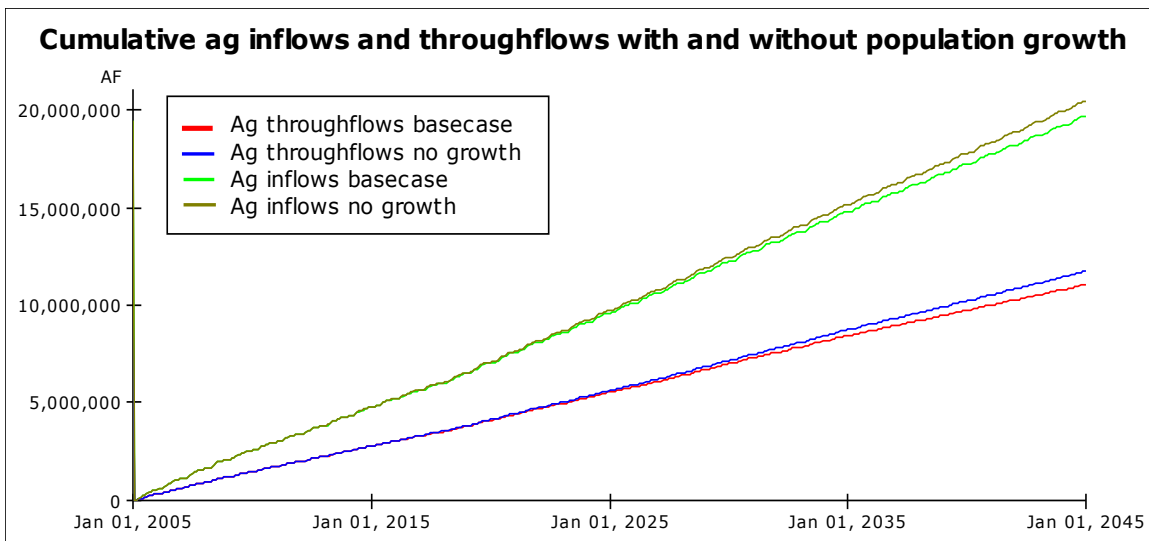
Figure 4-14. Cumulative agricultural inflows (total water available for agricultural use) and throughflows (water passing from one reach to the next in the agricultural conveyance system) for the reaches from Albuquerque to San Marcial during the scenario period. Differing ag throughflows explain almost all of the difference seen in inflows between the base case and no growth scenario conditions.
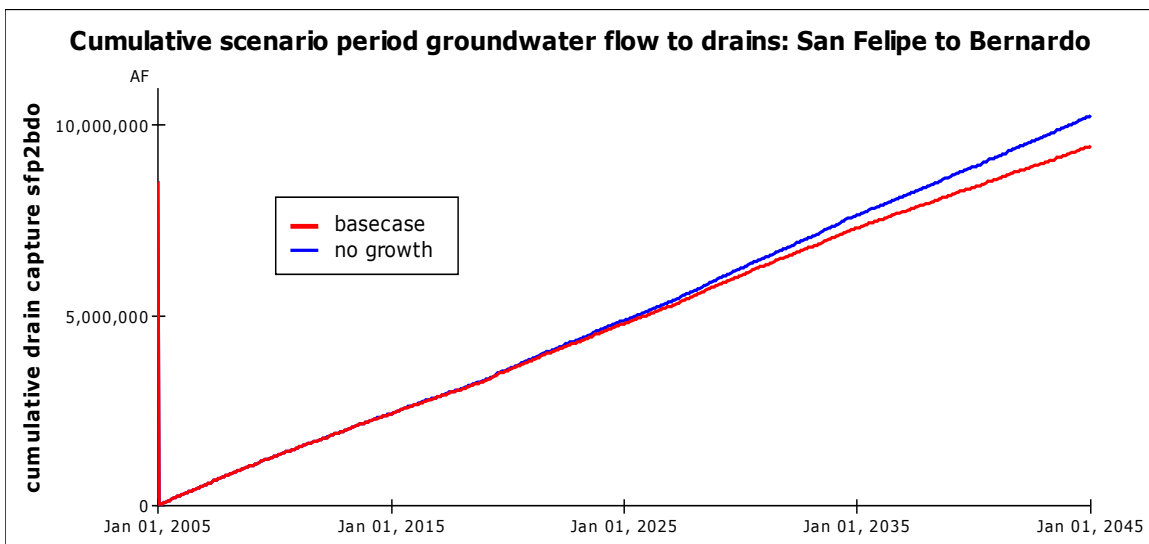
Figure 4-15. Cumulative groundwater flow to drains between San Felipe and Bernardo (containing the greater Albuquerque metro area) for basecase and no growth scenario conditions. Population growth drives increased well pumping, leading to decreased drain flows.

agriculture, a relatively large consumptive user of water, absorbing some of the pumping induced effects on surface water in this way, reservoir behavior and surface water flows are buffered somewhat from the effects of groundwater mining as seen in Sections 4.3.1, 4.3.2, and 4.3.4 above, and 4.3.6 below. Agriculture ends up absorbing municipal and industrial pumping effects because the model is set up to keep a specific percentage of agricultural return flows in the conveyance system for use in the next reach. As those return flows are impacted by groundwater pumping, the water available in theconveyance system downstream is impacted. In reality it seems the irrigators would divert more river water as available to make up for reductions in return flows. This reveals one of the weaknesses of the model in its current form. How the water is moved into and through the agricultural conveyance system is not well understood and modeled in the scenario period with overly simplified historical percentages, or fixed diversion amounts. In addition, the amount of water in a given reach that can be used by the irrigators is limited by a calibration factor (see Section 2.2.3.2.9 and Table 2-4). The model may be improved in the future with better understanding and modeling of agricultural conveyance system operation.

4.3.6 Rio Grande Compact Balance

As described in Section 2.2.3.5.3.8, the Rio Grande Compact legally divides the surface water of the Rio Grande system between Colorado, New Mexico, and Texas. Projections of the Rio Grande Compact balance as demands for the water continue to grow are of distinct interest to policy makers and planners. The ability to model New Mexico's compact balance during calibration and validation is discussed in Section 2.3.4.

The focus here will be the scenario period, however the historic compact balance behavior provides important context. Figure 4-16 shows New Mexico's compact balance as observed during the historic period, and modeled during the historic and scenario periods. There are two significant features apparent in Figure 4-16. The first is that New Mexico's compact balance is always positive during the calibration period, and often more positive than anytime in the history of the compact (Shafike, 2007). The second feature of note is that relative to the no growth scenario, population growth increases New Mexico's compact balance early in the scenario run, and decreases it later. Each of these features is discussed in further detail below.

The high compact balances compared to the historic range without an obvious physical explanation are intuitively unsettling. Interestingly, the trend is the same in the URGWOM model with the same climate sequence. This result has led some of the URGWOM developers to conclude that consumptive losses may be underestimated in URGWOM[10]. This is also a distinct possibility for the monthly model for at least two reasons. First, modeled flows at San Marcial (the last gage above Elephant Butte where the compact balance is tabulated) were consistently above gaged values during the 2000-2005 validation period as described in Section 2.3.1.4 and shown in Figure 2-36. Secondly, as described in Section 4.3.5 above, agricultural consumptive use may be underestimated during the scenario as a result of overly simple rules guiding conveyance system operations that may limit agricultural use despite available resources. However, it is also important to note that despite overestimates of flow compared to the gages during

---

[10] Personal communication with Nabil Shafike of the New Mexico Interstate Stream Comission, and URGWOM developer on February 21, 2007

New Mexico's Rio Grande Compact Balance
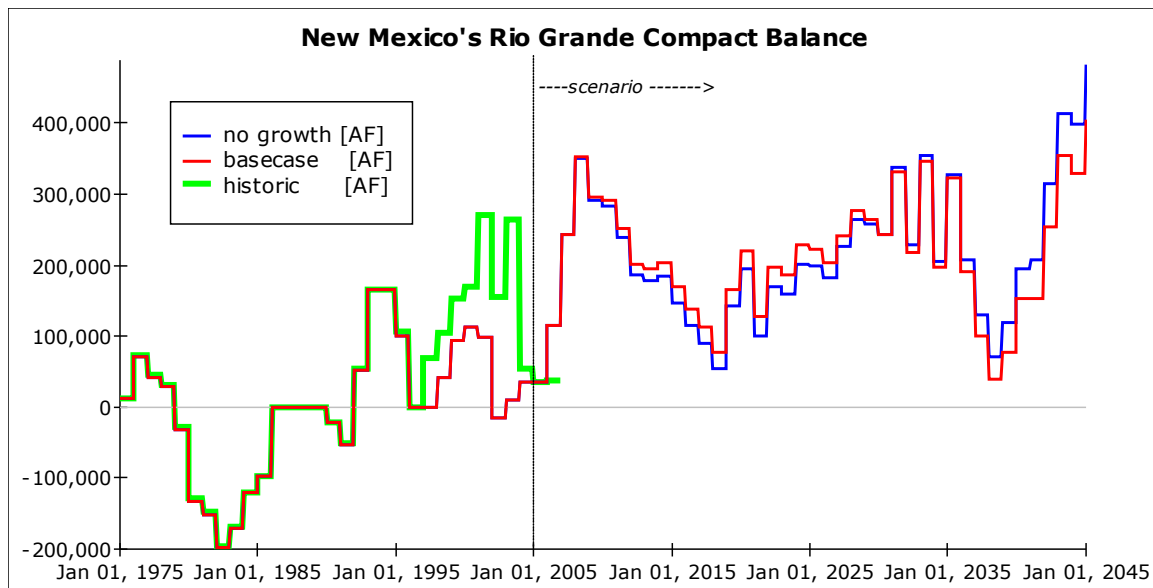
Figure 4-16. New Mexico's Rio Grande Compact balance for historic and scenario periods using the basecase URGWOPS climate scenario described in Section 4.2.2.1. The scenario balance is significantly positive, and population growth has a changing effect on the balance.

the validation period, the compact balance is consistently *underestimated* by the model during that period. In addition, as shown in Figure 2-54, the compact balance is relatively sensitive to minor differences in the two major drivers of the balance, the native flow at Otowi and the inflows to Elephant Butte. Thus, the compact balance is very sensitive to what happens to the water between these two points. If inflows to the river system between these reaches are unusually large, New Mexico will likely easily meet its delivery obligations at Elephant Butte. If inflows are unusually small, the opposite may be true. Using gaged tributary inflows as a proxy for overall surface water inflows to the system, a ratio of total gaged tributary flows to the Rio Grande between Otowi and Elephant Butte to the Otowi Index Supply (see Section 2.2.3.5.3.8) can be developed. Mathematically:

$$TROIS = \frac{Trib_{otw2eb}}{OIS} \hspace{4cm} (4\text{-}4)$$

where

$TROIS$	=	Tributary to Otowi Index Supply ratio. [-]
$Trib_{tow2eb}$	=	Gaged tributary inflows to the Rio Grande between Otowi and Elephant Butte corrected for Jemez reservoir storage. [L^3/T]
OIS	=	Otowi Index Supply as defined in equation 2-16.

Figure 4-17 plots *TROIS* against historic compact balance changes since 1975 in years when the accounting was not abnormal due to a reservoir spill or exchange of credits between states[11]. The TROIS metric could be improved as, in its described form, it does not account for the timing of inflows, which should also be important. Inflows during the winter for example would be subject to fewer losses as they move downstream, and thus effect New Mexico's compact balance in a more positive way than the same flows in the summer. However, the TROIS metric does show the intuitive result that New Mexico's Rio Grande Compact balance is sensitive to inflows, and by extension the climate between Otowi and Elephant Butte. The average TROIS metric for 1975 through 1999 is 8.5%, while for the 40 year URGWOPS sequence, though average tributary flow between Otowi and Elephant Butte decreases, the TROIS ratio increases to 8.9%. So though the URGWOPS sequence is drier than the 1975-1999 period from an absolute perspective, the TROIS ratio is higher.

Another way to look at the behavior of New Mexico's compact balance in relation to climate is simply to look at the compact changes associated with historic years in the

---

[11] The years 1985 through 1988, and 1995 were left out due to reservoir spills which dramatically change the way the compact is calculated. The years 2003, and 2004 were left out due significant accounting changes to New Mexico's credit balance as a result of credit relinquishment by New Mexico.

New Mexico's Rio Grande Compact change as a function of the TROIS ratio
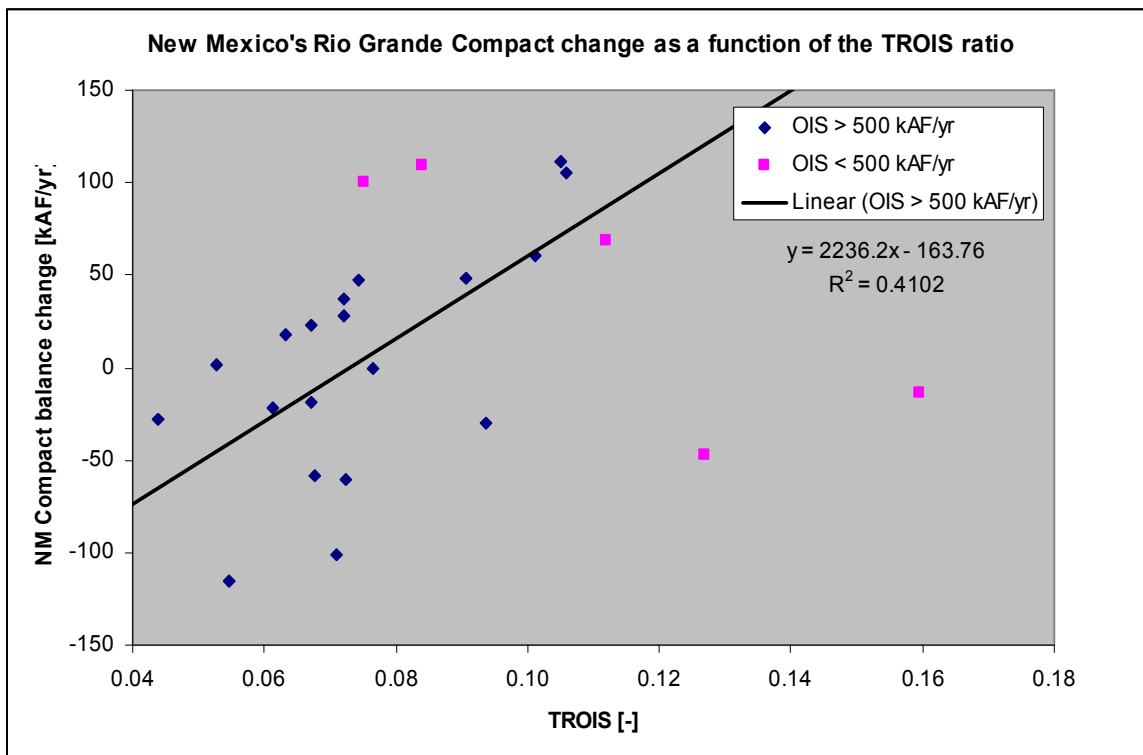
Figure 4-17. New Mexico's Rio Grande Compact balance change compared to the TROIS ratio from 1975 through 2004 exclusive of years where some sort of abnormal accounting occurred (see footnote). The linear relationship plotted was improved by not including any year in which the Otowi Index Supply was less than 500,000 AF. These outliers are shown as pink squares.

context of scenario climate sequences. Interestingly, although the URGWOPS climate sequence was selected to be representative of long term hydrology, as discussed in Section 4.2.2.1, the climate years used in the sequence happen to be years in which New Mexico's compact balance change was far more positive than normal. Part of this can be explained by the higer TROIS as discussed above. So while average Otowi Index flows in the URGWOPS sequence years were smaller than the 1975-1999 average as shown in Figure 4-1, the average historical change to New Mexico's compact balance in the years used in the URGWOPS sequence was nearly triple the 1975-1999 average. These results

are shown in Table 4-8. Two model runs with scenario inputs based on the URGWOPS

sequence and a loop of 1975-1999 historic data respectively, with all other inputs the

same are shown in Figure 4-18. New Mexico's compact balance is still predominately

positive, however significantly reduced from the values derived with the URGWOPS

sequence, and all within the range of values seen historically.

Table 4-8. Comparison of the change to New Mexico's compact balance between 1975 and 1999, and the historic years making up the URGWOPS climate sequence, all of which fall within the 1975 - 1999 period. The URGWOPS sequence happens to favor years that were historically beneficial to New Mexico from a compact perspective.

	Average New Mexico Rio Grande Compact balance change [AF/yr]	
	1975-1999	URGWOPS 40yr
All years	6308	23363
Filtered years*	8385	24635
* Filtered years do not include years associated with an historic spill or relinquishment		

The role of Elephant Butte storage on New Mexico's compact was also checked,

as large storage leads to large evaporation, which removes water from New Mexico's

effective delivery to Elephant Butte. However, the data did not show any relationship

between storage in Elephant Butte to start the year, and the change in New Mexico's

compact balance in the same year.

A final factor considered in the perceived high compact balances seen in the

scenario period is the release of San Juan Chama water for non consumptive use. In the

reservoir operations rules used in the model, if San Juan Chama water is available from

other contractors, the Bureau of Reclamation can use it to protect minimum stream flows

during dry periods. This is with recent historic precedent, and results in San Juan Chama
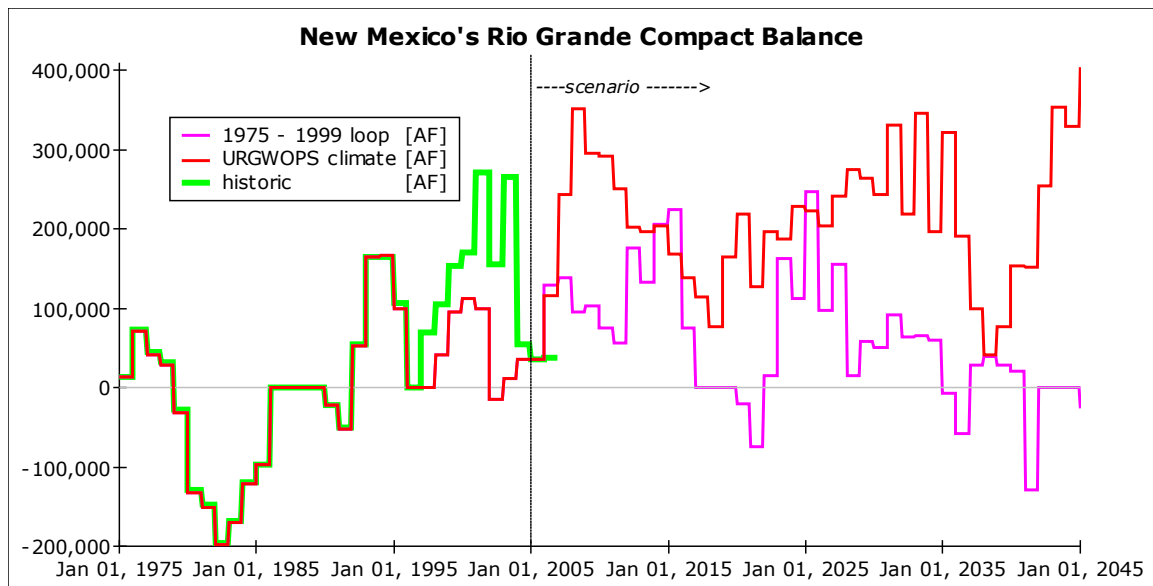
Figure 4-18. New Mexico's historic Rio Grande Compact balance compared to scenario projections based on two different climate scenarios. The URGWOPS sequence results in much higher predicted compact balances than a 1975-1999 historic loop. All other factors are the same as basecase for the two scenario runs.

water, which is not included in the Otowi Index Supply, and thus New Mexico's delivery obligation, flowing to Elephant Butte where it is counted as a delivery. These releases total about 240,000 AF for the 40 year basecase scenario, an average of about six thousand acre feet per year. This is a relatively small amount in the context of a balance that runs into the hundreds of thousands, but it is not negligible. So while underestimated consumptive losses remain a possible reason for the perceived high compact balances in the scenario period, the climate sequence likely plays a more significant role, with San Juan Chama water operations also playing a limited role.The second feature that stands out in Figure 4-16, is that population growth (or lack thereof) seems to have contradictory effects on the compact balance. The reason for this lies in the interactions between the surface water and groundwater systems. As population grows in the model, groundwater

extraction increases. Increased groundwater extraction has a lagged effect on river leakage and drain capture, with the net flux of surface water to groundwater slowly but cumulatively increasing to replace the water pumped out. Increased water use in cities with sewers discharging to the river also results in some fraction of groundwater pumping going immediately to the river. Figure 4-19 shows the difference between the groundwater pumped to the river (via the waste water treatment plant) in the Albuquerque groundwater basin, and the net river leakage in the same area. As population grows in the base case, the immediate effect of increased relative return flows to the river results in more surface water than in the no growth scenario. However, between 20 and 25 years into the scenario, the larger debt to the groundwater accrued in the basecase scenario is impacting the river sufficiently to finally reduce the surface water in the system compared to the no growth scenario, a trend that strengthens through the duration of the model run. This change in relative effect on the surface water is mirrored in New Mexico's Rio Grande compact balance as seen in Figure 4-16. It is the relative magnitude of instant increased return flows compared to lagged river leakage that results in the apparently contradictory effects of population growth on surface water flows.

4.3.7 Policy Related Sensitivity Analysis

To test model sensitivity to policy related parameters, the six model results discussed above (reservoir behavior, Caballo releases, groundwater mass balance, critical low flows, agricultural shortfalls, and the Rio Grande compact) were used to generate five model metrics for the scenario period. For consistency with the physical parameter

Albuquerque gw basin: GW pumped to Rio Grande minus net river leakage (5 year average)
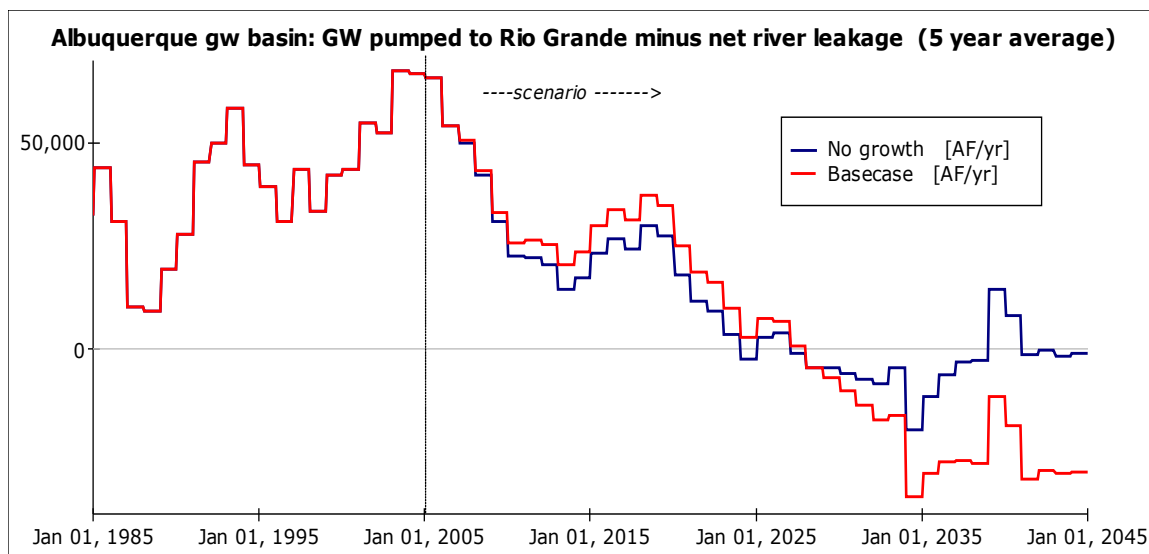
Figure 4-19. Groundwater pumped to the Rio Grande minus net river leakage (includes drain flow) for the bascase and no growth scenario conditions. Five year average annual data.

sensitivity analysis (see Section 2.3.5), reservoir behavior and Caballo releases were lumped into a single metric: the average change in reservoir storage plus the average Caballo releases for the forty year scenario period. Average scenario period groundwater storage change rate and average scenario period actual agricultural ET rate betweenCochiti and Elephant Butte were used as metrics for groundwater mass balance and agricultural shortfalls respectively. The highest of the three average expectations that the river will experience at least one zero flow event in a given year during the scenario period at Bernardo, San Acacia, or San Marcial is used as the critical flow metric. The average value of New Mexico's compact balance during the scenario period is used as the Rio Grande Compact metric. The policy related sensitivity analysis focuses on relative changes to these metrics, but for context the base case values of each of these metrics are shown in Table 4-9. To estimate the sensitivity of each metric to high level human

behavior related inputs, basecase population growth rates, irrigated agriculture area, and

indoor and outdoor per capita use values, were changed one at a time by -40%, -20%,

20%, and 40%, and the value of each of the five metrics at the end of the scenario

analysis period was recorded. Results of these runs are shown graphically in Figure 4-20.

*Table 4-9. Values for the sensitivity analysis metrics at the end of the basecase
scenario run.*

Sensitivity Analysis Metric	Base value	unit
Average scenario reservoir change plus Caballo releases	939	cfs
Average cumulative scenario groundwater storage change	-433	cfs
Average max expectation of a zero flow day at Bernardo, San Acacia, or San Marcial	48.7	%
Average scenario actual ag ET between Cochiti and Elephant Butte	271	cfs
Average scenario New Mexico Rio Grande Compact balance	250.7	kAF

Population growth rates have a very significant impact on the groundwater

resources which are used to support the growing demand. New Mexico's Rio Grande

Compact balance is also affected by population growth due to the effects of groundwater

use on surface flows as discussed in Section 4.3.6. Model responses to changes in

population growth rates are not linear because of the compounding nature of exponential

growth; increasing population growth rates by 40% leads to more than a 40% population

increase compared to base case.

Changes to per capita indoor use affect the model in a similar way to changes to

population growth rates, except that model response is linear. Note that Rio Grande

Compact balances increase as per capita indoor use increases because most of the water

used inside ends up back in the Rio Grande where it can add to New Mexico's compact

balance. The probability of a low flow event decreases slightly, and the surface water
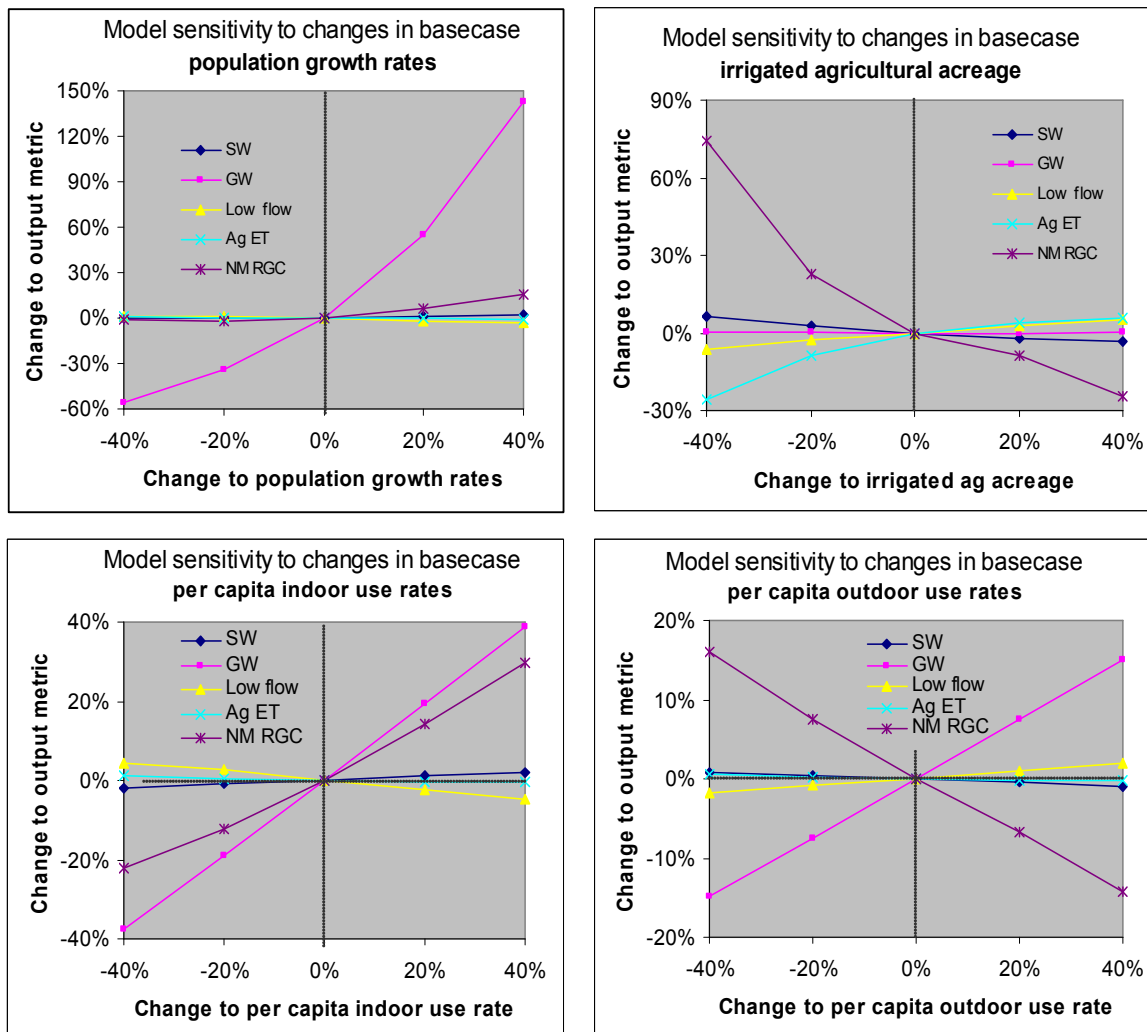
Figure 4-20. Model sensitivity to changes in four different human behavior related input parameters: population growth rates, irrigated agricultural area, and per capita indoor and outdoor water use. Each input parameter was varied from -40% to 40% of its base value and the percent change in each model metric base value (shown in Table 4-9) was recorded.

metric increases slightly with increases of per capita indoor use for the same reason.

Agricultural ET is not affected appreciably by changes in indoor water use.

Model response to increases or decreases in outdoor water use per person is

significantly different than the response to indoor use. The effect on groundwater is the

same for indoor or outdoor use because the demand is served largely by groundwater.

However, the fate of water used outdoor and indoors is extremely different. Because the water for both indoor and outdoor uses comes largely from mining of groundwater, both water uses enhance river leakage to the aquifer. However, most of the water used indoors ends up in the river, offsetting to some degree the pumping induced river leakage. Water used outdoors on the other hand, while contributing to pumping induced river leakage, does not return to the river. As a result, outdoor use of groundwater has exclusively adverse effects on surface water flows, and increased outdoor use leads to reductions in New Mexico's Rio Grande compact balance and the overall surface water metric. Increased outdoor use reduces surface water flows, and thus increases the likelihood of zero flow days. Like changes to indoor use, changes to outdoor use do not affect agricultural ET significantly because the impacts to the surface water system are small.

Changes in irrigated agricultural area affect actual agricultural ET in a non-linear fashion because of the model framework. A reduction in irrigated agricultural area of 40% reduces ag ET by less than 30% because the actual ag ET is less than potential ag ET in the basecase (see Figure 4-13). As a result, when agricultural area is reduced, a greater amount of potential ET can be served with the same amount of water. Small reductions in agricultural area result in small changes to actual ag ET as the actual ET on the remaining land gets closer to the potential ET. Once potential ET is fully satisfied, further reductions in agricultural area would have a more linear effect on changes to agricultural ET. When agricultural area is increased, the current model framework does not change the amount of water diverted to the agricultural conveyance system. The diversions to the conveyance system are based on a static diversion schedule as discussed

in Section 2.2.3.4.3 and shown in Table 2-14. Agricultural ET increases slightly with increases to agricultural area because water that might have been surplus in the conveyance system in the base case is used by the additional irrigated ag. The model can be improved conceptually by making agricultural diversions (and through flows from the upstream agricultural conveyance system as discussed in Section 4.3.5) a function of potential ag ET and conveyance system capacity, rather than static diversion targets (and static % through flows as discussed in Section 4.3.5). The Rio Grande compact changes dramatically with changes of agricultural area. The changes are proportional to changes in agricultural ET, suggesting that the compact is very sensitive to changes in consumptive agricultural water use between Otowi and Elephant Butte; an intuitive result.

To summarize model sensitivity to human behavioral related inputs: changes in population affect the groundwater and surface water systems directly by changing indoor and outdoor water use. Changes in indoor and outdoor water use affect the groundwater system directly through changes in groundwater pumping, and the surface water system indirectly through lagged groundwater pumping induced river leakage effects. Changes in indoor water use also affect the surface water system by changing waste water returns to the river. Changes in irrigated agricultural area affect the surface water system, but their effect is mediated by current static model structure governing the operation of agricultural conveyance systems.

4.4   Scenario Analysis Conclusions

The monthly timestep integrated model of the Rio Grande described in this dissertation was developed for scenario analysis, and this discussion has only scratched the surface of its potential in this regard. The model can quickly evaluate scenarios from a nearly infinite number of possibilities for users with different interests in and understandings of the system. High level results show the relationship between human water use patterns and model response. It is important to note that the scenario evaluation was limited to a 40 year horizon in this discussion; a typical planning horizon, but too short to see long term effects of groundwater pumping on the surface water system. Although the groundwater storage metric inherently includes information as to the debt due the groundwater system that surface water will have to pay, the surface water metrics developed do not. Scenario analysis should include analysis of groundwater effects with an understanding of their implication on future surface water flows unless the scenario is run until the long term groundwater system storage change is negligible.

The scenario analysis described here is preliminary and high level, covering only a base case scenario and a no growth equivalent, and overall model response to human water use both in a municipal and industrial context, and in an agricultural context. The results of this preliminary analysis show that the model is very effective for scenario analysis, and not surprisingly, that the feedbacks and competing effects between systems cannot be predicted without a numerical model. The model yields results that at first look may not make intuitive sense, but whose causes can be followed back until they are

indeed intuitive. The model is ready for more detailed scenario analysis to help evaluate

the myriad of ideas put forth by professionals and the interested public as they consider

the possible outcomes of current growth in demands on the finite and variable water

resources of the Rio Grande river system.

CHAPTER 5: CONCLUSIONS

5.1 Model Development Summary

The monthly timestep mass balance model of the Rio Grande basin in New Mexico above and including Caballo reservoir described in the previous chapters uses a system dynamics foundation, and is a fast, multidisciplinary, and basin scale model of the major systems whose interactions through time affect how water moves through the Rio Grande. A daily timestep surface water model, and three spatially distributed groundwater models were abstracted and combined on a software platform amenable to the creation of graphical user interfaces. The result is a basin scale monthly timestep integrated surface water groundwater model linked dynamically to a human behavioral model. The integrated model captures salient surface water and groundwater dynamics of the Rio Grande river system in New Mexico, and runs 40 year scenarios in a matter of seconds. The model interface and framework can accept any allowed range of changeable user inputs, and as a result, the model is a powerful tool for use both in public education and preliminary policy discussions and decisions. Scenario analysis presented here is preliminary, but shows the model capable of scenario analysis under a wide range of inputs. The model is ready for more detailed scenario analysis to help evaluate the myriad of ideas put forth by professionals and the interested public as they consider the possible outcomes of current growth in demands on the finite water resources of the Rio Grande river system.

5.2 Model Strengths

The strength and uniqueness of the upper Rio Grande monthly timestep model lies in its integration of basin scale multidisciplinary science into a computer based tool able to run physically meaningful scenarios in tens of seconds on a typical laptop computer. The resulting model behavior is potentially educational to a wide range of users from water professionals to the interested public. In this way the model serves as a bridge between scientists and modelers of different disciplines, as well as a bridge between science and policy. The qualitative policy proposals for the Rio Grande put forth by groups like 1000 Friends of New Mexico (Belin et al. 2002), as well as more general qualitative proposals suggested by the Bureau of Reclamation (2005) in the Water 2025 report can be evaluated quantitatively with this model. The model, in the Rio Grande at least, is a tool for "explaining, communicating, and educating water managers, decision makers, and members of the public", which as noted in Section 1.2 is the task that Jury and Vaux (2005) have charged to scientists and policy makers as critical in addressing the world's emerging water problems. And while this work has focused on the Rio Grande, the model components are modular enough, and the model approach general enough, that the lessons learned here may be applied rapidly to new problems in other basins.

5.3 Model Gaps and Significant Weaknesses

5.3.1 Land Surface Model

The largest gap in the current surface water model is the lack of a land surface model to transfer atmospheric precipitation to the surface water gages, ungaged tributaries, and groundwater system. Current work by Aragon and Vivoni is addressing this gap (Tidwell et al. 2006, Chapter 4), and will be built into future model versions.

5.3.2 Agricultural Water Deliveries

The most significant weakness of the physical hydrology model is in the calibration of the agricultural ET loss estimates discussed in Section 2.2.3.2.9. The understanding of how water deliveries are made to fields has significant impact on the amount of water that can by used towards the potential agricultural ET. The model version described here calibrated total agricultural ET losses by limiting deliveries to fields to a fixed percentage of the amount of water in the conveyance system in a given reach. The resulting methodology may underestimate agricultural losses in low water conditions as discussed in Sections 2.3.1.4 and 4.3.5. A similar problem exists with diversions from the river to the agricultural conveyance system, which are currently set to absolute numbers based on historic diversions. Future model versions should include logic to guide how agricultural deliveries are made, and river diversions should be determined based on actively irrigated agricultural acreage and conveyance system capacity as discussed in Section 4.3.5.

5.3.3 Scenario Options

The current scenario options, including changing agricultural area, population growth rates, indoor and outdoor use factors, and climate sequences cover a tremendous range of potential futures for the basin. However, more detailed demand related changes, such as improved agricultural efficiency, crop type changes, thinning of riparian vegetation, or urban rainwater harvesting to name just a few are policies that can be approximated only implicitly in the current model version by changing the high level options. Tidwell et al. (2004) and Yalcin and Lansey (2004) provide good examples of the numerous demand related inputs that can be provided to users for evaluation of a nearly infinite range of scenarios. Future model versions will continue to expand the explicit policy options provided as model inputs for scenario evaluation. Specifically, the ability to test the effect of direct diversions of San Juan Chama water from the Rio Grande by Espanola, San Juan Pueblo, and Santa Fe as discussed in Section 4.2.2.2.3 should be added explicitly to the model.

5.4 Future Work

5.4.1 Fixes and Enhancements

Future model development will start by addressing model weaknesses outlined in Section 5.3, specifically reworking rules determining how agricultural water is moved through the system, and enhancement of the scenario options provided to users. In addition to the land surface component currently being worked on for integration with the hydrology model as discussed in Section 5.3 above, a water quality component, an aquatic habitat component, and an economic component have also been developed for incorporation in the system dynamics model of the Rio Grande hydrological system (Tidwell et al. 2006).

5.4.2 Groundwater Improvements

In the current model reservoir rules, the city of Albuquerque and other contractors of San Juan Chama water are required to send water downstream to offset either groundwater pumping effects on the river, or surface water storage changes that affect New Mexico's ability to make Rio Grande Compact deliveries. These releases, called "letter water" releases because they are prompted by a letter from the New Mexico Office of the State Engineer to the Bureau of Reclamation are currently exogenous to the model, that is they are specified based on historic values or output from other analyses. The letter water releases for entities besides Albuquerque are relatively small at approximately 4600 AF/yr. Albuquerque letter water, used to offset pumping induced river leakage is a more significant term, with values as high as 25,000 AF/yr in the current model, based on URGWOM assumptions. The current groundwater model

cannot separate river leakage into that which is induced by Albuquerque pumps, and that which is not, because a base case model without pumping would have to be run for every climate sequence and surface water condition possible during the scenario period. Because river leakage is dependent on river stage, and river stage is strongly dependent on reservoir operations, which may change as a result of user inputs, the no pumping base case must be calculated for each scenario. To calculate a no pumping condition, a second groundwater model could be set up to run in parallel with the first, forced by all the same fluxes except for Albuquerque (or any other city or well group) pumping. In this way the no pumping base case could be subtracted from the actual model results to estimate pumping induced leakage. This improvement will help the model significantly as stakeholders use it to evaluate the impact of Albuquerque's direct use of San Juan Chama water for municipal supply.

5.4.3 Surface Water Stage Calculations Below Cochiti

As discussed in Section 2.2.3.2.8, Rio Grande area below Cochiti is estimated from flow rate as with empirical functions (Table 2-11) derived by URGWOM (USACE et al. 2002). Average river width as a function of flow can then be obtained by dividing river area by reach length (Table 2-4). URGWOM has also developed relationships between flow rate and average water velocity in each reach (ibid). If flow rate is divided by the product of velocity and width, the result is average stage. This fairly direct calculation of average stage might be more accurate than the current method of calculation using Manning's equation (discussed in Sections 3.4.1.1.3.2.2 and 3.4.3.1.3.2), and would be more consistent with existing surface water area calculations.

This has not been implemented in the current model because recalibration of groundwater parameters would be necessary, however such a change should be considered for future model versions.

5.4.4 Behavioral Model and Scenario Evaluation Enhancements

As mentioned in Section 5.3.3, the behavioral component of the current model iteration is very simple. Future work might include more realistic demand functions for indoor and outdoor domestic use by city and reach, as well as agricultural demand functions by reach. Once these demand functions are included, a valuation of water use in each sector from an economic perspective would be almost inevitable, followed by non market valuation of water left in the river. The research to include these functions exists with investigators such as Dr. Janie Chermak at the University of New Mexico, and Matt Weber at the University of Arizona respectively. The model framework is built for the incorporation of exactly this sort of data, which would add considerably to the model metrics that could be evaluated with scenario runs. An interesting metric for valuation of scenario analysis would be a comparison of actual consumptive water use compared to sustainable consumptive water use. Actual consumptive use would be measured by summing evapotranspiration from agricultural, municipal and industrial, riparian, and open water sources. Sustainable consumptive use would be estimated by summing groundwater recharge and surface water inflows less downstream delivery obligations.

5.4.5 Spatial Demand Forecasting

Spatial analysis was relied upon to generate reach based population estimates

from the 1990 and 2000 United States Census data as described in Section 4.2.2.2.1.

However, this analysis could be improved to be based on the groundwater model spatial

units rather than the surface water reach units. The spatial location of residents

connected to the city water supply and waste water treatment system have little impact on

the model because the city pumps and waste water treatment plant lump the demand and

return impacts of city residents at point locations. Residents with domestic wells and

septic tanks however have a spatially dependent effect on the groundwater model. For

this reason, population growth rates as a function of groundwater zone would be of more

use in the model than those used currently. In addition, spatial growth projections based

on build out of city zoning maps would provide a potentially more realistic population

growth projection than the extrapolation based on 1990 and 2000 census data currently

employed. The model framework would have to be adjusted slightly to handle

groundwater zone based information, but the changes would not be difficult, and would

simplify the existing structure somewhat.

5.4.6 Spatial Extent

The current model extent includes the Rio Grande river system from the Colorado

New Mexico border to Caballo reservoir (see Figure 2-1). It does not include the Rio

Grande river system in Colorado, or below Caballo. If the model is extended to include

the portions of the system in Colorado, and from Caballo to Fort Quitman Texas, it would

effectively capture all water use governed by the Rio Grande Compact between the states

of Colorado, New Mexico, and Texas, as well as the upper Rio Grande specific

agreements between the United States and Mexico, and be a truly basin scale model.

5.4.7 Climate Change Implications

The physical model developed here is by far the most sensitive to climate related

inputs as discussed in Section 2.3.5 and seen in Figure 2-55. Currently, the model can be

run with average historical inputs, a loop of sequential historic years, or a loop of

sampled historic years chosen to be representative of long term climate patterns in the

basin (Section 4.2.2.1). The option to make overall climate wetter, or drier, or make

spring runoff slightly earlier does not currently exist, but may be an interesting option in

the face of growing acceptance of and interest in probable impacts of global climate

change. As global climate models become more reliable, testing the sensitivity of the Rio

Grande model described here to changes considered likely by climate change scientists

will be a worthwhile task.

5.4.8 Public Availability

As they have been for thousands of years, water resources are an important reality

along the Rio Grande in New Mexico, especially as urban population growth stresses the

system. As a result, there are a large number of people in the region interested in water

resource issues. The model described here is for each and every one of them. Interface

work to make sure the model can be accessed at a very high level by first time users, but

"drilled into" by the return user or water professional is underway. Current collaborative

efforts with the URGWOM technical team as described in Section 1.3 should lead to a

visible role for this model in public education and outreach. Ideally, the model will be available on the web for download by the public, who can install a free version of the player required to view the model and change input and run individual scenarios. It is only in the running of thousands of scenarios for hundreds of users that the model can bring science to the public and integrated science to the water professionals, and this can only be done if these groups are aware of the model, and the model is readily available.

5.4.9 Scenario Analysis

As has been stated more than once in this document, the model developed here was developed for scenario analysis. There are an infinite number of scenarios to be tested, and ideas to be considered. Solutions to continued population growth in a semi-arid region served by finite, fully allocated, and variable future water supplies will not be easy to come by, but it is time to bring the available wealth of intelligence and creativity to bear on the problem by exploring a wide range of ideas with the upper Rio Grande basin simulation model.

APPENDIX A: ADDITIONAL GROUNDWATER DATA AND RESULTS
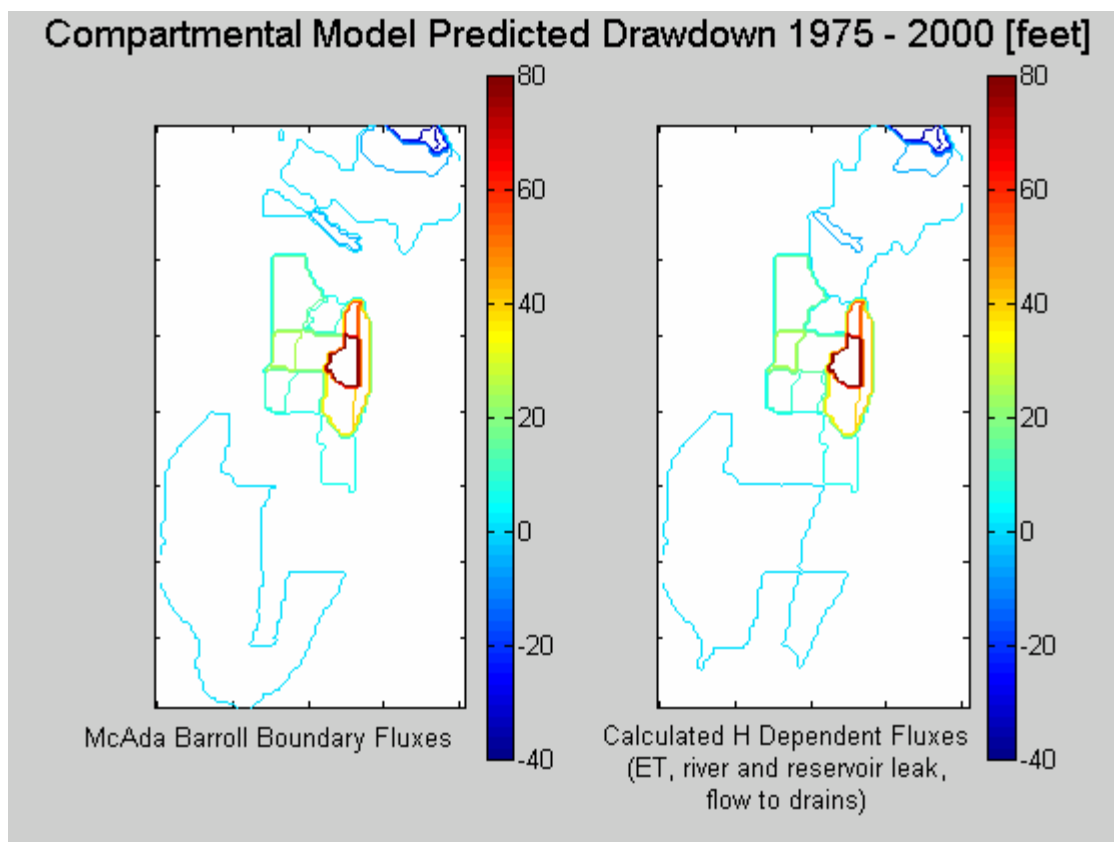
Figure A-1. Comparison of drawdown in models with head-dependent fluxes calculated internally by 51-zone model. Differences in zero level contour location are not important.
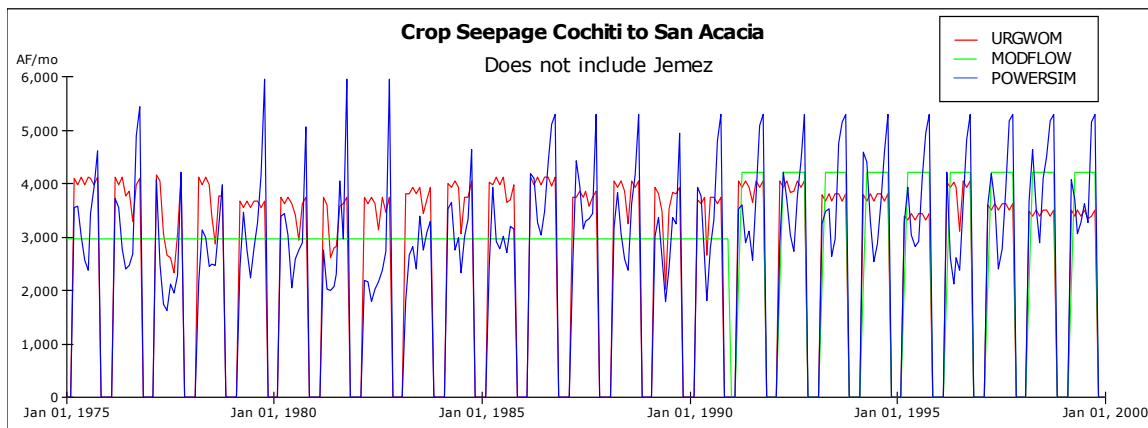
Figure A-2a. Crop seepage to the groundwater system for the Rio Grande reaches from Cochiti to San Acacia as modeled by the coupled monthly timestep model, the URGWOM surface water model, and the McAda and Barroll (2002) regional groundwater model.
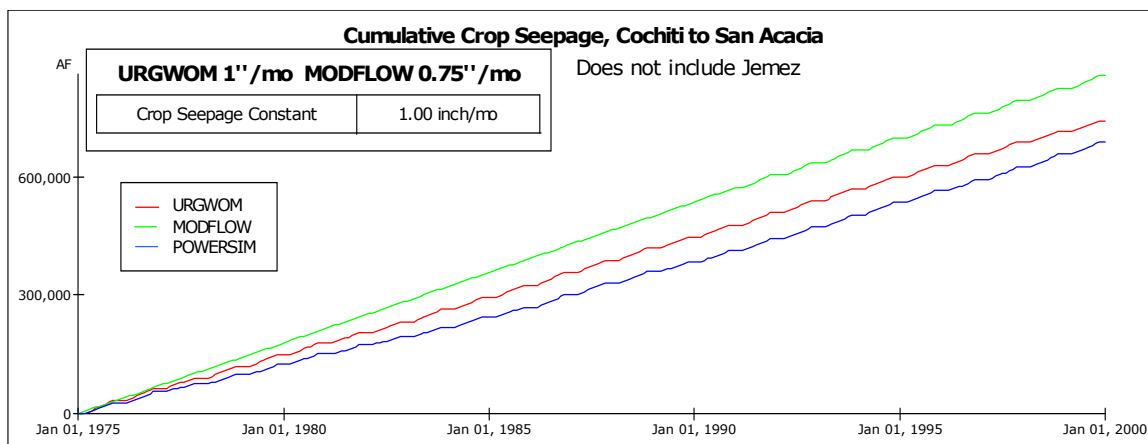
Figure A-2b. Cumulative crop seepage to the groundwater system for the Rio Grande reaches from Cochiti to San Acacia as modeled by the coupled monthly timestep model, the URGWOM surface water model, and the McAda and Barroll (2002) regional groundwater model.
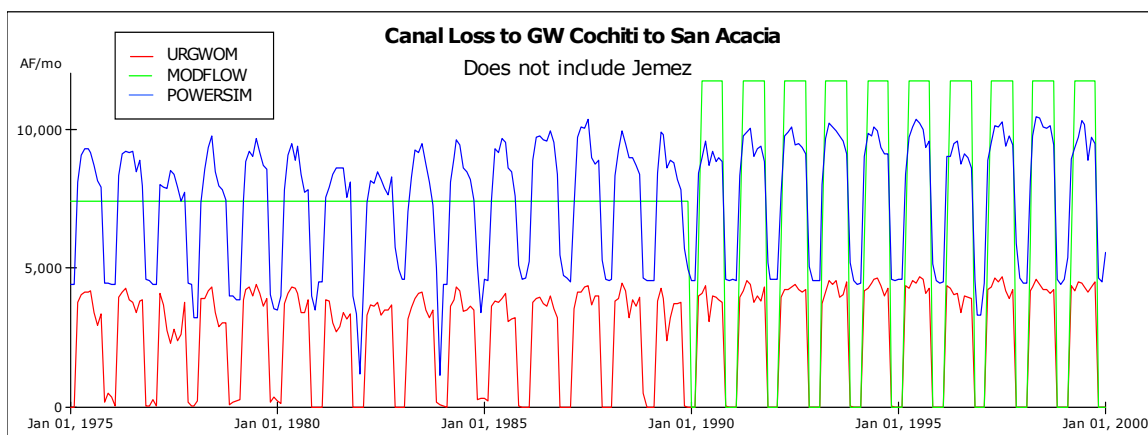
Figure A-3a. Canal seepage to the groundwater system for the Rio Grande reaches from Cochiti to San Acacia as modeled by the coupled monthly timestep model, the URGWOM surface water model, and the McAda and Barroll (2002) regional groundwater model.
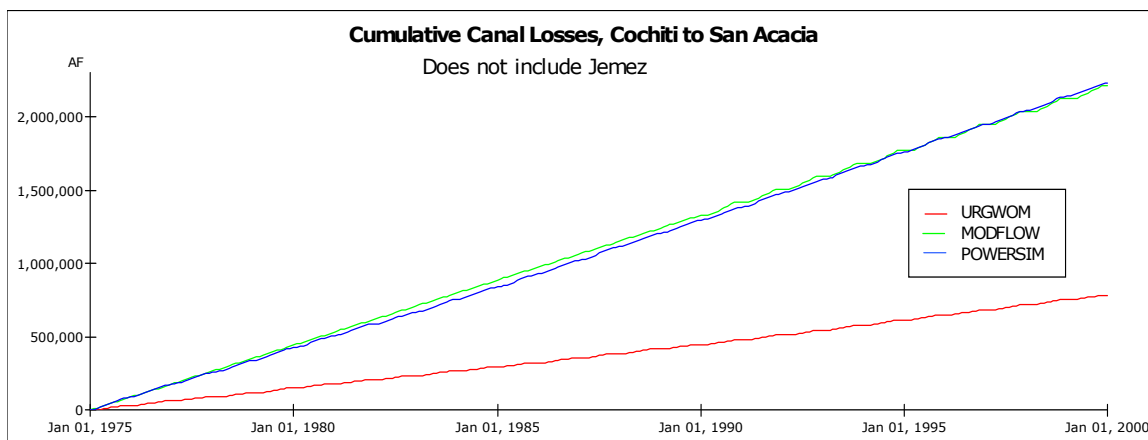
Figure A-3b. Cumulative canal seepage to the groundwater system for the Rio Grande reaches from Cochiti to San Acacia as modeled by the coupled monthly timestep model, the URGWOM surface water model, and the McAda and Barroll (2002) regional groundwater model.

309
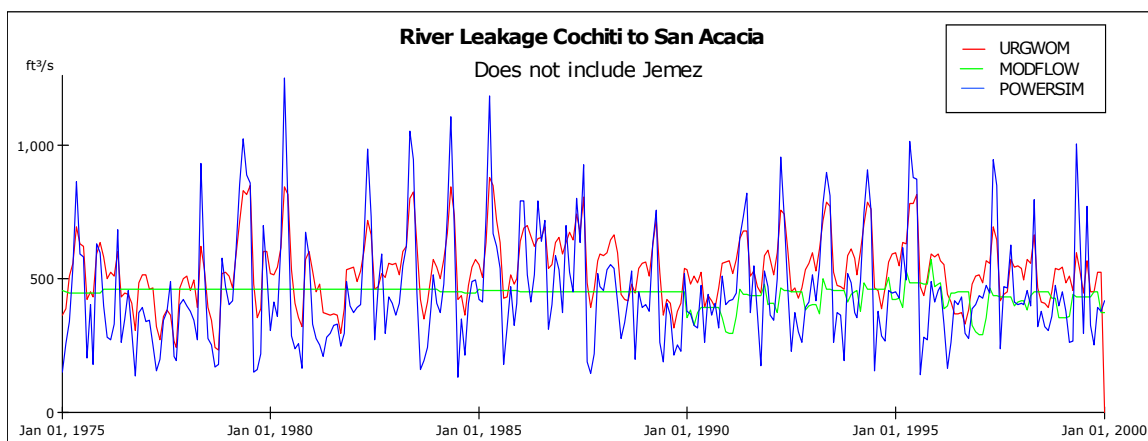
Figure A-4a. River leakage to the groundwater system for the Rio Grande reaches from Cochiti to San Acacia as modeled by the coupled monthly timestep model, the URGWOM surface water model, and the McAda and Barroll (2002) regional groundwater model.
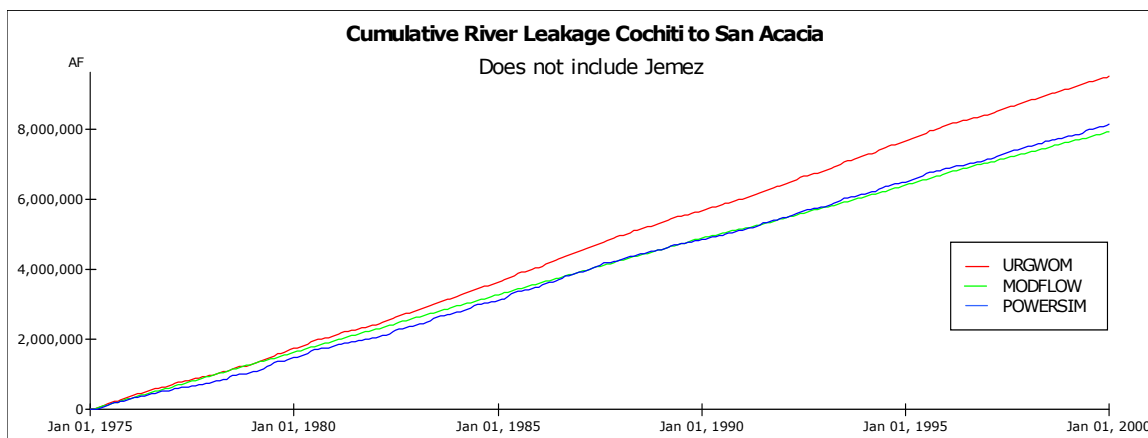
Figure A-4b. Cumulative river leakage to the groundwater system for the Rio Grande reaches from Cochiti to San Acacia as modeled by the coupled monthly timestep model, the URGWOM surface water model, and the McAda and Barroll (2002) regional groundwater model.
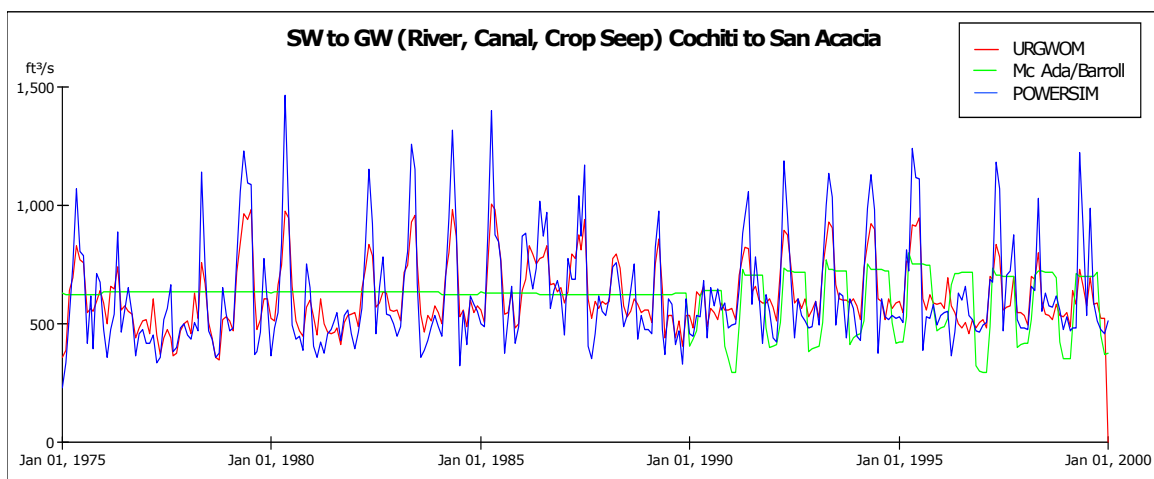
Figure A-5a. Fluxes to the groundwater system from the surface water system for the Rio Grande reaches from Cochiti to San Acacia as modeled by the coupled monthly timestep model, the URGWOM surface water model, and the McAda and Barroll (2002) regional groundwater model.
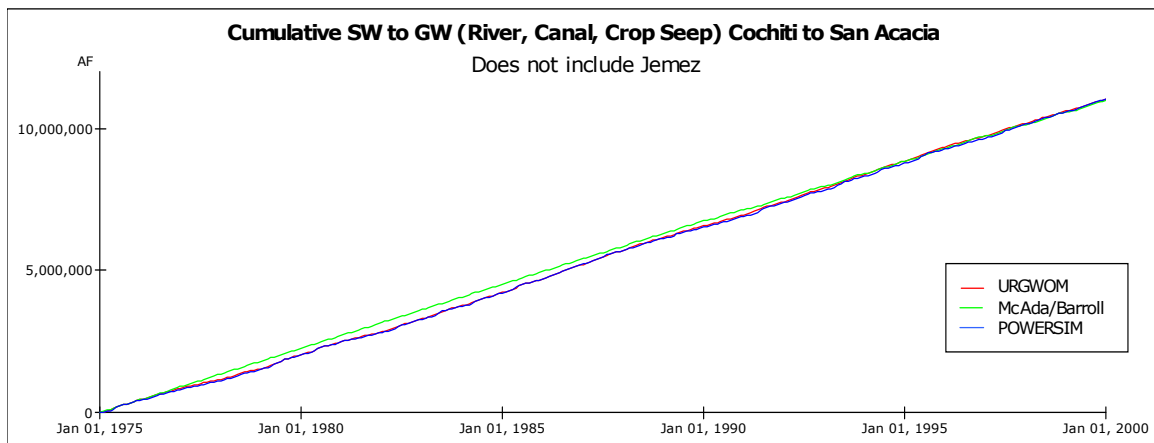
Figure A-5b. Cumulative fluxes to the groundwater system from the surface water system for the Rio Grande reaches from Cochiti to San Acacia as modeled by the coupled monthly timestep model, the URGWOM surface water model, and the McAda and Barroll (2002) regional groundwater model. Same as Figure 3-23.
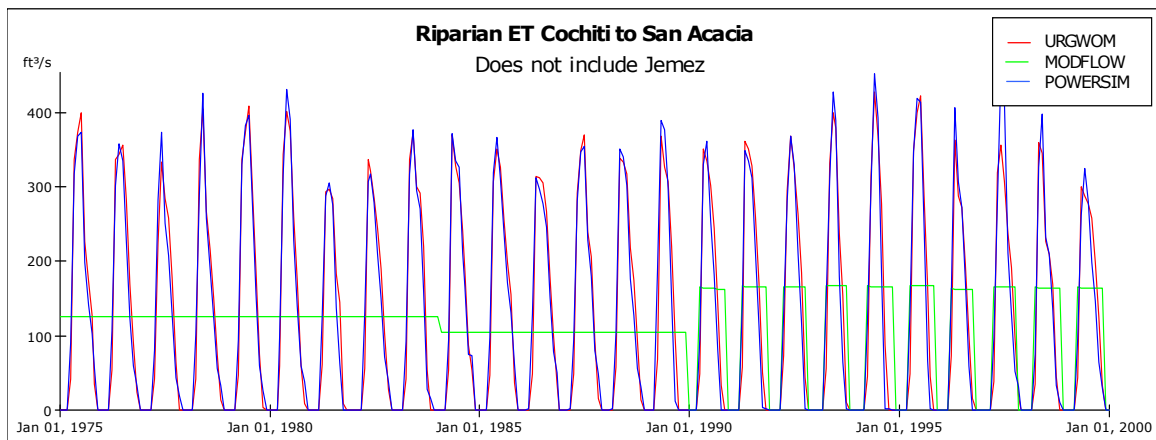
Figure A-6a. Riparian ET 1975–1999 for Rio Grande reaches from Cochiti to San Acacia as modeled by the coupled monthly timestep model, the URGWOM surface water model, and the McAda and Barroll (2002) regional groundwater model. Same as Figure 3-21.
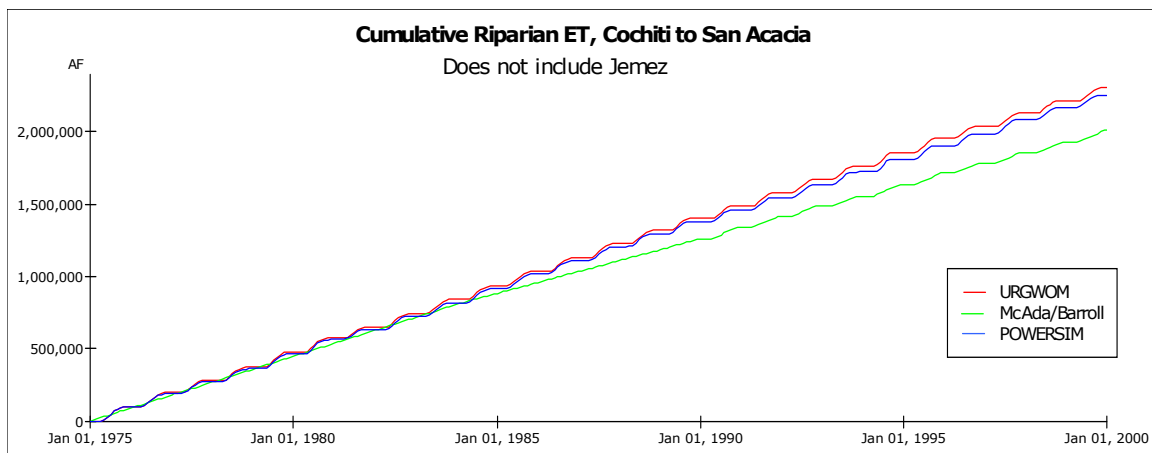
Figure A-6b. Cumulative riparian ET 1975–1999 for Rio Grande reaches from Cochiti to San Acacia as modeled by the coupled monthly timestep model, the URGWOM surface water model, and the McAda and Barroll (2002) regional groundwater model.
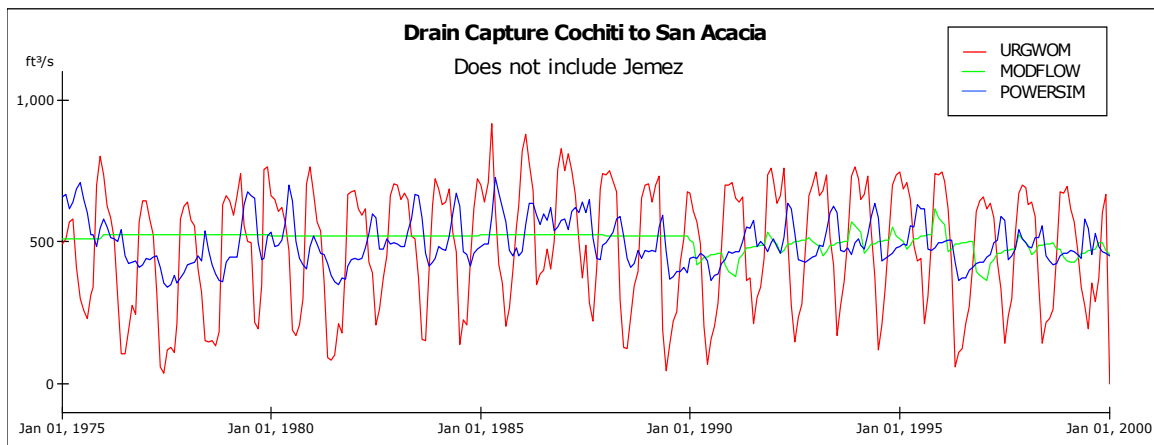
Figure A-7a. Losses from the groundwater system via drain flows for the Rio Grande reaches from Cochiti to San Acacia as modeled by the coupled monthly timestep model, the URGWOM surface water model, and the McAda and Barroll (2002) regional groundwater model.
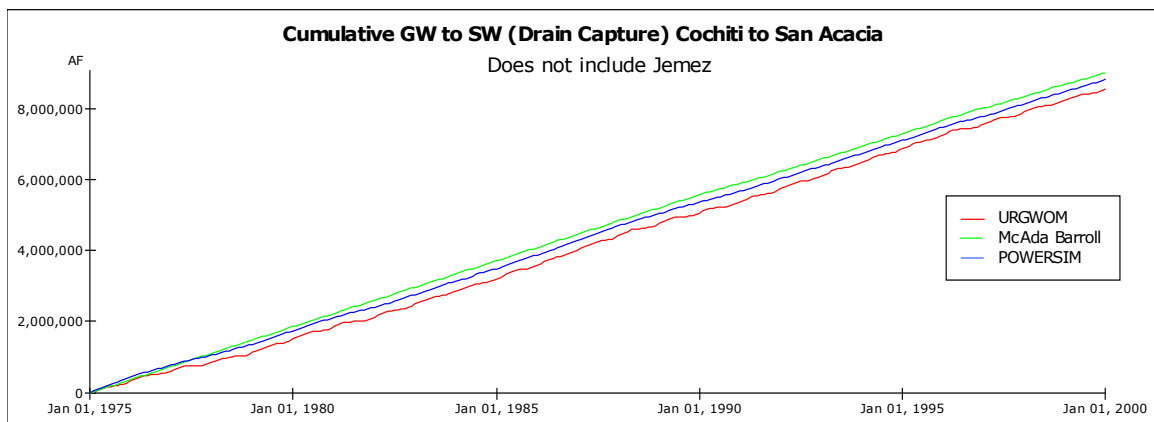
Figure A-7b. Cumulative losses from the groundwater system via drain flows for the Rio Grande reaches from Cochiti to San Acacia as modeled by the coupled monthly timestep model, the URGWOM surface water model, and the McAda and Barroll (2002) regional groundwater model.
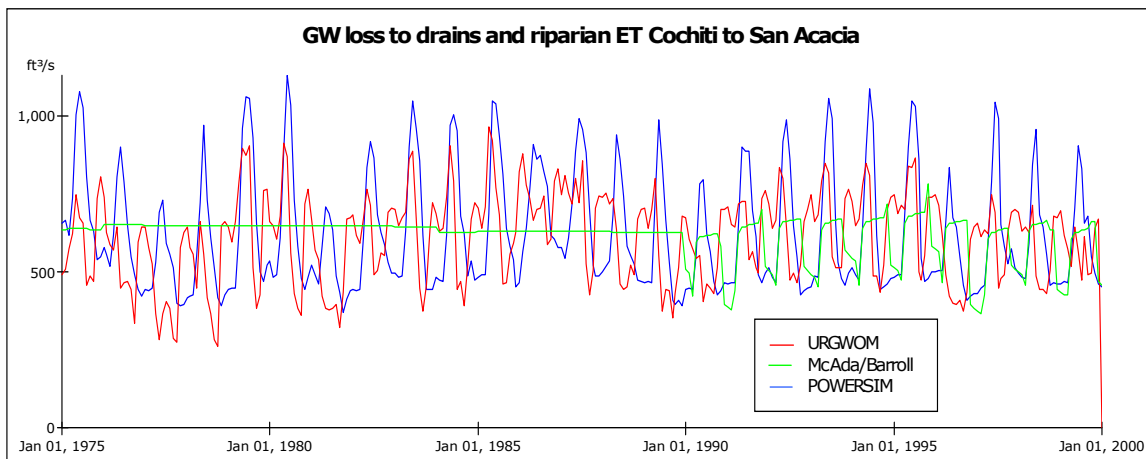
Figure A-8a. Fluxes out of the groundwater system via drains and riparian ET for the Rio Grande reaches from Cochiti to San Acacia as modeled by the coupled monthly timestep model, the URGWOM surface water model, and the McAda and Barroll (2002) regional groundwater model.
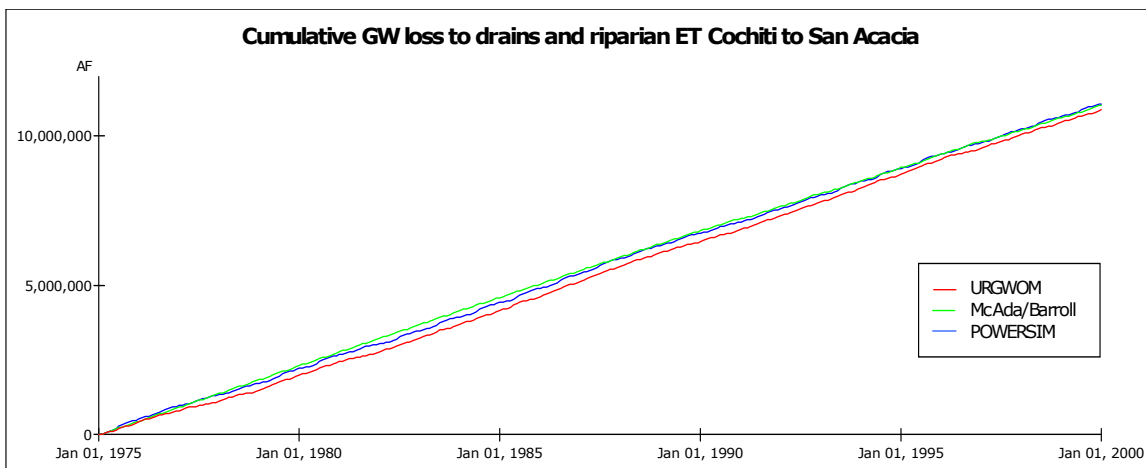
Figure A-8b. Cumulative fluxes out of the groundwater system via drains and riparian ET for the Rio Grande reaches from Cochiti to San Acacia as modeled by the coupled monthly timestep model, the URGWOM surface water model, and the McAda and Barroll (2002) regional groundwater model. Same as Figure 3-24.

Cumulative LFCC GW gains between San Acacia and Elephant Butte reservoir 1975-1999
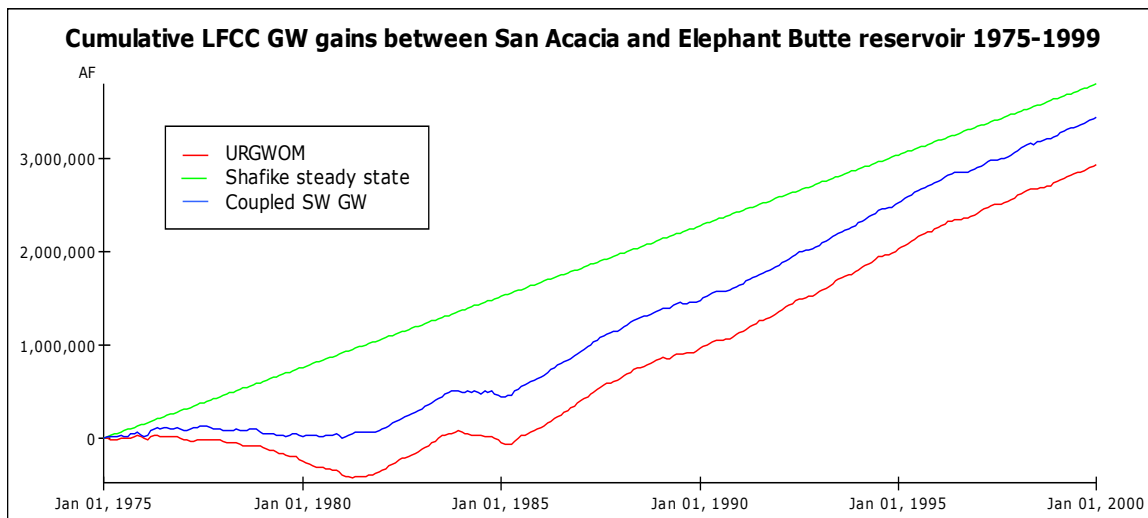
Figure A-9. *Cumulative fluxes out of the groundwater system to the low flow conveyance channel for Rio Grande reaches from San Acacia to Elephant Butte as modeled by the coupled monthly timestep model, the URGWOM surface water model, and steady state values reported by Shafike (2005).*

Cumulative river leakage between San Acacia and Elephant Butte reservoir 1975-1999
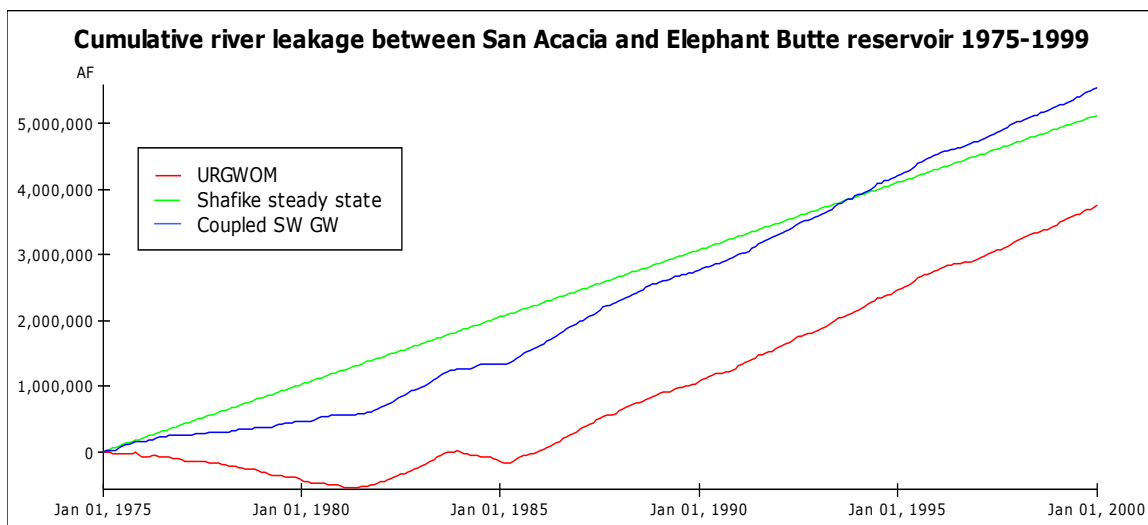
Figure A-10. *Cumulative river leakage for Rio Grande reaches from San Acacia to Elephant Butte as modeled by the coupled monthly timestep model, the URGWOM surface water model, and steady state values reported by Shafike (2005).*
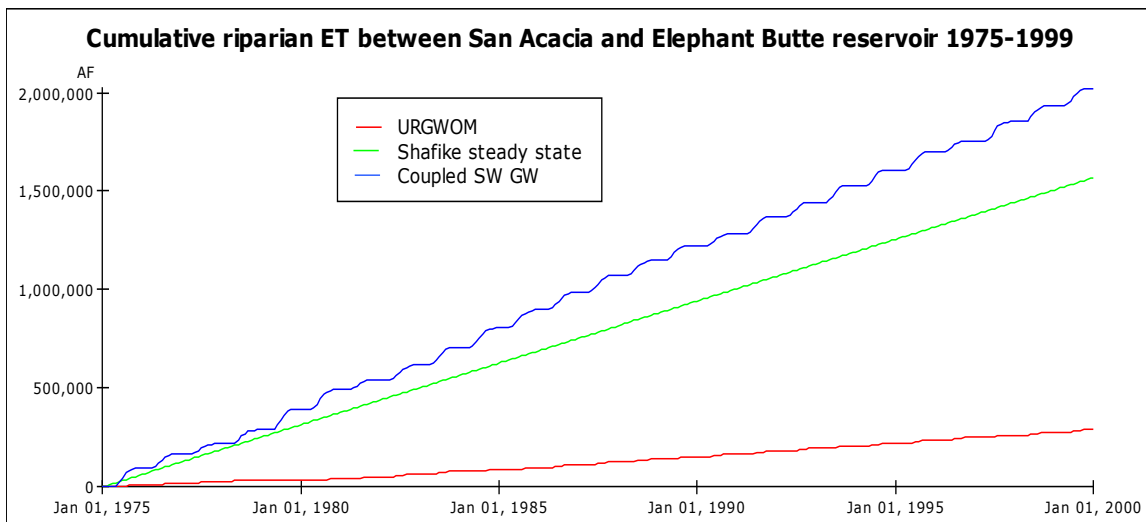
Figure A-11. Cumulative riparian evaportranspiration for Rio Grande reaches from San Acacia to Elephant Butte as modeled by the coupled monthly timestep model, the URGWOM surface water model, and steady state values reported by Shafike (2005).
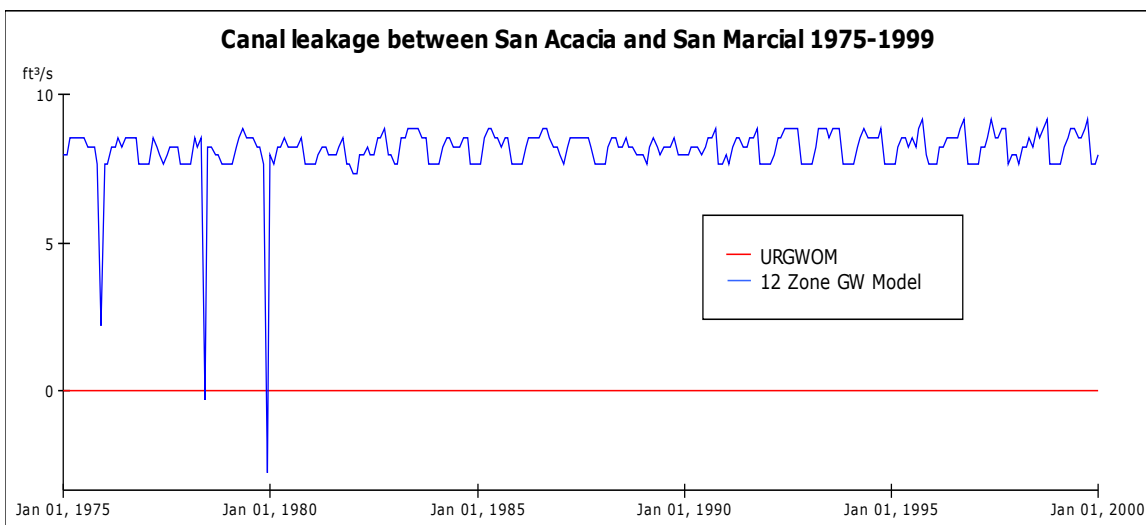
Figure A-12. Irrigation canal leakage between San Acacia and San Marcial as modeled by the coupled monthly timestep model. URGWOM does not track canal leakage in this reach.

Table A-1. Alpha matrix (connectivity and head dependent flow relations) for 51-zone Albuquerque Basin compartmental model [ft²/day]. Numbers represent flow in cubic feet per day from any given groundwater zone to any other groundwater zone for each foot of head difference between the given zones. See Section 3.4.1.1.2. Table continued on the next 10 pages.

Zone	1	2	3	4	5	6	7	8	9	10
1	0	3500	0	47721	0	0	0	0	0	0
2	3500	0	1429	0	95882	0	0	0	0	0
3	0	1429	0	0	0	3.00E+05	0	0	0	0
4	47721	0	0	0	31737	0	10520	0	0	0
5	0	95882	0	31737	0	15630	34374	0	3045	0
6	0	0	3.00E+05	0	15630	0	0	17819	0	16703
7	0	0	0	10520	34374	0	0	6721	0	0
8	0	0	0	0	0	17819	6721	0	0	0
9	0	0	0	0	3045	0	0	0	0	7487
10	0	0	0	0	0	16703	0	0	7487	0
11	0	0	0	0	0	0	0	0	0	0
12	0	0	0	0	0	0	0	0	0	0
13	0	0	0	0	0	0	0	1868	0	0
14	0	0	0	0	0	0	0	14221	0	0
15	0	0	478.9	0	0	0	0	0	0	0
16	0	0	0	0	0	0	0	0	0	0
17	0	0	0	0	0	0	0	0	0	0
18	0	0	0	0	0	7522	0	0	0	0
19	0	0	0	0	0	0	0	0	0	0
20	0	0	0	0	0	0	0	0	0	0
21	0	0	0	0	0	0	0	0	0	0
22	0	0	0	0	0	0	0	0	0	0
23	0	0	0	0	0	0	0	0	0	0
24	0	0	0	0	0	0	0	0	0	0
25	0	0	0	0	0	0	0	0	0	0
26	0	0	0	0	0	0	0	0	0	0

Table A-1 (continued). Alpha matrix (connectivity and head dependent flow relations) for 51-zone Albuquerque Basin compartmental model [ft^2/day]. Numbers represent flow in cubic feet per day from any given groundwater zone to any other groundwater zone for each foot of head difference between the given zones. See Section 3.4.1.1.2. Table continued on the next 9 pages.

Zone	11	12	13	14	15	16	17	18	19	20
1	0	0	0	0	0	0	0	0	0	0
2	0	0	0	0	0	0	0	0	0	0
3	0	0	0	0	478.9	0	0	0	0	0
4	0	0	0	0	0	0	0	0	0	0
5	0	0	0	0	0	0	0	0	0	0
6	0	0	0	0	0	0	0	7522	0	0
7	0	0	0	0	0	0	0	0	0	0
8	0	0	1868	14221	0	0	0	0	0	0
9	0	0	0	0	0	0	0	0	0	0
10	0	0	0	0	0	0	0	0	0	0
11	0	25.53	9790	0	0	0	0	0	0	0
12	25.53	0	0	25360	737.5	0	0	0	0	0
13	9790	0	0	2804	0	0	0	0	0	0
14	0	25360	2804	0	0	0	0	36728	0	0
15	0	737.5	0	0	0	750.1	0	4.00E+05	0	0
16	0	0	0	0	750.1	0	3220	0	5.00E+05	0
17	0	0	0	0	0	3220	0	0	0	3.00E+06
18	0	0	0	36728	4.00E+05	0	0	0	13173	0
19	0	0	0	0	0	5.00E+05	0	13173	0	57557
20	0	0	0	0	0	0	3.00E+06	0	57557	0
21	0	0	4247	8160	0	0	0	0	0	0
22	0	0	0	1387	0	0	0	0	5298	0
23	0	0	0	0	0	0	0	0	0	0
24	0	0	0	0	0	0	0	0	0	2092
25	0	0	0	0	0	0	0	0	0	0
26	0	0	0	0	0	0	0	1934	0	0

Table A-1 (continued). Alpha matrix (connectivity and head dependent flow relations) for 51-zone Albuquerque Basin compartmental model [ft²/day]. Numbers represent flow in cubic feet per day from any given groundwater zone to any other groundwater zone for each foot of head difference between the given zones. See Section 3.4.1.1.2. Table continued on the next 8 pages.

Zone	21	22	23	24	25	26	27	28	29	30
1	0	0	0	0	0	0	0	0	0	0
2	0	0	0	0	0	0	0	0	0	0
3	0	0	0	0	0	0	0	0	0	0
4	0	0	0	0	0	0	0	0	0	0
5	0	0	0	0	0	0	0	0	0	0
6	0	0	0	0	0	0	0	0	0	0
7	0	0	0	0	0	0	0	0	0	0
8	0	0	0	0	0	0	0	0	0	0
9	0	0	0	0	0	0	0	0	0	0
10	0	0	0	0	0	0	0	0	0	0
11	0	0	0	0	0	0	0	0	0	0
12	0	0	0	0	0	0	0	0	0	0
13	4247	0	0	0	0	0	0	0	0	0
14	8160	1387	0	0	0	0	0	0	0	0
15	0	0	0	0	0	0	0	0	0	0
16	0	0	0	0	0	0	0	0	0	0
17	0	0	0	0	0	0	0	0	0	700
18	0	0	0	0	0	1934	5416	0	0	0
19	0	5298	0	0	0	0	12161	0	0	0
20	0	0	0	2092	0	0	0	38966	0	0
21	0	3991	812.5	0	0	0	0	0	0	0
22	3991	0	3986	7479	0	0	0	0	0	0
23	812.5	3986	0	0	1050	0	0	0	0	0
24	0	7479	0	0	5517	0	0	0	0	0
25	0	0	1050	5517	0	0	0	0	0	0
26	0	0	0	0	0	0	0	0	0	0

Table A-1 (continued). Alpha matrix (connectivity and head dependent flow relations) for 51-zone Albuquerque Basin compartmental model [ft^2/day]. Numbers represent flow in cubic feet per day from any given groundwater zone to any other groundwater zone for each foot of head difference between the given zones. See Section 3.4.1.1.2. Table continued on the next 7 pages.

Zone	31	32	33	34	35	36	37	38	39	40
1	0	0	0	0	0	0	0	0	0	0
2	0	0	0	0	0	0	0	0	0	0
3	0	0	0	0	0	0	0	0	0	0
4	0	0	0	0	0	0	0	0	0	0
5	0	0	0	0	0	0	0	0	0	0
6	0	0	0	0	0	0	0	0	0	0
7	0	0	0	0	0	0	0	0	0	0
8	0	0	0	0	0	0	0	0	0	0
9	0	0	0	0	0	0	0	0	0	0
10	0	0	0	0	0	0	0	0	0	0
11	0	0	0	0	0	0	0	0	0	0
12	0	0	0	0	0	0	0	0	0	0
13	0	0	0	0	0	0	0	0	0	0
14	0	0	0	0	0	0	0	0	0	0
15	0	0	0	0	0	0	0	0	0	0
16	0	0	0	0	0	0	0	0	0	0
17	0	0	0	0	0	0	0	0	0	0
18	0	0	0	0	0	0	0	0	0	0
19	0	0	0	0	0	0	0	0	0	0
20	0	0	0	21074	0	0	0	0	0	0
21	0	0	0	0	0	0	0	0	0	0
22	0	0	0	0	0	0	0	0	0	0
23	0	0	0	0	0	0	0	0	0	0
24	0	0	0	0	0	0	0	10646	0	0
25	0	0	0	0	0	0	0	0	1049	0
26	0	0	0	0	0	0	0	0	0	0

Table A-1 (continued). Alpha matrix (connectivity and head dependent flow relations) for 51-zone Albuquerque Basin compartmental model [ft^2/day]. Numbers represent flow in cubic feet per day from any given groundwater zone to any other groundwater zone for each foot of head difference between the given zones. See Section 3.4.1.1.2. Table continued on the next 6 pages.

Zone	41	42	43	44	45	46	47	48	49	50	51
1	0	0	0	0	0	0	0	0	0	0	0
2	0	0	0	0	0	0	0	0	0	0	0
3	0	0	0	0	0	0	0	0	0	0	0
4	0	0	0	0	0	0	0	0	0	0	0
5	0	0	0	0	0	0	0	0	0	0	0
6	0	0	0	0	0	0	0	0	0	0	0
7	0	0	0	0	0	0	0	0	0	0	0
8	0	0	0	0	0	0	0	0	0	0	0
9	0	0	0	0	0	0	0	0	0	0	0
10	0	0	0	0	0	0	0	0	0	0	0
11	0	0	0	0	0	0	0	0	0	0	0
12	0	0	0	0	0	0	0	0	0	0	0
13	0	0	0	0	0	0	0	0	0	0	0
14	0	0	0	0	0	0	0	0	0	0	0
15	0	0	0	0	0	0	0	0	0	0	0
16	0	0	0	0	0	0	0	0	0	0	0
17	0	0	0	0	0	0	0	0	0	0	0
18	0	0	0	0	0	0	0	0	0	0	0
19	0	0	0	0	0	0	0	0	0	0	0
20	0	0	0	0	0	0	0	0	0	0	0
21	0	0	0	0	0	0	0	0	0	0	0
22	0	0	0	0	0	0	0	0	0	0	0
23	0	0	0	0	0	0	0	0	0	0	0
24	0	0	0	0	0	0	0	0	0	0	0
25	0	0	0	0	0	0	0	0	0	0	0
26	0	0	0	0	0	0	0	0	0	0	0

Table A-1 (continued). Alpha matrix (connectivity and head dependent flow relations) for 51-zone Albuquerque Basin compartmental model [ft^2/day]. Numbers represent flow in cubic feet per day from any given groundwater zone to any other groundwater zone for each foot of head difference between the given zones. See Section 3.4.1.1.2. Table continued on the next 5 pages.

Zone	1	2	3	4	5	6	7	8	9	10
27	0	0	0	0	0	0	0	0	0	0
28	0	0	0	0	0	0	0	0	0	0
29	0	0	0	0	0	0	0	0	0	0
30	0	0	0	0	0	0	0	0	0	0
31	0	0	0	0	0	0	0	0	0	0
32	0	0	0	0	0	0	0	0	0	0
33	0	0	0	0	0	0	0	0	0	0
34	0	0	0	0	0	0	0	0	0	0
35	0	0	0	0	0	0	0	0	0	0
36	0	0	0	0	0	0	0	0	0	0
37	0	0	0	0	0	0	0	0	0	0
38	0	0	0	0	0	0	0	0	0	0
39	0	0	0	0	0	0	0	0	0	0
40	0	0	0	0	0	0	0	0	0	0
41	0	0	0	0	0	0	0	0	0	0
42	0	0	0	0	0	0	0	0	0	0
43	0	0	0	0	0	0	0	0	0	0
44	0	0	0	0	0	0	0	0	0	0
45	0	0	0	0	0	0	0	0	0	0
46	0	0	0	0	0	0	0	0	0	0
47	0	0	0	0	0	0	0	0	0	0
48	0	0	0	0	0	0	0	0	0	0
49	0	0	0	0	0	0	0	0	0	0
50	0	0	0	0	0	0	0	0	0	0
51	0	0	0	0	0	0	0	0	0	0

Table A-1 (continued). Alpha matrix (connectivity and head dependent flow relations) for 51-zone Albuquerque Basin compartmental model [ft^2/day]. Numbers represent flow in cubic feet per day from any given groundwater zone to any other groundwater zone for each foot of head difference between the given zones. See Section 3.4.1.1.2. Table continued on the next 4 pages.

Zone	11	12	13	14	15	16	17	18	19	20
27	0	0	0	0	0	0	0	5416	12161	0
28	0	0	0	0	0	0	0	0	0	38966
29	0	0	0	0	0	0	0	0	0	0
30	0	0	0	0	0	0	700	0	0	0
31	0	0	0	0	0	0	0	0	0	0
32	0	0	0	0	0	0	0	0	0	0
33	0	0	0	0	0	0	0	0	0	0
34	0	0	0	0	0	0	0	0	0	21074
35	0	0	0	0	0	0	0	0	0	0
36	0	0	0	0	0	0	0	0	0	0
37	0	0	0	0	0	0	0	0	0	0
38	0	0	0	0	0	0	0	0	0	0
39	0	0	0	0	0	0	0	0	0	0
40	0	0	0	0	0	0	0	0	0	0
41	0	0	0	0	0	0	0	0	0	0
42	0	0	0	0	0	0	0	0	0	0
43	0	0	0	0	0	0	0	0	0	0
44	0	0	0	0	0	0	0	0	0	0
45	0	0	0	0	0	0	0	0	0	0
46	0	0	0	0	0	0	0	0	0	0
47	0	0	0	0	0	0	0	0	0	0
48	0	0	0	0	0	0	0	0	0	0
49	0	0	0	0	0	0	0	0	0	0
50	0	0	0	0	0	0	0	0	0	0
51	0	0	0	0	0	0	0	0	0	0

Table A-1 (continued). Alpha matrix (connectivity and head dependent flow relations) for 51-zone Albuquerque Basin compartmental model [ft²/day]. Numbers represent flow in cubic feet per day from any given groundwater zone to any other groundwater zone for each foot of head difference between the given zones. See Section 3.4.1.1.2. Table continued on the next 3 pages.

Zone	21	22	23	24	25	26	27	28	29	30
27	0	0	0	0	0	0	0	14399	4016	0
28	0	0	0	0	0	0	14399	0	2960	0
29	0	0	0	0	0	0	4016	2960	0	0
30	0	0	0	0	0	0	0	0	0	0
31	0	0	0	0	0	0	0	0	0	1836
32	0	0	0	0	0	0	0	0	0	0
33	0	0	0	0	0	0	0	0	0	0
34	0	0	0	0	0	0	0	0	0	2.00E+05
35	0	0	0	0	0	0	0	0	0	0
36	0	0	0	0	0	0	0	0	0	0
37	0	0	0	0	0	0	0	0	0	0
38	0	0	0	10646	0	0	0	0	0	0
39	0	0	0	0	1049	0	0	0	0	0
40	0	0	0	0	0	0	0	0	0	0
41	0	0	0	0	0	0	0	0	0	0
42	0	0	0	0	0	0	0	0	0	0
43	0	0	0	0	0	0	0	0	0	0
44	0	0	0	0	0	0	0	1559	2155	0
45	0	0	0	0	0	0	0	0	0	0
46	0	0	0	0	0	0	0	0	0	0
47	0	0	0	0	0	0	0	0	0	0
48	0	0	0	0	0	0	0	0	0	0
49	0	0	0	0	0	0	0	0	0	0
50	0	0	0	0	0	0	0	0	0	0
51	0	0	0	0	0	0	0	0	0	0

Table A-1 (continued). Alpha matrix (connectivity and head dependent flow relations) for 51-zone Albuquerque Basin compartmental model [ft²/day]. Numbers represent flow in cubic feet per day from any given groundwater zone to any other groundwater zone for each foot of head difference between the given zones. See Section 3.4.1.1.2. Table continued on the next 2 pages.

Zone	31	32	33	34	35	36	37	38	39
27	0	0	0	0	0	0	0	0	0
28	0	0	0	0	0	0	0	0	0
29	0	0	0	0	0	0	0	0	0
30	1836	0	0	2.00E+05	0	0	0	0	0
31	0	1612	0	0	2.00E+06	0	0	0	0
32	1612	0	952.5	0	0	3.00E+05	0	0	0
33	0	952.5	0	0	0	0	3.00E+05	0	0
34	0	0	0	0	6141	0	0	78761	0
35	2.00E+06	0	0	6141	0	16024	0	0	0
36	0	3.00E+05	0	0	16024	0	10111	0	0
37	0	0	3.00E+05	0	0	10111	0	0	0
38	0	0	0	78761	0	0	0	0	4651
39	0	0	0	0	0	0	0	4651	0
40	0	0	0	0	2.00E+05	0	0	4406	2164
41	0	0	0	0	0	0	0	0	512.8
42	0	0	0	0	0	50668	0	0	0
43	0	0	0	0	0	0	13360	0	0
44	0	0	0	16495	0	0	0	0	0
45	0	0	0	0	8794	0	0	0	0
46	0	0	0	0	0	20383	0	0	0
47	0	0	0	0	0	0	11638	0	0
48	0	0	950.8	0	0	0	0	0	0
49	0	0	0	0	0	0	5442	0	0
50	0	0	0	0	0	0	0	0	0
51	0	0	0	0	0	0	0	0	0

Table A-1 (continued). Alpha matrix (connectivity and head dependent flow relations) for 51-zone Albuquerque Basin compartmental model [ft^2/day]. Numbers represent flow in cubic feet per day from any given groundwater zone to any other groundwater zone for each foot of head difference between the given zones. See Section 3.4.1.1.2. Table continued on the next page.

Zone	40	41	42	43	44	45
27	0	0	0	0	0	0
28	0	0	0	0	1559	0
29	0	0	0	0	2155	0
30	0	0	0	0	0	0
31	0	0	0	0	0	0
32	0	0	0	0	0	0
33	0	0	0	0	0	0
34	0	0	0	0	16495	0
35	2.00E+05	0	0	0	0	8794
36	0	0	50668	0	0	0
37	0	0	0	13360	0	0
38	4406	0	0	0	0	0
39	2164	512.8	0	0	0	0
40	0	10433	6775	0	0	0
41	10433	0	465.4	879.1	0	0
42	6775	465.4	0	4857	0	0
43	0	879.1	4857	0	0	0
44	0	0	0	0	0	12079
45	0	0	0	0	12079	0
46	0	0	0	0	0	6504
47	0	0	0	0	0	0
48	0	0	0	0	0	0
49	0	0	0	0	0	0
50	0	201.7	0	38597	0	0
51	0	0	0	0	0	0

Table A-1 (concluded). Alpha matrix (connectivity and head dependent flow relations) for 51-zone Albuquerque Basin compartmental model [ft^2/day]. Numbers represent flow in cubic feet per day from any given groundwater zone to any other groundwater zone for each foot of head difference between the given zones. See Section 3.4.1.1.2

Zone	46	47	48	49	50	51
27	0	0	0	0	0	0
28	0	0	0	0	0	0
29	0	0	0	0	0	0
30	0	0	0	0	0	0
31	0	0	0	0	0	0
32	0	0	0	0	0	0
33	0	0	950.8	0	0	0
34	0	0	0	0	0	0
35	0	0	0	0	0	0
36	20383	0	0	0	0	0
37	0	11638	0	5442	0	0
38	0	0	0	0	0	0
39	0	0	0	0	0	0
40	0	0	0	0	0	0
41	0	0	0	0	201.7	0
42	0	0	0	0	0	0
43	0	0	0	0	38597	0
44	0	0	0	0	0	0
45	6504	0	0	0	0	0
46	0	4957	0	0	0	0
47	4957	0	0	0	0	1341
48	0	0	0	1.00E+05	0	0
49	0	0	1.00E+05	0	4934	6536
50	0	0	0	4934	0	0
51	0	1341	0	6536	0	0

Table A-2. Zone bottom elevations [ft above mean sea level],
areal extent [km^2], and initial heads [feet above mean sea level] for
the spatially aggregated Albuquerque Basin groundwater model.

Zone	Bottom Elevation [ft amsl]	Area [km^2]	Jan1975 Heads [ft]
1	5159.2	16	5239.7
2	5129.3	29	5209.5
3	5079.1	64	5158.4
4	2860.7	80	5252.6
5	2277.4	87	5219.1
6	-728.1	137	5162.5
7	1465	107	5227.4
8	-2661	183	5174.9
9	3899.2	79	5292.9
10	2617.8	94	5206.4
11	5316	83	5430.4
12	5083.4	41	5172.1
13	3182.4	305	5368.9
14	-68.441	231	5134.6
15	4987.3	100	5066.3
16	4918.4	56	4992
17	4887.2	74	4945.3
18	-751.43	182	5070.5
19	-6335.4	88	4988.1
20	-5916	106	4942.7
21	2519.3	122	5163.5
22	-966.25	206	5024.1
23	1635.3	153	5037.6
24	-2834.3	68	4955.1
25	1066.9	104	4965.2
26	2522.2	54	5226.9
27	780.59	36	4990.9
28	-2424	85	4928.8
29	3135.5	92	5020.5
30	4845.7	73	4920.3
31	4792.4	120	4874.2
32	4734.2	172	4819.2
33	4673.5	109	4756
34	-3002.2	108	4916
35	-4230.1	202	4874.1
36	-3833.2	265	4820.4
37	-1637.1	194	4759.5
38	-1127.3	67	4919.6
39	2358.3	116	4916
40	-2968.1	272	4873.5
41	-1289.6	756	4875
42	-4500.1	272	4822.2
43	-3190.2	213	4776
44	-2977.6	100	4922.5
45	-415.52	139	4894.1
46	-458.59	258	4836.3

Table A-2 continued: Zone bottom elevations [ft above mean sea level], areal extent [km²], and initial heads [feet above mean sea level] for the spatially aggregated Albuquerque Basin groundwater model.

Zone	Bottom Elevation [ft amsl]	Area [km2]	Jan1975 Heads [ft]
47	1364.6	205	4791
48	4627.7	69	4707.2
49	1888.4	140	4713.2
50	1817.5	104	4774.2
51	3417.6	65	4727.5

Table A-3. Calibration parameters for river and reservoir leakage for the spatially aggregated Albuquerque Basin groundwater model.

SW Reach	GW Zone# or Reservoir	Riverbed K/Thickness [day-1]	Riverbed Elevation [ft amsl]	River Slope [-]
CTI2SFP	2	0.1	5213	0.001389
CTI2SFP	3	0.1	5159	0.001389
Jemez	11	0.25	5430	0.003194
Jemez	12	0.25	5185	0.003194
SFP2ALB	15	0.1	5069	0.000976
SFP2ALB	16	0.1	4993	0.000976
SFP2ALB	17	0.02	4938	0.000976
ALB2BDO	30	0.1	4916	0.000797
ALB2BDO	31	0.1	4873.5	0.000797
ALB2BDO	32	0.1	4820	0.000797
ALB2BDO	33	0.1	4755	0.000797
BDO2SA	48	0.1	4704	0.00092
	Cochiti Reservoir	0.0006	5339	
	Jemez Reservoir	0.0012	5129	

Table A-4. Calibration parameters for flow to drains for
the spatially aggregated Albuquerque Basin groundwater model.

SW Reach	GW Zone#	K [ft/day]	Characteristic distance (x_i in Equation 3-15) [mile]	Drain Bed Elevation [ft amsl]
CTI2SFP	2	5	0.45	5208
CTI2SFP	3	5	0.55	5154
SFP2ALB	15	5	0.005	5064
SFP2ALB	16	5	0.2	4988
SFP2ALB	17	5	0.01	4933
ALB2BDO	30	5	0.05	4911
ALB2BDO	31	5	0.25	4868.5
ALB2BDO	32	5	0.2	4815
ALB2BDO	33	5	0.6	4750
BDO2SA	48	5	1.1	4699

Table A-5. Calibration parameters for riparian evapotranspiration from aquifer for
the spatially aggregated Albuquerque Basin groundwater model.

SW Reach	GW Zone#	Surface Elevation [ft amsl]
CTI2SFP	2	5221
CTI2SFP	3	5161.5
Jemez	11	5436
Jemez	12	5187
SFP2ALB	15	5072
SFP2ALB	16	4997
SFP2ALB	17	4941
ALB2BDO	30	4921
ALB2BDO	31	4879
ALB2BDO	32	4824
ALB2BDO	33	4763.5
BDO2SA	48	4716.5

Table A-6. Zone bottom elevations [ft above mean sea level],
areal extent [km^2], and initial heads [feet above mean sea level] for
the spatially aggregated Espanola Basin groundwater model.

Zone	Bottom Elevation [feet amsl]	Area [mile^2]	1975 Head [feet amsl]
1	355	74	5955
2	96	76	5696
3	401	44	6001
4	320	23	5920
5	96	52	5696
6	256	41	5856
7	611	77	6211
8	-111	90	5489
9	406	28	6006
10	963	70	6563
11	143	25	5743
12	551	77	6151
13	930	35	6530
14	5400	22	5600
15	5185	16	5385
16	5480	5	5680

Table A-7. Alpha matrix (connectivity and head-dependent flow relations) for 16-zone Espanola Basin compartmental model [ft^2/month].

Zone	1	2	3	4	5	6	7	8
1	0	0.00862	0	0.15229	0.0019	0	0	0
2	0.00862	0	0.0168	0	0.11299	0.02227	0.00673	0
3	0	0.0168	0	0	0	0	0.00533	0
4	0.15229	0	0	0	0.02389	0	0	0
5	0.0019	0.11299	0	0.02389	0	0.01754	0	0.01814
6	0	0.02227	0	0	0.01754	0	0.01527	0.0216
7	0	0.00673	0.00533	0	0	0.01527	0	0
8	0	0	0	0	0.01814	0.0216	0	0
9	0	0	0	0	0	0.05093	0	0.00922
10	0	0	0	0	0	0	0.01322	0
11	0	0	0	0	0	0	0	0.00806
12	0	0	0	0	0	0	0	0
13	0	0	0	0	0	0	0	0
14	0	0.0883	0	0	0.00104	0	0	0
15	0	0	0	0	0.01518	0	0	0.06972
16	0	0.23003	0	0	0	0	0.00116	0

Zone	9	10	11	12	13	14	15	16
1	0	0	0	0	0	0	0	0
2	0	0	0	0	0	0.0883	0	0.23003
3	0	0	0	0	0	0	0	0
4	0	0	0	0	0	0	0	0
5	0	0	0	0	0	0.00104	0.01518	0
6	0.05093	0	0	0	0	0	0	0
7	0	0.01322	0	0	0	0	0	0.00116
8	0.00922	0	0.00806	0	0	0	0.06972	0
9	0	0.01131	0	0.04091	0	0	0	0
10	0.01131	0	0	0.01298	0.06373	0	0	0
11	0	0	0	0.00466	0	0	0	0
12	0.04091	0.01298	0.00466	0	0.01615	0	0	0
13	0	0.06373	0	0.01615	0	0	0	0
14	0	0	0	0	0	0	0	0.00155
15	0	0	0	0	0	0	0	0
16	0	0	0	0	0	0.00155	0	0

Table A-8. Calibration parameters for stream-aquifer
interactions in spatially aggregated Espanola Basin groundwater model.

SW Reach	In GW Zone	Riverbed Conductance [feet^2/s]	Stream Stage [feet amsl]
Rio Grande north of Otowi	14	0.169	From SW model
Rio Grande south of Otowi	15	6.54	From SW model
Pojoaque River	16	0.5	5671.2
Rio Nambe & Rio Tesuque	7	0.039	6092.8

Table A-9. Head-dependent boundary flow parameters
for spatially aggregated Espanola Basin groundwater model.

Zone	Flow Description	Boundary Head [feet amsl]	Alpha Parameter [feet^2/day]
1	N boundary constant H	6119	392.3
2	N boundary constant H	5640.9	3562.7
3	N boundary constant H	5995.9	4194.9
14	N boundary constant H	6551	1.3
8	To Alb basin zone 1	Alb basin zone 1	265.2
8	To Alb basin zone 4	Alb basin zone 4	5656.8
11	To Alb basin zone 4	Alb basin zone 4	44.4

Table A-10. Alpha matrix (connectivity and head-dependent flow relations)
for 12-zone Socorro Basin for spatially aggregated groundwater model [acre/month].
SB signifies the south boundary, which is assumed to be Elephant Butte Reservoir
for all southern zones (3, 10-12).

Zone	1	2	3	4	5	6
1	0	0.7188	0	0	38.633	0
2	0.719	0	1.0625	0	0	0
3	0	1.0625	0	0	0	0
4	0	0	0	0	6.075	0
5	38.63	0	0	6.075	0	9.675
6	0	0	0	0	9.675	0
7	0	0	0	0.4219	0	0
8	0	33.367	0	0	0.1771	0
9	0	0	0	0	0	0.1194
10	0	0	0	0	0	0
11	0	0	13.5	0	0	0
12	0	0	0	0	0	0
SB	0	0	1.3333	0	0	0

Zone	7	8	9	10	11	12	SB
1	0	0	0	0	0	0	0
2	0	33.367	0	0	0	0	0
3	0	0	0	0	13.5	0	1.3333
4	0.4219	0	0	0	0	0	0
5	0	0.1771	0	0	0	0	0
6	0	0	0.1194	0	0	0	0
7	0	6.3917	0	0	0	0	0
8	6.3917	0	0	0	0.2708	0	0
9	0	0	0	0	0	0	0
10	0	0	0	0	1.4907	0	3.0962
11	0	0.2708	0	1.4907	0	0	0.25
12	0	0	0	0	0	0	0
SB	0	0	0	3.0962	0.25	0	0

Table A-11. Calibration parameters for low flow conveyance channel surface water – aquifer interactions, and riparian evapotranspiration for spatially aggregated Socorro Basin groundwater model. These values were found by calibration with all other source terms set to steady state values.

	Sub Reach	GW Zone #	LFCC char dist [mile]	Shallow Aquifer Ksat [ft/day]	LFCC Bed Elev [ft amsl]	LFCC Slope [-]
Aquifer Zone	SA2BDA	1	3	65	4576.1	0.00097
	BDA2SM	2	3	65	4495.4	0.00097
	SM2EB	3	3	65	4456.1	0.00097

	Sub Reach	GW Zone #	River bed K/Thick [day^{-1}]	River bed Elev [ft amsl]	River Slope [-]	Canal bed K/Thick [day-1]	Canal bed Elev [ft amsl]	Surf Elev [ft amsl]
Aquifer Zone	SA2BDA	1	0.1	4583	0.00079	0.1	4590	4586
	BDA2SM	2	0.1	4501	0.00079	NA	NA	4505.5
	SM2EB	3	0.1	4430	0.00096	NA	NA	4473

REFERENCES

Adar, E. M., and S. P. Neuman, 1986, The use of environmental tracers (isotopes and hydrochemistry) for quantification of natural recharge and flow components in arid basins, *Proceedings of the 5th International Symposium on Underground Tracing*, Athens, Greece: 235-253.

Adar, E., and S. Sorek, 1989, Multi-compartmental modeling for aquifer parameter estimation using natural tracers in non-steady flow, *Advances in Water Resources* Vol. 12: 84-89.

Adar, E. M., S. P. Neuman, and D. A. Woolhiser, 1988, Estimation of spatial recharge distribution using environmental isotopes and hydrochemical data. 1. Mathematical model and application to synthetic data, *Journal of Hydrology* Vol. 97: 251-277.

Albuquerque Bernalillo County Water Utility Authority, 2007, San Juan Chama Drinking Water Project. Website, accessed February 19, 2007 http://www.sjcdrinkingwater.org/

Barroll, P., and P. Burck, 2005, *Documentation of the OSE Taos Area Calibrated Groundwater Flow Model T17.0. Review Draft 11/08/2005*. New Mexico Office of the State Engineer, Water Resource Allocation Program, Technical Services Division, Hydrology Bureau Report, Santa Fe, New Mexico.

Bear, J., and A. Verruijt, 1987, *Modeling Groundwater Flow and Pollution*. Theory and Applications of Transport in Porous Media book series, J. Bear, ed. D. Reidel Publishing Company, Dordrecht, Holland.

Belin, A., C. Bokum, and F. Titus, 2002, Taking Charge of Our Water Destiny: A Water Management Policy Guide for New Mexico in the 21st Century. 1000 Friends of New Mexico. 1001 Marquette NW, Albuquerque NM 87102, (505) 848-8232

Bexfield, L.M., and D. P. McAda, 2003, *Simulated Effects of Ground-Water Management Scenarios on the Santa Fe Group Aquifer System, Middle Rio Grande Basin, New Mexico, 2001-40.* U.S. Geological Survey Water-Resources Investigations Report 03-4040, Albuquerque, New Mexico.

Brower, A., 2004, *ET Toolbox, Evapotranspiration Toolbox for the Middle Rio Grande. A Water Resources Decision Support Tool*, Water Resources Division Technical Service Center, Denver, Colorado, Bureau of Reclamation, United States Department of the Interior. http://www.usbr.gov/pmts/rivers/awards/ettoolbox.pdf

Campana, M. E., and E. S. Simpson, 1984, Groundwater residence times and recharge rates using a dicrete state compartmental model and C-14 data, *Journal of Hydrology* Vol.72: 171-185.

Campana, M. E., G. A. Harrington, and L. Tezcan, 2001, Environmental Isotopes in the Hydrological Cycle: Principles and Applications, W. Mook, ed. UNESCO/IAEA, Vol. VI, pp. 37-73. http://www.iaea.org/programmes/ripc/ih/volumes/volumes.htm

Carter, R.W., J. Davidian, 1968, General procedure for gaging streams. USGS—TWRI Book 3, Chapter A6. http://pubs.usgs.gov/twri/

Clark, I.G., 1987. Water in New Mexico: A History of Its Management and Use. University of New Mexico Press. Albuquerque

Colorado, New Mexico, and Texas, the states of, 1938. Rio Grande Compact. Public Act No. 96, 76th Congress. Approved by the President May 31, 1939.

Colorado, New Mexico, and Texas, the states of, 1948. Resolution Adopted by Rio Grande Compact Commission at the Annual Meeting Held at El Paso, Texas, February 22-24, 1948, Changing Gaging Stations and Measurements of Deliveries by New Mexico.

Fetter, C. W., Jr., 1980, Applied Hydrogeology. Charles E. Merrill Publishing Co., Columbus, Ohio.

Ford, A. 1996. *Testing the Snake River Explorer*. System Dynamics Review, *12*(4), 305-329

Forrester, J.W. 1961. Industrial dynamics. Waltham, MA: Pegasus Communications.

Forrester, J. W. 1987. *Lessons from system dynamics modeling*. System Dynamics Review, *3*(2), 136-149.

Frenzel, P. F., 1995, *Geohydrology and Simulation of Groundwater Flow near Los Alamos, North-Central New Mexico*. United States Geological Survey Water Resources Investigations Report 95-4091, Albuquerque, New Mexico.

Gardner, S. E., 2006, *Water for Endangered Silvery Minnow Considered a Beneficial Use. Mississippi-Alabama Sea Grant Legal Program.* University, Mississippi. Accessed February 28, 2007 from http://www.olemiss.edu/orgs/SGLC/MS-AL/Water%20Log/23.2minnow.htm

Gelhar, L. W., and J. L. Wilson, 1974, *Ground-Water Quality Modeling*, Ground Water, Vol. 12, no. 6, pp. 399-408.

Gleick, P., W.C.G. Burns, E.L. Chalecki, M. Cohen, K.K. Cushing, A.S. Mann, R. Reyes, G.H. Wolff, and A.K. Wong, 2003. The World's Water; The Biennial Report on Freshwater Resources 2002-2003. Pacific Institute for Studies in Development, Environment, and Security. Oakland, California. Island Press, Washington D.C.

Grant, D. M., and B. D. Dawson, 1997, *Isco Open Channel Flow Measurement Handbook, Fifth Edition*. Isco Inc., Lincoln, Nebraska.

Harbaugh, A. W., 1990, *A Computer Program for Calculating Subregional Water Budgets Using Results from the U.S. Geological Survey Modular Three-dimensional Finite-difference Ground-water Flow Model*. U.S. Geological Survey Open-File Report 90-392.

Harris, B. IT Goes Strategic. A new decision-making role emerges for information technology. Government Technology's Public CIO. Winter 2004. URL accessed March 2007: http://govtech.public-cio.com

Hearne, G. A., and J. D. Dewey, 1988, *Hydrologic Analysis of the Rio Grande Basin North of Embudo, New Mexico, Colorado and New Mexico*. United States Geological Survey Water Resources Investigations Report 86-4113, Denver, Colorado.

Horgan, P. 1954, Great River: The Rio Grande in North American History/2 Volumes in 1/Vol 1 Indians and Spain, Vol 2 Mexico and the United States. Wesleyan University Press. Published by University Press of New England, Hanover, NH 03755

Jemez y Sangre Water Planning Council, 2003, *Jemez y Sangre Regional Water Plan*. Prepared by Daniel B. Stephens and Associates, Albuquerque, New Mexico, in association with Amy C. Lewis, Santa Fe, New Mexico. Available October 2006 at http://www.ose.state.nm.us/water-info/NMWaterPlanning/regions/jemezysangre/jys_sec1-5.pdf

Jensen, M. E., 1998, *Coefficients for Vegetative Evapotranspiration and Open Water Evaporation for the Lower Colorado River Accounting System*. Report prepared for the U.S. Bureau of Reclamation, Boulder City, Nevada.

Jury, W. A., and H. Vaux, 2005, The role of science in solving the world's emerging water problems, *Proceedings of the National Academy of Sciences*, Vol. 102, no. 44, 15715-15720. http://www.pnas.org/cgi/doi/10.1073/pnas.0506467102

Konikow, L. F., and J. D. Bredehoeft, 1992, *Ground-water models cannot be validated*, Advances in Water Resources, Vol. 15, no. 1, 75-83.

Kumar, M., G. Bhatt, Y. Qu, and C. J. Duffy, 2006, *Coupling hydrological processes across different spatio-temporal scales: The Juniata River Basin,* Eos Trans. AGU, 87(52), Fall Meet. Suppl., Abstract H31H-07

338

Lyons, M. 2004, Insights from complexity: organisational change and systems modelling. Chapter 2 in Systems Modelling: Theory and Practice. Michael Pidd (Editor). Wiley Publishing, Indianapolis IN. ISBN: 978-0-470-86731-0

McAda, D. P., and M. Wasiolek, 1988, *Simulation of the Regional Geohydrology of the Tesuque Aquifer System near Santa Fe, New Mexico*. U.S. Geological Survey Water-Resources Investigations Report 87-4056, Albuquerque, New Mexico.

McAda, D. P., and P. Barroll, 2002, *Simulation of Ground-Water Flow in the Middle Rio Grande Basin Between Cochiti and San Acacia, New Mexico*. U.S. Geological Survey Water-Resources Investigations Report 02-4200, Albuquerque, New Mexico.

McDonald, M. G., and A. W. Harbaugh, 1988, *A modular three-dimensional finite-difference ground-water flow model: U.S. Geological Survey Techniques of Water Resources Investigations*, Book 6, Chapter A1, 14 ch.

Miller, L., and J. Stiles, 2006, *Water Resources Data, New Mexico, Water Year 2005*. Water-Data Report NM-05-1. United States Geological Survey, New Mexico Water Science Center, Albuquerque, New Mexico. http://pubs.usgs.gov/wdr/2005/wdr-nm-05-1/

Neuman, S. P., and P. J. Wierenga, 2003, *A Comprehensive Strategy of Hydrogeologic Modeling and Uncertainty Analysis for Nuclear Facilities and Sites*. Prepared for Division of Systems Analysis and Regulatory Effectiveness, Office of Nuclear Regulatory Research, U.S. Nuclear Regulatory Commission, Washington D.C. 20555-0001. NRC Job Code W6790. NUREG/CR-6805.

Rio Grande Compact Commission, 1976-2006, *Report(s) of the Rio Grande Compact Commission 1975-2005 to the Governors of Colorado, New Mexico, and Texas*. (31 different reports)

Rosegrant, M. W., X. Cai, and S. A. Cline, 2002. *World water and food to 2025: dealing with scarcity*. Washington, DC: International Food Policy Research Institute (www.ifpri.org).

Roybal, F. E., 1991, *Groundwater Resources of Socorro County, New Mexico*. U.S. Geological Survey Water Resources Investigation Report 89-4083, Albuquerque, New Mexico.

The Santa Fe New Mexican, 2005, *Deal clears way for Espanola, N.M. water plant*. July 23, 2005. http://ww.santafenewmexican.com

Shafike, N. G., 2005, *Linked Surface Water and Groundwater Model for Socorro and San Marcial Basins between San Acacia and Elephant Butte Reservoir. Appendix J in Upper Rio Grande Water Operations Review DEIS*, pp. J-59 to J-94.

http://www.spa.usace.army.mil/urgwops/deis/URGWOPS%20DEIS%20Volume%202/URGWOPS%20Appendix%20J.pdf

Shafike, N. G., 2007, Spreadsheet of New Mexico Rio Grande Compact balance figures from 1941 to 2005. Personal communication.

Simonovic, S. P. and H. Fahmy, 1999, *A new modeling approach for water resources policy analysis.* Water Resources Research, 35(1) 295-304

Smith, G. A., 2001, *The Volcanic Foundation of Cochiti Dam, Sandoval County, New Mexico. New Mexico Decision-Makers Field Guide No. 1: Water, Watersheds, and Land Use in New Mexico. Impacts of Population Growth on Natural Resources. Santa Fe Region*, P. S. Johnson (ed.). New Mexico Bureau of Mines and Mineral Resources.
http://geoinfo.nmt.edu/publications/decisionmakers/2001/dmfg2001_complete.pdf

Tetratech Inc., 2003, *Rio Grande Seepage Study Report, Taos Box Canyon.* Final Report for United States Bureau of Reclamation. Tetra Tech ISG Project No. P06000-0023-01, April 2003.

Tidwell, V.C., H. D. Passell, S. H. Conrad, and R. P. Thomas, 2004, System Dynamics Modeling for Community-Based Water Planning: An Application to the Middle Rio Grande. *Journal of Aquatic Sciences*.

Tidwell, V.C., L.A. Malczynski, H.D. Passell, W.J. Peplinski, M.D. Reno, J. Chermak, D. Brookshire, J. Thacher, K. Grimsrud, C. Broadbent, J. Hanson, J.D. Roach, E. Vivoni, C. Aragon, H. Hallett, K. Cockerill, and D. Coursey, 2006. *Integrated System Dynamics Toolbox for Water Resources Planning.* Sandia Report SAND2006-7676. Sandia National Laboratories, Albuquerque New Mexico 87185.

United States Army Corps of Engineers (USACE), United States Geological Survey (USGS), United States Bureau of Reclamation (BoR), United States Fish and Wildlife Service (USFWS), United States Bureau of Indian Affairs (BIA), and the International Boundary and Water Commission (IBWC), 2002, *Upper Rio Grande Water Operations Model*, Model Documentation, Draft by the Technical Review Committee. http://www.spa.usace.army.mil/urgwom/docintro.asp

United States Army Corps of Engineers (USACE), United States Department of the Interior (USDoI) Bureau of Reclamation (BoR) and New Mexico Interstate Stream Commission (NMISC), 2006. *Draft Environmental Impact Statement (DEIS) Upper Rio Grande Basin Water Operations Review.* URL accessed January 29, 2007: http://www.spa.usace.army.mil/urgwops/drafteis.asp

United States Army Corps of Engineers (USACE), 2007, Shared Vision Planning Website. URL accessed March 1, 2007. http://www.svp.iwr.usace.army.mil/svppage.htm

United States Census Bureau, 2007, City, county, and state population estimates for New Mexico, 1990, 2000, and 2005. URL accessed February 14, 2007: http://www.census.gov

United States Department of Agriculture (USDA), 2007. Natural Resources Conservation Service. National Water and Climate Center. Snow water equivalent readings for Elk Cabin, Lat 35.7043 Long -105.80675. URL accessed February 16, 2007: http://www.wcc.nrcs.usda.gov/snotel/snotel.pl?sitenum=921&state=nm ftp://ftp.wcc.nrcs.usda.gov/data/snow/snow_course/table/history/new_mexico/05p04.txt

United States Department of Agriculture (USDA), Forest Service Southwest Region, and United States Department of the Interior (USDoI) Bureau of Land Management New Mexico State Office, 2004. Draft Environmental Impact Statement of the Buckman Water Diversion Project. Santa Fe National Forest and Taos Field Office of the BLM in Santa Fe County, New Mexico. Website accessed February 19, 2007. http://www.nm.blm.gov/tafo/buckman_eis/docs/draft_eis/Cover%20thru%20Exec%20Summary.pdf

United States Department of the Interior (USDoI), Bureau of Reclamation (BoR), 2006, *Environmental Assessment: San Juan-Chama Water Contract Amendments with City of Santa Fe, County of Santa Fe, County of Los Alamos, Town of Taos, Village of Taos Ski Valley, Village of Los Lunas, and City of Espanola*. Prepared by Aspen Environmental Group for BoR Albuquerque Area Office, May 19, 2006. http://www.usbr.gov/uc/albuq/envdocs/ea/sanjuanchama/finalEA.pdf

United States Department of Interior, Bureau of Reclamation (BoR), 2005, *Water 2025 Preventing Crises and Conflict in the West*, accessed July 17, 2006, at http://www.doi.gov/water2025.

United States Department of the Interior (USDoI) Bureau of Reclamation (BoR), 2002, *Biological Assesment: Effects of LFCC Experimental Operations: Water Diversions from the Rio Grande and Parrot Feather Removal*. Albuquerque Area Office, Albuquerque, New Mexico. http://www.usbr.gov/uc/albuq/library/eis/pdfs/ba_lfcc_mar_2002.pdf

United States Department of the Interior (USDoI), Fish and Wildlife Service (FWS), 2003a, *Endangered and Threatened Wildlife and Plants; Designation of Critical Habitat for the Rio Grande Silvery Minnow; Final Rule.* 50 CFR Part 17 Federal Register, Vol. 68, No. 33, Wednesday February 19, 2003 URL accessed February 22, 2007: http://www.fws.gov/policy/library/03-3255.pdf

United States Department of the Interior (USDoI), Fish and Wildlife Service (FWS), 2003b, *Biological and Conference Opinions of the Effects of Actions Associated with the Programmatic Biological Assessment of Bureau of Reclamation's Water and River Maintenance Operations, Army Corps of Engineers' Flood Control Operation, and Related Non-Federal Actions on the Middle Rio Grande, New Mexico.* Cons. #2-22-03-F-0129 Dated March 17, 2003. FWS P.O.Box 1306, Albuquerque, New Mexico, 87103-1306

van den Belt, M., 2004, <u>Mediated Modeling: A System Dynamics Approach to Environmental Consensus Building</u>. Island Press, Washington D.C.

Ward, F. A., R. Young, R. Lacewell, J. P. King, M. Frasier, J. T. McGuckin, J. Booker, J. Ellis, R. Srinivasan, 2001, *Institutional Adjustments for Coping with Prolonged and Severe Drought in the Rio Grande Basin.* Technical Completion Report Account Number 01423937. New Mexico Water Resources Research Institute. URL accessed February 2007 http://wrri.nmsu.edu/publish/techrpt/tr317/front.pdf

Wells, S. M., 2002, *Watermaster's Report Rio Chama Mainstream 2002.* State of New Mexico, Office of the State Engineer, Santa Fe, New Mexico.

Wilkins, D. W., 1986, *Geohydrology of the Southwest Alluvial Basins Regional Aquifer-Systems Analysis, parts of Colorado, New Mexico, and Texas.* United States Geological Survey Water Resources Investigations Report 84-4224, Albuquerque, New Mexico.

Wilkins, D. W., 1998, *Summary of the southwest alluvial basins regional aquifer-system analysis in parts of Colorado, New Mexico, and Texas.* U. S. Geological Survey Professional Paper 1407A, 49 pp.

Wilkins, D. W., 2006, *Summary data for the 2001-2004 Middle Valley model run using the calibrated URGWOM.* Personal communication.

Wilson, B. C., 1992, *Water Use by Categories in New Mexico Counties and River Basins, and Irrigated Acreage in 1990.* New Mexico State Engineer Office, Technical Report 47

Wolf, A. T., 1999, *Water and Human Security.* AVISO: An Information Bulletin on Global Environmental Change and Human Security. Issue #3, June 1999

Yalcin Sumer, D. and K. Lansey, 2004, *Evaluation of conservation measures in the Upper San Pedro Basin.* Proceedings of the World Water and Environmental Resources Congress. June 27 – July 1, 2004. Salt Lake City, Utah.

Zehnder, A. J. B., H. Yang, and R. Schertenleib 2003, *Water issues: the need for action at different levels.* Aquatic Sciences 65(2003) 1-20